universität wien

DISSERTATION

Titel der Dissertation

„Synthesis and Evaluation of Chiral Cation and Zwitterion Exchanger Materials for Chromatography“

Verfasser

Dipl.-Chem. Christian Hoffmann

angestrebter akademischer Grad

Doktor der Naturwissenschaften (Dr. rer.nat.)

Wien, 2008

Studienkennzahl lt. Studienblatt:	A 091 419
Dissertationsgebiet lt. Studienblatt:	Chemie
Betreuer:	Prof. Wolfgang Lindner

Table of Contents

Appendices:

Publications I-III, Manuscript Draft I, Publication IV, Manuscript Draft II-III, Experimental Section on SO-SA Complex Crystallization

Danksagung

Abstract

Zusammenfassung

curriculum vitae

1 Introduction

1.1 Definitions

Chirality, or often called handedness, is derived from the greek word for hand and represents the geometrical property of a given object to be not superimposable with its mirror image. Two chiral molecules that are related to each other like image and mirror image and are not superimposable are called enantiomers. The composition of a mixture of enantiomers is described by the enantiomeric excess (% ee) and refers to the fraction of the sample that leads to optical activity. A racemate is referred to a stoichiometric 1:1 mixture of two enantiomers, is not optically active and has an ee of 0%. The term stereoisomer is used for molecules that have the same atom-to-atom connections and thus, constitution. However, their atoms or atom groups are oriented differently in three-dimensional space. Besides enantiomers also diastereoisomers are stereoisomers. However, the latter are not like image and mirror image. In an achiral environment, enantiomers have identical physicochemical properties (except their interaction with linear polarized light) and cannot be distinguished from each other. In contrast, diastereomers have distinct physicochemical properties and can be differentiated in an achiral environment.

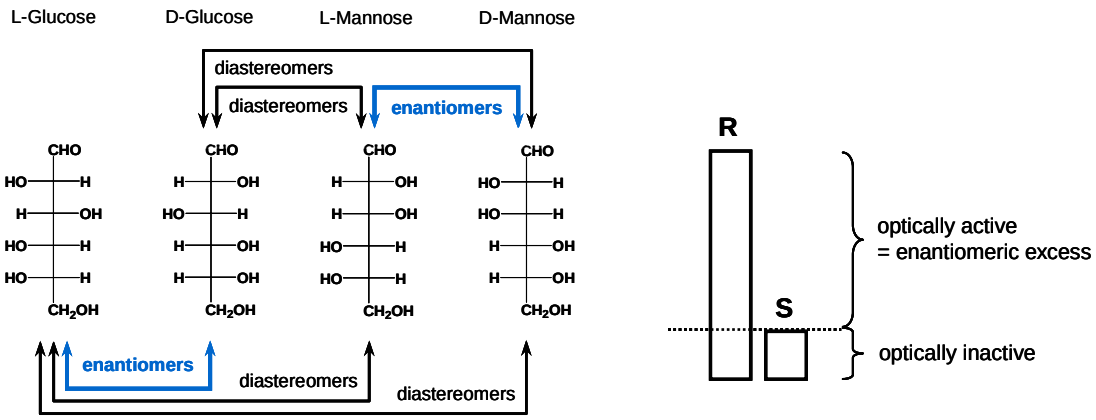

Figure 1. Schematic illustration of enantiomer and diastereomer (left) and enantiomeric excess (right).

1.2 Importance of Chirality

Chirality is an essential and ubiquitous property of living nature since their fundamental building blocks, amino acids and carbohydrates, are chiral and thus, also all resulting

biological macromolecules like DNA, RNA, proteins, and polysaccharides. Hence, biological processes that are mediated by or involve these chiral molecules like e.g. receptor-ligand interactions or enzymatically catalyzed biotransformations can be stereoselective. Therefore, the two enantiomers of a given racemate can interact differently with this chiral environment, leading to distinct biological activities of the two isomers. There are a number of "combinations" described in this context, and scheme 1 depicts a selection thereof.[1]

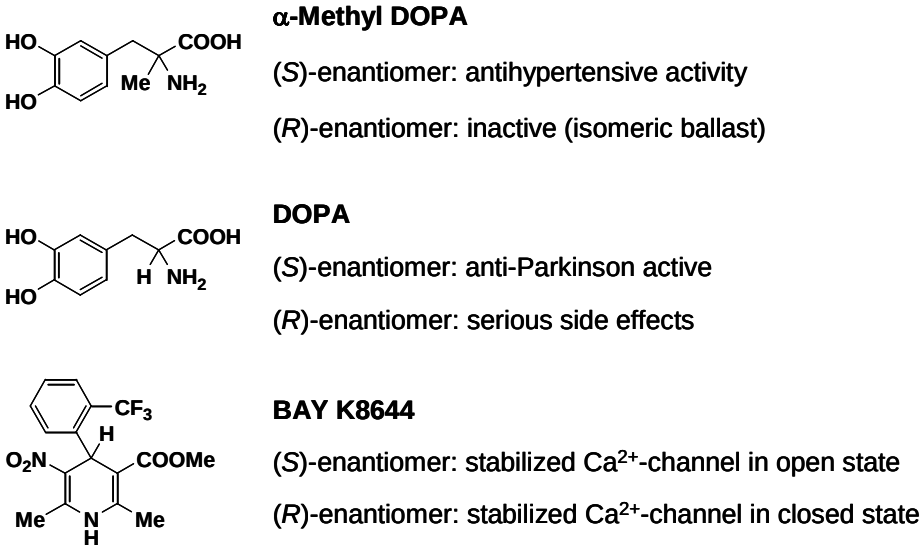

Scheme 1. Combinations of pharmacological activities of the enantiomers of exemplary racemates (adopted from M.Lämmerhofer, lecture on drug- and toxine analysis, 2007).

Consequently, the two enantiomers must be regarded as two separate, individual compounds. This aspect of chirality has major implications in particular for pharmaceutical and agrochemical sciences. In both fields of application xenobiotica, such as drugs, drug-candidates, herbicides, fungicides, and pesticides interact with living systems, and an increasing number of their active compounds employed are chiral. For example, during the different stages of drug discovery and development ranging from early preparation and screening of drug-candidates to pharmacological as well as toxicological studies in the clinical trials, both enantiomers of a given chiral compound and their racemate have to be tested separately. These demands, which are also enforced by the regulatory institutions, require appropriate methodologies both for

making the enantiomeric compounds available as well as for their subsequent monitoring by means of analytical techniques.[2,3]

1.3 Impact of LC Enantiomer Separation

In particular enantioselective liquid chromatographic (LC) techniques can be applied for both analytical and preparative separation challenges today due to its good scalability.

For analytical purposes enantioselective LC is the method of choice besides GC- and CE-based separation techniques, ranging from chip- and capillary-based micro-scale to standard HPLC applications e.g. in pharmaceutical industry for high-throughput monitoring alongside pharmacological and toxicological investigations, in quality control during production of chiral drug substances and their formulations. Also in asymmetric synthesis and catalysis enantioselective HPLC is frequently used. At first, as a convenient tool to measure the outcome of a stereoselective reaction by assessing the enantiomeric excess of the products in the course of investigating and improving enantioselective reactions. In addition, also the determination of the enantiomeric purity of the employed chiral reagents, synthons, and catalysts themselves is important for reliable results. Under the name dynamic HPLC (DHPLC) enantioselective HPLC has also evolved as a method for the characterization of stereolabile substances e.g. in view of determination of enantiomerization barriers and the corresponding kinetic parameters. DHPLC allows to investigate those interconversion processes that happen at the time scale of the chromatographic separation process, and for that purpose employs the variation of experimental parameters like column temperature (from -80 to +80 °C) and flow rate.[4]

On a preparative level, LC enantioseparations are used besides enantioselective and biotechnological synthesis and other separation techniques like crystallization and membrane-based methods. In particular, enantioselective LC is feasible to give rapid access to mg-kg quantities of both enantiomers in highly pure form e.g. at early drug discovery and development stages and for clinical trials. In that way, enantioselective synthesis of small amounts of large numbers of compounds can be avoided, and instead, racemic protocols may be used. Also for the large-scale production of tons of chiral active compound as well as for “polishing” of enantioenriched samples obtained by other approaches, enantioselective LC became applicable. However, at these stages the concert of a number of aspects like cost efficiency, overall productivity, production

of waste (non-utilized enantiomer), and others makes it a case-to-case decision which approach is to be taken.[3]

1.4 Concepts of Chromatographic Enantiomer Separations

The indirect approach implies covalent chemical modification of the enantiomeric mixture with a chiral auxiliar (chiral derivatizing agent, CDA) of high enantiomeric purity. Thereby, a pair of diastereomers is formed that can be separated using standard achiral separation techniques. In preparative applications the chiral auxiliar is removed after successful separation to afford the initial compounds again, now in their enantiomerically pure form. Over the years the indirect enantiomer separation approach became well established but it also holds a series of inherent drawbacks.[5] Most importantly, two additional, ideally high-yielding and racemization-free chemical modifications including subsequent purifications of the product stereoisomers are required. Furthermore, the enantiomeric impurity of the CDA may lead to two pairs of diastereomers and the corresponding enantiomers will coelute during separation. If the separation has preparative focus, the coeluted stereoisomer will end as enantiomeric impurity in the product. Kinetic resolution phenomena, which may occur if rate constants for the two analyte enantiomers are different ($k_R \neq k_S$) and the derivatization reaction is stopped before completion, are a serious complication in analytical applications. These and other shortcomings limit the applicability of the indirect enantiomer separation. Moreover, it is generally desired to avoid time consuming pre-column derivatization schemes to minimize potential sources of inaccuracy and errors in an analytical method.

Thus, the preferred method for chromatographic enantioseparation today is the direct approach, in particular by using chiral stationary phases (CSPs). In general, the chiral auxiliar for the creation of a diastereomeric relationship in the direct CSP approach is bound as a so called chiral selector (SO) onto the surface of a chromatographic solid support. The process of enantiomer separation is now described by the formation of transient, noncovalent diastereomeric associates of the two analyte enantiomers (selectants, SAs) with the SO as the chiral environment of the CSP. The enantioselectivity α is expressed by the differences in free energy of the two diastereomeric complexes, according to the following equations, and manifests in different elution times, respective retention factors of both SA enantiomers.

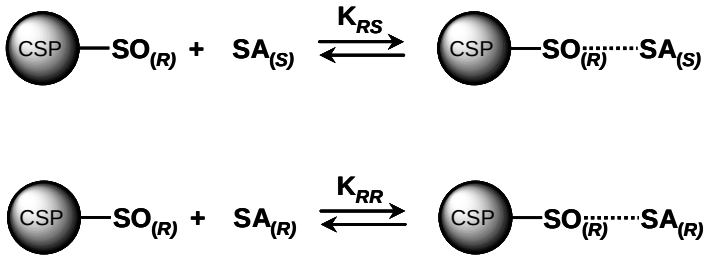

Be SA_R the stronger bound enantiomer, i.e. $K_{RR} > K_{RS}$, and the retention factor k given by the product of the phase ratio Φ and the equilibrium constant of the SO-SA interaction

$$k = \Phi \cdot K$$

and the enantioselectivity α as the ratio of retention factors of second to first eluted enantiomer

$$\alpha = \frac{k_R}{k_S}$$

it follows

$$\Delta\Delta G_{R/S} = \Delta G_{RR} - \Delta G_{RS} = -RT \cdot \ln\left(\frac{K_{RR}}{K_{RS}}\right) = -RT \cdot \ln \alpha$$

Obviously, the chiral SO has to be enantioenriched in order to afford an observable selectivity, and ideally is of high enantiomeric purity. Other than with CDAs however, the magnitude of enantiomeric excess of the SO principally has no impact on the peak purity of the fractionated analyte enantiomers (prepartive LC) and on the determined enantiomer ratio (analytical LC) as long as a baseline separation can be achieved.[6]

If SA retention is exclusively caused by specific interaction with the SO the obtained enantioselectivity represents the true value of the thermodynamic enantiorecognition process. Additional, nonspecific interactions of the SA e.g. with the chromatographic support material could also take place. These interactions would be the same for both enantiomers, thus affecting the retention factor of the first eluting enantiomer relatively stronger than that of the second eluted enantiomer. Accordingly, the ratio of retention factors of second and first eluted enantiomer k_2 and k_1, including specific and

nonspecific contributions k_{sp} and k_{nsp}, would lead to an apparent enantioselectivity α_{app}, expressed by

$$\alpha_{app} = \frac{k_2}{k_1} = \frac{\left(k_{2,nsp} + k_{2,sp}\right)}{\left(k_{1,nsp} + k_{1,sp}\right)}$$

Nonspecific interactions between SA and stationary phase are dependent on the physicochemical properties of the chromatographic system and the particular SA (e.g. ionic interaction between basic SAs and weakly acidic bare silica surfaces), and therefore, appropriate experimental conditions have to be selected for CSP operation in order to minimize these nonspecific contributions to analyte retention.[7,8]

1.5 Chiral Stationary Phases (CSPs)

1.5.1 General Concepts

A large variety of different types of CSPs has been described in the literature[9-12], and they can be classified according to several aspects and common features. Very generally, CSPs typically rely on the one hand on chiral polymers that can either be used as porous bulk material or bound to a chromatographic solid support like silica. On the other hand, individual chiral compounds, covalently linked to silica to afford a surface with separate, distinct SO sites represent the group of brush-type CSPs. CSPs can also be distinguished according to the size of their chiral selectors (macromolecules: synthetic polymers, DNA, RNA, polysaccharides and proteins; low molecular mass selectors ranging from macrocyclic antibiotics and cyclodextrins to small molecules), the source of their chiral entities (natural, semi-synthetic, totally synthetic), or according to their general working principles and the types of intermolecular interactions that they mainly employ (e.g. π-donor/acceptor, hydrogen bonding, metal chelation, ion exchange etc.) which have implications on their general application range in terms of types of analytes as well as on the mobile phase conditions and additives that are then typically employed (nonpolar normal phase, polar organic mode, aqueous reversed-phase).

1.5.2 Polysaccharide-type CSPs

Numerous types of CSPs have also been commercialized. The most wide spread and successfully employed type of commercially available CSPs, both on an analytical as well as on a preparative level, are polysaccharide-based CSPs[3] which were introduced in 1973[13] with microcrystalline cellulose triacetate (CTA-I, see Fig. 2). The pioneering contributions of Okamoto lead to a series of additional, nowadays most common CSPs based on the tribenzoates and trisphenylcarbamates of cellulose and amylose (see Figure 2) with excellent and often complementary enantioseparation abilities towards a broad range of chiral analytes.[14,15]

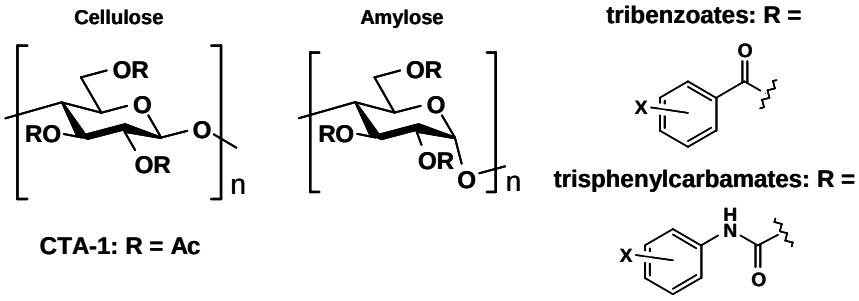

Figure 2. Chemical structures of common polysaccharide-based CSPs (adopted from ref. [15]).

While these CSPs initially were adsorbed onto silica solid support and therefore could solely be operated in very a narrow range of solvents to avoid column degradation, recent introduction of polysaccharide-CSP versions with covalently immobilized polymers led to a further expansion of their applicability. The helical superstructure of the modified polysaccharides and the π-acidity/basicity of the aromatic substituents, affecting the polarity of the benzoate and carbamate groups, was reported to be fundamental for the enantiodiscrimination properties.[16,17] Still, a more detailed picture of the enantiorecognition process of polysaccharide-type CSPs on a molecular level or a generalized binding model seems difficult to be derived.[18] For example, the macromolecules may present not one particular but several different binding sites that might also vary from analyte to analyte, which hampers also spectroscopic investigations of SO-SA interaction.

1.5.3 Brush-type CSPs and Enantioselective Molecular Recognition

A rationale of the process of enantioselective recognition and what leads on a molecular level to a tighter binding of one enantiomer and a less tighter binding of the opposite enantiomer, however, is desirable due to several reasons: It facilitates the finding of an appropriate separation system in terms of type of CSP and operation condition for a new racemate and can replace a trial-and-error approach. A consistent binding mechanism for a series of structurally related analytes supports the prediction of separation properties in the context of indirect assignment of absolute configurations. In addition, it can rationally guide an improvement of the separation properties of a given CSP by chemical modifications.

For a number of CSPs their molecular recognition mechanisms have been successfully investigated in greater detail. Most frequently, such CSPs employed distinct low molecular mass SO entities,[19] like Pirkle-type π-donor/acceptor selectors,[20] cyclodextrins,[21-24] macrocyclic antibiotics-type,[25,26] crown ether-type,[27-31] and also chiral ligand-exchange-type SOs[32-34] (for a selection of these chiral SOs, see Figure 3).

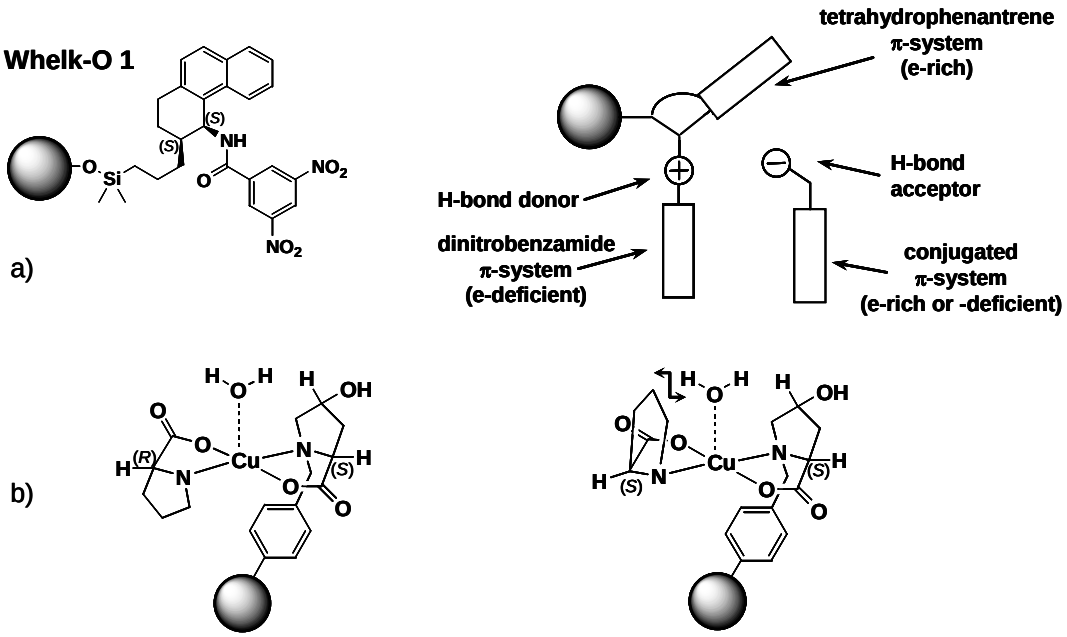

Figure 3. a) Chemical structure of the p-donor/acceptor-type Whelk-O1 CSP (left), and generalized SO-SA interaction prerequisites for successful enantioseparation. b) Chemical structures of SO-proline Cu(II) complexes and enantiodiscrimination model on a chiral ligand-exchange-type CSP (CLEC) based on (*S*)-hydroxyproline (adopted from ref. [10]).

As low molecular mass chiral SOs are either prepared by totally synthetic or semisynthetic protocols they are not seldom available in both enantiomeric forms. This allows to select the analyte's elution order simply by switching to the CSP of opposite configuration and is an important benefit e.g. in preparative applications, or for determination and for the quantification of low abundant enantiomeric impurities.[22,35] In this case, the enantiomer of interest can eluted first via selection of the corresponding CSP configuration. In addition, the synthetic approach to low molecular mass chiral SOs allows to enhance or even tailor their molecular recognition capabilities towards a selected target analyte due to structural modifications. In this context, the successful combination of combinatorial synthesis to provide larger numbers of potential SOs and appropriate read-out systems to screen the SOs for their enantioselective properties have been reported.[19,36-38] Besides other conceptual approaches, SO libraries have frequently been screened, according to the reciprocal recognition of SO and SA, by using the immobilized-target approach ("analyte-type" CSPs) or CE based methodologies that require only low amounts of SO substance to be carried out.[8,39]

1.5.4 *Cinchona*-carbamate based Weak Anion Exchanger CSPs

Typical representatives of CSPs based on the above described low molecular mass SOs are the weak anion exchanger (WAX) type CSPs of the *Cinchona* alkaloid family (Figure 4). These semi-synthetic SOs employ *Cinchona* alkaloid scaffolds that are also successfully and widely used in another field of stereoselective molecular recognition, that is, organocatalysis and catalysis.[40] This class of CSPs has been reported to allow the enantioseparation of a large variety of chiral acidic compounds as its prime class of target analytes. CSPs based on the O9-*tert*butyl carbamates of quinine (QN) and quinidine (QD) have been commercialized as Chiralpak QN-AX and QD-AX[41] (Fig. 4) and, due to the availability of pseudoenantiomeric forms QN and QD, basically allow a switch of analyte elution order.

The general working principle of *Cinchona*-carbamate type CSP is based on an ion pairing process between the protonated quinuclidine amine of the SO and the dissociated acidic function of the analyte as the primary interaction that brings SO and SA in close contact. At this stage, further intermolecular interactions like hydrogen bonding, π-π stacking, steric interactions and others may come into play to afford enantiodiscrimination. During the course of inventing, developing and exploring this

class of SOs and CSPs a comprehensive set of investigations has been conducted which successfully provide more detailed insights into the enantiorecognition mechanism in action.[42]

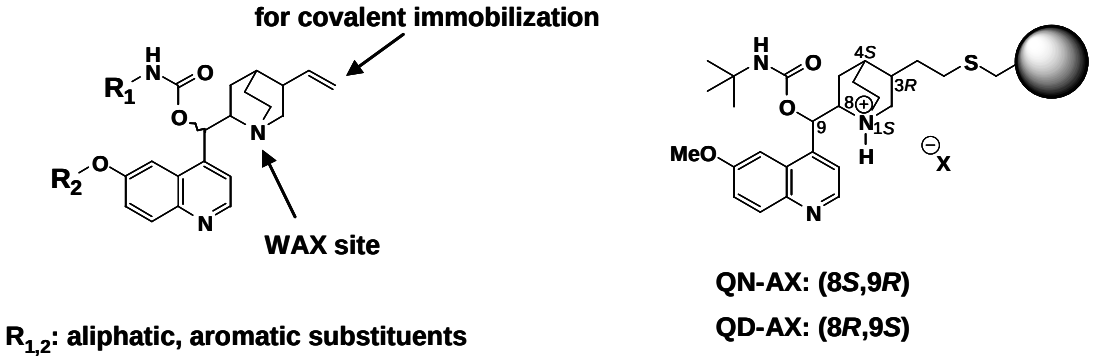

Figure 4. Schematic structure of carbamoylated *Cinchona* alkaloid weak anion exchanger (WAX) SOs with sites for chemical modification (left). Chemical structures of commercially available Chiralpak QN-AX and QD-AX CSPs (right).

Several systematic studies on the structures of SO and SA in LC have been carried out. For example, the influence of both the type of N-derivatizing group and the type of substituent in α-position of N-blocked amino acids was extensively tested, thereby mapping the binding cleft of the chiral SO.[43-46] The DNB-amide group was found to be exceptionally useful to enhance enantioselectivity. Correspondingly, the SO structure was methodically modified around different sets of analytes in order to reveal the parts of SO and SA that interact and to enhance enantioselectivity.[44,47,48] For example, testing of various substituents introduced at O9- and O6'-position of the alkaloid could increase enantioselectivity for model analytes such as DNB-Leu to very high values.[6,49] NMR investigations of selected SO-SA complexes in solution corresponded to the observations in LC and revealed the differential binding of the weaker and stronger bound enantiomers and were supported both by X-ray crystallographic data and theoretical calculations.[49-53] Solid state NMR experiments of the true CSP with model analytes confirmed the findings of the solution studies.[54] Hence, the following tentative binding model was proposed (scheme 2).[43,44]

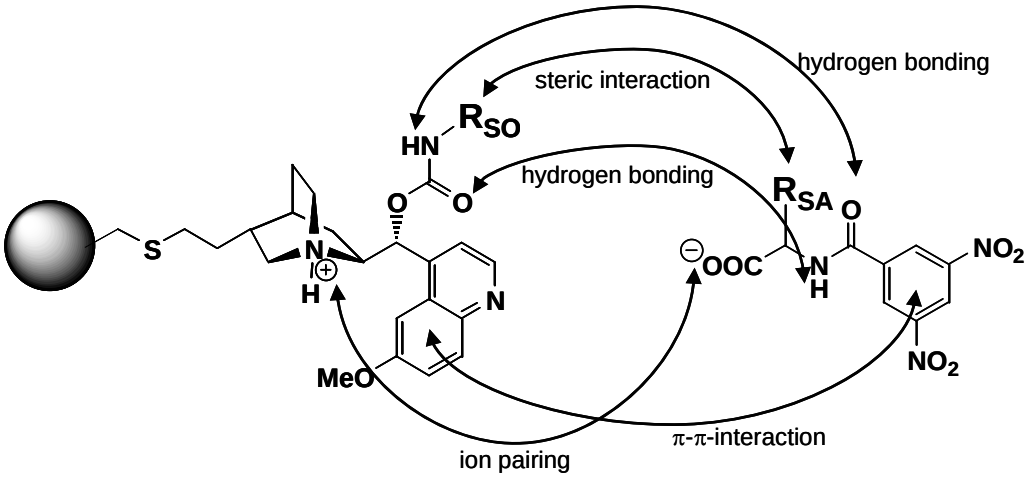

Scheme 2. Chemical structure of the carbamoylated quinine QN-AX CSP and postulated binding model of DNB amino acids (adopted from ref. [43]).

While this particular model has been derived for N-blocked amino acids, it was found to be generally useful guideline also for the study of other chiral acidic compounds, e.g. peptide enantiomers,[45,49-51] chiral auxiliars,[55,56] and xenobiotica[57] and was also employed for the indirect assignment of absolute configurations.[58]

From the several other anion exchanger CSP systems derived from *Cinchona* alkaloids like dimers[59] and hybrids with calixarenes[60,61] the phthalazine-type CSPs[49,62] stand out with remarkably high enantioselectivities (Figure 5).

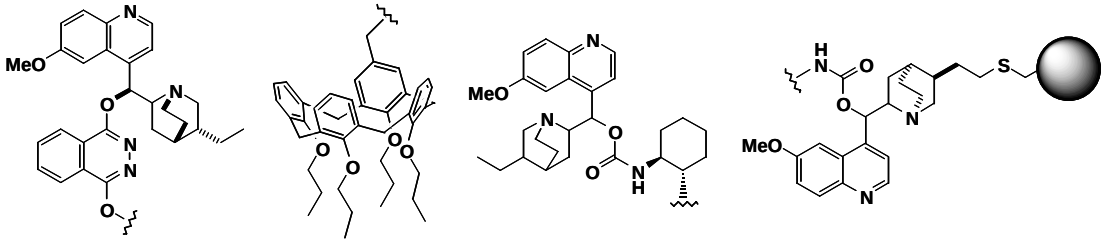

Figure 5. Chemical structures of *Cinchona* WAX CSPs: derived from bis-1,4-(dihydroquinidinyl)phthalazine (left), hybrids with calixarenes (middle), and dimeric selectors (right).

In summary, the extensively investigated *Cinchona* alkaloid derived chiral SOs and CSPs exemplarily depict the potential of the concept of low-molecular mass synthetic

enantioselective recognition entities in general and that of chiral ion exchangers in particular.

1.5.5 Retention mechanism on Ion Exchanger CSPs

Ionic interaction between the protonated amine-type SO and a dissociated acidic analyte is regarded as the main process in SO-SA interaction and analyte retention on the above described weak anion exchanger-type CSPs and is the initial event for the formation of diastereomeric complexes and thus, enantiodiscrimination. At the same time, these ionic interactions are largely responsible for analyte retention. Analyte elution on the other hand is effected by the action of anionic counterions that are added to the mobile phase. The counterions displace the analyte from the oppositely charged SO-site competitively according to a stoichiometric displacement model[63,64] that is expressed by the following equation

$$\log k = \log K_Z - Z \cdot \log[CI]$$

where k is the retention factor, [CI] is the counterion concentration, and Z as the slope is the ratio of effective charges of SA and counterion under the given conditions. The intercept log K_Z represents the log k at a molar concentration of 1 mol/l. This inherent virtual constant K_Z combines several parameters including SO density on the surface and the equilibrium constant of SO-SA ion pairing. Typically, linear relationships between log k and log [CI] are observed for an ion exchange dominated retention mechanism. The effectiveness of a counterion in terms of elution strength is both given by the intercept and the slope. For example, a stronger counterion can be applied in a lower concentration than a weaker counterion in order to afford similar retention factors. Typically, the principal ion exchange processes are identical for both enantiomers which manifests itself in an almost unchanged enantioselectivity alongside changes in counterion concentration.

Obviously, the ionization states of SO, SA and counterion play an important role in the ion exchange process and are determined by the pH or the apparent proton activity pH_a of the mobile phase. The effects of pH are thus superimposed to the ion exchange equilibria. A theoretical model according to the mass action relationship can describe pH-dependencies in ion exchange processes according to the following equation

$$k = \phi \cdot \frac{1}{[CI]} \cdot K \cdot \alpha^*_{SO} \cdot \alpha^*_{SA} \cdot [SO]_{tot}$$

where α^* are the dissociation states of SO and SA, K the ion-exchange equilibrium constant, [CI] the counterion concentration, and $[SO]_{tot}$ the total ion-exchange capacitiy of the stationary phase.[65] From this equation it follows that maximum retention is observed at a pH where there is maximum overlap of dissociation of both SO and SA. From a practical point of view the retention of the analytes can properly be adjusted by selection of the type and concentration of the counterion as well as by the mobile phase pH_a.

1.5.6 Nonenantioselective Characteristics of Ion Exchanger CSPs

The chemical structure of *Cinchona* carbamate-type CSPs comprises besides the anion exchanger site further polar and hydrophobic parts (see Figure 4). When being operated in aqueous reversed-phase conditions these CSPs can be regarded as a mixed mode type stationary phase where both polar and ionic adsorption interactions as well as hydrophobic partitioning processes can take place. These chromatographic mixed mode properties lead to the development of a simplified SO that combined a hydrophobic alkyl chain with a weak anion exchanger site (RP/WAX, see Figure 6) and is particularly useful for the analysis of highly polar, acidic compounds that are difficult to retain e.g. on RP packing materials.[66]

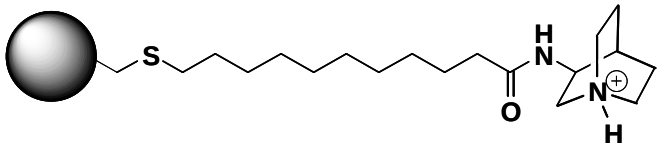

Figure 6. Chemical structure of the mixed-mode reversed-phase/weak anion exchanger (RP/WAX) stationary phase based on N-(10-undecenoyl)-3-aminoquinuclidine.

Several applications in metabolic and toxicological studies proved the potential of the mixed mode RP/WAX concept and also illustrate the versatility of chiral ion exchangers as chromatographic separation materials.[67] Hence, in the course of developing novel ion

exchanger type CSPs also the characterization of their nonenantioselective chromatographic properties becomes appropriate in order to open up new fields of application.

1.5.7 Cation Exchanger CSPs

Recently, and in a complementary fashion to the *Cinchona*-based WAX-type CSPs, also corresponding cation exchanger (CX) type SOs and CSPs have been developed. As prime target analytes these CX-type CSPs conceptually address chiral amine-type compounds which includes the large group of chiral basic drugs. Amino acids and peptides represented the chiral entities of these synthetic low molecular mass chiral CX-SOs which would eventually allow a systematic and straightforward optimization of the SO structure (Figure 7).[68-71] A detailed comparison of carboxylate, phosphonate, and sulfonate functionalities to serve as the cation exchange site of the SO confirmed the sulfonate group as the motif of choice with both broadest scope of applicability as well as widest range of useful experimental conditions that are practical for CSP operation.[69]

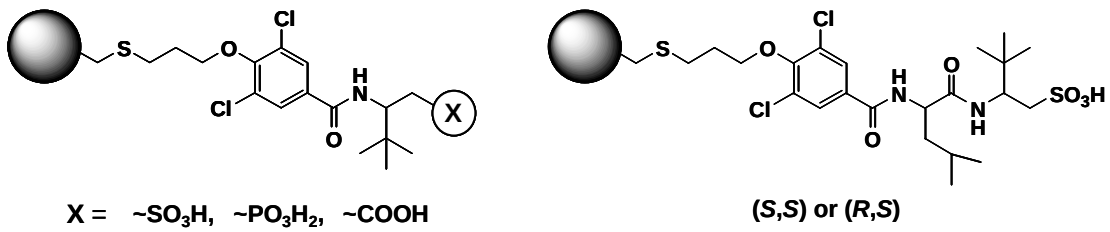

Figure 7. Chemical structures of CX-type CSPs based on amino acids and dipeptides (adopted from ref. [69,71])

These CX-type SOs have been successfully applied for the enantiomer separation of numerous chiral basic drugs and related compounds but so far only in capillary format using capillary electrochromatography (CEC) and capillary liquid chromatography (CLC) methodologies. However, application and evaluation in standard HPLC columns, where peak efficiencies are principally lower as opposed to CEC techniques and therefore overall higher enantioselectivities are required for baseline enantioseparation, of such CX-type CSPs was still to be realized when this thesis was started.

1.5.8 Zwitterionic Chiral Solutes and Packing Materials

As pointed out above, ion exchanger type CSPs have so far been reported to enable enantiomer separations of many chiral basic and acidic compounds. On the other hand the large group of chiral amphoteric substances like amino acids do not seem to be their prime target analytes because up to now only two corresponding studies were reported that show enantiomer separations of amino acids using a QN-AX CSP.[72,73] Nevertheless, ion exchanger CSPs appear conceptually suited for enantioselective amino acid analysis since compounds of this class are *per se* ionized. Furthermore, the enantioselective analysis of amino acid enantiomers is becoming an increasingly relevant task, in particular in the context of determination and quantification of low abundant D-amino acids in mammalian tissues in order to study their biochemical functions,[74-76] in food stuffs to perform quality control and to investigate food processing,[77,78] and to date chronological ages of bones and teeth by determination of the degree of amino acid racemization.[79,80]

For the direct liquid chromatographic enantiomer separation of underivatized amino acids CSPs based on macrocyclic antibiotics,[26,81-84] crown ethers,[85-87] proteins,[88] RNA aptamers,[89,90] α-CD,[91] and chiral ligand-exchange[32-34] have been reported, with the macrocyclic antibiotics CSPs being the most successful and widely used. However, these packing materials rely mainly on other types of SO-SA interaction than classical ion exchange such as metal chelation and multiple hydrogen bonding. In 1989 Hartwick et.al. showed in a single preliminary example the separation of phenylalanine and tryptophan enantiomers using a chiral stationary phase made up of a zwitterionic alanine derivative (Figure 8) – only to provide evidence for a postulated double ionic interaction between the zwitterionic stationary phase and zwitterionic analytes in nonenantioselective separations.[92] Yet, it seems that this report has hardly been recognized as no further, eventually systematic, study appeared to date on the enantioselective properties towards amino acid enantiomers of comparable, covalently immobilized zwitterionic packing materials. Merely the separation of tryptophan enantiomers by means of a (L)-Leu-(L)-Leu-(L)-Leu tripeptide adsorbed onto octadecylsilane modified silica was reported in 1982[93] and further investigated in 2000[94].

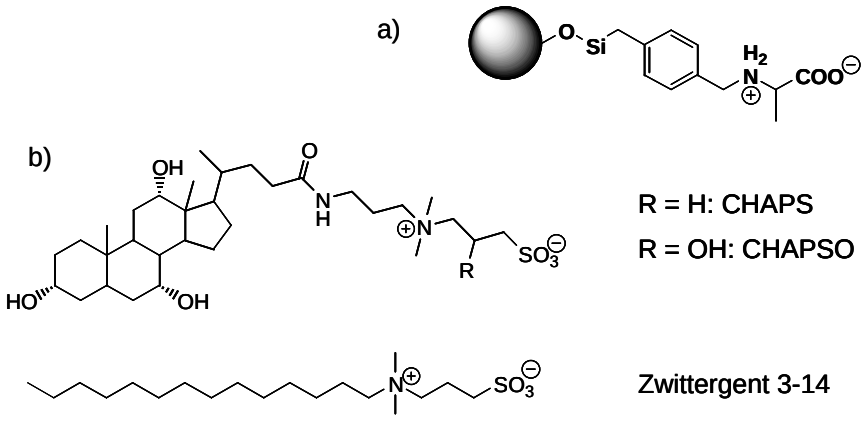

Figure 8. Chemical structures of a) the chiral weak zwitterion exchanger described by Hartwick et.al. (adopted from ref. [92]), b) the surfactants that were used for the preparation of zwitterionic stationary phases by coating onto octadecylsilica for electrostatic ion chromatography EIC (adopted from ref. [95]).

On the other hand, zwitterionic stationary phases of various kinds (Nesterenko review) become more and more popular in the last decade in several areas of nonstereoselective liquid chromatography. In particular, zwitterionic surfactants like Chaps and Chapso, adsorbed onto C18-modified silica, were used in ion chromatography IC for the separation of inorganic ions (Figure 9).[96-100] In addition, mainly Irgum et.al. described polymer-based zwitterionic stationary phases (see Figure 10) that have been applied in IC, but most importantly for hydrophilic interaction liquid chromatography (HILIC) separations of – often amphoteric – peptides and proteins.[101-107]

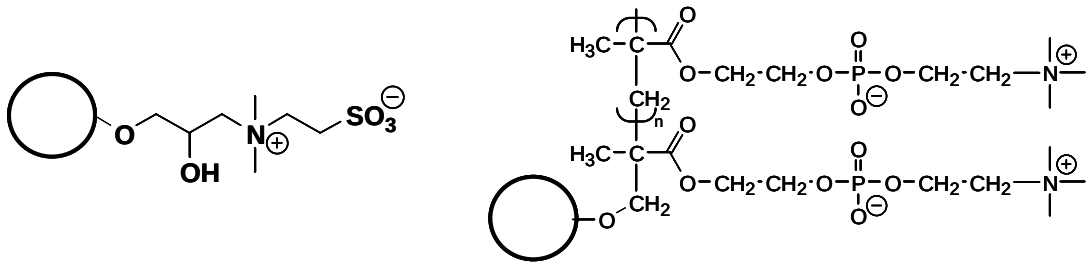

Figure 9. Chemical structures of zwitterionic stationary phases based on sulfobetaine-type copolymers (left) and phosphorylcholine-type polymer grafts (adopted from ref. [101, 106]).

Finally, immobilized artificial membrane chromatography IAM based on covalently attached cell membrane phospholipids to chromatographic solid supports have been

described as a useful tool to study ion exchange and hydrophobic properties of cell membranes and analyte partitioning between liquid phase and the membranes.[95,108-111] In this context, NMR investigations stated the simultaneous double ion pairing of tryptophan and an IAM made up from zwitterionic phospholipids.[112]

Apparently, there are indications for that point towards the applicability of ion exchanger CSPs in the context of zwitterionic chiral analytes that still have to be tested.

2 Aims of the Thesis

The aims of the present thesis were the design and the synthesis of novel chiral selectors, based on low molecular mass ion exchangers, and corresponding CSPs followed by their evaluation for the liquid chromatographic enantiomer separation.

In particular, a new approach to novel cation exchanger CSPs was to be developed to afford the enantioseparation of chiral basic drugs and related compounds by HPLC employing an ion exchange mechanism. Therefore, a modular synthesis scheme was created that could give access to systematically varied selector structures, and would eventually allow to prepare larger numbers of selectors according to combinatorial synthesis protocols for target-analyte oriented selectors screening.

Furthermore, ion exchanger based selectors and CSPs were to be designed that would address the amphoteric character of amino acids and other chiral zwitterionic compounds as a principal molecular recognition feature for their successful enantioseparation. In doing so, conceptually all types of ionizable chiral compounds would be made susceptible to enantioselective ion exchange.

The chromatographic evaluation of the novel packing materials focused on enantioselectivity in order to assess their enantiorecognition capabilities and to allow to draw conclusions on the molecular recognition processes being in function. Nevertheless, detailed investigations of the overall chromatographic properties of the newly prepared ion exchanger type CSPs were to be carried out in order to determine the underlying retention mechanisms, and to describe experimental conditions for their successful operation – also in nonenantioselective applications.

3 Results and Discussion

3.1 General Aspects

In this chapter mainly those results will be presented that afforded either manuscripts that were already published or manuscript drafts that were ready for submission at the time of writing this thesis. Abstract pages are included in this chapter to allow fluent reading. In order to avoid extensive repetition, however, the content of the articles and drafts is only mentioned briefly herein, together with additional results, to put the articles and drafts in context. For the complete information it is therefore referred to the full articles and manuscript drafts that are given in the appendices.

3.2 Cation Exchanger type SOs and CSPs

3.2.1 SO and CSP Design and Synthesis

Generally, the low molecular mass chiral CX-type SOs described until now employed various amino acids as building blocks, either as a single compound or in form of dipeptides.[68-71] In that way, incremental contributions to enantioselectivity could be derived for instance to a particularly bulky amino acid side chain.[71] Nevertheless, no structural motif with fundamental significance for enantioselectivity towards chiral basic analytes (i.e. reasonably large α-values for a wider range of chiral bases) could be identified. It was therefore important to examine further types of building blocks that are readily accessible in larger quantities. While previously reported CX-type CSPs (see above) were mainly based on α-amino acids, β-amino acids have not been fully evaluated yet in this context.[69] β-Amino acids however have received a lot of interest in synthetic chemistry and especially the conformations of their peptidic derivatives differ significantly from those comprised of α-amino acids.[113-116] Since in the amino acid-derived CX-SOs the amino groups were typically modified as amides, β-amino acids were selected herein to be examined as building blocks in CX-type SOs. Furthermore, sulfonates were found to be the most promising functionalities for the cation exchange process.[69] However, in the sulfonate-based CX-CSPs prepared so far the cation exchange site was always attached at an achiral methylene-group and the closest chiral center was at least one bond further away (e.g. cysteic acid). It may be expected that close proximity of the ion exchange site to a center of chirality can be beneficial for the

enantioselective interaction of SO and analyte. In addition to the beta-amino acid scaffold the attachment of the sulfonate group directly at a chiral center thus became a prerequisite for the CX-type SOs to be developed herein.

The following modular synthesis scheme had been designed to give access to novel CX-type SOs and their systematic structural variation (scheme 3).

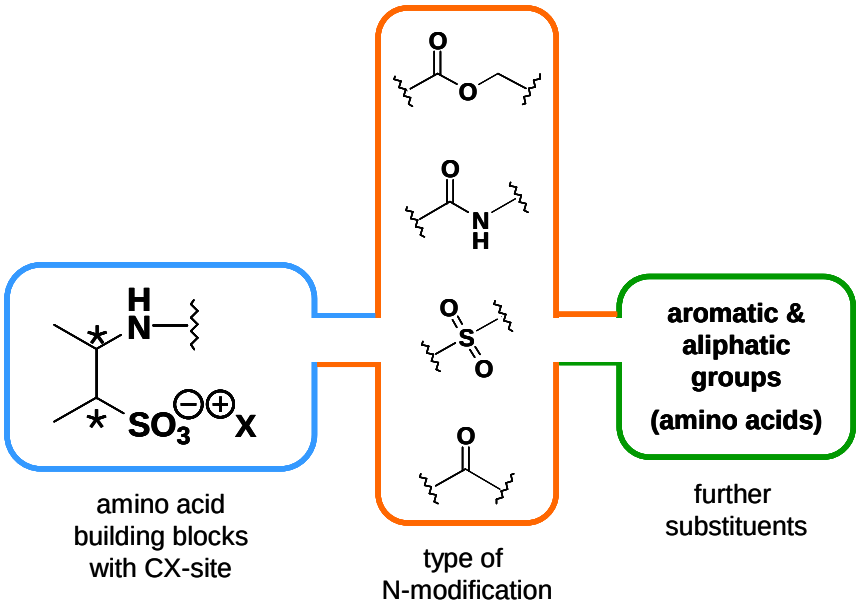

Scheme 3. Modular synthesis scheme for the preparation of structurally divers CX-type chiral SOs.

Starting points represented the β-aminosulfonic acid building blocks with the sulfonate as the site for ionic interaction with the basic analyte and the β-amino group for chemical modification. As N-derivatizations, carboxylic amides, sulfonamides, carbamates, and ureas were envisioned for providing e.g. various donor/acceptor patterns for hydrogen bonding among SO and SA, as well as different geometry and distance between the aminosulfonic acid and further substituent groups. As substituents aromatic moieties of altered size and π-acidity/basicity and aliphatic groups of diverse steric demand were possible. Both N-derivatization and the further substituents were to be introduced in one step by reaction with alkyl- and aryl-sulfonyl chlorides, -chloroformates, -isocyanates and -carboxylic acids and acid chlorides. Immobilization to the silica chromatographic support could either occur via additional appropriate functional groups at the aminosulfonic acid building blocks or at the N-modification, thereby employing well established protocols.[47,117] In the first place, it was planned to

prepare CX-type SOs consisting solely of one amino acid unit, but eventually, also peptidic modifications at the β-amino group might be carried out.

Conceptually, a racemic and therefore straightforward route for the preparation of the sulfonic acid based chiral SOs was preferred due to the following reasons. With the potent AX-type CSPs of the *Cinchona* carbamate type in hand, purification of the acidic SO enantiomers prior to immobilization guarantees high enantiomeric purity and reproducibility while in addition enantioselective synthesis is not required and no precautions concerning racemization during synthesis have to be taken into consideration. Furthermore, both enantiomeric forms of the SOs become available in the same time. This gives access to CSPs of opposite absolute configuration, and therefore the elution order of analytes to be enantioseparated later on can be reversed simply by switching from one enantiomeric CSP to the other. Finally, a rather simple and fast synthesis route to racemic SOs – according to a modular synthesis scheme appropriate also for combinatorial synthesis – is ideally suited for generating a library or a larger set of structurally divers SOs which then can be directly screened for their enantioselective properties, for example towards a target analyte, using CE techniques (see above).

β-Aminosulfonic acids with the acid group being at a chiral center were not commercially available. Several synthetic approaches that give access to chiral β-aminosulfonic acids have been described in the literature and essentially employed the corresponding amino alcohols as starting material. Subsequent functional group interconversion of the alcohol lead to the desired amino acids.[118-124] If the amino alcohols were not directly available they had to be prepared – from the corresponding epoxide or even from the alkene itself. A rather different approach represented the direct amino-sulfonation of alkenes by sulfur trioxide SO_3 in the presence of nitriles which is also used for the industrial production of acrylamidosulfonic acid monomers. Only recently, Cordero et. al. adopted this three-component reaction for a laboratory scale by substituting liquid SO_3 or oleum by a commercially available, solid SO_3•DMF complex.[125] The postulated reaction mechanism is depicted in the scheme 4. Addition of SO_3 to the alkene affords a β-sultone that reacts in situ by nucleophilic attack of acetonitrile to give an oxathiazine that hydrolyses upon addition of water to give a N-acetyl-β-aminosulfonic acid. In a subsequent step hydrolysis affords the amphoteric β-aminosulfonic acid. If the alkene was not terminal the amino-sulfonation

stereoselectively lead to *anti* addition of amino and sulfonic acid groups. The presence of trifluoromethane sulfonic acid TfOH was found to enhance the reaction rate as well as the yield of the product.

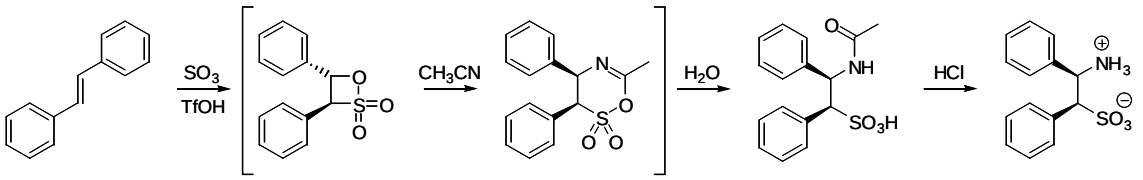

Scheme 4. Reaction scheme of the direct amino-sulfonation of alkenes (adopted from ref. [125]).

Principally, this amino-sulfonation reaction appeared feasible for our purposes for several reasons.[125] It involves as a starting material alkenes which are commercially available in a broad structural range. Both functional groups that were required in the β-aminosulfonic acid building block are formed in one step. The reaction is stereoselective, however not enantioselective. Thus, racemic products are obtained but not a more complex mixture of stereoisomers. Finally, access is given to sulfonic acid groups that are directly attached at chiral centers. Therefore, the three-component direct amino-sulfonation reaction was employed in the following to initially provide access to different chiral β-aminosulfonic acids.

3.2.2 Evaluations of SCX-type SOs and CSPs

The above described approach to novel low molecular mass chiral SOs for cation exchanger type CSPs has been applied for the preparation of a series of racemic SCX-SOs on a mg-scale. Their screening for enantioselectivity towards a target chiral basic compound was also carried out. However, this chiral basic compound was investigated in cooperation with an industrial partner and due to confidentiality agreements and patent issues no particular results can be shown here, but will be presented after release by the industrial partner. Nevertheless, from one of these racemic SCX-SOs the corresponding enantiomeric CSPs have been prepared and evaluated for the enantiomer separation of a number of nonrestricted chiral basic drugs for HPLC. The resultant findings were reported in the following publication (C. Hoffmann et. al., Journal of Chromatography A 2007, 1161, p. 242-251; for the complete article, see Appendix P-I):

Novel strong cation-exchange type chiral stationary phase for the enantiomer separation of chiral amines by high-performance liquid chromatography

Christian V. Hoffmann, Michael Lämmerhofer, Wolfgang Lindner*

Christian Doppler Laboratory for Molecular Recognition Materials, Department of Analytical Chemistry
and Food Chemistry, University of Vienna, Währinger Strasse 38, A-1090 Vienna, Austria

* Corresponding author

Abstract
The preparation of novel brush-type chiral cation-exchange materials based on *de novo* designed synthetic low molecular mass selectors (SOs) and their evaluation for enantioselective separation of chiral amines by HPLC are presented. The SO as the functional unit for enantioselectivity contains a β-aminocyclohexanesulfonic acid moiety and is readily accessible via straightforward synthesis in both enantiomeric forms yielding chiral stationary phases (CSPs) with opposite configurations, CSPs **1** and **2**, and reversed elution orders. For the evaluation of these novel CSPs by HPLC a sound set of chiral amines, mainly amino-alcohol type drug molecules, was selected. The chromatographic evaluations were carried out using polar organic mobile phase conditions. All of the analytes could be baseline separated, compared to common CSPs in parts with excellent peak efficiencies (up to 70000 theoretical plates per meter for the second eluted enantiomer). A number of experimental parameters have been varied to look at and prove the underlying ion-exchange process on CSPs **1** and **2**, and to reveal suitable conditions for their operation. In this context, the influence of proton activity in the mobile phase and the effects of varying concentration and type of the counterion as well as type of co-ion and of bulk solvent components were thoroughly investigated.

Keywords: Enantiomer separation; Chiral stationary phase; Cation exchanger; Liquid chromatography; Chiral amines; β-Aminosulfonic acid. doi:10.1016/j.chroma.2007.05.092

Received: 26 April 2007; Accepted: 31 May 2007.

The chiral SO **1** that was employed in the article reported above (Figure 11) was also investigated for microscale enantioseparations of racemic basic drug analytes. For that purpose, **1** was covalently immobilized onto thiol-modified silica monoliths in fused-silica capillaries. At first, these monolithic SCX-type CSPs were studied in a direct comparison of capillary electrochromatoraphy (CEC) and capillary LC (CLC) as separation techniques in enantioselective chromatography (B. Preinerstorfer et. al., Electrophoresis 2008, 29, p. 1626-1637; for the complete article, see Appendix P-II). The same monolithic CSPs were applied for an investigation of the electrokinetic and chromatographic processes that effect analyte migration in stereoselective cation exchange CEC (B. Preinerstorfer et. al., Journal of Separation Science 2008, 29, p. 3065-3078; for the complete article, see Appendix P-III).

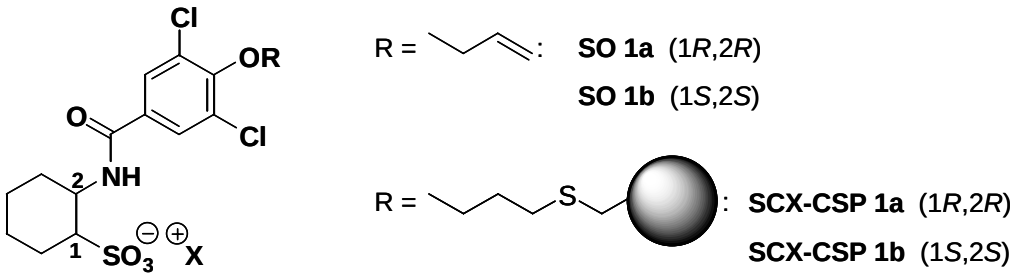

Figure 10. Chemical structures of the b-aminosulfonic acid based **SOs 1a**,**b** and the corresponing SCX-type **CSPs 1a**,**b**.

Enantioselective silica-based monoliths modified with a novel aminosulfonic acid-derived strong cation exchanger for electrically driven and pressure-driven capillary chromatography

Beatrix Preinerstorfer[1], Christian Hoffmann[1], Dieter Lubda[2], Michael Lämmerhofer[1]*, Wolfgang Lindner[1]

[1]Christian Doppler Laboratory for Molecular Recognition Materials, Department of Analytical Chemistry & Food Chemistry, University of Vienna, Vienna, Austria
[2]Performance & Life Science Chemicals, Merck KGaA, Darmstadt, Germany

*Correspondence to Michael Lämmerhofer

Abstract
Silica monoliths modified with trans-(1*S*,2*S*)-2-(N-4-allyloxy-3,5-dichlorobenzoyl)amino cyclohexanesulfonic acid were tested for enantioselective separations of various chiral bases by aqueous and nonaqueous CEC as well as nano-HPLC. The optimization of the immobilization procedure showed that an intermediate selector (SO) coverage, as does result from a single static immobilization cycle in the capillary at 60°C with an 8% (m/v) SO solution in methanol, affords maximal EOF and optimal enantioselectivity values, while a second immobilization cycle does not lead to any improvements. Furthermore, the mobile phase composition was examined regarding the effectiveness of aqueous phases (ACN/water and methanol/water) compared to nonaqueous eluents (ACN/methanol) in terms of separation selectivity and efficiency. Additionally, different acids of varying strengths were tested as co-ions in the ion-exchange process, including formic acid, acetic acid, methanesulfonic acid, and TFA (pK_a from 4.75 to 0.5). It turned out that the effects regarding EOF and enantioselectivity were largely negligible. The chromatographic efficiencies of the new capillary columns were compelling and remarkable for bases. H-u curves established for mefloquine revealed a C-term contribution (resistance to mass transfer) by a factor of about six lower in CEC than in nano-HPLC and an A-term (flow maldistribution) about three times lower in the CEC mode. Theoretical plate heights as low as around 3-5 μm could be obtained in CEC over a wide flow range (0.5-1.5 mm/s). Run-to-run repeatabilities like in HPLC and excellent system stability promise the practical usefulness of the novel monolithic capillary column for enantiomeric composition analysis of pharmaceuticals by CEC.

Keywords: Capillary electrochromatography / Capillary liquid chromatography / Chiral stationary phase / Silica monolith / Sol-gel process DOI 10.1002/elps.200700525

Received: July 19, 2007; Revised: September 14, 2007; Accepted: October 7, 2007.

Deconvolution of electrokinetic and chromatographic contributions to solute migration in stereoselective ion-exchange capillary electrochromatography on monolithic silica capillary columns

Beatrix Preinerstorfer[1], Michael Lämmerhofer[1], Christian V. Hoffmann[1], Dieter Lubda[2], Wolfgang Lindner[1]

[1]Department of Analytical and Food Chemistry, Christian Doppler Laboratory for Molecular Recognition Materials, University of Vienna, Vienna, Austria
[2]Performance and Life Science Chemicals, Merck KGaA, Darmstadt, Germany

*Correspondence to Michael Lämmerhofer

Abstract
A monolithic silica stationary phase functionalized with an enantioselective strong cation exchanger based on an aminosulfonic acid derivative was used for chiral separations of basic test solutes by nonaqueous CEC and capillary LC. The effects of the applied electric field as well as the ionic strength in the eluent on electrokinetic and chromatographic contributions to the overall separation performance in the electrically driven mode were investigated. Hence, under the utilized experimental conditions, *i. e.*, at an electric field strength in the range of l120–720 V/cm (applied voltages 4–24 kV) and an ionic strength of the counterion between 5 and 25 mM (at constant acid-to-base, *i. e.*, co- to counterion ratio of 2:1), no deviations from the expected linearity of the EOF were observed. This led to the conclusion that an occurrence of the so-called electrokinetic effects of the second kind resulting from electric double layer overlap inside the mesopores of the monolithic stationary phase and concentration polarization phenomena were largely negligible. Additional support to this conclusion was inferred from the observed independence of CEC retention factors on the electric field strength across the investigated ionic strength range of the BGE. As a consequence, a simple framework allowing for calculation of the CEC mobilities from the individual separation contributions, *viz*. electroosmotic and electrophoretic mobilities as well as retention factors, could be applied to model CEC migration. There was a reasonable agreement between calculated and experimental CEC mobility data with deviations typically below 5%. The deconvolution of the individual contributions to CEC migration and separation is of particular value for the understanding of the separation processes in which electrophoretic migration of ionic sample constituents plays a significant role like in ion-exchange CEC and may aid the optimization procedure of the BGE and other experimental conditions such as the optimization of the surface chemistry of the stationary phase. In combination with the remarkable column performance evident from the low theoretical plate heights observed under CEC conditions for all test solutes (3.5–7.5 μm in the flow rate range of 0.4–1.2 mm/s, corresponding to (130000–300000 plates *per* meter), the presented framework provides an attractive tool as the basis for the assessment of chromatographic selectivities in a miniaturized CEC screening of new selectors and chiral stationary phases (CSPs), respectively, from experimental CEC data and known CE mobilities.

Keywords: Concentration polarization / Electric double layer overlap / Enantiomer separation / Silica monolith / Strong cation exchanger DOI 10.1002/jssc.200700572

Received: November 6, 2007; revised: December 12, 2007; accepted: December 12, 2007.

In order to assign the absolute configuration of the two chiral centers in the 2-amidocyclohexanesulfonate moiety of SO **1** the elution order of its enantiomers on a *tert*butyl carbamoyl quinine-type QN-AX CSP could be brought into play since this

type of CSP had been employed for their preparative enantiomer separation (α = 6.0, R_S = 12, using a mobile phase of 65 mM NH_4OAc in MeOH/HOAc 98/2 v/v). For the *Cinchona* carbamate WAX CSPs a tentative analyte binding model had been described earlier for N-blocked α-amino acids which stated that the D-forms (resp. (*R*) configuration) of N_α-acyl α-amino acids were eluted *first* and the L-forms (resp. (*S*) configuration) were eluted *second* on a quinine-based QN-AX CSP. On a corresponding pseudoenantiomeric quinidine-based QD-AX CSP elution orders were reversed.[43,44] This model was shown to be applicable to β-amino acids as well.[126,127] Thus, by applying this binding model the elution order of SO **1** enantiomers on the QN-AX CSP was preliminarily predicted to be (*R*) before (*S*). Since the configuration of the two substituents on the cyclohexane ring were postulated to be *trans*,[125] the absolute configuration of the two chiral centers followed to be (1*R*,2*R*) for the *first* and (1*S*,2*S*) for the *second* eluted enantiomer of SO **1**.

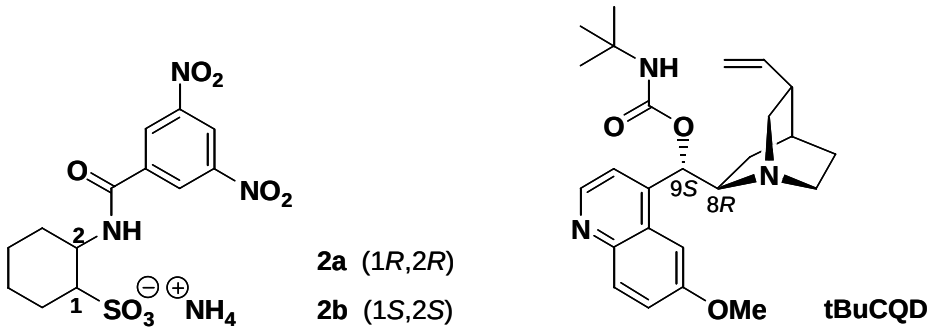

Figure 11. Chemical structures of DNB-homologues of **SO 1a**,**b** (left) and *tert*butyl carbamoyl quinidine (tBuCQD, right).

For assessment of these predictions, including the provisional expansion of the binding model of *Cinchona* carbamate CSP from N_α-acyl α-amino acids to β-amidosulfonic acids, X-ray diffraction analysis of a diastereomeric salt of a *Cinchona* carbamate SO and the stronger bound enantiomer of SO **1** seemed to be suitable. However, it was reported for QN-AX type CSPs to show particularly high enantioselectivities for amino acids derivatized with the N-3,5-dinitrobenzoyl (DNB) group.[43,44] Therefore, a structural DNB-homologue of SO **1** appeared better suited for salt crystallization with a *Cinchona* type SO than SO **1** itself owing to increased binding strength, and was therefore prepared (Figure 11; for experimental details, see Appendix. Exp-I).

Sulfonic acid **2** cannot be readily immobilized to serve as a chiral SO due to the lack of an appropriate functional group but, as expected, its racemate could be enantioseparated on a QN-AX CSP with significantly higher selectivity (α = 11.4) than that of SO **1** (α = 6.0). Hence, the weaker bound sulfonic acid enantiomer **2a** eluted first on a QN-AX CSP was crystallized with the amine-type SO of the pseudoenantiomeric QD-AX CSP to obtain the stronger binding ion pair. Single crystals of the sulfonic acid-tBuQD salt suitable for X-ray diffraction analysis could be grown (for experimental details, see Appendix Exp-I) and the following crystal structure of the salt of DNB-derivatized aminosulfonic acid **2a** and *tert*butyl-carbamoyl quinidine could be solved (Figure 12).

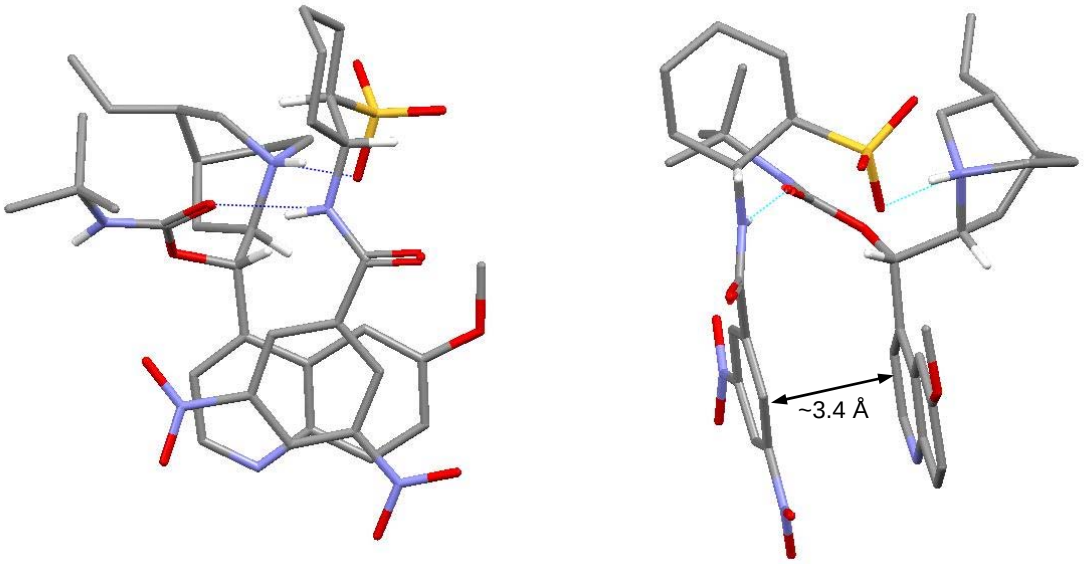

Figure 12. Different views of the crystal structure of an ion pair between tBuCQD and sulfonic acid **2a**. H-bonds and H-bonding supported ionic interactions are indicated by dashed blue lines.

First of all, the crystal structure confirmed the absolute configuration of the known quinidine derivative (1*S*,3*R*,4*S*,8*R*,9*S*). Additionally, the absolute configuration of the sulfonic acid **2a** was (1*R*,2*R*), and thus, the absolute configuration of the enantiomeric acid **2b** could be assigned as (1*S*,2*S*). In other words, the first eluted **2a** on a QN-AX CSP has (1*R*,2*R*) configuration while on the pseudoenantiomeric QD-AX CSP the first eluted enantiomer is **2b** with (1*S*,2*S*) configuration. Thereby, the initial prediction of the elution order and the absolute configuration by employing the tentative binding model described for *Cinchona* carbamate CSPs could be confirmed. Furthermore, the crystal

structure gave insights into the molecular recognition between SO and SA, which was strikingly similar to previously described SO-SA interactions for *Cinchona* carbamate CSPs with DNB-derivatized amino acids.[43-45,49,50,52] Interactions like hydrogen bond-mediated ion pairing between the sulfonic acid and the quinuclidine amine (N-H···O 2.71 Å, 169.8°), hydrogen bond interaction between the carbamate carbonyl oxygen and the amide NH (C=O···N 2.86 Å), and π-π stacking interaction between the DNB- and the quinoline-group (face-to-face ~3.4 Å) illustrated why the present SO-SA complex was found to be the stronger bound in LC. Moreover, the quinidine derivative adopted its *anti-open* conformation which is also in agreement with general molecular recognition mechanism of *Cinchona* carbamate CSPs (see scheme 5).[50,52] Obviously, the binding model described for *Cinchona* carbamate CSPs could also be expanded to β-amidocyclohexanesulfonic acids.

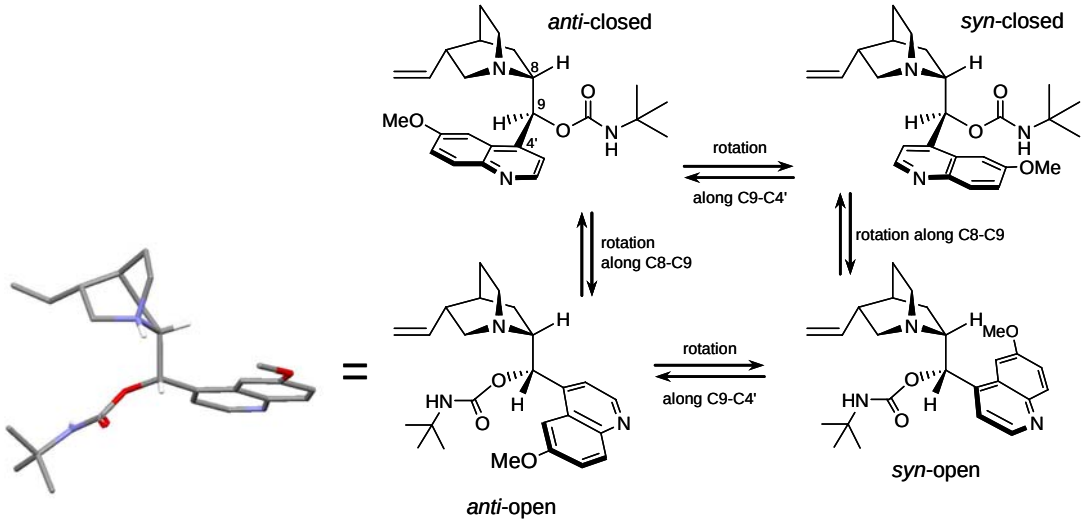

Scheme 5. Conformers of tBuCQD and comparison with its conformation in the SO-SA ion pair crystal structure from Fig. 12.

The substituents on the cyclohexane ring were in their energetically favored equatorial position and trans to each other which was also in accordance with the postulated outcome of the amino-sulfonation reaction.[125]

Finally, the initial purpose of these detailed investigations of intermolecular interactions between a QD-AX-type SO and sulfonic acid **2a**, i.e. the determination of the absolute configuration of the enantiomers of SO **1**, could be fulfilled by extrapolation from their

structural homologue **2a**. Therefore, the first eluted enantiomer of SO **1** on a QN-AX CSP has been ascribed the (1*R*,2*R*)-configuration.

3.2.3 Nonenantioselective Application of a SCX-type CSP

In the course of developing and exploring ion exchanger type stationary phases as functional materials for chromatography, the synthetic work in our laboratory usually involved acidic and basic compounds, i.e. SOs and their precursors or test analytes. Due to the potentially ionic character of these substances home-made CX- and AX-type stationary phases were predominantly employed for their chromatographic analysis like determination of the enantiomeric purity, reaction monitoring, and purity control, and often also for their preparative purification. For example, the herein developed SCX-type CSPs based on SOs **1** were found to be particularly useful as a chromatographic tool for the quality control (identitiy and purity) of *Cinchona* alkaloids employed for preparing chiral AX-type materials. In order to report our findings we decided to carry out a dedicated study on the HPLC separation of natural *Cinchona* alkaloids and several synthetic derivatives thereof by using the SCX-type CSP **1** (C. Hoffmann et.al., manuscript draft; for the complete version, see Appendix M-I). For a better illustration of the characteristics of the sulfonic acid based column packing material also a commercially available racemic SCX-type stationary phase (PolySulfoethyl-A, PolyLC Inc.) and an octadecylsilane column (Zorbax Eclipse RP C18-XBR, Agilent Techn.), which is typically employed for *Cinchona* alkaloid analysis, were included in this study.

Separation of *Cinchona* Alkaloids on a novel Strong Cation Exchange type Chiral Stationary Phase – Comparison with commercially available Strong Cation Exchanger and Reversed-Phase Packing Materials

Christian V. Hoffmann, Michael Lämmerhofer, Wolfgang Lindner*

University of Vienna, Christian Doppler Laboratory for Molecular Recognition Materials, Department of Analytical Chemistry & Food Chemistry, Währinger Strasse 38, A-1090 Vienna, Austria

*corresponding author

Abstract

A recently reported chiral strong cation exchanger (cSCX) type stationary phase was investigated for the LC separation of a series of *Cinchona* alkaloids and synthetic derivatives thereof to test its usefulness as alternative methodology for the separation of those important pharmaceuticals. The cSCX column packing material was qualitatively compared on the one hand against a commercially available nonenantioselective SCX-material,

PolySULFOETHYL-A, and on the other hand against a modern C18 reversed-phase stationary phase which is commonly employed for *Cinchona* alkaloid analysis. Both SCX columns showed no pronounced peak tailing phenomena which typically hamper their RP analysis and require specific optimization. Thus, the cSCX-based assay provided new feasibilities for the separation of the *Cinchona* alkaloids in polar organic mode as opposed to conventional reversed-phase methodologies. In particular, a method for the simultaneous determination of eight *Cinchona* alkaloids (quinine, quinidine, cinchonine, cinchonidine, and their corresponding dehydro analogs) using the cSCX column in HPLC has been developed and exemplarily applied to impurity profiling of a commercial alkaloid sample. Furthermore, both SCX materials allowed successful separation of C9-epi and 10,11-didehydro derivatives from their respective educts in an application in synthetic *Cinchona* alkaloid chemistry.

*Keywords:*Column liquid chromatography, *Cinchona* alkaloid, reversed-phase, cation exchanger, packing materials.

3.3 Zwitterionic SOs and CSPs

3.3.1 Development and Characterization of Zwitterionic CSPs

As already mentioned before, Knox and Jurant and later Hartwick reported first on selected enantiomer separations of amino acids by means of zwitterionic stationary phases.[92,93] Although these systems have not been investigated in greater detail for their enantioselective properties these early findings clearly pointed the way how enantioselective recognition of chiral amphoteric compounds could principally be accomplished with an ion exchanger concept, namely by zwitterion exchange. With molecular entities of proven enantioselective properties in hand like the *Cinchona* alkaloid derivatives for anion exchange and now also β-aminosulfonic acids for cation exchange, the circumstances seemed favorable to address chiral amino acids and related amphoteric compounds as prime analytes for ion exchanger CSPs. As a consequence, by fusing parts of previously established AX- and CX-type SOs to afford defined synthetic low molecular mass zwitterionic chiral SOs, a novel type of ion exchanger CSP was presented (Scheme 6).

In particular, the β-aminocyclohexanesulfonic acid building block from SCX-type CSP **1** was introduced at the C9-position of the *Cinchona* alkaloid via carbamate formation.

Therefore, the sites for anion and cation exchange were linked along several chiral centers in combination with relatively rigid groups like the cyclohexane ring, the carbamate, and the quinuclidine ring system, putting the oppositely charged atoms at a distance of eight atoms. On the contrary, in typically reported zwitterionic materials the two charges were rather close together (2-4 atoms in-between) and linked via flexible

alkyl chains.[92,93,101,106] The design of the *Cinchona* alkaloid-based zwitterionic CSPs with its relatively large distance between the charges though aimed at reducing the electrostatic repulsions of similarly charged groups in both SO and SA upon binding, thereby also supporting intermolecular interactions other than ion pairing.

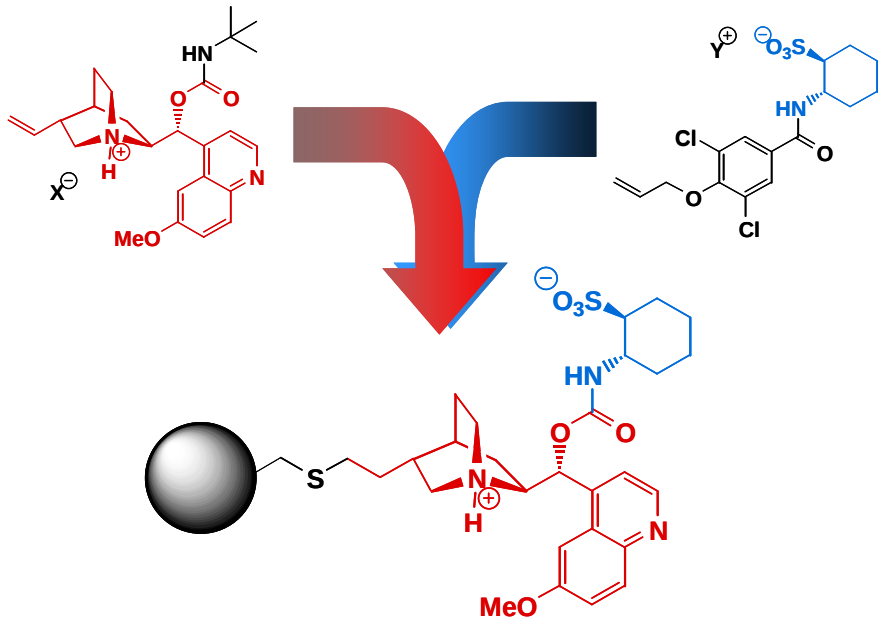

Scheme 6. Design of zwitterionic CSPs by fusion of parts of low molecular mass chiral SOs of the AX- and CX-type.

Due to the combination of anion and cation exchanger sites in one CSP, the novel zwitterionic CSPs could conceptually be operated in three different enantioselective ion exchange modes: anion, cation, and zwitterion exchange (AX, CX, ZX) (see Scheme 7). However, other than on the parent, pure AX- and CX-type CSPs further characteristics may arise on zwitterionic CSPs. In the AX mode for example, the intramolecular acid group could act as a counterion in the anion exchange process (and *vice versa*, the amino group in the cation exchange process). Thus, in the ZX mode both charged groups in the zwitterionic SO could function both as ion pairing sites and also as intramolecular counterions. Particular attention was therefore directed to retention behavior of zwitterionic CSPs in comparison to their parent AX- and CX-type packing materials.

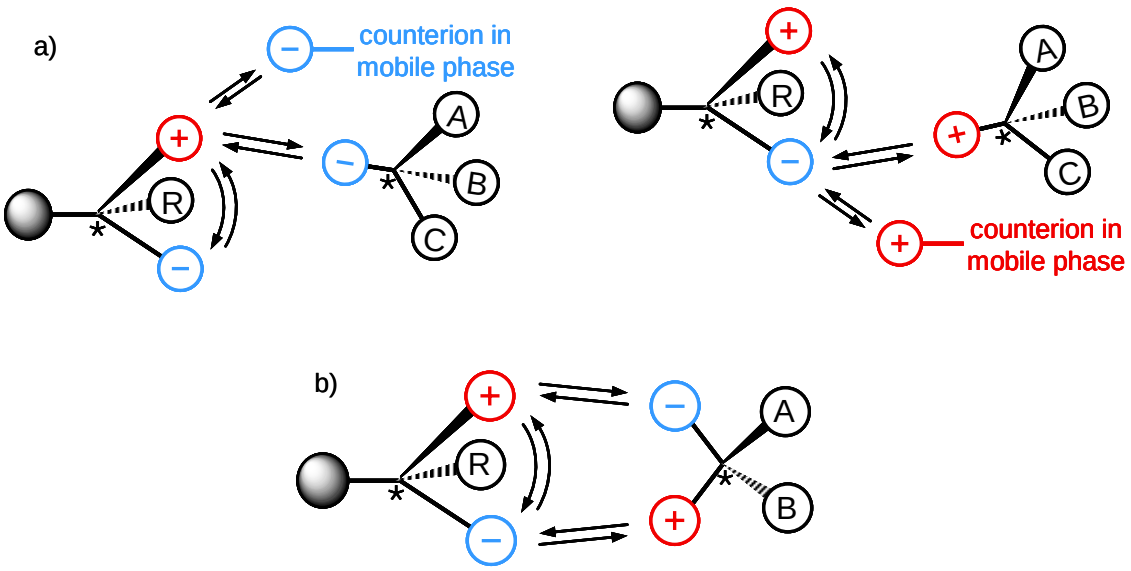

Scheme 7. a) Anion exchanger mode (left) and cation exchanger mode (right), supported by the intramolecular counterion, on zwitterionic CSPs (schematic). Co-ions in the mobile phase were omitted for the benefit of clarity. b) Proposed zwitterion exchanger mode, supported by the intramolecular counterions, for amphoteric analytes on zwitterionic CSPs (schematic).

The design of zwitterionic ion exchanger-type CSPs represented a significant expansion of the concept of chiral ion exchangers. Both novel enantioselective properties as well as particularities for the chromatographic operation were indicated. But first of all, it was essential to evaluate the concept of a combined anion and cation exchanger CSP, and most importantly, to assess the proposed model of enantioselective zwitterion exchange. For that purpose, a systematic study on the overall enantioselective properties of zwitterionic ion exchanger-type CSPs for chiral acids, bases, and amino acids was carried out and reported in the following article (C. Hoffmann et.al., Analytical Chemistry 2008, in press; for the complete article, see Appenix P-IV):

Synergistic Effects on Enantioselectivity of Novel Zwitterionic Chiral Stationary Phases for Separations of Chiral Acids, Bases, and Amino Acids by HPLC

Christian V. Hoffmann, Reinhard Pell, Michael Lämmerhofer, Wolfgang Lindner*

Christian Doppler Laboratory for Molecular Recognition Materials, Department of Analytical Chemistry & Food Chemistry, University of Vienna, Währinger Strasse 38, A-1090 Vienna, Austria.

*Author for correspondence

Abstract
In an attempt to overcome the limited applicability scope of earlier proposed *Cinchona* alkaloid based chiral weak anion exchangers (WAX) and recently reported aminosulfonic acid based chiral strong cation exchangers (SCX), which are conceptionally restricted to oppositely charged solutes, their individual chiral selector (SO) subunits have been fused in a combinatorial synthesis approach into single, now zwitterionic, chiral SO motifs. The corresponding zwitterionic ion-exchange type chiral stationary phases (CSPs) in fact combined the applicability spectra of the parent chiral ion-exchangers allowing for enantioseparations of chiral acids and amine-type solutes in liquid chromatography using polar organic mode with largely rivalling separation factors as compared to the parent WAX and SCX CSPs. Furthermore, the application spectrum could be remarkably expanded to various zwitterionic analytes like α- and β-amino acids and peptides. A set of structurally related yet different CSPs consisting of either a quinine or quinidine alkaloid moiety as anion-exchange subunit and various chiral or achiral amino acids as cation-exchange subunits enabled to derive structure-enantioselectivity relationships which clearly provided strong unequivocal evidence for synergistic effects of the two oppositely charged ion-exchange subunits being involved in molecular recognition of zwitterionic analytes by zwitterionic SOs driven by double ionic coordination.

Keywords: Enantiomer separation; Chiral stationary phase; Anion exchanger; Cation exchanger; Zwitterion; Liquid chromatography; Chiral acids; Amino acids; Chiral amines; Peptides.

After confirmation that enantioselective anion, cation, and zwitterion exchange was available with *Cinchona* alkaloid based zwitterionic CSPs, an additional subtype of such CSPs was contributed by Norbert N. Maier and is shown in Figure 14. As opposed to the existing zwitterionic SOs that contain the cation exchanger site as a C9-carbamate modification, in the novel subtype the achiral acidic side chains had been introduced to the alkaloid scaffold at its C6'-position.

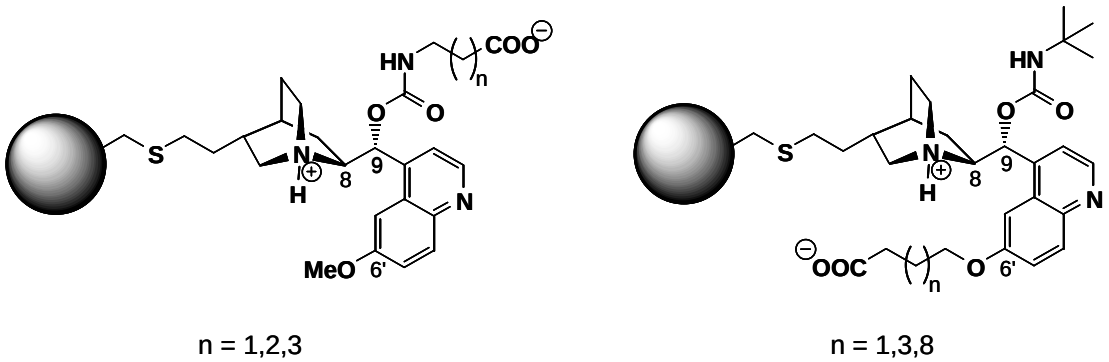

Figure 13. Comparison of the chemical structures of zwitterionic CSPs with the CX-site either in 9- or 6'-position of the quinine alkaloid.

These C6'-type zwitterionic CSPs were included in the following studies in order to examine the effects of an alternative arrangement of AX- and CX-sites within the SOs

on the overall ion exchange properties of zwitterionic column packing materials in comparison to their C9-modified congeners.

As pointed out earlier herein, in the course of developing new CSPs it is also of vital importance to evaluate these functional materials for their common chromatographic properties and characteristics. Most importantly, the chromatographic parameters such as k and α should be evaluated in dependence of the primary operation conditions (i.e. mobile phase variables like type of solvent system, pH and others) in order to derive the major influencal factors and support the general understanding of the working principles of the CSPs. Additionally, such evaluations lead to the description of experimental conditions that enable successful CSP operation. As a consequence, a further study was conducted that focused on the ion exchange retention mechanisms underlying the enantioselective recognition processes, and on the effects of the intramolecular counterions in this context. Finally, the effects of the variation of experimental parameters related to the mobile phase composition on the overall column performance were evaluated. Both investigations have been summarized in the following manuscript drafts (C. Hoffmann et.al., manuscript drafts; for the complete versions, see Appendices M-II and M-III).

Stationary Phase-related Investigations of Quinine-based Zwitterionic Chiral Stationary Phases operated in Anion, Cation, and Zwitterion Exchange Processes

Christian Hoffmann, Roland Reischl, Norbert M. Maier, Michael Lämmerhofer, Wolfgang Lindner*

Christian Doppler Laboratory for Molecular Recognition Materials, Department of Analytical Chemistry & Food Chemistry, University of Vienna, Währinger Strasse 38, A-1090 Vienna, Austria.

*Author for correspondence:

Abstract

The concept of recently introduced *Cinchona* alkaloid-type zwitterionic chiral stationary phases (CSPs) is based on fusing key cation and anion exchanger (CX, AX) moieties in one single low-molecular mass chiral selector (SO) with the resulting CSPs allowing enantiomer separations of a wide range of chiral ionizable analytes comprising acids, bases, and zwitterionic compounds. Herein, we report principal, systematic investigations of the ion exchange-type retention mechanisms available with the novel zwitterionic CSPs in nonaqueous polar organic mode. Typical CX and AX processes, corresponding to the parent single ion exchangers, are confirmed also for zwitterionic CSPs. The mechanism leading to recognition and retention of zwitterions was also found to be ion exchange mediated in a zwitterion exchange (ZX) mode. In both AX and CX mode the additional ionizable group within the SO besides the site responsible for the respective ion exchange process could be

characterized as an intramolecular counterion (IMCI) that effectively participates in the ion exchange equilibria and thus, contributes to solute elution. In ZX mode both oppositely charged groups of the zwitterionic SO were found not only to be the sites for simultaneous ion pairing with the analyte but also functioned as IMCIs in the same time. The main practical consequences of the IMCI feature were significant reduction of the amounts and even elimination of acidic and basic additives required in the eluent systems to afford analyte elution while still providing faster analysis than the parent single ion exchanger-type CSPs. The set of ten structurally different zwitterionic CSPs employed in this study also allowed correlations between chromatographic behavior of the CSPs with particular SO elements, thereby supporting the understanding of the working principles of these novel packing materials on a molecular level.

Keywords: Chiral stationary phase; Anion exchanger; Cation exchanger; Zwitterion; Liquid chromatography; Retention mechanism; Chiral acids; Amino acids; Chiral amines; Zwitterionic surface.

Investigations of Mobile Phase Contributions to Enantioselective Anion and Zwitterion Exchange Modes on Quinine-based Zwitterionic Chiral Stationary Phases

Christian Hoffmann, Roland Reischl, Norbert M. Maier, Michael Lämmerhofer, Wolfgang Lindner*

Christian Doppler Laboratory for Molecular Recognition Materials, Department of Analytical Chemistry & Food Chemistry, University of Vienna, Währinger Strasse 38, A-1090 Vienna, Austria.

*Author for correspondence:

Abstract

Novel chiral stationary phases (CSPs) based on zwitterionic *Cinchona* alkaloid-type low-molecular mass chiral selectors (SOs), as they have been reported recently, were principally investigated in HPLC towards effects on their chromatographic behavior by mobile phase composition. Mobile phase characteristics like acid-to-base ratio and type of acidic and basic additives as well as effect of type of bulk solvents in nonaqueous polar organic and aqueous reversed-phase (RP) eluent systems were varied in order to illustrate the variability and applicability of zwitterionic CSPs with regard to mobile phase aspects. Chiral SOs of the five zwitterionic CSPs investigated herein contained weak and strong cation exchanger (WCX, SCX) sites at C9- and C6'-position of the *Cinchona* alkaloid scaffold which itself accomodated the weak anion exchanger (WAX) site. The study focused on zwitterion exchange (ZX) operational mode and chiral amino acids as target analytes. Besides, also the anion exchange (AX) mode for chiral N-blocked amino acid analytes was considered, because of the intramolecular counterion (IMCI) property available in AX mode. Overall, most general and successful conditions in ZX mode were found to be weakly acidic methanolic mobile phases. In aqueous eluents RP contributions to retention came into play but only at low organic modifier content because of the highly polar character of zwitterionic analytes. At higher acetonitrile content HILIC-related retention phenomena were observed. When using weakly basic eluent system in AX mode remarkably fast enantiomer separations involving exclusion phenomena were possible with one enantiomer eluting before and the other after void volume.

Keywords: Chiral stationary phase; Ion exchange; Zwitterion; Liquid chromatography; Mobile phase composition; Polar organic mode.

3.3.2 On the Mechanism of Enantioselective ZX Mode

Although all investigated zwitterionic CSPs were found to enantioseparate at least a few amphoteric chiral compounds like α-methyl tryptophan or tryptophan, there are pronounced differences in the overall enantiorecognition capabilities among the ten packing materials towards a larger, more diverse set of amphoteric chiral analytes (see also Appendix P-IV). In particular, the arrangement of AX- and CX-sites in the C6'-modified CSPs showed only limited separation potential, followed by the 6-aminohexanoic acid-based C9-type CSP. The C9-type zwitterionic CSPs with less flexible β- and γ-amino acid moieties as CX-sites finally afforded broad applicability in the enantioselective ZX mode, thereby indicating the requirement of a rather rigid connection of AX- and CX-sites. Currently available data on these C9-type zwitterionic CSPs do not allow to postulate a general mechanism for the enantiorecognition of chiral amino acids. In addition, one should be careful with deducing selective molecular interaction processes from low enantioselectivities. Nevertheless, a few conclusions might be drawn at this point to set up a tentative model that can be used to direct further variations of analyte and selector structure and to interpret observations thereof.

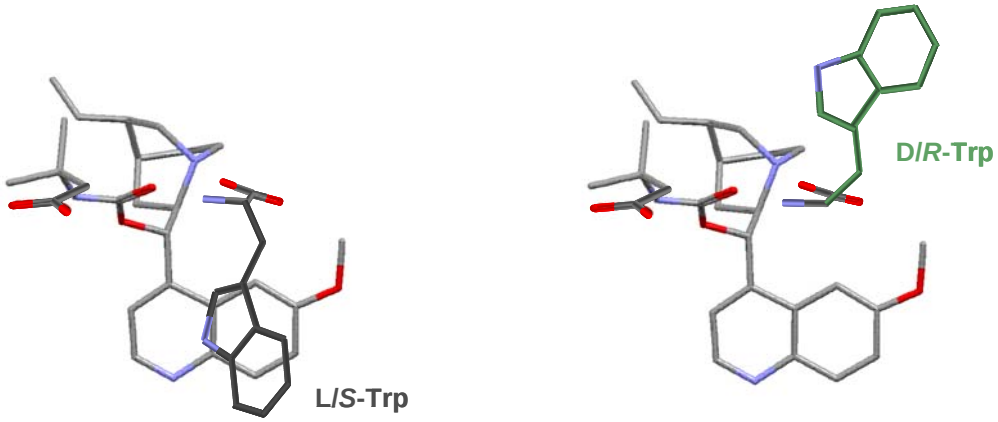

Scheme 8. Schematic illustration of a tentative model for the formation of diastereomeric SO-SA complexes of zwitterionic analytes (here: Trp) with a zwitterionic SO (here: b-valine-modified QD) in ZX mode. Hydrogens are omitted for clarity.

Relatively consistent elution orders between the ZX mode for aromatic α-amino acids like the phenylalanines, tyrosines, and tryptophanes and the AX mode for N-derivatized amino acids were found, e.g. on QN-type CSPs D- or *R*-enantiomers eluted first while on QD-type CSPs elution order was typically reversed. Based on these common elution

orders a recognition mode for the ZX mode can be derived that is principally similar to the AX mode where the alkaloid is present in its preferred *anti-open* conformation (Scheme 8, with a β-valine-modified QD selector, for comparison see also Scheme 5).

Also the amino acid analyte could take a position relative to the alkaloid scaffold that is comparable to the binding model in AX mode with the acidic function just above the C7'-position and in-between C9 and the methoxy group (see Scheme 8, with Trp as a representative amphoteric analyte). In the AX mode the amide nitrogen of the N-derivatized amino acid exhibits a hydrogen bond to the carbamate carbonyl oxygen (e.g. see above Figure 13). In the ZX mode the ammonium group of the amino acid would be at a similar position like the amide nitrogen before, but now could undergo an ionic interaction with the acidic function at the C9-carbamate position of the zwitterionic selector. Depending on the configuration at the analyte's chiral center the side chain could now point towards the quinoline plane (L- or *S*-enantiomer in Scheme 8) or straight away from the selector (D- or *R*-enantiomer in Scheme 8). In the latter arrangement the side chain would experience less steric hindrance, and therefore, would enable stronger binding to the selector.

With this proposed SO-SA-binding mechanism at least the elution order of aromatic α-amino acid enantiomers and several other amphoteric analytes as well as the similarities to the elution orders in AX mode could be rationalized. On the other hand, on the present zwitterionic selectors there may be completely different geometries of diastereomeric SO-SA complexes possible. Even single ion pairing which could be regarded as nonspecific interaction with respect to the enantioselective double ion pairing process. Thus, it is not surprising that the suggested binding model does not cope for instance with cyclic amino acids. However, a universal model seems unrealistic, especially in view of the various analyte structures. Despite these limitations the tentative model presented here could be employed for example to guide spectroscopic studies on the enantioselective ZX mode or could be probed by specific modifications of the zwitterionic selector structure.

4 Summary and Concluding Remarks

In this work a series of novel ion exchanger-type CSPs based on low molecular mass chiral selectors have been designed, prepared and evaluated for their enantioselective and nonenantioselective chromatographic properties.

With **SO 1** a novel β-aminosulfonic acid-based SCX-type selector was presented that allowed the successful enantioseparation – in parts with excellent peak efficiencies – of a number of chiral basic compounds in HPLC and capillary-based separation techniques. Its ready and straightforward synthetic availability according to a modular synthesis concept indicated the potential for the development of further SCX CSPs with improved enantiorecognition properties. Thereby, the preparation of the β-aminosulfonic acid building blocks by means of the direct amino-sulfonation reaction on alkenes proved principally worthwhile.

With the help of an X-ray crystal structure of an ion pair of a cation exchanger-type selector analog **SO 2a** and an anion exchanger-type selector tBuCQD descriptive insight into their intermolecular interactions could be provided. In addition, the absolute configuration of the SCX-type **SOs 1a** and **1b** could be derived thereof, and the binding model for *Cinchona* carbamate-type AX CSPs was confirmed – this time for a trans-β-amidocyclohexanesulfonic acid.

Moreover, the novel SCX CSP could be successfully applied for the HPLC analysis of natural *Cinchona* alkaloids and related synthetic derivatives. In particular, a method for the simultaneous HPLC separation of the four major *Cinchona* alkaloids quinine, quinidine, cinchonine, cinchonidine, and their dihydro derivatives on the SCX CSP was developed. A comparison to a octadecylsilane-based RP column showed that the SCX-concept circumvents a common drawback of RP packing materials, that is, peak tailing due to ion exchange type interactions with residual silanol groups on the silica surface.

The β-aminocyclohexanesulfonic acid building blocks were not only the central structural elements of the novel SCX CSPs. Also among the novel zwitterionic chiral selectors and corresponding CSPs, which were prepared by fusion of parts of both anion and cation exchanger entities in one selector, the β-aminocyclohexanesulfonate-based representatives turned out to be most successful. For example, they were found to essentially provide the combined enantiorecognition properties of their parent, pure anion and cation exchanger column packing materials now with one CSP by allowing enantioseparations of both chiral acidic and basic analytes.

Most importantly however, enantioselective zwitterion exchange of amphoteric chiral analytes like amino acids as a separate recognition process on *Cinchona* alkaloid-based zwitterionic CSPs could be described that is mediated by simultaneous double ion pairing of analyte and selector. Basis for these findings were the investigations of ten structurally different, yet closely related CSPs towards a large and diverse set of chiral analytes. In this context, it was found that the particular selector structure had marked influence on the extent of the enantioseparation capabilities. Thus, C6'-type zwitterionic CSPs could enantioseparate only a limited number of amino acids while especially one β-aminocyclohexanesulfonate based CSP turned out to be advantageous both in terms of number of different analytes separated as well as thereby observed enantioselectivities. Opposite elution orders of amino acid and dipeptide enantiomers were observed on pseudoenantiomeric CSPs based on quinine and quinidine which indicated that the *Cinchona* alkaloid scaffolds in the zwitterionic selectors dominated the enantioselective molecular recognition process. As a result, also a tentative binding model mainly for aromatic α-amino acids was proposed to support future investigations on enantioselective zwitterion exchange on *Cinchona* alkaloid-based zwitterionic CSPs.
Besides assessing their enantiorecognition properties, the zwitterionic CSPs were evaluated for their overall chromatographic characteristics by variation of experimental parameters like proton activity and elution strength of the mobile phase, and type of bulk solvents and acidic and basic additives. In that way, ion exchange was confirmed as the fundamental process of chromatographic retention of chiral acidic, basic and amphoteric analytes. Due to their zwitterionic nature, the novel chiral packing materials offered several additional features that distinguished them from their parent, pure anion and cation exchanger CSPs. Hence, in view of the selector coverage, retention times were generally shorter on zwitterionic CSPs owing to the intramolecularly present counterion. As a consequence, the amounts of mobile phase additives that were required to afford analyte elution in reasonable time frames could be significantly reduced as compared to the parent ion exchangers, and even additive-free elution could be carried out. Moreover, by appropriate selection of the proton activity of the eluent system, particular elution phenomena of acidic analytes were observable where one enantiomer was excluded by the stationary phase due to electrostatic repulsion while the other was retained by the CSP. Finally, the zwitterion exchange mode was found to be highly sensitive to the protic character of the mobile phase that was determined by the bulk solvents. In particular, the use of acetonitrile lead to HILIC-related retention behavior.

5 Future Perspectives

In the context of cation exchanger-type CSPs and the optimization of their enantiorecognition properties, focus should be kept on providing additional chiral aminosulfonic acid building blocks in order to further exploit the modular synthesis approach. Thereby, peptidic selector scaffolds could be considered more closely as they offer a wide range of structural variations. Furthermore, in peptidic structures the cation exchanger site could be located rather in the center of the selector than at a terminal position as it has been done so far. Finally, in a similar fashion to the RP/WAX mixed mode stationary phase, a corresponding SCX-type packing material could be investigated in more detail for nonenantioselective applications.

The introduction of novel zwitterionic selectors and CSPs herein opened up new perspectives for further materials development and raised several questions. Particularly relevant appear spectroscopic investigations of SO-SA complexes that are vital for more insights into enantioselective amino acid recognition and to confirm the simultaneous double ion pairing. In order to improve or adjust enantioselectivity in the zwitterion exchange mode testing of additional chiral acidic subunits at the C9-position are required, but also the alkaloid scaffold still offers a number of possibilities for systematic structural modifications. Quaternizing the quinuclidine amine in accordance to successful *Cinchona*-based catalysts and organocatalysts, epimerization of the chiral center at C9-position which would lead to a significant change of the binding area, and utilization of the C6’-position to increase or decrease steric demand are therefore suggested. Studies on the loadability of zwitterionic CSPs could assess their potential for preparative enantioseparations, i.e. in the zwitterion exchange mode for amino acid and peptide enantiomers. To see whether faster analysis time and lower amounts of additives due to the intramolecular counterion can indeed lead to higher productivity of zwitterionic CSPs in the anion exchange mode for acidic analytes, a direct comparison to the parent pure anion exchanger-type packing material will be necessary. Finally, the zwitterionic packing materials could be evaluated for nonenantioselective purposes following the fundamental chromatographic characterization presented herein, also in view of the increased hydrophobicity of the *Cinchona* alkaloid based selectors with their quinoline and quinuclidine moieties relative to other, commercially available zwitterionic stationary phases.

6 References

(1) Wainer, I. W. *Drug Stereochemistry - Analytical methods and Pharmacology*, 2nd ed.; Marcel Dekker: New York, 1993.

(2) Maier, N. M.; Lindner, W. In *Chirality in Drug Research*; Francotte, E., Lindner, W., Eds.; Wiley-VCH: Weinheim, Germany, 2006; Vol. 33.

(3) Francotte, E. R. *Journal of Chromatography A* **2001**, *906*, 379-397.

(4) D'Acquarica, I.; Gasparrini, F.; Pierini, M.; Villani, C.; Zappia, G. *Journal of Separation Science* **2006**, *29*, 1508-1516.

(5) Lindner, W. In *Stereoselective Synthesis*, 4th ed.; Helmchen, G., Hoffmann, R. W., Mulzer, J., Schaumann, E., Eds.; Thieme: Stuttgart, 1995; Vol. E21a, pp 225-252.

(6) Levkin, P.; Maier, N. M.; Schurig, V.; Lindner, W.; poster, 19th International Symposium on Chirality ISCD: San Diego, 2007.

(7) Gotmar, G.; Fornstedt, T.; Guiochon, G. *Chirality* **2000**, *12*, 558-564.

(8) Lammerhofer, M.; Zarbl, E.; Piette, V.; Crommen, J.; Lindner, W. *Journal of Separation Science* **2001**, *24*, 706-716.

(9) Subramanian, G. *Chiral Separation Techniques - a practical approach*, 2nd ed.; Wiley-VCH: Weinheim, 2001.

(10) Lämmerhofer, M.; Lindner, W. In *Separation Methods in Drug Synthesis and Purification (Book series: Handbook of Analytical Separations)*; Valko, K., Ed.; Elsevier: Amsterdam, 2000; Vol. 1, pp 337-437.

(11) Pirkle, W. H.; Pochapsky, T. C. *Chemical Reviews* **1989**, *89*, 347-362.

(12) Ward, T. J.; Baker, B. A. *Analytical Chemistry* **2008**, *80*, 4363-4372.

(13) Hesse, G.; Hagel, R. *Chromatographia* **1976**, *9*, 62-68.

(14) Okamoto, Y.; Kaida, Y. *Journal of Chromatography A* **1994**, *666*, 403-419.

(15) Yashima, E. *Journal of Chromatography A* **2001**, *906*, 105-125.

(16) Yashima, E.; Yamamoto, C.; Okamoto, Y. *Journal of the American Chemical Society* **1996**, *118*, 4036-4048.

(17) Okamoto, Y.; Yashima, E. *Angewandte Chemie - International Edition* **1998**, *37*, 1021-1043.

(18) Maier, N. M.; Franco, P.; Lindner, W. *Journal of Chromatography A* **2001**, *906*, 3-33.

(19) Gasparrini, F.; Misiti, D.; Villani, C. *Journal of Chromatography A* **2001**, *906*, 35-50.

(20) Welch, C. J. *Journal of Chromatography A* **1994**, *666*, 3-26.

(21) Chankvetadze, B.; Endresz, G.; Blaschke, G. *Chemical Society Reviews* **1996**, *25*, 141-&.

(22) Chankvetadze, B.; Schulte, G.; Blaschke, G. *Journal of Chromatography A* **1996**, *732*, 183-187.

(23) Chankvetadze, B.; Blaschke, G. *Journal of Chromatography A* **2001**, *906*, 309-363.

(24) Chankvetadze, B. In *Chiral Separations Methods and Protocols*; Gübitz, G., Schmid, M. G., Eds.; Humana Press: Totowa, NJ, United States, 2004; Vol. 243, pp 387-399.

(25) Cavazzini, A.; Nadalini, G.; Dondi, F.; Gasparrini, F.; Ciogli, A.; Villani, C. *Journal of Chromatography A* **2004**, *1031*, 143-158.

(26) Ilisz, I.; Berkecz, R.; Peter, A. *Journal of Separation Science* **2006**, *29*, 1305-1321.

(27) Cram, D. J.; Helgeson, R. C.; Sousa, L. R.; Timko, J. M.; Newcomb, M.; Moreau, P.; Dejong, F.; Gokel, G. W.; Hoffman, D. H.; Domeier, L. A.; Peacock, S. C.; Madan, K.; Kaplan, L. *Pure and Applied Chemistry* **1975**, *43*, 327-349.

(28) Dotsevi, G.; Sogah, Y.; Cram, D. J. *Journal of the American Chemical Society* **1975**, *97*, 1259-1261.

(29) Helgeson, R. C.; Koga, K.; Timko, J. M.; Cram, D. J. *Journal of the American Chemical Society* **1973**, *95*, 3021-3033.

(30) Kyba, E. B.; Koga, J.; Sousa, L. R.; Siegel, M. G.; Cram, D. J. *Journal of the American Chemical Society* **1973**, *95*, 2692-2693.

(31) Hyun, M. H.; Jin, J. S.; Lee, W. J. *Journal of Chromatography A* **1998**, *822*, 155-161.

(32) Davankov, V. A.; Rogozhin, S. V. *Journal of Chromatography* **1971**, *60*, 280-&.

(33) Davankov, V. A.; Bochkov, A. S.; Kurganov, A. A.; Roumeliotis, P.; Unger, K. K. *Chromatographia* **1980**, *13*, 677-685.

(34) Davankov, V. A. *Journal of Chromatography A* **1994**, *666*, 55-76.

(35) Bicker, W.; Hebenstreit, D.; Lämmerhofer, M.; Lindner, W. *Electrophoresis* **2003**, *24*, 2532-2542.

(36) Welch, C. J. *J. Chromatogr. A* **1994**, *666*, 3-26.

(37) Wu, Y. Q.; Wang, Y.; Yang, A. L.; Li, T. Y. *Analytical Chemistry* **1999**, *71*, 1688-1691.

(38) Lewandowski, K.; Murer, P.; Svec, F.; Frechet, J. M. J. *Journal of Combinatorial Chemistry* **1999**, *1*, 105-112.

(39) Piette, V.; Lammerhofer, M.; Lindner, W.; Crommen, J. *Journal of Chromatography A* **2003**, *987*, 421-427.

(40) Kacprzak, K.; Gawronski, J. *Synthesis - Stuttgart* **2001**, 961-998.

(41) Inc., C. T.

(42) Lämmerhofer, M.; Lindner, W. In *Advances in Chromatography*; Grushka, E., Grinberg, N., Eds.; CRC Ress, Taylor & Francis Group: Boca Raton, 2008; Vol. 46, pp 1-109.

(43) Lämmerhofer, M.; Lindner, W. *Journal of Chromatography A* **1996**, *741*, 33-48.

(44) Mandl, A.; Nicoletti, L.; Lämmerhofer, M.; Lindner, W. *Journal of Chromatography A* **1999**, *858*, 1-11.

(45) Czerwenka, C.; Lammerhofer, M.; Lindner, W. *Journal of Separation Science* **2003**, *26*, 1499-1508.

(46) Oberleitner, W. R.; Maier, N. M.; Lindner, W. *Journal of Chromatography A* **2002**, *960*, 97-108.

(47) Maier, N. M.; Nicoletti, L.; Lammerhofer, M.; Lindner, W. *Chirality* **1999**, *11*, 522-528.

(48) Lammerhofer, M.; Franco, P.; Lindner, W. *Journal of Separation Science* **2006**, *29*, 1486-1496.

(49) Czerwenka, C.; Lammerhofer, M.; Maier, N. M.; Rissanen, K.; Lindner, W. *Analytical Chemistry* **2002**, *74*, 5658-5666.

(50) Czerwenka, C.; Zhang, M. M.; Kahlig, H.; Maier, N. M.; Lipkowitz, K. B.; Lindner, W. *Journal of Organic Chemistry* **2003**, *68*, 8315-8327.

(51) Czerwenka, C.; Maier, N. M.; Lindner, W. *Anaytical and Bioanalytical Chemistry* **2004**, *379*, 1039-1044.

(52) Maier, N. M.; Schefzick, S.; Lombardo, G. M.; Feliz, M.; Rissanen, K.; Lindner, W.; Lipkowitz, K. B. *Journal of the American Chemical Society* **2002**, *124*, 8611-8629.

(53) Lah, J.; Maier, N. M.; Lindner, W.; Vesnaver, G. *Journal of Physical Chemistry B* **2001**, *105*, 1670-1678.

(54) Hellriegel, C.; Skogsberg, U.; Albert, K.; Lammerhofer, M.; Maier, N. M.; Lindner, W. *Journal of the American Chemical Society* **2004**, *126*, 3809-3816.

(55) Akasaka, K.; Gyimesi-Forras, K.; Lammerhofer, M.; Fujita, T.; Watanabe, M.; Harada, N.; Lindner, W. *Chirality* **2005**, *17*, 544-555.

(56) Gyimesi-Forras, K.; Akasaka, K.; Lammerhofer, M.; Maier, N. M.; Fujita, T.; Watanabe, M.; Harada, N.; Lindner, W. *Chirality* **2005**, *17*, S134-S142.

(57) Bicker, W.; Chiorescu, I.; Arion, V. B.; Lammerhofer, M.; Lindner, W. *Tetrahedron: Asymmetry* **2008**, *19*, 97-110.

(58) Lammerhofer, M.; Hebenstreit, D.; Gavioli, E.; Lindner, W.; Mucha, A.; Kafarski, P.; Wieczorek, P. *Tetrahedron: Asymmetry* **2003**, *14*, 2557-2565.

(59) Franco, P.; Lammerhofer, M.; Klaus, P. M.; Lindner, W. *Journal of Chromatography A* **2000**, *869*, 111-127.

(60) Krawinkler, K. H.; Maier, N. M.; Sajovic, E.; Lindner, W. *Journal of Chromatography A* **2004**, *1053*, 119-131.

(61) Krawinkler, K. H.; Maier, N. M.; Ungaro, R.; Sansone, F.; Casnati, A.; Lindner, W. *Chirality* **2003**, *15*, S17-S29.

(62) Gavioli, E.; Maier, N. M.; Minguillon, C.; Lindner, W. *Analytical Chemistry* **2004**, *76*, 5837-5848.

(63) Kopaciewicz, W.; Rounds, M. A.; Fausnaugh, J.; Regnier, F. E. *Journal of Chromatography* **1983**, *266*, 3-21.

(64) Lämmerhofer, M.; Lindner, W. In *Advances in Chromatography*; Grinberg, N., Grushka, E., Eds.; CRC Press LLC: Boca Raton, FL, USA, 2007; Vol. in press.

(65) Sellergren, B.; Shea, K. J. *Journal of Chromatography A* **1993**, *654*, 17-28.

(66) Nogueira, R.; Lammerhofer, M.; Lindner, W. *Journal of Chromatography A* **2005**, *1089*, 158-169.

(67) Bicker, W.; Lammerhofer, M.; Lindner, W. *Analytical and Bioanalytical Chemistry* **2008**, *390*, 263-266.

(68) Tobler, E.; Lämmerhofer, M.; Wuggenig, F.; Hammerschmidt, F.; Lindner, W. *Electrophoresis* **2002**, *23*, 462-476.

(69) Zarbl, E.; Lämmerhofer, M.; Woschek, A.; Hammerschmidt, F.; Parenti, C.; Cannazza, G.; Lindner, W. *Journal of Separation Science* **2002**, *25*, 1269-1283.

(70) Constantin, S.; Bicker, W.; Zarbl, E.; Lammerhofer, M.; Lindner, W. *Electrophoresis* **2003**, *24*, 1668-1679.

(71) Hebenstreit, D.; Bicker, W.; Lammerhofer, M.; Lindner, W. *Electrophoresis* **2004**, *25*, 277-289.

(72) Gika, H.; Lämmerhofer, M.; Papadoyannis, I.; Lindner, W. *Journal of Chromatography B* **2004**, *800*, 193-201.

(73) Sardella, R.; Lämmerhofer, M.; Natalini, B.; Lindner, W. *Chirality* **2008**, *20*, 571-576.

(74) Morikawa, A.; Hamase, K.; Inoue, T.; Konno, R.; Niwa, A.; Zaitsu, K. *Journal of Chromatography B* **2001**, *757*, 119-125.

(75) Hamase, K.; Morikawa, A.; Zaitsu, K. *Journal of Chromatography B* **2002**, *781*, 73-91.

(76) Hamase, K.; Tojo, Y.; Miyoshi, Y.; Morikawa, A.; Etoh, S.; Mita, M.; Kaneko, T.; Lindner, W.; Zaitsu, K. *Amino Acids* **2007**, *33*, V-VI.

(77) Marchelli, R.; Dossena, A.; Palla, G. *Trends in Food Science & Technology* **1996**, *7*, 113-119.

(78) Friedman, M. *Journal of Agricultural and Food Chemistry* **1999**, *47*, 3457-3479.

(79) Lubec, G.; Lubec, B. *Amino Acids* **1993**, *4*, 1-3.

(80) Meyer, V. R. *ACS Symposium Series* **1991**, *471*, 217-227.

(81) D'Acquarica, H.; Gasparrini, F.; Misiti, D.; Zappia, G.; Cimarelli, C.; Palmieri, G.; Carotti, A.; Cellamare, S.; Villani, C. *Tetrahedron: Asymmetry* **2000**, *11*, 2375-2385.

(82) D'Acquarica, I. *Journal of Pharmaceutical and Biomedical Analysis* **2000**, *23*, 3-13.

(83) Berthod, A.; Yu, T.; Kullman, J. P.; Armstrong, D. W.; Gasparrini, F.; D'Acquarica, I.; Misiti, D.; Carotti, A. *Journal of Chromatography A* **2000**, *897*, 113-129.

(84) Berthod, A.; Chen, X. H.; Kullman, J. P.; Armstrong, D. W.; Gasparrini, F.; D'Acquarica, I.; Villani, C.; Carotti, A. *Analytical Chemistry* **2000**, *72*, 1767-1780.

(85) Shinbo, T.; Yamaguchi, T.; Nishimura, K.; Sugiura, M. *Journal of Chromatography* **1987**, *405*, 145-153.

(86) Hyun, M. H.; Han, S. C.; Lipshutz, B. H.; Shin, Y. J.; Welch, C. J. *Journal of Chromatography A* **2001**, *910*, 359-365.

(87) Berkecz, R.; Ilisz, I.; Fulop, F.; Pataj, Z.; Hyun, M. H.; Peter, A. *Journal of Chromatography A* **2008**, *1189*, 285-291.

(88) Franco, E. J.; Hofstetter, H.; Hofstetter, O. *J. Sep. Sci.* **2006**, *29*, 1458-1469.

(89) Ravelet, C.; Boulkedid, R.; Ravel, A.; Grosset, C.; Villet, A.; Fize, J.; Peyrin, E. *Journal of Chromatography A* **2005**, *1076*, 62-70.

(90) Ruta, J.; Grosset, C.; Ravelet, C.; Fize, J.; Villet, A.; Ravel, A.; Peyrin, E. *Journal of Chromatography B-Analytical Technologies in the Biomedical and Life Sciences* **2007**, *845*, 186-190.

(91) Ilisz, I.; Sapi, J.; Tourwe, D.; Armstrong, D. W.; Peter, A. *Chromatographia* **2006**, *63*, S23-S27.

(92) Yu, L. W.; Hartwick, R. A. *Journal of Chromatographic Science* **1989**, *27*, 176-185.

(93) Knox, J. H.; Jurand, J. *Journal of Chromatography* **1982**, *234*, 222-224.

(94) Kaufman, D. B.; Hayes, T.; Buettner, J.; Hammond, D. J.; Carbonell, R. G. *Journal of Chromatography A* **2000**, *874*, 21-26.

(95) Nesterenko, P. N.; Haddad, P. R. *Analytical Sciences* **2000**, *16*, 565-574.

(96) Hu, W. Z.; Takeuchi, T.; Haraguchi, H. *Analytical Chemistry* **1993**, *65*, 2204-2208.

(97) Hu, W. Z.; Tao, H.; Haraguchi, H. *Analytical Chemistry* **1994**, *66*, 2514-2520.

(98) Hu, W. Z.; Haraguchi, H. *Analytical Chemistry* **1994**, *66*, 765-767.

(99) Hu, W. Z.; Haddad, P. R. *Trac-Trends in Analytical Chemistry* **1998**, *17*, 73-79.

(100) Cook, H. A.; Hu, W. Z.; Fritz, J. S.; Haddad, P. R. *Analytical Chemistry* **2001**, *73*, 3022-3027.

(101) Jiang, W.; Irgum, K. *Analytical Chemistry* **1999**, *71*, 333-344.

(102) Jiang, W.; Irgum, K. *Analytical Chemistry* **2001**, *73*, 1993-2003.

(103) Viklund, C.; Sjogren, A.; Irgum, K.; Nes, I. *Analytical Chemistry* **2001**, *73*, 444-452.

(104) Jiang, W.; Irgum, K. *Analytical Chemistry* **2002**, *74*, 4682-4687.

(105) Hemstrom, P.; Irgum, K. *Journal of Separation Science* **2006**, *29*, 1784-1821.

(106) Jiang, W.; Fischer, G.; Girmay, Y.; Irgum, K. *Journal of Chromatography A* **2006**, *1127*, 82-91.

(107) Appelblad, P.; Jonsson, T.; Jiang, W.; Irgum, K. *Journal of Separation Science* **2008**, *31*, 1529-1536.

(108) Ong, S. W.; Cai, S. J.; Bernal, C.; Rhee, D.; Qiu, X. X.; Pidgeon, C. *Analytical Chemistry* **1994**, *66*, 782-792.

(109) Pidgeon, C.; Ong, S.; Choi, H. S.; Liu, H. L. *Analytical Chemistry* **1994**, *66*, 2701-2709.

(110) Pidgeon, C.; Ong, S. W.; Liu, H. L.; Qiu, X. X.; Pidgeon, M.; Dantzig, A. H.; Munroe, J.; Hornback, W. J.; Kasher, J. S.; Glunz, L.; Szczerba, T. *Journal of Medicinal Chemistry* **1995**, *38*, 590-594.

(111) Ong, S. W.; Liu, H. L.; Pidgeon, C. *Journal of Chromatography A* **1996**, *728*, 113-128.

(112) Ong, S. W.; Qiu, X. X.; Pidgeon, C. *Journal of Physical Chemistry* **1994**, *98*, 10189-10199.

(113) Seebach, D.; Overhand, M.; Kuhnle, F. N. M.; Martinoni, B.; Oberer, L.; Hommel, U.; Widmer, H. *Helvetica Chimica Acta* **1996**, *79*, 913-941.

(114) Abele, S.; Seebach, D. *European Journal of Organic Chemistry* **2000**, 1-15.

(115) Seebach, D.; Beck, A. K.; Bierbaum, D. J. *Chemistry & Biodiversity* **2004**, *1*, 1111-1239.

(116) Seebach, D.; Hook, D. F.; Glattli, A. *Bioploymers* **2006**, *84*, 23-37.

(117) Kacprzak, K. M.; Maier, N. M.; Lindner, W. *Tetrahedron Letters* **2006**, *47*, 8721-8726.

(118) Higashiura, K.; Morino, H.; Matsuura, H.; Toyomaki, Y.; Ienaga, K. *Journal of the Chemical Society-Perkin Transactions 1* **1989**, 1479-1481.

(119) Gude, M.; Piarulli, U.; Potenza, D.; Salom, B.; Gennari, C. *Tetrahedron Letters* **1996**, *37*, 8589-8592.

(120) Braghiroli, D.; DiBella, M. *Tetrahedron Letters* **1996**, *37*, 7319-7322.

(121) Braghiroli, D.; DiBella, M. *Tetrahedron: Asymmetry* **1996**, *7*, 2145-2150.

(122) Braghiroli, D.; Mussati, E.; DiBella, M.; Saladini, M. *Tetrahedron: Asymmetry* **1996**, *7*, 831-836.

(123) Gennari, C.; Ceccarelli, S.; Piarulli, U.; Montalbetti, C.; Jackson, R. F. W. *Journal of Organic Chemistry* **1998**, *63*, 5312-5313.

(124) Xu, J. X.; Xu, S. *Synthesis-Stuttgart* **2004**, 276-282.

(125) Cordero, F. M.; Cacciarini, M.; Machetti, F.; de Sarlo, F. *European Journal of Organic Chemistry* **2002**, 1407-1411.

(126) Zarbl, E.; Lammerhofer, M.; Hammerschmidt, F.; Wuggenig, F.; Hanbauer, M.; Maier, N. M.; Sajovic, L.; Lindner, W. *Analytica Chimica Acta* **2000**, *404*, 169-177.

(127) Lammerhofer, M.; Zarbl, E.; Lindner, W.; Simov, B. P.; Hammerschmidt, F. *Electrophoresis* **2001**, *22*, 1182-1187.

7 List of Publications and Manuscript Drafts

Appendix #1: P-I

Christian Hoffmann, Michael Lämmerhofer, Wolfgang Lindner: „Novel strong cation-exchange type chiral stationary phase for the enantiomer separation of chiral amines by high-performance liquid chromatography", Journal of Chromatography A 1161 (2007), 242-251.

Appendix #2: P-II

Beatrix Preinerstorfer, Christian Hoffmann, Dieter Lubda, Michael Lämmerhofer, Wolfgang Lindner: „Enantioselective silica-based monoliths modified with a novel aminosulfonic acid-derived strong cation exchanger for electrically driven and pressure-driven capillary chromatography", Electrophoresis 29 (2008), 1626-1637.

Appendix #3: P-III

Beatrix Preinerstorfer, Michael Lämmerhofer, Christian Hoffmann, Dieter Lubda, Wolfgang Lindner: „Deconvolution of electrokinetic and chromatographic contributions to solute migration in stereoselective ion-exchange capillary electrochromatography on monolithic silica capillary columns", Journal of Separation Science 31 (2008), 3065-3078.

Appendix #4: M-I

Christian Hoffmann, Michael Lämmerhofer, Wolfgang Lindner: „Separation of *Cinchona* Alkaloids on a novel Strong Cation Exchange type Chiral Stationary Phase – Comparison with commercially available Strong Cation Exchanger and Reversed-Phase Packing Materials".

Appendix #5: P-IV

Christian Hoffmann, Reinhard Pell, Michael Lämmerhofer, Wolfgang Lindner: „Synergistic Effects on Enantioselectivity of Novel Zwitterionic Chiral Stationary Phases for Separations of Chiral Acids, Bases, and Amino Acids by HPLC", Analytical Chemistry in press.

Appendix #6: M-II

Christian Hoffmann, Roland Reischl, Norbert M. Maier, Michael Lämmerhofer, Wolfgang Lindner: „Stationary Phase-related Investigations of Quinine-based Zwitterionic Chiral Stationary Phases operated in Anion, Cation, and Zwitterion Exchange Processes".

Appendix #7: M-III

Christian Hoffmann, Roland Reischl, Norbert M. Maier, Michael Lämmerhofer, Wolfgang Lindner: „Investigations of Mobile Phase Contributions to Enantioselective Anion and Zwitterion Exchange Modes on Quinine-based Zwitterionic Chiral Stationary Phases".

Appendix #1

Publication P-I

Available online at www.sciencedirect.com
ScienceDirect
Journal of Chromatography A, 1161 (2007) 242–251
JOURNAL OF CHROMATOGRAPHY A
www.elsevier.com/locate/chroma

Novel strong cation-exchange type chiral stationary phase for the enantiomer separation of chiral amines by high-performance liquid chromatography

Christian V. Hoffmann, Michael Laemmerhofer, Wolfgang Lindner *

Christian Doppler Laboratory for Molecular Recognition Materials, Department of Analytical Chemistry and Food Chemistry, University of Vienna, Währinger Strasse 38, A-1090 Vienna, Austria

Received 26 April 2007; accepted 31 May 2007
Available online 6 June 2007

Abstract

The preparation of novel brush-type chiral cation-exchange materials based on *de novo* designed synthetic low molecular mass selectors (SOs) and their evaluation for enantioselective separation of chiral amines by HPLC are presented. The SO as the functional unit for enantioselectivity contains a β-aminocyclohexanesulfonic acid moiety and is readily accessible via straightforward synthesis in both enantiomeric forms yielding chiral stationary phases (CSPs) with opposite configurations, CSPs **1** and **2**, and reversed elution orders. For the evaluation of these novel CSPs by HPLC a sound set of chiral amines, mainly amino-alcohol type drug molecules, was selected. The chromatographic evaluations were carried out using polar organic mobile phase conditions. All of the analytes could be baseline separated, compared to common CSPs in parts with excellent peak efficiencies (up to 70 000 theoretical plates per meter for the second eluted enantiomer). A number of experimental parameters have been varied to look at and prove the underlying ion-exchange process on CSPs **1** and **2**, and to reveal suitable conditions for their operation. In this context, the influence of proton activity in the mobile phase and the effects of varying concentration and type of the counterion as well as type of co-ion and of bulk solvent components were thoroughly investigated.

Keywords: Enantiomer separation; Chiral stationary phase; Cation exchanger; Liquid chromatography; Chiral amines; β-Aminosulfonic acid

1. Introduction

An ever-increasing number of pharmaceuticals are marketed in their enantiomerically pure rather than their racemic form [1,2]. This can be attributed to the fact that the two enantiomers of the same compound can act differently in a chiral environment such as living organisms. Adequate methodologies for enantiomer analysis and purification are therefore required in the course of drug discovery and quality control. Enantioselective chromatography employing chiral stationary phases (CSPs) is a major technique for the separation of enantiomers [3,4]. At an analytical level enantioselective chromatography is a powerful tool for the analysis of racemic or enantio-enriched mixtures and for the determination of enantiomeric excess. Preparative chromatography is also becoming increasingly important, in particular in the early stages of drug development, as a complementary way to biocatalytic and asymmetric syntheses to obtain the desired bulk quantities of enantiopure compounds. It has been even adopted for industrial production of single enantiomer drugs using the simulated moving bed (SMB) technology [5]. Consequently, continued development of new CSPs and their improvement in terms of selectivity, stability, and capacity are worthwhile exercises, both from an industrial but also from an academic point of view.

Among the large pool of chiral low molecular mass drugs there are many basic amine compounds. For their chromatographic enantioseparation numerous and different types of CSPs are commercially available, whereupon polysaccharide based materials are most prominent due to their very broad spectrum of enantioselectivity towards different classes of chiral compounds [6–8]. But also CSPs that employ, e.g. proteins [9,10], synthetic polymers [11,12], macrocyclic antibiotics [13,14], crown ethers [15–17], cyclodextrins [18], neutral syn-

* Corresponding author. Tel.: +43 1 4277 52300; fax: +43 1 4277 9523.
E-mail address: Wolfgang.Lindner@univie.ac.at (W. Lindner).

0021-9673/$ – see front matter © 2007 Elsevier B.V. All rights reserved.
doi:10.1016/j.chroma.2007.05.092

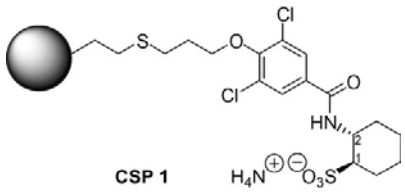

Fig. 1. Chemical structure of novel chiral strong cation exchanger material CSP **1** being of (1*R*,2*R*)-configuration. CSP **2** is of opposite configuration.

thetic ligands [19,20] and chelating compounds [21], etc. as selectors (SO) are commonly used in complementary fashion. Chiral basic molecules, which act as cationic species upon protonation, on the other hand, seem to be very well suited for an enantioselective cation-exchange process. Therefore, corresponding chiral cation exchangers are supposed to be similarly successful for chiral bases [22–25] as the earlier developed and commercialized cinchona-type weak anion-exchange (WAX) phases for the separation of chiral acidic molecules [26–29].

To realize this concept for HPLC, we herein present the development of brush-type strong cation-exchange (SCX) CSPs for the successful chromatographic enantiomer separation of a variety of chiral amines by HPLC.

As depicted in Fig. 1, the novel materials CSPs **1** and **2** consist of low molecular mass *de novo* designed chiral β-aminosulfonic acid SO that are covalently attached to a chromatographic support. The present β-amino acid motif has two centers of chirality with the sulfonate anion as the functionality for prime ionic interaction with the cationic analyte being attached to one chiral center. Furthermore, the β-amino acid is part of a conformationally restrained cyclohexane, a motif, which is similar to 1,2-functionalized cycloalkanes commonly used for chiral building blocks and auxiliaries or ligands in asymmetric synthesis [30–32]. It was conceived that such rigid and conformationally well defined cyclohexane scaffolds might be beneficial for enantioselective molecular recognition in liquid chromatography.

For HPLC evaluation of the novel CSPs under nonaqueous polar organic mobile phase conditions a comprehensive set of chiral basic analytes, mainly common drugs, has been studied (Fig. 2).

2. Experimental

2.1. Materials

The preparation of the achiral compound used as a linker, namely 4-allyloxy-3,5-dichlorobenzoic acid is described elsewhere [22]. Thiol-modified silica gel was prepared from Daisogel (pore size 120 Å, particle size 5 μm, Daiso, Japan), similar to a previously published procedure [27] yielding a SH-group grafting level of 940 μmol/g. All chemicals used for synthesis were of reagent grade quality or higher, purchased from Sigma–Aldrich (Vienna, Austria) and were used without further purification. Methanol and acetonitrile as solvents for HPLC were of HPLC-grade from Merck (Darmstadt, Germany). Mobile phase additives like acetic acid (HOAc), formic acid (FA), trifluoroacetic acid (TFA), racemic 2-amino-1-butanol (AB), diethylamine (DEA), diisopropylethylamine (DIEA), and ammonium acetate (NH_4OAc) were of analytical grade (Sigma–Aldrich, Austria). Thin-layer chromatography was performed on TLC aluminium sheets silica gel 60 F_{254} from Merck. The chiral basic analytes used in this study were either commercially available or were kind gifts from pharmaceutical companies.

2.2. Instrumentation

^1H and ^{13}C NMR spectra were acquired on a Bruker DRX 400 MHz spectrometer. The chemical shifts are given in parts per million (δ ppm) using tetramethylsilane as internal standard. Mass spectrometry was performed on a PESciex API 365 triple quadrupole mass spectrometer (Applied Biosystems/MDS Sciex, Concord, Canada) equipped with a standard electrospray source. Specific optical rotation values were measured on a Polarimeter 341 from Perkin-Elmer (Vienna, Austria). Elemental analysis was carried out with an EA 1108 CHNS-O from Carlo Erba. Calculations of pK_a values were performed using ACD/pKa DB 7.0 software from ACDLabs (Advanced Chemistry Development, Ontario, Canada). All chemical reactions were carried out under anhydrous conditions using nitrogen atmosphere and oven-dried glassware unless otherwise stated.

2.3. Synthesis of CSPs

CSPs **1** and **2** were prepared as depicted in Fig. 3. Detailed experimental procedures are given below.

2.3.1. *trans*-2-Aminocyclohexanesulfonic acid **3** [33]

To a stirred solution of SO_3·DMF complex (1.53 g, 10 mmol) in acetonitrile (10 ml) on a water bath (20 °C) was added trifluoromethanesulfonic acid (880 μl, 10 mmol). To this solution cyclohexene **1** (1.0 ml, 10 mmol) was added dropwise over 10 min. The resulting mixture was stirred for 3 h. Then water (180 μl, 10 mmol) was added dropwise. A fine white precipitation formed and stirring was maintained for 4 h. The precipitate was collected by filtration and washed with acetonitrile (3 × 5 ml) to afford *trans*-2-*N*-acetylaminocyclohexanesulfonic acid **2** which was dissolved in a 10% aqueous solution of HCl (10 ml) and heated under reflux overnight. The solution was concentrated in vacuo to yield a solid that was recrystallized (acetonitrile/water) affording off-white racemic *trans*-2-aminocyclohexanesulfonic acid **3** (1.20 g, 67%). ^1H NMR [D_2O]: $\delta = 3.40$ (dt, $J = 4.3$, 11.4 Hz, 1H), 2.95 (dt, $J = 3.8$, 11.4 Hz, 1H), 2.30-2.15 (m, 2H), 1.85-1.79 (m, 2H), 1.57-1.25 (m, 4H). ^{13}C NMR: $\delta = 60.25$ (CH), 50.79 (CH), 30.61 (CH_2), 26.78 (CH_2), 23.95 (CH_2), 23.87 (CH_2). MS (electrospray ionization, ESI, positive): 180.3 $[M+H]^+$, 197.2 $[M+NH_4]^+$, 202.2 $[M+Na]^+$, 359.3 $[2M+H]^+$, 376.4 $[2M+NH_4]^+$, 381.3 $[2M+Na]^+$.

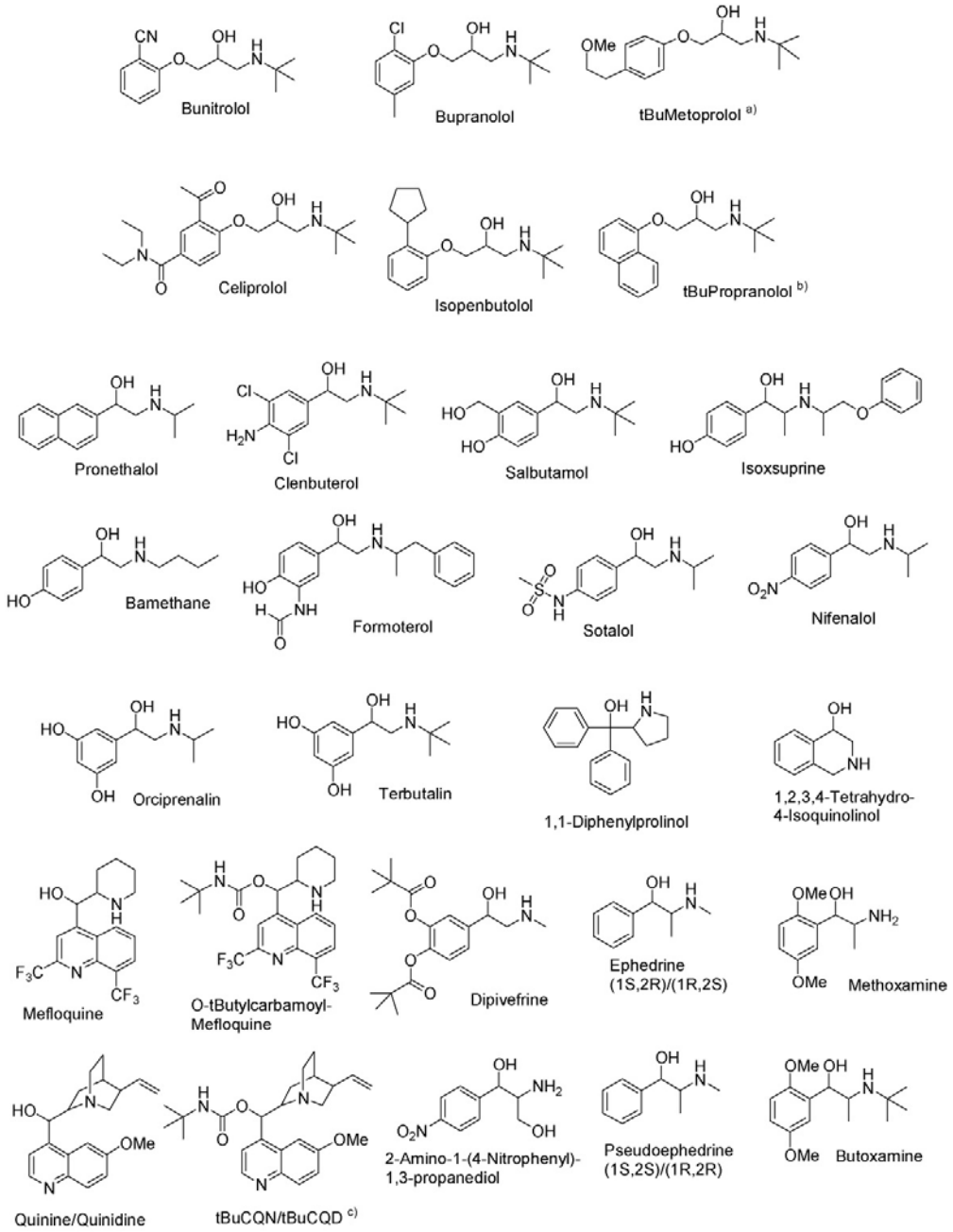

a) N-Deisopropyl-N-*tert*butyl-Metoprolol
b) N-Deisopropyl-N-*tert*butyl-Propranolol
c) O-tertbutylcarbamoyl-Quinine/Quinide

Fig. 2. Overview of chiral basic analytes used in the presented study.

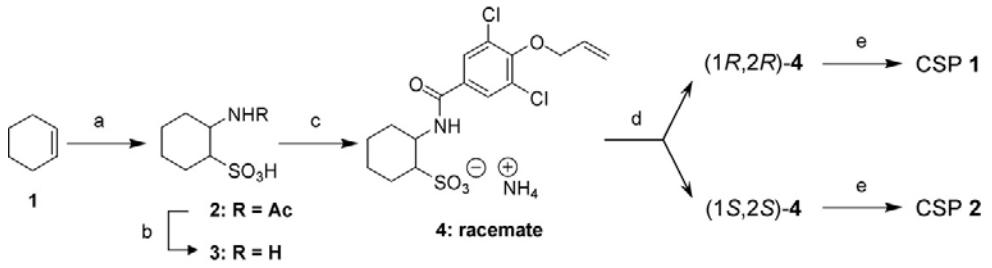

Fig. 3. Synthesis of novel CSP **1** and **2**. (a) SO_3·DMF complex, CH_3CN, 20 °C, 3 h; then H_2O, 20 °C, 4 h; (b) 10% aqueous HCl, 110 °C, 18 h (overall yield 67%). (c) 4-Allyloxy-3,5-dichlorobenzoic acid, DIEA, EEDQ, DMF, 25 °C, 24 h; (d) preparative enantiomer separation on tBuCQN-CSP, methanol/HOAc (98/2, vol.) with 0.13 M NH_4OAc (overall yield 52%, >99% ee). (e) Thiol-modified silica gel (120 Å, 5 μm), AIBN, MeOH, 65 °C, 6 h (SO coverage 190–220 μmol/g).

2.3.2. Ammonium trans-2-(N-4-allyloxy-3,5-dichlorobenzoyl)-aminocyclohexanesulfo-nate 4

To a solution of aminosulfonic acid **3** (715 mg, 4.0 mmol) and 4-allyloxy-3,5-dichlorobenzoic acid (900 mg, 3.65 mmol) in DMF (35 ml) was added DIEA (2.0 ml, 12 mmol) followed by addition of *N*-ethoxycarbonyl-2-ethoxy-1,2-dihydroquinoline (1.0 g, 4.05 mmol). The resulting suspension was stirred at 25 °C overnight while becoming a clear solution. Concentration in vacuo afforded a brown oil that was dissolved in dichloromethane (30 ml) and extracted once with aqueous NaOH (10 ml, 0.5 M). The aqueous layer was concentrated in vacuo to afford a pale white solid that was directly submitted to preparative chromatographic enantiomer separation (see below) which yielded **4** in both configurations as their ammonium salts (combined 810 mg, 52%, >99% ee each). $[\alpha]_D^{20} = -68.8°$ (MeOH, 1.0 g/100 ml, first eluted enantiomer), $[\alpha]_D^{20} = +63.3°$ (MeOH, 1.0 g/100 ml, second eluted enantiomer). ^{1}H NMR [CD_3OD]: $\delta = 7.87$ (s, 2H), 6.13 (m, $J = 5.8$, 10.4, 17 Hz, 1H), 5.41 (d, $J = 1.3$, 17 Hz, 1H), 5.25 (d, $J = 1.3$, 10,4 Hz, 1H), 4.60 (d, $J = 1.3$, 5.8 Hz, 2H), 4.15 (dt, $J = 4.0$, 11.0 Hz, 1H), 2.88 (dt, $J = 3.5$, 11.0 Hz, 1H), 2.44-2.24 (m, 2H), 1.86–1.74 (m, 2H), 1.64-1.28 (m, 4H). ^{13}C NMR: $\delta = 133.20$ (CH), 132.93 (C), 129.68 (C), 128,38 (CH), 118.12 (CH_2), 74.49 (CH_2), 61.43 (CH), 51.69 (CH), 32.79 (CH_2), 28.21 (CH_2), 25.20 (CH_2), 24.85 (CH_2). MS (ESI, negative): 406.2 $[M-H]^-$, 364.9 $[M-\text{Allyl}]^-$.

2.3.3. Preparative enantiomer separation

Chromatographic resolution of racemic **4** was performed with a Bischoff system (Leonberg, Germany) consisting of a HPD Pump Multitherm 200 XL pump, a Lamda 1010 UV/Vis detector, a LC-CaDI 22-14 interface and a manual injection valve with a 10 ml sample loop. The employed CSP was a *tert*-butyl carbamoylated quinine (tBuCQN) modified silica (15 μm particle size, commercially available as Chiralpak QN-AX, Chiral Technologies Europe, Illkirch, France) that was packed in house into a stainless steel column (150 mm × 16 mm I.D.). As mobile phase methanol/HOAc (98/2, vol.) with 0.13 M NH_4OAc was used. The crude racemic sulfonic acid **4** was dissolved in methanol/HOAc (98/2, vol.), yielding concentrations of approximately 15 mg/ml. Sample amounts injected onto the column reached up to 100 mg. The flow was set to 10 ml/min and the separations were carried out at ambient temperature. The separately collected fractions of the respective enantiomers were pooled and concentrated in vacuo. Residual NH_4OAc was removed by sublimation at 50 °C under high vacuum. The enantiomeric purity of the collected enantiomers of the SOs was assessed analytically using similar conditions (Chiralpak QN-AX; 150 mm × 4 mm I.D., 5 μm particle size; methanol/HOAc 98/2, vol., with 0.13 M NH_4OAc). The first eluted (−)-enantiomer was assigned the (1*R*,2*R*)-configuration and accordingly, the second eluted (+)-enantiomer the (1*S*,2*S*)-configuration as was established by single crystal X-ray diffraction analysis which will be described in detail elsewhere [34].

2.3.4. SO immobilization and column packing

The SO enantiomers where separately immobilized according to the following procedure: Oven-dried thiol-modified silica gel (2.20 g, 940 μmol/g SH-grafting level, 5 μm particle size) was suspended in methanol (10 ml) and SO (380 mg, 0.89 mmol) dissolved in methanol (5 ml) and α,α-azobisisobutyronitrile (30 mg, 0.18 mmol) were added. The suspension was stirred under reflux for 6 h. After filtration the silica gel was washed with methanol (3 × 20 ml), diethylether (2 × 20 ml), and dried in vacuo at 60 °C to yield the new CSPs **1** and **2**. The SO coverage was calculated from the nitrogen content obtained by elemental analysis (wt.% C 8.99, wt.% H 1.70, wt.% N 0.56) which represents a value of 221 μmol SO per gram CSP for CSP **2** (1*S*,2*S*). For the enantiomeric CSP **1** (1*R*,2*R*) the coverage was 189 μmol/g. CSPs **1** and **2** were slurry packed into stainless steel columns (150 mm × 4 mm I.D.) at VDS Optilab (Berlin, Germany).

2.4. Chromatography

Chromatographic measurements were accomplished on a 1100 Series HPLC system from Agilent Technologies (Waldbronn, Germany) consisting of a solvent degasser, a pump, an autosampler, a column thermostat and an UV–vis detector. Data aquisition and analysis was carried out with ChemStation chromatographic data software from Agilent Technologies. Additionally, a Jasco OR-990 optical rotation detector (Jasco, Gross-Umstadt, Germany) was used online to assess the elution order of solute enantiomers. Elution was performed in the iso-

cratic mode and the mobile phase flow rate was 1 ml/min. If not otherwise stated, column temperature was 20 °C and detection was performed by UV at selected wavelengths between 220 and 280 nm. The void volumes of the columns were determined by injecting acetone with detection at 280 nm. All analytes were applied as methanolic solutions of 0.5–1.0 mg/ml.

3. Results and discussion

3.1. Preparation of CSPs *1* and *2*

Strong cation exchangers CSPs **1** and **2** were prepared as outlined in Fig. 3, relying on established methodologies. At first, the achiral precursor cyclohexene **1** was converted into racemic *trans-N*-acetylaminosulfonic acid **2** via direct stereoselective aminosulfonation [33]. Consecutive acid hydrolysis yielded zwitterionic aminosulfonic acid **3**. Acylation of **3** with 4-allyloxy-3,5-dichlorobenzoic acid [22] provided the target acid **4**. Conceptually, this SO provides as primary interaction site an anionic sulfonate group for ion pairing with the cationic analyte. Furthermore, the π-acidic aromatic moiety can take part in π–π interactions while the amide group can serve as a donor/acceptor site for H-bonding in the course of the formation of diastereomeric complexes of chiral selectands (SAs) and the chiral SO. The racemic mixture **4** was resolved chromatographically by employing cinchona-based weak anion exchanger CSPs. On analytical scale the resolution of racemic **4** using a polar organic mobile phase provided excellent selectivity ($\alpha = 6.0$, $R_S = 12.0$) and the transfer of these conditions to a preparative level allowed high sample loading of 100 mg crude racemate and more per injection while baseline separation was still maintained. Thus, the collected fractions were virtually enantiopure (data not shown). Finally, the SOs were covalently attached to thiol-functionalized silica gel by means of radical addition reaction yielding SO loadings of around 200 μmol per gram CSP.

This synthetic route via racemic intermediates and enantioselective chromatography offers major advantages: the synthesis is straightforward; the necessary SO purification before immobilization is integrated in the final enantioselective chromatographic step; furthermore, chromatography guarantees for controlled and high enantiomeric purity of the SO which is essential for a successful and reproducible CSP production; lastly, both enantiomeric forms of the SO and thus of the CSP can be obtained meaning that the elution order of the analytes on the resulting CSP can be selected deliberately.

3.2. Chromatographic evaluation of CSPs

3.2.1. General aspects

The chiral stationary phases CSPs **1** and **2** were evaluated by HPLC for enantiomer separations of a set of chiral bases (Fig. 2). Polar organic mode was chosen for these studies. This nonaqueous operation mode features polar organic bulk solvents like methanol and acetonitrile together with various acidic and basic additives as co- and counterions that support and balance, respectively, via competitive equilibria the otherwise too strong ionic interactions between charged SO and analyte moieties. The benefits of this system compared to reversed phase conditions consist primarily of lowered impairment of enantioselectivity due to substantial reduction of nonspecific interactions [29]. Secondly, mass transfer of the solute in the intraparticulate pores is improved which leads to better peak efficiency [29]. In this study influences of the mobile phase composition concerning acid-to-base ratio as a substitute for proton activity, protic-to-aprotic solvent ratio, and co- and counterion variation on the overall chromatographic performance were investigated in order to reveal the ion exchange process as the main mechanism for retention and to map the conditions under which this new material can be successfully operated. These aspects will be discussed in detail in the following sections.

3.2.2. Variation of the counterion concentration

It is a peculiarity of the investigated CSPs that an ion pairing process is dominating the retention of basic analytes. Slightly acidic polar organic mobile phase systems (i.e. 50 mM acid and 25 mM base in acetonitrile–methanol mixtures) have been applied because under such conditions the basic analytes (calculated pK_a 8.8–10.0, for diluted aqueous solutions) are protonated while the sulfonic acid as the negatively charged SO site (calculated pK_a 1.78 ± 0.40, for diluted aqueous solutions) is expected to be dissociated. Therefore, a long-range ionic interaction between cationic analyte and anionic SO should be the primary interaction that causes retention of the analyte and the formation of transient diastereomeric noncovalent complexes, which are the basis for enantiomer discrimination. If ion pairing of SO and solute takes place, counterions in the solvent system will competitively interfere with these interactions and thus control the retention. In order to evaluate the presence of ion-pairing, the counterion concentration was varied in a range of 12.5–50 mM (note: the acid-to-base molar ratio was kept constant). The obtained results are depicted as plots of the logarithm of the retention factors ($\log k_1$) versus the logarithm of counterion concentration of the first eluted enantiomer ($\log c$) (Fig. 4a).

A linear relationship between $\log k_1$ and $\log c$ was observed with a decrease in retention upon increasing the counterion concentration. This is a clear indication that an ion exchange type process takes place on the novel CSPs that mainly accounts for the analytes' retention according to a stoichiometric displacement model [29,35]. The slopes of the plots are given by the ratio of effective charges of solute and counterion. Under the given mobile phase conditions of acid excess it can be expected that both counterion and analytes are protonated and have comparable net charges close to 1. The chromatographic data support this as the analytes show very similar slopes of $\log k_1$ versus $\log c$ plots of 0.93–0.95. Although the selected analytes have the ethanolamine motif in common they differ, i.e. in steric demand of the *N*-alkyl substituents and carry various functional groups. Different intercepts observed for the analytes due to different ion exchange equilibrium constants reflect these structural differences. First and second eluting enantiomers show almost identical slopes (data not shown) indicating that both enantiomers encounter the same type and quality of ion exchange

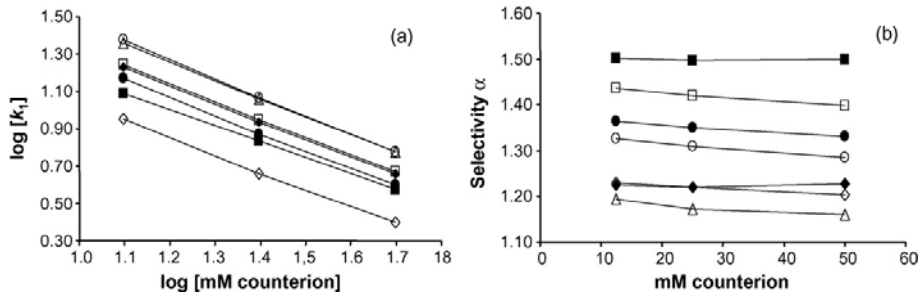

Fig. 4. Influence of the counterion concentration on (a) retention of the first eluting enantiomer, and (b) selectivity. Data of seven representative chiral analytes are shown. (◊, Butoxamin; □, clenbuterol; ◯, mefloquine; ■, *O*-*t*butylcarbamoyl-mefloquine; ●, nifenalol; ♦, pronethalol; △, salbutamol). CSP **2**; *T*: 20 °C, flow 1.0 ml/min, UV detection at 254 nm, mobile phase: DEA (12.5, 25, 50 mM) and FA (25, 50, 100 mM) in acetonitrile–methanol (9/1, vol.).

process and that they respond equally to changes in counterion concentration. Consequently, enantioselectivites do not significantly change when the counterion concentration is changed (Fig. 4b). The independence of enantioselectivity on counterion concentration is a unique feature of these CSPs that relies on ion exchange processes and allows adjustment of retention times without affecting selectivity, as has also been previously shown for the chiral anion exchangers [29,36].

3.2.3. Variation of the acid-to-base ratio

An ion exchange process (that is at work on CSPs **1** and **2** as verified above) also depends on the proton activity of the mobile phase [36], regulating the dissociation states of solute and SO. In order to map suitable operation conditions the dependence of the overall performance of CSPs **1** and **2** on distinct acid-to-base ratios as a measure of proton activity under nonaqueous conditions was investigated. For this purpose four different acid-to-base (i.e. co-ion-to-counterion) molar ratios of the mobile phase additive components were selected using FA and AB in an acetonitrile/methanol solvent system. Besides equimolar conditions basic conditions were represented by a ratio of 0.2/1 of acid to base (2 mM FA, 10 mM AB). On contrary, acidic conditions employed acid excess with ratios of 5/1 and 10/1 (50 mM and 100 mM FA, and 10 mM AB each). Fig. 5 depicts the observations on retention and efficiency for different acid-to-base ratios for representative basic analytes.

It can be seen that for the majority of analytes retention remains largely unchanged upon various acidic and basic conditions but constant concentration of the basic counterion (Fig. 5a). The strongly acidic ion exchange sites on CSPs **1** and **2** are retaining their ion exchange capacities as may have been expected for strong cation exchangers. Furthermore, enantioselectivity and resolution are affected only to minor extents as well (data not shown). In contrast, both basic and increasingly acidic conditions improve peak shape compared to equimolar conditions (Fig. 5b). However, basic mobile phases should be avoided as it may affect column lifetime. Hence, a mobile phase containing two equivalents of acidic additive per counterion represents a good compromise and has been applied for all further experiments. It can be derived from Fig. 5 that strong cation exchangers like CSPs **1** and **2** have a broad window of operation in terms of proton activity of the mobile phase for the analysis of basic compounds.

3.2.4. Variation of the type of basic counterion

Counterions in the mobile phase play a crucial role for the ion-exchange process. They act as a competitor for the ion-pairing of solute and SO in the ion-exchange equilibrium. For this reason and as already shown in a previous section, retention can be controlled by means of changing counterion concentration. However, not only the concentration, but also the type of the counterion can affect the chromatographic behavior. In

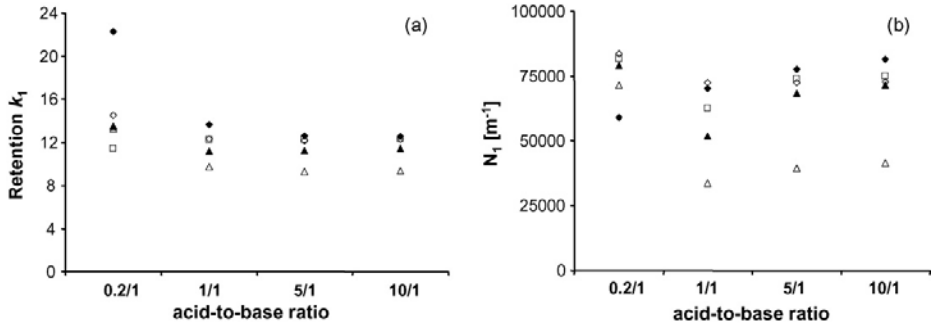

Fig. 5. Effect of the acid-to-base molar ratio on (a) retention and (b) plate numbers of the first eluting enantiomer. Data of five representative chiral analytes are shown (△, celiprolol; ◊, clenbuterol; □, pronethalol; ▲, *tert*butyl-propranolol; ♦, salbutamol). CSP **1**; *T*: 20 °C, flow 1.0 ml/min, UV detection at 254 nm, mobile phase: AB (10 mM) and FA (2, 10, 50, 100 mM) in acetonitrile–methanol (4/1, vol.).

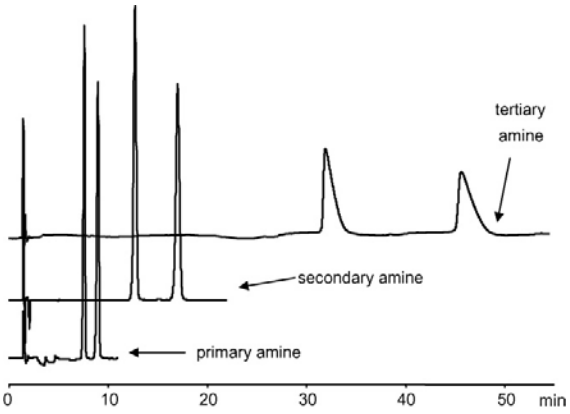

Fig. 6. Effect of the nature of the counterion being a primary, secondary, or tertiary alkyl ammonium ion. Data of a representative chiral analyte Clenbuterol is shown (α = 1.23 for AB, 1.38 for DEA, and 1.45 for DIEA). CSP **1**; *T*: 20 °C, flow 1.0 ml/min, UV detection at 254 nm, mobile phase: AB, DEA, and DIEA (25 mM) and FA (50 mM) in acetonitrile–methanol (9/1, vol.).

studies on a weak anion exchanger CSP of the quinine-type a pronounced influence of various counterion acids on retention, selectivity and resolution was found and attributed to acid strength [37].

Consequently, different types of basic counterions were tested on SCX CSPs **1** and **2** at identical concentrations, namely 2-amino-1-butanol (AB, calc. pK_a 9.25) as a primary amine, diethylamine (DEA, calc. pK_a 10.76) as a secondary, and diisopropylethylamine (DIEA, calc. pK_a 10.98) as a tertiary amine (note: calculated pK_a for diluted aqueous solutions). As expected, retention displayed a strong dependence on the type of counterion (Fig. 6). The elution strength increases in the following order: tertiary, secondary, primary amine.

The elution strengths of the counterions do not simply follow their basicity but structural parameters that influence the affinity of the counterion to the ion exchange site also seem to play a role. In any case, a higher affinity of the counterion to the SO is associated with higher elution strength. Decreased affinity of the ammonium cation to the SO sulfonate anion due to steric demand of a second or third alkyl group in the process of displacing the analyte bound to the SO should also be considered.

As a result of different elution strengths of various amine counterions, isoelutropic mobile phase conditions can be obtained, e.g. with a decreased concentration of the stronger eluting type of counterion. Furthermore, as a consequence of the ion exchange process, the retention of the analyte can be regulated either with changes of the counterion type or its concentration. Alongside retention also selectivity and resolution are affected by the variation of the type of counterion, although to a smaller extent. Selectivity improves in the following order: primary, secondary, tertiary amine, i.e. for Clenbuterol with α = 1.23, 1.38, 1.45 (Fig. 6). The highest peak efficiencies and resolutions were obtained for DEA, which also provides a good compromise between retention and selectivity. DEA therefore represents an optimum type of counterion for the selected group of chiral analytes.

3.2.5. Variation of the type of acidic co-ion

In a further experiment the acidic co-ion component of the mobile phase was varied in order to test its influence on the chromatographic performance of CSPs **1** and **2**. Formic acid was replaced by a weaker acid, acetic acid, and by a stronger acid, trifluoroacetic acid while the acid-to-base ratio was kept at 2/1 (50 mM acid, 25 mM AB). Our observations suggest rather analyte specific and no marked general effect of acid strength neither on selectivity, nor resolution or retention (data not shown), corresponding to the above discussed influence of proton activity of the mobile phase. Overall, formic acid yielded the best peak efficiencies and was hence applied in further investigations.

3.2.6. Influence of protic and aprotic solvent components

Acetonitrile and methanol represent the preferred bulk solvents in the employed nonaqueous polar organic mode. Acetonitrile is an aprotic solvent that is known to disrupt aromatic π–π interactions [38]. Methanol, however, is a protic solvent that can therefore interfere with H-bonds. Hence, it is of great interest to investigate whether the bulk solvents have an impact on the chromatographic behavior of CSPs **1** and **2** type strong cation exchangers.

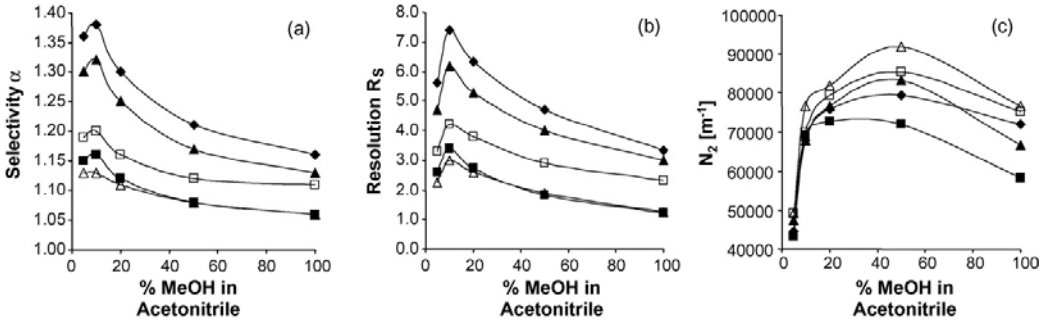

Fig. 7. Impact of the proportion of methanol in the bulk solvent (mixture of acetonitrile and methanol) on (a) selectivity, (b) resolution, and (c) plate numbers of the second eluting enantiomer. Data of five representative chiral analytes are shown (♦, clenbuterol; ▲, nifenalol; □, pronethalol; △, ephedrine; ■, salbutamol). CSP **2**; *T*: 20 °C, flow 1.0 ml/min, UV detection at 254 nm, mobile phase: DEA (25 mM) and FA (50 mM) in methanol–acetonitrile (5:95, 10:90, 20:80, 50:50, 100:0, vol.).

Table 1
HPLC enantiomer separation of various basic analytes on CSP **2**[a]

Analyt[b]	k'_1	k'_2	α	R_S	N_1 (m^{-1})	N_2 (m^{-1})
2-Amino-1-(4-nitrophenyl)-1,3-propanediol[c]	14.24	16.00	1.12	2.66	64533	62000
Bamethane	12.69	13.59	1.07	1.61	69000	68733
Bunitrolol	5.31	5.76	1.09	1.71	63600	63467
Bupranolol	6.12	6.71	1.10	1.93	63933	63733
Butoxamine	5.10	6.28	1.23	4.21	62200	61000
Celiprolol	6.83	7.37	1.08	1.52	56733	55533
Clenbuterol	9.64	13.85	1.44	8.02	63533	62933
1,1-Diphenylprolinol[d]	7.50	8.16	1.09	1.88	69000	66533
Dipivefrin	6.15	6.85	1.11	2.23	59933	61867
Ephedrine	7.77	8.94	1.15	3.30	73400	75000
Formoterol	18.19	20.54	1.13	2.71	59133	59333
Isopentbutolol	7.02	7.75	1.10	2.09	61400	62000
Isoxsuprine	7.14	8.68	1.22	4.18	63267	61400
Mefloquine	12.30	16.25	1.32	5.88	54000	56400
*O-tert*butylcarbamoyl-mefloquine	7.16	10.73	1.50	7.71	50533	48533
Methoxamine	11.62	12.91	1.11	2.43	67600	67133
Nifenalol	8.15	11.05	1.36	6.69	63467	63733
Orciprenalin	16.74	17.96	1.07	1.61	64467	60133
Pronethalol	9.67	11.86	1.23	4.76	67667	72467
Pseudo-Ephedrine	7.10	7.59	1.07	1.58	76867	74067
Quinine/Quinidine	9.45	10.91	1.15	2.96	55867	53867
Salbutamol	12.53	14.72	1.17	3.78	68467	67800
Sotalol	8.40	9.49	1.13	2.66	62800	62867
tBuCQD/CQN[e]	2.82	9.34	3.31	19.30	49600	46067
tBuMetoprolol[f]	5.23	5.70	1.09	1.75	60800	61200
tBuPropanolol[g]	7.66	8.49	1.11	2.22	63600	62733
Terbutalin	15.55	17.46	1.12	2.58	60800	58133
1,2,3,4-Tetrahydro-4-isoquinolinol	9.45	10.28	1.09	1.93	70067	66267

[a] *Conditions*: stationary phase: CSP **2**, (1S, 2S)-configuration, 150 × 4 mm I.D.; mobile phase: 50 mM FA and 25 mM DEA in acetonitrile–methanol (9/1; vol.); flow: 1.0 ml/min; *T*: 25 °C; t_0 = 1.39 min.
[b] Elution order (−)–(+) unless otherwise noted.
[c] Elution order (R)–(S).
[d] Elution order (+)–(−).
[e] *O-tert*butylcarbamoyl-quinidine/quinine, elution order (+)–(−).
[f] *N*-deisopropyl-*N-tert*butyl-metoprolol.
[g] *N*-deisopropyl-*N-tert*butyl-propranolol.

For this purpose, the proportions of acetonitrile and methanol in the mobile phase were varied (100, 50, 20, 10, 5, and 0% methanol in acetonitrile) under otherwise identical conditions. Our observations for the case of very high acetonitrile contents (100%: data not shown because of analyte specific inconsistencies; and 95%: Fig. 7) indicate that such conditions are not beneficial for CSPs that operate upon an ion-exchange mechanism like CSPs **1** and **2**, because mainly decreased peak efficiencies are yielded (Fig. 7c).

A protic solvent like methanol seems to be essential for properly balanced ion-exchange processes and acid–base-equilibria between SO, analyte, and modifier components. Once there is a protic solvent present in sufficient amounts (e.g. 10% methanol) the CSPs work properly. On the other hand, it seems that there is a dependency on acetonitrile content of opposite trend superimposed for CSPs **1** and **2**: Steadily increasing acetonitrile content (from 0% up to 90%) leads to markedly increased selectivity and resolution until the effects of very high acetonitrile contents come into play (Fig. 7a and b). This indicates that for the type of SO present in CSPs **1** and **2** π–π interactions with the solute are of moderate importance for enantiodiscrimination. Because increasing methanol content yields lower selectivities it seems that H-bonding is clearly involved in the differential binding of the solute enantiomers. Additionally, the elution strength of acetonitrile and methanol was also assessed (data not shown). No general trend or dependency can be observed that is valid for all analytes tested. There are rather three groups of analytes showing similar behavior: one group shows a steady increase in retention with increasing amount of methanol, one group behaves just the opposite, and one group shows similar retention towards the pure solvents together with increased retention for solvent mixtures.

To summarize, for the given set of analytes protic solvents are required when operating chiral SCX CSPs **1** and **2** but polar aprotic modifiers like acetonitrile generally improve the CSPs' performance and can be used in portions up to 90% of mobile phase suggesting that H-bonding rather than aromatic interactions between solute and SO account for enantiodiscriminating properties of CSPs **1** and **2**.

3.2.7. Enantiomer separation of a set of chiral amines and elution order

In the sections above a systematic investigation of the mobile phase composition in terms of proton activity, concentration of

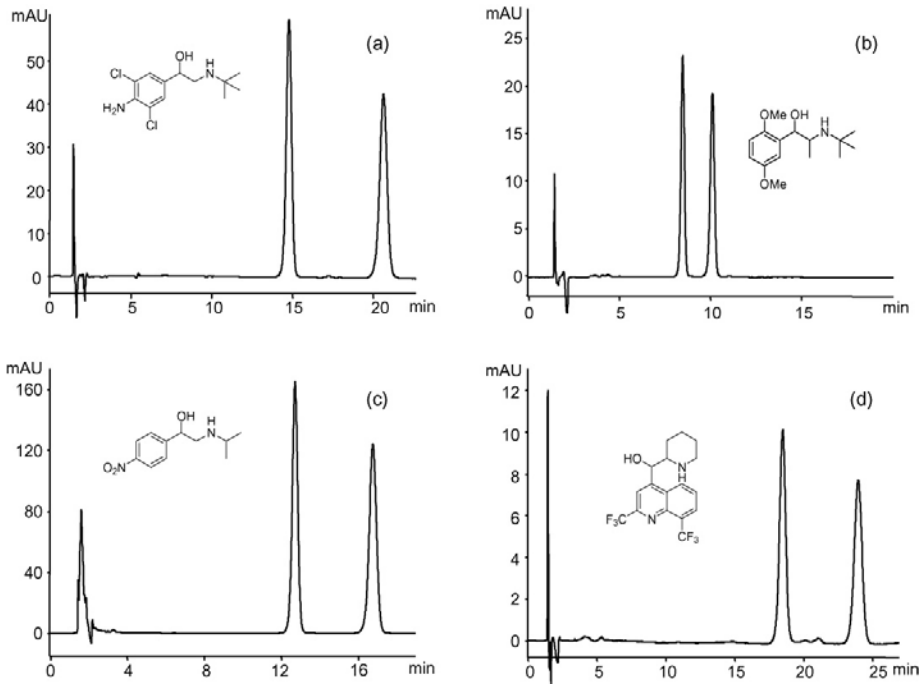

Fig. 8. HPLC chromatograms of four racemic drug analytes on CSP **2**: (a) clenbuterol; (b) butoxamine; (c) nifenalol; (d) mefloquine. Mobile phase: 50 mM FA and 25 mM DEA in acetonitrile–methanol (9/1; vol.). Flow rate 1.0 ml/min, *T*: 25 °C, UV detection at 254 nm.

counterion, type of co- and counterion, and protic and aprotic bulk solvent proportions, was presented revealing the chromatographic window of successful operation of the novel CSPs **1** and **2** in great detail. Optimized conditions obtained from these studies were applied to the separation of a set of more than 20 chiral basic drugs and other chiral amines (Fig. 2) to point out the scope of applicability of CSPs **1** and **2**. Table 1 depicts the obtained chromatographic data. Although being no essential prerequisite for a successful separation the amino-alcohol substructure is favorable for enantioseparation. Fig. 8 shows four representative chromatograms of enantiomer separations. All four racemates are base-line separated with high selectivity and resolution (i.e. mefloquine: $\alpha = 1.23$, $R_S = 5.8$) and excellent peak efficiencies (i.e. >60 000 theoretical plates per meter for butoxamine, clenbuterol and nifenalol).

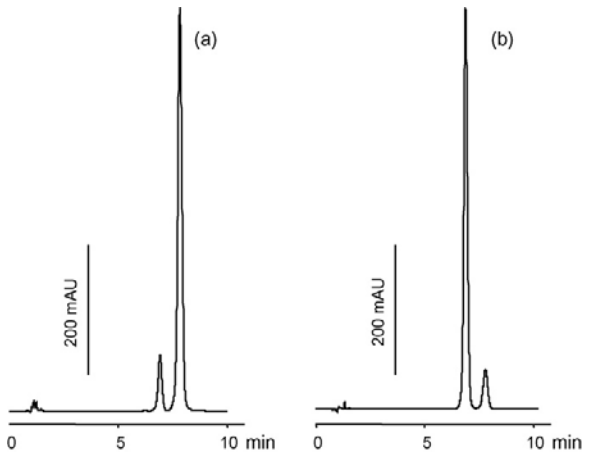

Fig. 9. Switch in elution order of the analyte enantiomers when changing the configuration of the SO as shown with (a) CSP **1**, and (b) CSP **2**, with a non-racemic sample of clenbuterol as a chiral analyte. Flow rate: 1.0 ml/min, *T*: 25 °C, UV detection at 254 nm, mobile phase: NH_4OAc (25 mM) in methanol.

As outlined in Fig. 3 the synthetic pathway yields the CSPs in both configurations, CSP **1** in (1*R*,2*R*)- and CSP **2** in (1*S*,2*S*)-configuration. Consequently, the elution order of the solute enantiomers upon operation of the CSPs can be reversed. This is of practical relevance, for instance for enantiomeric purity profiling where recoveries, accuracy and correct quantitation benefit from the fact that the enantiomeric purity can be eluted first by selection [39]. Fig. 9 exemplarily proves the switch of elution order of enantiomers of a parent compound when analyzing on CSPs of opposite configuration, CSPs **1** and **2**.

4. Conclusion

Successful brush-type CSPs for the enantiomer separation of chiral amines in HPLC acting as a cation exchanger in concert with additional intermolecular interactions have been developed and described. These CSPs are based on simple low molecular mass SO of the β-aminocyclohexanesulfonic acid type and were prepared via non-enantioselective synthesis followed by preparative enantioseparation yielding CSPs of both configurations. Chromatographic evaluation of the novel CSPs was carried out in nonaqueous polar organic mobile phase conditions where

detailed investigations of the operating conditions in terms of proton activity, type of co- and counterion, concentration of the counterion, and type of bulk solvent were accomplished. Thereby, ion pairing and ion exchange was determined as the dominant process for solute retention and insights into the mechanism of enantiodiscrimination of CSPs **1** and **2** were provided. Furthermore, generally optimized mobile phase conditions were established and applied for a larger set of drug analytes. The findings presented here are promising and demonstrate the potential of enantioselective strong cation exchanger type CSPs based on synthetic low molecular mass SOs. A dedicated program to further elucidate the future of cation exchanger materials with improved properties in terms of selectivity and applicability ranges is in progress.

Acknowledgements

The financial support of this research project by the Austrian Christian Doppler Research Society and the industrial partners AstraZeneca (Mölndal, Sweden) and Merck (Darmstadt, Germany) is gratefully acknowledged. The authors thank the Microanalysis Services team of the Faculty of Chemistry, University of Vienna, for providing elemental analysis and C. Cerwenka for his comments while carefully reading this manuscript.

References

[1] I. Agranat, H. Caner, J. Caldwell, Nat. Rev. Drug Discov. 1 (2002) 753.
[2] N.M. Maier, P. Franco, W. Lindner, J. Chromatogr. A 906 (2001) 3.
[3] N.M. Maier, W. Lindner, E. in, W. Francotte, Lindner (Eds.), Chirality in Drug Research, Wiley-VCH, Weinheim, 2006, pp. 189–260.
[4] M. Lämmerhofer, W. Lindner, in: K. Valko (Ed.), Recent Developments in Liquid Chromatographic Enantioseparation, Elsevier, Amsterdam, 2000, p. 337.
[5] M. Schulte, J. Strube, J. Chromatogr. A 906 (2001) 399.
[6] R.W. Stringham, in: P.R. Brown, E. Grushka (Eds.), The Use of Polysaccharide Phases in the Separation of Enantiomers, CRC Press, Boca Raton, FL, 2006, p. 257.
[7] B. Chankvetadze, in: G. Gübitz, M.G. Schmid (Eds.), Enantioseparation in Capillary Chromatography and Capillary Electrochromatography using Polysaccharide-Type Chiral Stationary Phases, Humana Press, Totowa, NJ, 2004, p. 387.
[8] Y. Okamoto, E. Yashima, Angew. Chem. Int. Ed. 37 (1998) 1021.
[9] J. Haginaka, J. Chromatogr. A 906 (2001) 253.
[10] E.J. Franco, H. Hofstetter, O. Hofstetter, J. Sep. Sci. 29 (2006) 1458.
[11] S.G. Allenmark, S. Andersson, P. Moeller, D. Sancher, Chirality 7 (1995) 248.
[12] G. Blaschke, W. Fraenkel, W. Broeker, J. Kinkel. Optically active stationary phase for chromatographic resolution of racemic mixtures, 1987; Vol. Ger. Offen. DE 3619303 A1.
[13] D.W. Armstrong, Y. Tang, S. Chen, Y. Zhou, C. Bagwill, J.-R. Chen, Anal. Chem. 66 (1994) 1473.
[14] I. Ilisz, R. Berkecz, A. Peter, J. Sep. Sci. 29 (2006) 1305.
[15] M.H. Hyun, Y.J. Cho, Y. Song, H.J. Choi, B.S. Kang, Chirality 19 (2007) 74.
[16] Y. Machida, H. Nishi, K. Nakamura, H. Nakai, T. Sato, J. Chromatogr. A 805 (1998) 85.
[17] R.J. Steffek, Y. Zelechonok, K.H. Gahm, J. Chromatogr. A 947 (2002) 301.
[18] C.R. Mitchell, D.W. Armstrong, in: G. Gübitz, M.G. Schmid (Eds.), Cyclodextrin-Based Chiral Stationary Phases for Liquid Chromatography: a Twenty-Year Overview, Humana Press, Totowa, NJ, 2004, p. 61.
[19] C.J. Welch, J. Chromatogr. A 666 (1994) 3.
[20] G. Cancelliere, I. D'Acquarica, F. Gasparrini, M. Maggini, D. Misiti, C. Villani, J. Sep. Sci. 29 (2006) 770.
[21] V.A. Davankov, J. Chromatogr. A 666 (1994) 55.
[22] E. Tobler, M. Lämmerhofer, F. Wuggenig, F. Hammerschmidt, W. Lindner, Electrophoresis 23 (2002) 462.
[23] E. Zarbl, M. Lämmerhofer, A. Woschek, F. Hammerschmidt, C. Parenti, G. Cannazza, W. Lindner, J. Sep. Sci. 25 (2002) 1269.
[24] S. Constantin, W. Bicker, E. Zarbl, M. Lämmerhofer, W. Lindner, Electrophoresis 24 (2003) 1668.
[25] D. Hebenstreit, W. Bicker, M. Lämmerhofer, W. Lindner, Electrophoresis 25 (2004) 277.
[26] M. Lämmerhofer, W. Lindner, J. Chromatogr. A 741 (1996) 33.
[27] A. Mandl, L. Nicoletti, M. Lämmerhofer, W. Lindner, J. Chromatogr. A 858 (1999) 1.
[28] N.M. Maier, L. Nicoletti, M. Lämmerhofer, W. Lindner, Chirality 11 (1999) 522.
[29] M. Lämmerhofer, W. Lindner, in: N. Grinberg, E. Grushka (Eds.), Liquid Chromatographic Enantiomer Separation and Chiral Recognition by Cinchona Alkaloid-Derived Enantioselective Separation Materials, CRC Press, Boca Raton, FL, 2007, in press.
[30] Y.L. Bennani, S. Hanessian, Chem. Rev. 97 (1997) 3161.
[31] D.J. Ager, I. Prakash, D.R. Schaad, Chem. Rev. 96 (1996) 835.
[32] F. Fache, E. Schulz, M.L. Tommasino, M. Lemaire, Chem. Rev. 100 (2000) 2159.
[33] F.M. Cordero, M. Cacciarini, F. Machetti, F. de Sarlo, Eur. J. Org. Chem. (2002) 1407.
[34] C.V. Hoffmann, M. Laemmerhofer, W. Lindner, in preparation.
[35] W. Kopaciewicz, M.A. Rounds, F. Fausnaugh, F.E. Regnier, J. Chromatogr. 266 (1983) 3.
[36] M. Lämmerhofer, N.M. Maier, W. Lindner, Am. Lab. 30 (1998) 71.
[37] K. Gyimesi-Forrás, K. Akasaka, M. Lämmerhofer, N.M. Maier, T. Fujita, M. Watanabe, N. Harada, W. Lindner, Chirality 17 (2005) S134.
[38] C.A. Hunter, K.R. Lawson, J. Perkins, C.J. Urch, J. Chem. Soc., Perkin Trans. 25 (2001) 651.
[39] W. Bicker, D. Hebenstreit, M. Lämmerhofer, W. Lindner, Electrophoresis 24 (2003) 2532.

Appendix #2

Publication P-II

Beatrix Preinerstorfer[1]
Christian Hoffmann[1]
Dieter Lubda[2]
Michael Lämmerhofer[1]
Wolfgang Lindner[1]

[1]Christian Doppler Laboratory for Molecular Recognition Materials, Department of Analytical Chemistry & Food Chemistry, University of Vienna, Vienna, Austria
[2]Performance & Life Science Chemicals, Merck KGaA, Darmstadt, Germany

Received July 19, 2007
Revised September 14, 2007
Accepted October 7, 2007

Research Article

Enantioselective silica-based monoliths modified with a novel aminosulfonic acid-derived strong cation exchanger for electrically driven and pressure-driven capillary chromatography

Silica monoliths modified with *trans*-(1*S*,2*S*)-2-(*N*-4-allyloxy-3,5-dichlorobenzoyl)amino cyclohexanesulfonic acid were tested for enantioselective separations of various chiral bases by aqueous and nonaqueous CEC as well as nano-HPLC. The optimization of the immobilization procedure showed that an intermediate selector (SO) coverage, as does result from a single static immobilization cycle in the capillary at 60°C with an 8% (m/v) SO solution in methanol, affords maximal EOF and optimal enantioselectivity values, while a second immobilization cycle does not lead to any improvements. Furthermore, the mobile phase composition was examined regarding the effectiveness of aqueous phases (ACN/water and methanol/water) compared to nonaqueous eluents (ACN/methanol) in terms of separation selectivity and efficiency. Additionally, different acids of varying strengths were tested as co-ions in the ion-exchange process, including formic acid, acetic acid, methanesulfonic acid, and TFA (pK_a from 4.75 to 0.5). It turned out that the effects regarding EOF and enantioselectivity were largely negligible. The chromatographic efficiencies of the new capillary columns were compelling and remarkable for bases. *H–u* curves established for mefloquine revealed a C-term contribution (resistance to mass transfer) by a factor of about six lower in CEC than in nano-HPLC and an A-term (flow maldistribution) about three times lower in the CEC mode. Theoretical plate heights as low as around 3–5 μm could be obtained in CEC over a wide flow range (0.5–1.5 mm/s). Run-to-run repeatabilities like in HPLC and excellent system stability promise the practical usefulness of the novel monolithic capillary column for enantiomeric composition analysis of pharmaceuticals by CEC.

Keywords:
Capillary electrochromatography / Capillary liquid chromatography / Chiral stationary phase / Silica monolith / Sol–gel process DOI 10.1002/elps.200700525

1 Introduction

Microscale separation techniques such as capillary LC (CLC) and CEC are in the focus of modern analytical methods in particular in the field of bioanalytics and life science. While the driving force for miniaturization of the column inner diameter, id, compared to conventional scale HPLC is the usually limited sample amount, CLC can also benefit from supplementary advantages such as higher separation efficiencies, decreased solvent consumption and increased mass sensitivity [1]. CEC as a hybrid method between LC and CE has received a lot of interest in recent years [2–6]. As a result of the flat plug-like flow profile of the mobile phase generated by the EOF and often also due to accelerated mass transfer, CEC usually features much higher peak efficiencies than are obtainable in LC which in turn leads to better peak resolution capacities. In combination with the outstanding and versatile selectivity of the stationary phase typical for HPLC, CEC stands for an extraordinary powerful technique, which has also found numerous use in enantioselective separations [7–12].

Correspondence: Professor Michael Lämmerhofer, Christian Doppler Laboratory for Molecular Recognition Materials, Department of Analytical Chemistry & Food Chemistry, University of Vienna, Währinger Strasse 38, A-1090 Vienna, Austria
E-mail: Michael.Laemmerhofer@univie.ac.at
Fax: +43-1-4277-9523

Abbreviations: AB, 2-amino-1-butanol; **CLC,** capillary liquid chromatography; **CSP,** chiral stationary phase; **DPDS,** di-2-pyridyl disulfide; **FA,** formic acid; **FS,** fused-silica; **MSA,** methanesulfonic acid; **SCX,** strong cation exchange; **SO,** selector

However, from a viewpoint of practical simplicity and universality neither CLC nor CEC do yet offer an adequate alternative to conventional HPLC. In this context, a crucial point is the choice of the capillary column used with regard to column stability and longevity as well as ease of fabrication. Various types of columns have been used for capillary techniques, *viz*. open-tubular [13–15], particle-packed [16, 17], and monolithic capillary columns [18–22]. Owing to several major advantages stationary phases based on monolithic materials received a lot of interest over the last few years and seem to have become the support of choice for capillary technologies. Most important for this development is, on the one side, the ease of preparation by usually well-reproducible *in situ* polymerization of monomer solutions directly within the capillary and, on the other side, the good column robustness especially in comparison to particle-packed capillary columns.

Nowadays, the most often used types of monolithic phases are (i) organic acrylamide-, methacrylate- or styrene-based polymers as well as materials prepared by ring-opening metathesis polymerization (ROMP) [23–25], (ii) inorganic silica-based polymers prepared by the sol–gel process [26–29], and (iii) particle-fixed materials which comprise silica particle-sintered monoliths and particle-entrapped or -loaded monoliths made from spherical chromatographic materials which are incorporated into inorganic gels or organic polymer matrices [11, 26]. All three types of supports have also been applied to enantioselective separations by capillary technologies.

Organic polymer monoliths based on polyacrylamides and polymethacrylates have been used for enantioseparations mainly by CEC employing diverse chiral selectors (SOs) such as CDs [30–32], crown ethers [33], "Pirkle"-phases [34], macrocyclic antibiotics [35], proteins [36], chiral ion exchangers [37–39], and ligand-exchange-type phases [40].

A lot of work in the field of enantioseparations by capillary technologies has also been done with inorganic silica-monoliths which are prepared by sol–gel process based upon the *in situ* polycondensation of alkoxysilanes [41]. The chiral SOs employed ranged from proteins [14, 42, 43], CDs [44, 45], and cellulose derivatives [46] to ligand-exchange-type phases [47–50] and chiral cation exchangers [51]. In most cases, the SOs have been attached onto the silica monolith in a second step by in-column modification [44–51] or by physical adsorption [14]. Kato *et al*. [42, 43] used an *in situ* encapsulation technique for the preparation of chiral protein-modified silica monoliths. Several groups compared the enantioseparation performance of their monolithic silica capillary columns in the pressure-driven (CLC) and the electrically driven mode (CEC) [14, 47, 49].

Recently, enantioselective separations by CEC have also been performed with particle-loaded and particle-sintered monolithic phases. As chiral SOs CDs [52, 53], Pirkle-phases [54], and macrocyclic antibiotics [55] have been used. Wistuba *et al*. used monolithic capillaries with sintered [52] or sol–gel-glued [53] CD-modified particles for CEC as well as for CLC.

In the present paper, we report on the advancement of previously proposed SO and monolithic column technology for the preparation of a chiral stationary phase (CSP) which was utilized for enantioseparations by both CEC and CLC. A siliceous monolith was prepared by the sol–gel process and subsequently functionalized with a novel strong cation exchange (SCX)-type chiral SO derived from *trans*-(1*S*,2*S*)-2-aminocyclohexanesulfonic acid. Thus, the monolithic phase was first modified with 3-mercaptopropyl trimethoxysilane in order to generate reactive sulfhydryl groups which were then used as anchor moieties for the immobilization of the SO by radical addition reaction. The influence of the SO coverage of this new CSP (Fig. 1) on retention, enantioselectivity, and resolution in both CEC and nano-HPLC separations was investigated employing a set of eight chiral bases (Fig. 2). Furthermore, aqueous and nonaqueous mobile phases were tested and the effect of the strength of different acids used as co-ions was examined.

2 Materials and methods

2.1 Instrumentation

All CEC and CE experiments were performed on an Agilent HP^{3D} CE system (Agilent, Waldbronn, Germany) equipped with a DAD and an external pressurization system. During electrochromatographic runs an external pressure of 6 bar was applied on both inlet and outlet end of the capillary. Samples were injected electrokinetically for 10 s. Voltages applied are specified in the figure legends. The monolithic

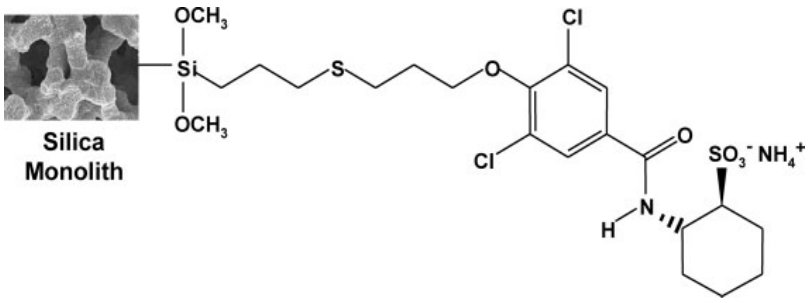

Figure 1. Structure of the siliceous monolithic enantioselective stationary phase carrying the aminosulfonic acid-derived cation-exchange-type chiral SO.

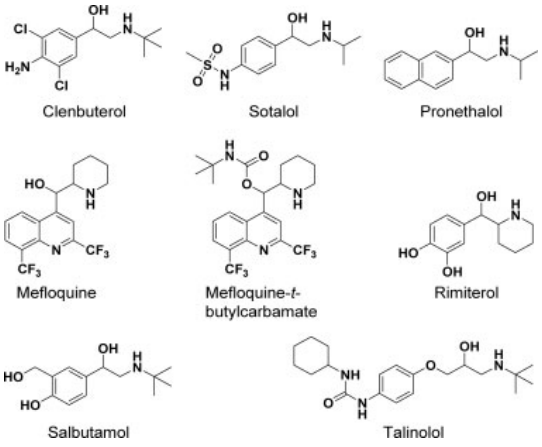

Figure 2. Chemical structures of the racemic basic drug analytes employed in this study.

capillary columns with inner diameter of 100 μm had a total length of 33.5 cm and were filled with the monolithic silica plug over the entire length. The effective length from injection to detection was 25 cm (long-end injection) or 8.5 cm (short-end injection). UV detection was carried out through the monolithic silica bed. A detection window of about 1.5 mm width was made by removing the polyimide-coating of the fused-silica (FS) capillaries using a razor blade. The data were processed with the HP^{3D} CE ChemStation software.

CLC experiments were performed on an UltiMate dual-gradient nano-LC system (LC Packings/Dionex, Amsterdam, The Netherlands) coupled to a FAMOS well plate autosampler (LC Packings/Dionex) equipped with a 1.0 μL injection loop. Injection was carried out by partial loop filling, and the injection volume was 0.1 μL. Flow rates are specified in the figure legends. The effective length of the capillaries was 33.5 cm, unless otherwise stated. Data processing was done by the Chromeleon chromatography management system, version 6.60 (Dionex, Sunnyvale, CA, USA).

For the rinsing and washing steps in the course of the chemical modifications of the monolithic capillaries a syringe pump (model 100, kd Scientific, New Hope, PA, USA) and a HPLC pump (model 2250, Bischoff Chromatography, Leonberg, Germany) were employed. The flow of the HPLC pump was split with a T-connector, the split ratio was adjusted by the length of a 50 μm id open FS capillary. For immobilization of the chiral SO by radical addition reaction a water bath model M12 from Lauda (Lauda-Koenigshofen, Germany) and an HPLC column thermostat model Jetstream 2 Plus from Alltech (Unterhaching, Germany) were used.

2.2 Materials and chemicals

The chiral SO *trans*-(1*S*,2*S*)-2-(*N*-4-allyloxy-3,5-dichlorobenzoyl)aminocyclohexanesulfonic acid was synthesized as described elsewhere [56].

Solvents (toluene, ACN, and methanol) were of analytical or HPLC gradient grade from Fisher Chemicals (Loughborough, UK) or Merck (Darmstadt, Germany). 3-Mercaptopropyl trimethoxysilane was from ABCR (Karlsruhe, Germany). (*R*,*S*)-2-Amino-1-butanol (AB), tris(2-carboxyethyl)phosphine (TCEP), di-2-pyridyl disulfide (DPDS), and formic acid (FA) were purchased from Sigma–Aldrich (Steinheim, Germany). α,α′-Azoisobutyronitrile (AIBN) and methanesulfonic acid (MSA) were supplied by Merck–Schuchardt (Hohenbrunn, Germany). 4-(2-Hydroxyethyl)piperazine-1-ethanesulfonic acid (HEPES), TFA, and acetic acid were purchased from Fluka (Buchs, Switzerland). Chiral test substances have either been synthesized in-house or were gifts from various drug companies.

2.3 Preparation of the chirally modified monolithic capillary columns

The silica monoliths were prepared as research samples at Merck in FS capillaries (from Polymicro Technologies, Phoenix, AZ, USA) of 100 μm id and about 60 cm length by sol–gel process following a protocol proposed by Ishizuka *et al.* [57]. The bonding of reactive sulfhydryl groups at the monolith surface by reaction with 3-mercaptopropyl trimethoxysilane and the quantitation of the generated thiols directly within the capillary by spectrophotometric assay employing DPDS were performed as described in ref. [51].

An about ten-fold molar excess (in relation to the concentration of reactive thiols determined at the monolith surface) of the chiral SO, *trans*-(1*S*,2*S*)-2-(*N*-4-allyloxy-3,5-dichlorobenzoyl)aminocyclohexanesulfonic acid, was dissolved in 120 μL methanol. AIBN (10 mol%) related to the SCX SO was added as radical initiator. The monolithic capillaries were rinsed with this solution by means of a Hamilton syringe and a syringe pump at a flow rate of 75 μL/h for about 1 h. After sealing both ends with rubber GC-septa the capillary columns were submerged in a water-bath. The immobilization was allowed to proceed for 24 h at 65°C.

In a distinct second approach, another monolith was modified by "flow-through immobilization". For that purpose, the capillary was rinsed with the SO–AIBN solution using the syringe pump at a flow rate of 20 μL/h for 4 h, while the capillary was housed in a HPLC column oven at 75°C.

After the immobilization process, the capillaries were always carefully washed with methanol by use of a HPLC pump.

3 Results and discussion

3.1 Column parameters

3.1.1 Chemical derivatization of the silica monolith and influence of the SO coverage

In our previous study on enantioselective phosphonic acid-derived SCX silica monolith capillaries [51] we did not pay

much attention neither to the silane bonding density nor the SO coverage. However, both are regarded to be of prime importance for the chromatographic performance of the monolithic columns. The first goal in the present study was therefore the investigation and optimization of the two-step chemical derivatization of the silica monolith comprising both the silylation reaction as well as the radical addition immobilization of the chiral SO.

First, the effectiveness of the silylation reaction of the monolith surface with 3-mercaptopropyl trimethoxysilane was examined. For this purpose, the concentration of reactive sulfhydryl groups in the capillary generated by the silylation reaction was determined spectrophotometrically by a disulfide exchange reaction using DPDS as reagent which yields 2-pyridinethione in equimolar amounts to the sulfhydryls following a protocol as described previously [58]. The silylation reaction was carried out in the flow-through mode by rinsing the pure monolithic capillaries that were housed in an HPLC oven with a 3 vol% solution of 3-mercaptopropyl trimethoxysilane in toluene for 3 h at enhanced temperature (60°C). Another capillary was treated with a two-fold and yet another third capillary with a four-fold increased silane reagent concentration under otherwise identical experimental conditions. In spite of the higher silane concentration the subsequent thiol quantitation by the DPDS method did not indicate significantly altered concentrations for these capillaries. The original procedure with a single immobilization cycle was therefore maintained.

In the next step, the surface coverage with SO moieties was optimized. For that purpose, three distinct capillaries with varying SO coverage were fabricated. In one case, the capillary was filled with a methanolic solution of the vinyl group-containing aminosulfonic acid-derived SO (ten-fold molar excess to thiols) containing 10 mol% AIBN and the radical addition reaction was carried out in a water bath for 24 h at 65°C. The yield of immobilization could be assessed by quantitation of sulfhydryl groups by the DPDS method before and after the reaction. Since a certain fraction of the remaining nonreacted thiol groups may have been inactivated during the radical addition reaction through the formation of disulfides, a reduction with TCEP was performed prior to quantitation. About 37% (corresponding to 13 nmol/cm monolithic bed) of the originally available thiol groups still reacted with the DPDS reagent after SO immobilization, indicating that a maximum of 63% (corresponding to 22 nmol/cm) of the sulfhydryls could be derivatized with the chiral SO. The second capillary was identical to the first except that it was – after completion of the experimental studies (see below) – subjected to a second radical immobilization step under identical conditions. According to the DPDS method the amount of remaining thiols was thus reduced to about 18% of the originally available sulfhydryls, *i.e.*, the SO coverage could be enhanced from 63 to 82% (29 nmol/cm). A third capillary was prepared by an alternative flow-through immobilization approach. Thus, a thiol-modified monolith with similar SH concentration was rinsed with the methanolic SO–AIBN solution for 4 h at 75°C. By this shortened derivatization process an SO coverage of about 12 nmol/cm was determined by the DPDS method.

These three new monolithic CSPs were then characterized by CEC with a set of eight basic test substances. Nonaqueous mobile phase conditions were employed as previously optimized for the corresponding aminophosphonic acid-based silica monolithic CSP [51], *i.e.*, an acidic eluent made up of a mixture of ACN and methanol (80:20, v/v) containing 25 mM FA as co-ion and 12.5 mM AB as counterion.

In Fig. 3, the results obtained with the three phases regarding mobility of the EOF and the analytes, separation factors (calculated as ratios of the retention times), resolution and efficiency are compared for three representative analytes, mefloquine, clenbuterol, and pronethanol. All three aminosulfonic acid-based CSPs exhibited a strong and stable cathodic EOF which was only slightly raising with increasing SO coverage from 1.38×10^{-4} $cm^2V^{-1}s^{-1}$ for the lowest coverage obtained by the flow-through immobilization to 1.41×10^{-4} and 1.47×10^{-4} $cm^2V^{-1}s^{-1}$ for the monolith treated once and twice, respectively, by the static immobilization procedure in the water bath (Fig. 3a). Thus, it becomes evident that the EOF cannot be much accelerated with further increase in the SO coverage.

While the effect of surface SO density on EOF was negligible, the observed mobilities in CEC were, as expected, significantly lower at elevated SO concentrations owing to the stronger chromatographic retention (Fig. 3a). Clenbuterol and pronethalol migrated before the EOF marker on the column with the lowest SO density, yet were strongly retained on the other two columns eluting after the flow marker. While the elution time in nano-HPLC was further increased when the SO coverage was elevated from 22 to 29 nmol/cm by performing a second immobilization cycle (data not shown), under CEC conditions the enhanced EOF compensated for the stronger adsorption so that even slightly higher observed mobilities of the analytes were measured on the monolith with an SO coverage of 29 nmol/cm compared to the column with 22 nmol/cm (Fig. 3a).

All tested analytes showed optimal separation factors at an intermediate SO density (Fig. 3b). If the monolith surface is covered by a larger number of SO molecules, more ion-exchange sites are available for stereoselective interactions, while nonstereoselective adsorption at the (thiol-modified) support becomes less influential which may lead to an increase in α values. If the SO-moieties are grafted too densely, access of the solute to the regions of the SO where stereodistinction takes place may be blocked by adjacent SO moieties while ion-exchange sites may still be active. The outcome may be a retention increase in a nonstereoselective manner and thus a drop in α values. Figures 3c and d show that the optimum in terms of resolution and efficiency is also obtained at an intermediate SO coverage. Plate counts of the capillary prepared by a single immobilization step ranged

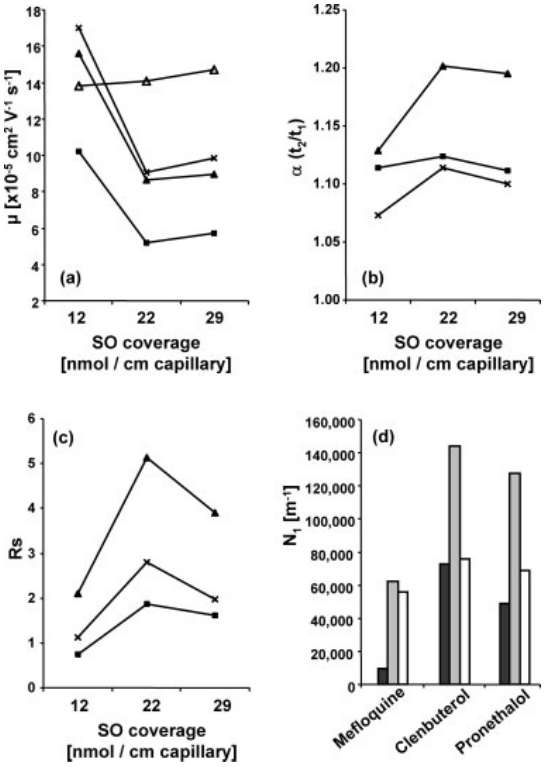

Figure 3. Influence of the SO coverage of the monolithic CSPs used for CEC separations on (a) the mobility μ of the EOF (Δ) and the first eluted enantiomers of mefloquine (■), clenbuterol (▲) and pronethalol (**x**), (b) the selectivity factor α, (c) the resolution *Rs*, and (d) the efficiency *N* (plate counts *per* meter). Notation on (d), SO coverage 12 (black bars), 22 (gray bars), and 29 (white bars) nmol/cm capillary. Experimental conditions: mobile phase, ACN/MeOH (80:20; v/v) containing 25 mM FA and 12.5 mM AB; voltage, +7 kV; electrokinetic injection for 10 s; UV detection at 216 nm; capillary temperature, 20°C.

between 60 000 and 150 000 *per* meter. It can therefore be concluded that the single static immobilization procedure represents a good choice and neither the dynamic flow-through immobilization nor the second immobilization cycle brings about any improvements.

3.1.2 Column length

The present capillary columns do not feature the dual architecture of typical CEC columns comprising a packed and an open segment. On contrary, the monolithic stationary phase is contained in the capillary over the entire length. In general, this departure from the dual architecture and the open segment resulted in more robust CEC methods. Moreover, either an 8.5 or a 25 cm effective bed length can flexibly be selected for the analysis without replacing

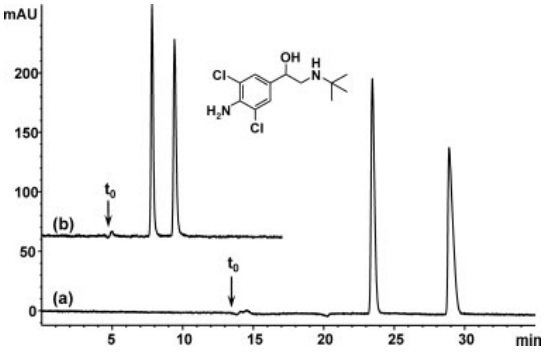

Figure 4. Enantioseparation of clenbuterol by CEC with SCX-modified silica monoliths of (a) 25 and (b) 8.5 cm effective bed length. Experimental conditions: same as in Fig. 3; SO coverage, 22 nmol/cm capillary.

the capillary cassette depending on what the separation problem demands leading to either faster separation (on the 8.5 cm side) or higher resolution (on the 25 cm side). In fact, by using the "short-end" injection the run times could be lowered by a factor of about three (Table 1 and Fig. 4). Although resolution was lower for all analytes on the short-end monolith, still five of the eight samples could be baseline-resolved.

3.2 Mobile phase effects

3.2.1 Aqueous *versus* nonaqueous mobile phases

In our studies we investigated nonaqueous eluents comprised of ACN and methanol in ratios of 80:20 and 20:80 (v/v) in comparison to aqueous mobile phases made up of ACN/water and methanol/water (80:20, v/v), respectively. All eluents contained 25 mM FA and 12.5 mM AB as electrolytes. Excess of acid should certify that the amine is fully protonated. Thus, the counterion concentration is comparable in the four mobile phases. In Figs. 5 and 6 the results regarding mobilities, retention factors (as determined by the chromatographic formalism k $(t_R - t_0)/t_0$), separation factors (as calculated by electrophoretic formalism $\alpha = t_2/t_1$ and chromatographic equation $\alpha = k_2/k_1$, respectively) and resolution obtained with these four eluents under CEC and CE as well as nano-HPLC conditions are shown. Two analytes, mefloquine-*t*-butylcarbamate and clenbuterol were chosen as representative examples for the presentation and discussion of the obtained results. Within the investigated series, the relative trend of EOF in CEC parallels that observed in CE with a blank FS tube of the same dimensions and identical BGE (Figs. 5a and b). This may lead to the conclusion that upon exchange of BGE solvents the variations of EOF in the present CEC separations are mainly a consequence of the alteration of the ε/η ratio. Both nonaqueous eluents provided a stronger EOF than the aqueous mobile phases.

Table 1. Enantioseparation of chiral bases by CEC on aminosulfonic acid-derived SCX-type monolithic silica of varying effective bed length[a)]

Analyte	Effective bed length [cm]	t_1 [min]	t_2 [min]	μ_1 [$\times 10^{-5}$ $cm^2V^{-1}s^{-1}$]	μ_2 [$\times 10^{-5}$ $cm^2V^{-1}s^{-1}$]	α (t_2/t_1)	*Rs*	N_1 [m^{-1}]	N_2 [m^{-1}]
Mefloquine	25	30.30	35.24	5.76	4.95	1.16	6.25	111,500	104,800
	8.5	13.06	14.68	5.19	4.62	1.12	1.87	62,100	39,900
Mefloquine-*t*-butylcarbamate	25	26.18	31.00	7.62	6.43	1.18	5.89	65,900	92,400
	8.5	8.56	9.97	7.92	6.80	1.16	4.50	55,500	56,400
Clenbuterol	25	23.44	28.89	8.51	6.90	1.23	9.99	180,200	128,000
	8.5	7.84	9.42	8.65	7.20	1.20	5.14	144,100	151,300
Pronethalol	25	21.64	24.37	9.21	8.18	1.13	6.42	253,800	149,500
	8.5	7.47	8.32	9.08	8.15	1.11	2.80	127,600	129,500
Salbutamol	25	26.81	29.41	7.44	6.78	1.10	3.40	99,500	78,700
	8.5	9.10	9.87	7.45	6.87	1.08	1.95	126,200	97,100
Talinolol	25	42.64	44.99	4.68	4.43	1.06	1.67	76,300	51,500
	8.5	13.60	14.23	4.99	4.76	1.05	0.52	43,500	16,800
Sotalol	25	21.42	22.04	9.31	9.05	1.03	1.70	338,400	162,000
	8.5	7.34	7.56	9.24	8.97	1.03	1.03	285,600	183,000
Rimiterol	25	34.44	37.33	5.79	5.34	1.08	1.58	26,300	23,200
	8.5	11.90	12.78	5.70	5.30	1.07	1.25	63,900	64,100

a) Experimental conditions: SO coverage of the monolith, 22 nmol/cm; mobile phase, ACN-MeOH (80:20; v/v) containing 25 mM formic acid and 12.5 mM 2-amino-1-butanol; voltage, +7 kV; electrokinetic injection for 10 s; UV detection at 216 nm; capillary temperature, 20°C. μ_{EOF} (25 cm) = 1.46 $\times$ 10^{-4} $cm^2V^{-1}s^{-1}$, μ_{EOF} (8.5 cm) = 1.41 $\times$ 10^{-4} $cm^2V^{-1}s^{-1}$.

On the other hand, it becomes evident that the observed mobilities of the solutes in CEC are altered in the same way, but inversely, as the chromatographic retention (Fig. 5a): For clenbuterol, both ACN-rich eluents and the nonaqueous methanol-rich mobile phase (*i.e.*, all eluents with ACN) exhibit similar and low retention factors and thus high mobilities in CEC (Figs. 5a and c). With the methanol-rich aqueous eluent the chromatographic interaction is significantly stronger and hence mobility in CEC lower. Strengthened hydrophobic and/or π–π interactions between solute and sorbent in the latter eluent may largely explain this trend. For mefloquine-*t*-butylcarbamate the tendencies are quite similar, except that a strong increase in retention and a reduction in mobilities, respectively, is found also for the methanol-rich nonaqueous conditions. Furthermore, the mobilities in the ACN-rich hydroorganic mixture is significantly higher than in the corresponding nonaqueous eluent mainly due to a lower retention but also owing to a higher electrophoretic mobility. Obviously, the chromatographic ion-exchange process exerts a dominating effect on CEC mobilities, while the electrophoretic mobility contribution has only modulating effects (Figs. 5b and c).

Regarding enantioselectivity (Figs. 6a and b) and resolution (Figs. 6c and d) the results for the tested analytes showed to some extent considerable differences. Thus, selectivity factor α and resolution for the separation of the mefloquine-*t*-butylcarbamate-enantiomers were significantly higher in the aqueous mobile phases which differs remarkably from the behavior of the other analytes, including mefloquine, and points towards stereoselective hydrophobic interactions in the aqueous eluents for this analyte. Hence, it is worthwhile investigating also aqueous mobile phases in combination with the present enantioselective SCX CSPs in the course of method development. In Figure 7, the chromatograms obtained with the distinct eluents for mefloquine under CLC conditions are illustrated.

3.2.2 Effect of co-ion type

Our previous studies with SCX-type chiral SOs based on both organic as well as inorganic silica monolithic stationary phases indicated that strong counterions are needed in order to allow the elution of the analytes in the ion-exchange retention mode with short run times and with satisfactory efficiencies [39, 51]. Under these premises AB proved to be well suited although it reduces the EOF and to some extent also the enantioselectivity compared to less efficient counterions such as the secondary or tertiary amines diethylamine, triethylamine, and Hünig base. It was thus used in the following studies at a constant concentration of 12.5 mM. At that point, another interesting task, previously ignored, was to examine the effect of the co-ion. It has been used in excess to the counterion to assure protonation of the basic solutes. Such acidic conditions turned out to be favorable in the present SCX system, while retention, enantioselectivity, resolution, and efficiency were all significantly lowered when excess of base was used (data not shown).

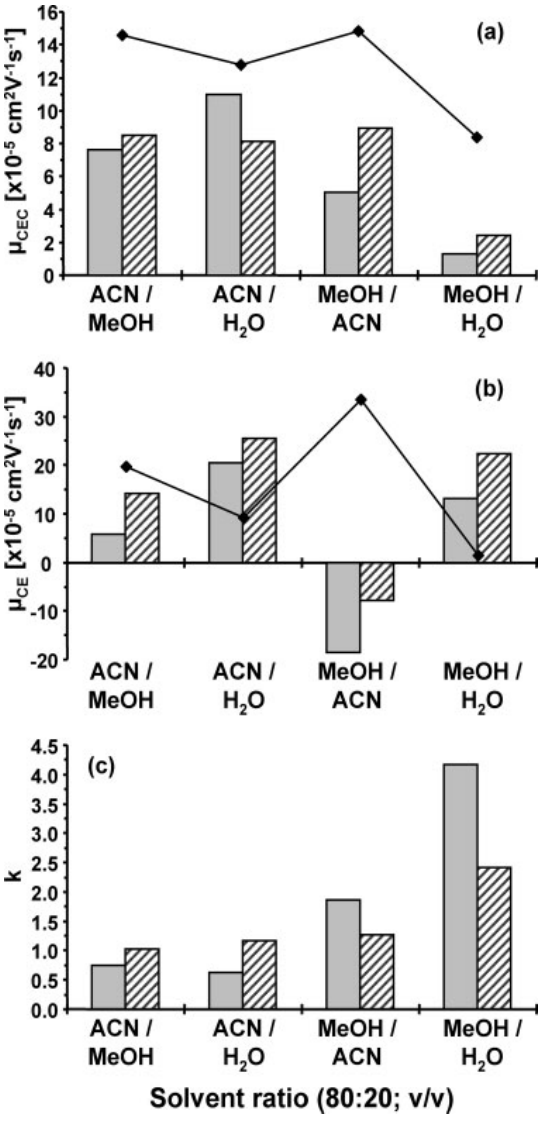

Figure 5. Enantioseparation of mefloquine-*t*-butylcarbamate (gray bars) and clenbuterol (shaded bars) by CEC, CE, and CLC using different nonaqueous and aqueous mobile phases. (a) Mobilities of the EOF (◆) and the first-eluted enantiomers under CEC conditions. (b) Electroosmotic (◆) and effective electrophoretic mobilities as measured in an open FS tube of identical dimensions. (c) Retention factors k (=($t_R - t_0$)/t_0) of the first-eluted enantiomers as measured by CLC. Experimental conditions: electrolytes, 25 mM FA and 12.5 mM AB; UV detection at 216 nm; capillary temperature, 20°C. (a, b) Applied voltages, +7 kV for all eluents except for MeOH-H_2O (+13 kV); electrokinetic injection for 10 s. (c) Flow rate, 0.35 μL/min; injection volume, 0.1 μL. (Note: negative electrophoretic % mobilities in (b) for the MeOH/ACN (80:20 v/v) eluent probably arise due to overlapped adsorption phenomena of the cationic solutes on the negatively charged silanol wall).

In our studies, we examined four distinct organic acids with varying acidity as co-ion: acetic acid (pK_a 4.75), FA (pK_a 3.75), MSA (pK_a 1.75), and TFA (pK_a 0.53) (pK_a values correspond to aqueous solutions). As we were interested in a comparison of electrically and pressure-driven chromatography we used methanol/water (80:20, v/v) based eluents due to the better enantioselectivity and resolution under nano-HPLC conditions (*vide supra*). All mobile phases contained 25 mM of the acid and AB as counterion at an acid-to-base ratio of 2:1. In order to minimize the elution times under CEC conditions we employed short-end injection, *i.e.*, effective bed length was 8.5 cm. Figure 8 depicts the results regarding retention, enantioselectivity, and resolution as obtained for the separation of mefloquine under CEC and CLC conditions. For all other tested analytes, largely the same trends were observed. For the purpose of straightforward comparison the retention factors are shown in Fig. 8a instead of electrochromatographic mobilities, and accordingly separation factors were calculated by the ratio of the k values of the enantiomers.

Overall, it is seen that the co-ion influence is relatively negligible, both in CEC (Fig. 8a) and CLC (Fig. 8b). Only minute effects are observed. It is noticeable, because it is somewhat counterintuitive, that upon exchange of the weaker acetic acid and FA co-ions by the stronger MSA and TFA co-ions the EOF remains essentially the same. Obviously, due to the constant counterion concentration the ζ-potential of the sulfonic acid surface remains nearly constant. More important is the co-ion effect on retention factors: In CLC, they are increasing in the order $k_{MSA} < k_{TFA} < k_{AcOH} < k_{FA}$. This trend roughly follows the ion-pairing tendencies of the co-ions. It might thus be explained by ion-pairing between co-ion and solute cation in the mobile phase which may be established as a competitive equilibrium to ion-pairing of the solute with the fixed ion-exchange sites of the sorbent weakening its adsorption. It is well known that TFA and MSA have good ion-pairing capacities, while FA exhibits no significant ion-pairing properties. In CEC the calculated retention factors are smaller than in CLC in any case, which originates from the superimposed codirectional electrophoretic migration contribution. As a consequence, the α values calculated by chromatographic formalism are slightly higher in CEC than in CLC. Otherwise, the same relative trends with regards to co-ion variation seem to be obeyed in CEC as in CLC except that the retention factors with MSA as co-ion are larger than those with TFA and the α value with TFA is significantly enhanced in comparison to those obtained with the other co-ions. These two effects are not well understood. With regards to resolution, the co-ion effect is also not very striking, although it may be significant because of its influence on peak shapes. In conclusion, the co-ion effects are rather negligible as opposed to the counterion effects [51], and not much can be gained by exchange of the common FA or acetic acid co-ion by other stronger acids such as TFA and MSA.

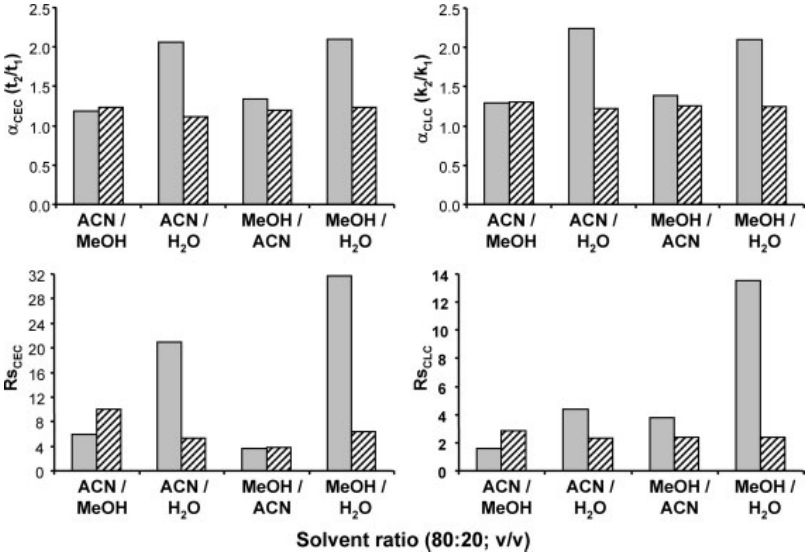

Figure 6. Enantioseparation of mefloquine-*t*-butylcarbamate (gray bars) and clenbuterol (shaded bars) by (a, c) CEC and (b, d) CLC using different nonaqueous and aqueous mobile phases. Comparison of the enantioselectivity α and the resolution *Rs* (c, d). ($\alpha = t_2/t_1$ for CEC, and k_2/k_1 for CLC). Experimental conditions as in Fig. 5.

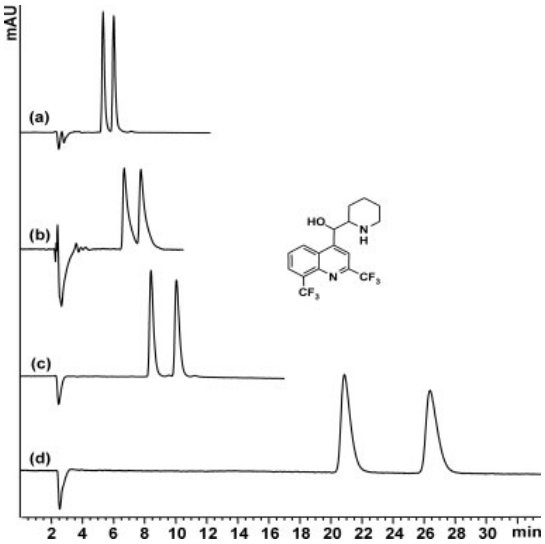

Figure 7. Enantioseparation of mefloquine by nano-HPLC with the SCX-modified silica monolith using nonaqueous and aqueous mobile phases. Eluents: (a) ACN-MeOH, (b) ACN-H_2O, (c) MeOH-ACN, and (d) MeOH-H_2O, always 80:20 (v/v). Other experimental conditions as in Fig. 5.

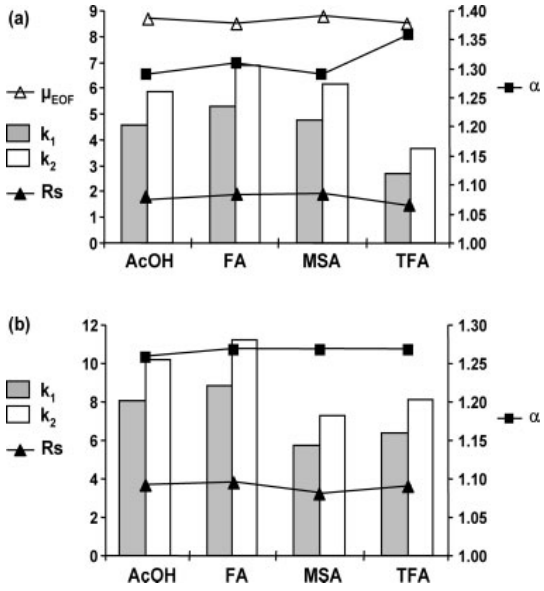

Figure 8. Enantioseparation of mefloquine using diverse acids as co-ions by (a) CEC and (b) nano-HPLC. Influence on the EOF ($\mu_{EOF} \times 10^{-5}$ $cm^2V^{-1}s^{-1}$, Δ), the retention factors k_1 (gray bars) and k_2 (white bars) and the resolution (▲) (all left ordinate) and the selectivity factor ($\alpha = k_2/k_1$, ■, right ordinate). Experimental conditions: mobile phase, MeOH-H_2O (80:20; v/v) containing 25 mM acid and 12.5 mM AB; UV detection at 216 nm; capillary temperature, 20°C. CEC: effective length, 8.5 cm; applied voltages: +10 kV (AcOH, pK_a 4.75 and FA, pK_a 3.75) and +7 kV (MSA, pK_a 1.75 and TFA, pK_a 0.53); electrokinetic injection for 10 s. nano-HPLC: effective length, 33. cm; flow rate, 0.35 μL/min; injection volume, 0.1 μL.

3.3 Kinetic behavior under electrically and pressure-driven capillary chromatography conditions

The most appealing driving force to use CEC instead of HPLC is, by theory, its amazing efficiency gain. This may indeed be extremely valuable for chiral separations where

not seldom poor peak performance is observed by HPLC. However, in practice the announced high plate numbers could often not be realized in many CEC separations reported in the literature. Here we wish to demonstrate the kinetic performance and the capability of the present sulfonic acid-based chiral cation exchanger to achieve high plate counts which may make CEC of real help for some specific enantiomer separation problems.

In order to facilitate the comparison of efficiencies obtained under electrically driven and pressure-driven conditions, CLC experiments were also performed in the electrophoresis instrument utilizing the available external pressurization system implemented with a nitrogen gas bottle. This system enables the application of pressures up to 12 bar which led to linear flow rates very similar to those obtained in CEC (in the range of ~0.2–1.2 mm/s). By performing the CLC experiments in a similar instrumental environment as the CEC separations extracolumn band broadening processes, as are usually not completely eliminated in a conventional nano-HPLC system, are excluded. Hence, the direct comparison of the obtained plate heights can be assumed to be valid, as they solely reflect peak broadening contributions arising in the column in both techniques.

In Fig. 9, the Van Deemter plots (*H*–*u* curves) obtained for the separation of the mefloquine enantiomers under CEC and CLC conditions are shown. As a result of the improved mass transfer and the plug-like flow profile of the electroosmotically driven mobile phase much lower theoretical plate heights *H* were obtained under CEC conditions, *i.e.*, the number of plates *per* unit length was significantly higher compared to capillary HPLC conditions, as claimed by theory. Thus, in CEC theoretical plate heights of about 3.5–9.5 μm were obtained corresponding to plate counts in the range of 295 000 and 105 000 *per* meter, while *H* values were significantly higher under pressure-driven conditions (between 11.5 and 16.5 μm, corresponding to plate counts of 60 000–90 000/m). While the graphs for the CLC separations have the common shape showing a minimum at a very slow linear flow velocity of 0.4–0.5 mm/s (4–6 bar), the *H*–*u* plots for the CEC separations display a plateau for the plate heights at linear flow velocities above ~0.5 mm/s (corresponding to an applied voltage of ~10 kV). The estimated coefficients *A* and *C* for the fitted Van Deemter curves $H = A + B/u + C \times u$ depicted in Fig. 9 differed significantly for the two graphs. The A-term contribution (flow maldistribution by Eddy diffusion) to band broadening was by a factor of about three lower in CEC compared to CLC. An even more pronounced improvement resulted for mass transfer resistance (C-term contribution), which was by a factor of about six lower in the electrically driven mode. Due to this insignificant C-term contributions and the low A-term contribution plate heights as low as ~3.5 μm were afforded over a wide flow rate range (at least between 0.5 and 1.5 mm/s) under CEC conditions. This is in particular remarkable for an enantioselective separation system which is based on multiple simultaneous interactions, involving besides others, ionic interactions which are commonly known to be associated with slow adsorption/desorption kinetics especially if occurring together with other interactions.

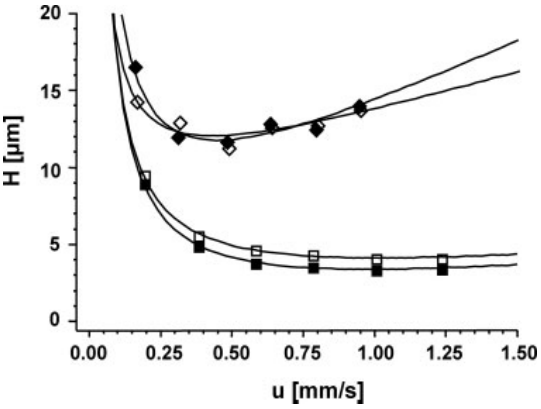

Figure 9. Van Deemter plots for the first (closed symbols) and second (open symbols) eluted enantiomer of mefloquine under CEC (squares) and CLC (rhombi) conditions. Experimental conditions: mobile phase, ACN/MeOH (80:20; v/v) containing 25 mM FA and 12.5 mM AB; electrokinetic injection at 10 kV for 10 s; capillary temperature, 20°C; UV detection at 216 nm. CEC: applied voltages: +4 to +24 kV. CLC: applied pressures: 2–12 bar.

According to the generally higher efficiencies found for the CEC separations also enantioresolutions were better in the electrically driven mode, even when short-end injection was used. In Figure 10, some exemplary electrochromatograms are compared with the CLC-chromatograms received under identical experimental conditions with the nano-HPLC system.

In sharp contrast to the irreproducible separations of basic compounds on SCX-columns in CEC mode in the early days of this technique [59], the CEC separations with the present monolithic capillary column, once optimized, were highly repeatable (Table 2). For example, RSD for t_0, $t_{1,2}$, and also α of about 0.1% (n = 10) could be afforded. This is well in the order of common RP-HPLC separations. Even resolution showed an RSD value <1%. Such excellent system stability and repeatabilities promise practical applicability for solving challenging real-life problems.

4 Concluding remarks

In the present paper, we described the behavior and performance of a new enantioselective silica-based monolithic stationary phase with novel surface chemistry for enantiomer separations by CEC and high-performance CLC. The monolith was prepared by the sol–gel process and subsequently functionalized with a novel SCX-type chiral SO. The chemical modification involved the derivatization of the pure silica monolith surface by silylation reaction with 3-mercaptopro-

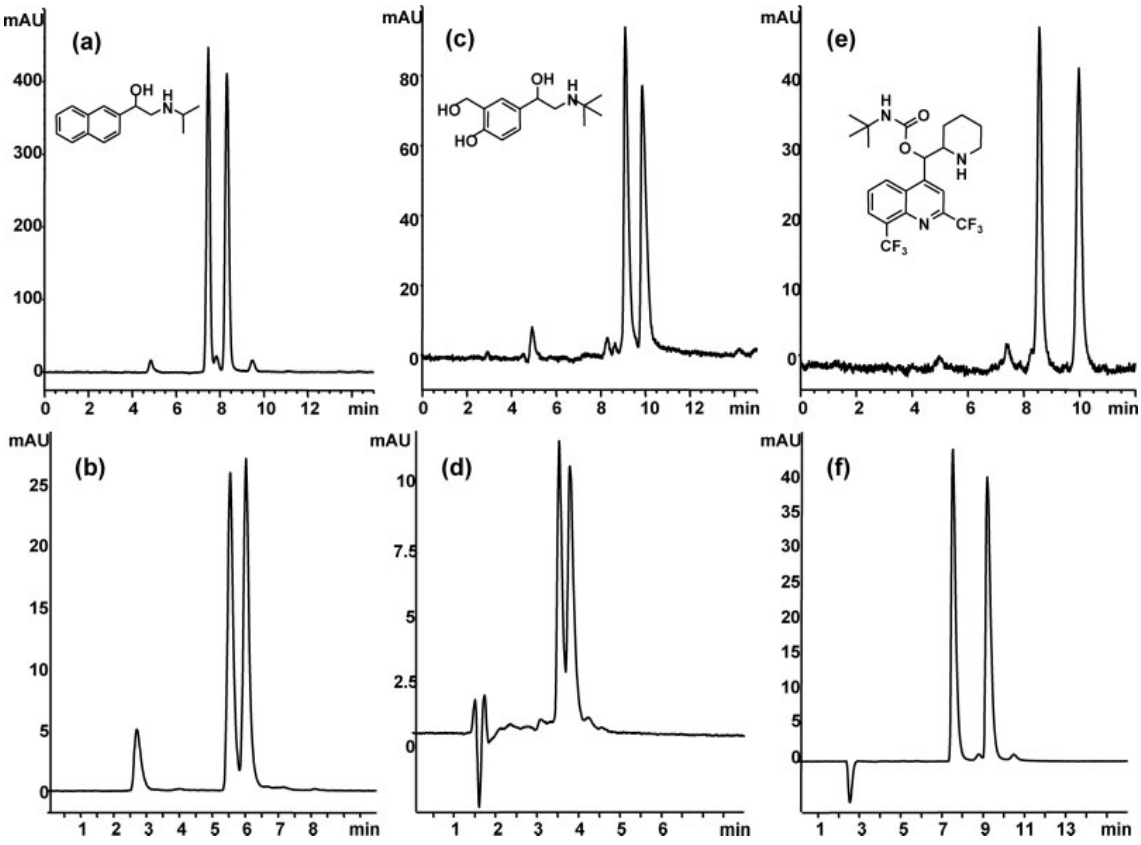

Figure 10. Enantioseparation of (a, b) pronethalol, (c, d) salbutamol, and (e, f) mefloquine-*t*-butylcarbamate by CEC (a, c, e) and nano-HPLC (b, d, f). Experimental conditions as in Fig. 9. CEC: effective length, 8.5 cm; applied voltage +7 kV, electrokinetic injection for 10 s. nano-HPLC: effective length, 33.5 cm; flow rate, 0.35 μL/min; injection volume, 0.1 μL.

Table 2. Run-to-run repeatability of the separation of mefloquine enantiomers on the chirally modified monolithic silica stationary phase under CEC conditions[a)]

	Mean[b)]	% RSD
t_0 [min]	4.79	0.11
t_1 [min]	7.28	0.10
t_2 [min]	8.01	0.07
α (t_2/t_1)	1.29	0.14
Rs	2.81	0.70

a) Experimental conditions: mobile phase, ACN-MeOH (80:20, v/v) containing 25 mM formic acid and 12.5 mM 2-amino-1-butanol; voltage, +20 kV; electrokinetic injection for 5 s; temperature, 20°C; UV detection at 216 nm.

b) $n = 10$.

pyl trimethoxysilane creating a reactive thiol surface followed by immobilization of the *trans*-(1*S*,2*S*)-2-(*N*-4-allyloxy-3,5-dichlorobenzoyl)aminocyclohexanesulfonic acid SO by radical addition reaction. Both the silylation and the radical addition reactions were thoroughly studied and the effect of the SO coverage on the separation of a number of basic test substances was examined in both electrically- and pressure-driven mode. As expected, by an increase in the concentration of SO moieties at the monolithic stationary phase enantioselectivity and resolution could be first enhanced, but they diminished again probably due to inaccessibility of the binding sites when chromatographic ligands are too close to each other. In the course of the study of the mobile phase composition nonaqueous eluents were compared to aqueous mobile phases and the performance was studied again for CEC as well as CLC. Overall, the performance turned out to be solute-dependent, as expected. For some analytes (those which apparently involve hydrophobic interactions) highest selectivity factors and resolutions were observed under aqueous conditions in both CEC and nano-HPLC. Furthermore, by investigating the influence of the co-ion which was

always applied in excess, FA proved to be the co-ion of choice with regards to enantioselectivity and resolution for both separation techniques, although with stronger acids, *e.g.*, TFA, separations were faster.

Overall, it can be concluded that the present new silica-based monolithic CSP is well suited for the separation of a number of chiral bases including a variety of pharmaceuticals such as β-blockers and β-sympathomimetics. Under repeated injections the monolithic phase showed excellent system robustness and run-to-run repeatability with RSDs far below 1% for elution times, α values and resolutions as well. Due to its rigidity, incompressibility and overall good column robustness the developed enantioselective SCX-type monolithic capillary column can be readily utilized not only in CEC, but also in pressure-driven CLC.

We gratefully acknowledge the financial support by the Austrian Christian Doppler Research Society and the industry partners AstraZeneca (Mölndal, Sweden) and Merck KGaA (Darmstadt, Germany).

The authors have declared no conflict of interest.

5 References

[1] Vallano, P. T., Chirica, G. S., Remcho, V. T., *Encyclopedia of Analytical Chemistry: Applications, Theory and Instrumentation*, Wiley, Chichester 2000, Vol. 13, pp. 11402–11428.

[2] Deyl, Z., Svec, F. (Eds.), *J. Chromatogr. Lib.*, Vol. 62, Elsevier, Amsterdam 2001.

[3] Svec, F., *Adv. Biochem. Eng./Biotechnol.* 2002, *76*, 1–47.

[4] Lämmerhofer, M., Lindner, W., in: Svec, F., Tennikova, T. B., Deyl, Z. (Eds.), *Monolithic Materials*, Elsevier, Amsterdam 2003, Vol. 67, pp. 489–559.

[5] Jiskra, J., Claessens, H. A., Cramers, C. A., *J. Sep. Sci.* 2003, *26*, 1305–1330.

[6] Eeltink, S., Kok, W. Th., *Electrophoresis* 2006, *27*, 84–96.

[7] Wistuba, D., Schurig, V., *Electrophoresis* 2000, *21*, 4136–4158.

[8] Lämmerhofer, M., Svec, F., Fréchet, J. M. J., Lindner, W., *Trends Anal. Chem.* 2000, *19*, 676–698.

[9] Chankvetadze, B., Blaschke, G., *J. Chromatogr. A* 2001, *906*, 309–363.

[10] Fanali, S., Catarcini, P., Blaschke, G., Chankvetadze, B., *Electrophoresis* 2001, *22*, 3131–3151.

[11] Gübitz, G., Schmid, M. G., *Electrophoresis* 2004, *25*, 3981–3996.

[12] Lämmerhofer, M., *J. Chromatogr. A* 2005, *1068*, 31–57.

[13] Jinno, K., Sawada, H., *TrAC* 2000, *19*, 664–675.

[14] Liu, Z., Wu, R. A., Zou, H., *Electrophoresis* 2002, *23*, 3954–3972.

[15] Guihen, E., Glennon, J. D., *J. Chromatogr. A* 2004, *1044*, 67–81.

[16] Colon, L. A., Maloney, T. D., Fermier, A. M., *J. Chromatogr. Lib.* 2001, *62*, 111–164.

[17] Fujimoto, C., *Chromatography* 2001, *22*, 145–150.

[18] Zou, H., Huang, X., Ye, M., Luo, Q., *J. Chromatogr. A* 2002, *954*, 5–32.

[19] Lämmerhofer, M., Lindner, W., in: Svec, F., Tennikova, T. B., Deyl, Z. (Eds.), *Monolithic Materials: Preparation, Properties and Applications*, Elsevier, Amsterdam 2003, p. 489.

[20] Legido-Quigley, C., Marlin, N. D., Melin, V., Manz, A., Smith, N. W., *Electrophoresis* 2003, *24*, 917–944.

[21] Svec, F., Tennikova, T. B., Deyl, Z. (Eds.), *J. Chromatogr. Lib.*, Vol. 67, Elsevier, Amsterdam 2003.

[22] Svec, F., *J. Sep. Sci.* 2005, *28*, 729–745.

[23] Bedair, M., El Rassi, Z., *Electrophoresis* 2004, *25*, 4110–4119.

[24] Hilder, E. F., Svec, F., Fréchet, J. M. J., *J. Chromatogr. A* 2004, *1044*, 3–22.

[25] Buchmeiser, M. R., Sinner, F., Mupa, M., *Macromol. Symp.* 2001, *163*, 25–34.

[26] Allen, D., El Rassi, Z., *Electrophoresis* 2003, *24*, 3962–3976.

[27] Siouffi, A. M., *J. Chromatogr. A* 2003, *1000*, 801–818.

[28] Tanaka, N., Motokawa, M., Kobayashi, H., Hosoya, K., Ikegami, T., in: Svec, F., Tennikova, T. B., Deyl, Z. (Eds.), *Monolithic Materials: Preparation, Properties and Applications. J. Chromatogr. Library*, Elsevier, Amsterdam 2003, Vol. 67, pp. 173–196.

[29] Tanaka, N., Kobayashi, H., Ishizuka, N., Minakuchi, H. *et al.*, *J. Chromatogr. A* 2002, *965*, 35–49.

[30] Koide, T., Ueno, K., *J. High Resolut. Chromatogr.* 2000, *23*, 59–66.

[31] Vegvari, A., Foldesi, A., Hetenyi, C., Kocnegarova, O. *et al.*, *Electrophoresis* 2000, *21*, 3116–3125.

[32] Zeng, H.-L., Li, H.-F., Lin, J.-M., *Anal. Chim. Acta* 2005, *551*, 1–8.

[33] Koide, T., Ueno, K., *J. Chromatogr. A* 2001, *909*, 305–315.

[34] Peters, E. C., Lewandowski, K., Petro, M., Svec, F., Fréchet, J. M. J., *Anal. Commun.* 1998, *35*, 83–86.

[35] Kornysova, O., Jarmalaviciene, R., Maruska, A., *Electrophoresis* 2004, *25*, 2825–2829.

[36] Machtejevas, E., Maruska, A., *J. Sep. Sci.* 2002, *25*, 1303–1309.

[37] Lämmerhofer, M., Peters, E. C., Yu, C., Svec, F. *et al.*, *Anal. Chem.* 2000, *72*, 4614–4622.

[38] Lämmerhofer, M., Tobler, E., Zarbl, E., Lindner, W. *et al.*, *Electrophoresis* 2003, *24*, 2986–2999.

[39] Preinerstorfer, B., Lindner, W., Lämmerhofer, M., *Electrophoresis* 2005, *26*, 2005–2018.

[40] Schmid, M. G., Grobuschek, N., Lecnik, O., Gübitz, G. *et al.*, *Electrophoresis* 2001, *22*, 2616–2619.

[41] Nakanishi, K., Soga, N., *J. Non-Cryst. Solids* 1992, *139*, 14.

[42] Kato, M., Sakai-Kato, K., Matsumoto, N., Toyo'oka, T., *Anal. Chem.* 2002, *74*, 1915–1921.

[43] Kato, M., Matsumoto, N., Sakai-Kato, K., Toyo'oka, T., *J. Pharm. Biomed. Anal.* 2003, *30*, 1845–1850.

[44] Kang, J., Wistuba, D., Schurig, V., *Electrophoresis* 2002, *23*, 1116–1120.

[45] Chen, Z., Ozawa, H., Uchiyama, K., Hobo, T., *Electrophoresis* 2003, *24*, 2550–2558.

[46] Chankvetadze, B., Yamamoto, C., Tanaka, N., Nakanishi, K., Okamoto, Y., *J. Sep. Sci.* 2004, *27*, 905–911.

[47] Chen, Z., Hobo, T., *Electrophoresis* 2001, *22*, 3339–3346.

[48] Chen, Z., Hobo, T., *Anal. Chem.* 2001, *73*, 3348–3357.

[49] Chen, Z., Uchiyama, K., Hobo, T., *J. Chromatogr. A* 2002, *942*, 83–91.

[50] Chen, Z., Nishiyama, T., Uchiyama, K., Hobo, T., *Anal. Chim. Acta* 2004, *501*, 17–23.

[51] Preinerstorfer, B., Lubda, D., Lindner, W., Lämmerhofer, M., *J. Chromatogr. A* 2006, *1106*, 94–105.

[52] Wistuba, D., Schurig, V., *Electrophoresis* 2000, *21*, 3152–3159.

[53] Wistuba, D., Banspach, L., Schurig, V., *Electrophoresis* 2005, *26*, 2019–2026.

[54] Kato, M., Dulay, M. T., Bennett, B., Chen, J.-R., Zare, R. N., *Electrophoresis* 2000, *21*, 3145–3151.

[55] Schmid, M. G., Koidl, J., Freigassner, C., Tahed, S. *et al.*, *Electrophoresis* 2004, *25*, 3195–3203.

[56] Hoffmann, C. V., Lämmerhofer, M., Lindner, W. T., *J. Chromatogr. A* 2007, *1161*, 242–251.

[57] Ishizuka, N. K. H., Minakuchi, H., Nakanishi, K., Hirao, K. *et al.*, *J. Chromatogr. A* 2002, *960*, 85–96.

[58] Preinerstorfer, B., Bicker, W., Lindner, W., Lämmerhofer, M., *J. Chromatogr. A* 2004, *1044*, 187–199.

[59] Smith, N. W., Evans, M. B., *Chromatographia* 1995, *41*, 197–203.

Appendix #3

Publication P-III

Beatrix Preinerstorfer[1]
Michael Lämmerhofer[1]
Christian V. Hoffmann[1]
Dieter Lubda[2]
Wolfgang Lindner[1]

[1]Department of Analytical and Food Chemistry, Christian Doppler Laboratory for Molecular Recognition Materials, University of Vienna, Vienna, Austria
[2]Performance and Life Science Chemicals, Merck KGaA, Darmstadt, Germany

Original Paper

Deconvolution of electrokinetic and chromatographic contributions to solute migration in stereoselective ion-exchange capillary electrochromatography on monolithic silica capillary columns

A monolithic silica stationary phase functionalized with an enantioselective strong cation exchanger based on an aminosulfonic acid derivative was used for chiral separations of basic test solutes by nonaqueous CEC and capillary LC. The effects of the applied electric field as well as the ionic strength in the eluent on electrokinetic and chromatographic contributions to the overall separation performance in the electrically driven mode were investigated. Hence, under the utilized experimental conditions, *i.e.*, at an electric field strength in the range of ~120 – 720 V/cm (applied voltages 4 – 24 kV) and an ionic strength of the counterion between 5 and 25 mM (at constant acid-to-base, *i.e.*, co- to counterion ratio of 2:1), no deviations from the expected linearity of the EOF were observed. This led to the conclusion that an occurrence of the so-called electrokinetic effects of the second kind resulting from electric double layer overlap inside the mesopores of the monolithic stationary phase and concentration polarization phenomena were largely negligible. Additional support to this conclusion was inferred from the observed independence of CEC retention factors on the electric field strength across the investigated ionic strength range of the BGE. As a consequence, a simple framework allowing for calculation of the CEC mobilities from the individual separation contributions, *viz*. electroosmotic and electrophoretic mobilities as well as retention factors, could be applied to model CEC migration. There was a reasonable agreement between calculated and experimental CEC mobility data with deviations typically below 5%. The deconvolution of the individual contributions to CEC migration and separation is of particular value for the understanding of the separation processes in which electrophoretic migration of ionic sample constituents plays a significant role like in ion-exchange CEC and may aid the optimization procedure of the BGE and other experimental conditions such as the optimization of the surface chemistry of the stationary phase. In combination with the remarkable column performance evident from the low theoretical plate heights observed under CEC conditions for all test solutes (3.5 – 7.5 μm in the flow rate range of 0.4 – 1.2 mm/s, corresponding to (130 000 – 300 000 plates *per* meter), the presented framework provides an attractive tool as the basis for the assessment of chromatographic selectivities in a miniaturized CEC screening of new selectors and chiral stationary phases (CSPs), respectively, from experimental CEC data and known CE mobilities.

Keywords: Concentration polarization / Electric double layer overlap / Enantiomer separation / Silica monolith / Strong cation exchanger

Received: November 6, 2007; revised: December 12, 2007; accepted: December 12, 2007

DOI 10.1002/jssc.200700572

1 Introduction

Although CEC [1] has evolved into a powerful high-performance analytical separation technique over the past decade, it is far from being on a par with capillary LC (CLC) or CE. Amongst the major impediments to further

Correspondence: Dr. Michael Lämmerhofer, Department of Analytical and Food Chemistry, Christian Doppler Laboratory for Molecular Recognition Materials, University of Vienna, Währinger Strasse 38, A-1090 Vienna, Austria.
E-mail: michael.laemmerhofer@univie.ac.at
Fax: +43-1-4277-9523

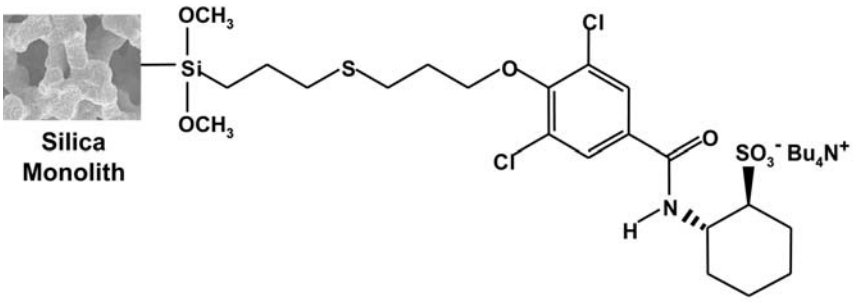

Figure 1. Structure of the monolithic silica-supported enantioselective stationary phase carrying the aminosulfonic acid-derived cation-exchange type chiral SO.

expand the scope of CEC applications are still deficits in column technologies and a continuous lack of theoretical understanding of the interplay of electrokinetic and chromatographic processes which exist despite a remarkable and increasing number of studies published over the last years reporting on fundamental aspects of this highly promising technique. For instance, several papers dealt with the modeling of solute migration in CEC or pressure-assisted CEC [2 – 22]. For stereoselective separation systems such attempts are unfortunately missing almost completely [23, 24].

Thus, it is the aim of the present paper, in which we report on extensive studies of the behavior of a silica-based monolithic capillary column in both electrically driven as well as pressure-driven enantioselective ion-exchange chromatography, to deconvolute the individual contributions to solute migration in CEC, *viz*. electroosmotic and electrophoretic mobility as well as chromatographic retention. The monolithic chiral stationary phase (CSP) was prepared by the sol – gel process and functionalized with a cation exchange type chiral selector (SO) based on the aminosulfonic acid derivative *trans*-(1*S*,2*S*)-2-(*N*-4-allyloxy-3,5-dichlorobenzoyl)aminocyclohexanesulfonic acid (Fig. 1). It was evaluated for the enantioselective separation of three test solutes, mefloquine, mefloquine-*O*-*tert*-butylcarbamate, and pronethalol (Fig. 2), by CEC and CLC. Electrophoretic mobilities were determined by means of CE using identical BGEs. The contributions of the individual separation processes in CEC were derived in dependence of the applied electric field strength and the ionic strength of the eluent, respectively, in order to assess whether nonlinear electrokinetic effects resulting from concentration polarization (CP) phenomena occur under the herein utilized experimental conditions [25 – 29]. The knowledge of the individual migration contributions in CEC should give better insight into the separation mechanism of charged solutes in stereoselective ion-exchange CEC [30 – 34] and may provide a fundamental basis for the optimization of enantiomer separations especially if complex mixtures are to be separated where besides adequate stereoselectivity a sufficient chemoselectivity is required as well (*e.g.*, when chiral drugs and their metabolites need to be analyzed simultaneously).

2 Theoretical background

The migration velocity of ionic analytes in CEC and pressure-assisted CEC (v_{CEC}) can, as a first approximation, be simply defined as a linear combination of all migration contributions (v_{tot}) weighted by a chromatographic retardation term as given by [21]

$$v_{CEC} = v_{tot}\left(\frac{1}{1+k_{CLC}}\right)$$

$$= \left(v_{eo} + v_{ep,eff} + v_{press}\right)\left(\frac{1}{1+k_{CLC}}\right) \quad (1)$$

wherein v_{eo}, $v_{ep,eff}$, and v_{press} are the linear velocities of the bulk EOF, the effective electrophoretic migration of the ionic sample and the pressurized flow, respectively, and k_{CLC} is the chromatographic retention factor under given experimental conditions.

In the absence of pressurized flow v_{press}, Eq. (1) can be expressed as

$$v^*_{CEC} = \mu^*_{CEC}E^* = \left(v^*_{eo} + v_{ep,eff}\right)\left(\frac{1}{1+k_{CLC}}\right)$$

$$= \frac{(\mu^*_{eo} + \mu_{ep,eff})E^*}{1+k_{CLC}} \quad (2)$$

wherein E is the electric field strength and μ_{CEC}, μ_{eo}, and $\mu_{ep,eff}$ are the observed mobility of the ionic solute in CEC, the electroosmotic mobility in CEC, and the effective electrophoretic mobility of the ionic solute, respectively.

Eq. (2) is employed herein as a framework to deconvolute individual migration/separation contributions in stereoselective ion-exchange CEC arising from electroosmosis, electrophoresis, and chromatographic retention.

Thereby, the * indicates that actual interstitial velocities and mobilities, respectively, as well as the actual field strength in the packing, considering the tortuosity of the flow channels, are used for the calculations (note, effective electrophoretic mobilities, as determined in the conventional way in an open tube, represent actual interstitial velocities and do not require for correction) [35]. The actual interstitial electroosmotic mobilities μ^*_{eo} were determined as suggested by [35]

$$\mu_{eo}^{*} = \frac{L_{act}^{2}}{t_0 V} \tag{3}$$

where L_{act} defines the length of the actual flow path of the tracer through the pores of the stationary phase. It can be calculated from the currents flowing in an open tube i_{open}, and a fully packed column of the same dimension i_{packed} of the length L_{tot} and identical BGE upon application of a voltage V as follows

$$L_{act} = L_{tot}\sqrt{\frac{i_{open}}{i_{packed}}} \tag{4}$$

The L_{act}/L_{tot} ratio and thus the square root of the i_{open}/i_{packed} ratio is also known as the tortuosity τ of the packing. In analogy to Eq. (3), the actual interstitial mobility of an ionic sample component under CEC conditions μ_{CEC}^{*} can be expressed by

$$\mu_{CEC}^{*} = \frac{L_{act}^{2}}{t_R V} \tag{5}$$

Further, it is assumed that k_{CLC}, as determined by HPLC and calculated by common chromatographic formalism, $k = (t_R - t_0)/t_0$, is not altered by the influence of the external electric field.

As the occurrence of an EOF results from the formation of an electric double layer (EDL) near charged surfaces, the mobility of the EOF depends according to the von Smoluchowski relationship amongst others on the properties of this EDL, which is characterized by the zeta potential ζ [36]

$$\zeta = \frac{\sigma_0 \delta}{\varepsilon_0 \varepsilon} \tag{6}$$

In this expression, σ_0 is the charge density at the surface and δ is the thickness of the EDL. δ is defined as the distance from the surface at which the potential drops to $1/e$ (~0.37) of its value at the surface and can be calculated by [16]

$$\delta = \sqrt{\frac{\varepsilon_0 \varepsilon RT}{2IF^2}} = \frac{1}{\kappa} \tag{7}$$

where I is the ionic strength of the electrolytes and κ is the Debye–Hückel parameter. Combining Eqs. (6) and (7) with the well-known von Smoluchowski equation yields Eq. (8) which describes the electroosmotic mobility μ_{eo} inter alia as the function of the ionic strength

$$\mu_{eo} = \sigma_0 \sqrt{\frac{\varepsilon_0 \varepsilon_r RT}{2F^2}} \frac{1}{\sqrt{I}} \tag{8}$$

Typical values for δ are much smaller than the average dimensions of the interparticulate spaces in CEC columns packed with commonly used chromatographic silica particles. Also for monolithic stationary phase supports, the mean macropore radius is generally orders of magnitude larger than the thickness of the occurring EDL. However, the intraparticle pore size of today most commonly used porous packing materials as well as the mean mesopore radius of bimodally structured monolithic stationary phases may already lie within the common EDL scale. As a consequence, inside these smaller pores EDL overlap may occur, which has already been reported for the first time in 1965 by Rice and Whitehead [37] and which was the object of several studies in recent years [3, 25–28, 38–44]. Significant effects of EDL overlap emerge when the ratio of pore channel radius to double layer thickness is close to unity or smaller. Besides the pore diameter and surface charge density, especially the ionic strength of the mobile phase decides whether significant EDL overlap takes place, as the thickness of the EDL depends inversely proportional on the square root of the ionic strength (Eq. 7). As a consequence of overlapped EDLs in the mesopores of the silica skeleton, they become charge-selective in both particulate and monolithic stationary phases and thus develop ion-permselectivity which means that they exclude coions and enrich counterions [25]. Upon application of high voltages typically used in CEC the phenomenon of CP arises, resulting in the formation of concentration gradients in the neighboring electrolyte solution of the ion-permselective mesopores, leading to nonlinear electrokinetic effects, the so-called effects of the second kind as described in detail by Tallarek and coworkers [25–29] in a series of papers. EDL overlap and CP affect the EOF which not only shows nonlinear electric field dependency, but also the retention factors of charged solutes in the CEC process which are not constant anymore but change with the field strength. Moreover, EOF of the second kind has been demonstrated to reduce plate heights and thus improve efficiencies. In such cases when CP is significant, Eqs. (1) and (2), respectively, are no longer applicable.

Effective electrophoretic mobilities $\mu_{ep,eff}$ under given conditions as determined by CE are, in case of a weak electrolyte, related to the actual mobilities of the fully charged ion $\mu_{act,i}$ by the degree of dissociation α. According to theory of ion conductance $\mu_{ep,eff}$ should, like actual ionic mobilities, drop with the square root of the ionic strength [45]

$$\mu_{act,i} = \mu_{0,i} - \left[\frac{8.204 \times 10^5}{(\varepsilon T)^{3/2}}\mu_{0,i} + \frac{4.275}{\eta(\varepsilon T)^{1/2}}\right]\sqrt{I} \tag{9}$$

where T is the absolute temperature and $\mu_{0,i}$ is the ion mobility at infinite dilution.

On the other hand, ion-exchange processes of small ions are commonly described by a stoichiometric displacement model [2, 46].

$$k = K_z[C]^{-\frac{x}{y}} \text{ or } \log k = \log K_z - \frac{x}{y}\log[C] \tag{10}$$

wherein C is the counterion concentration, K_Z a constant depending amongst others on parameters of the station-

ary phase and the ion-exchange equilibrium constant under given conditions, and x and y are the charge numbers of solute ion (x) and counterion (y), respectively. Although this is an empirical relationship which has been critically assessed [46, 47], it is assumed to be accurate enough for the present purpose.

3 Materials and methods

3.1 Instrumentation

All CEC and CE experiments were performed on an Agilent HP^{3D} CE system (Agilent, Waldbronn, Germany) equipped with a diode array detector and an external pressurization system. The data were processed with the HP^{3D} CE Chemstation software. Samples were injected electrokinetically for 10 s. Voltages applied are specified in the figure legends. The capillary cassette was thermostated at 20°C throughout the experiments.

The monolithic capillary columns with inner diameter (id) of 100 µm had a total length of 33.5 cm and were filled with the monolithic silica plug over the entire length. The effective length from injection to detection was 25 cm. UV detection was carried out through the monolithic silica bed for which purpose a detection window of about 1.5 mm width was made by removing the polyimide-coating of the fused-silica (FS) capillaries using a razor blade. CE experiments were carried out in a 100 µm id bare FS capillary of the same dimensions (*i.e.*, L_{tot} = 33.5 cm, L_{eff} = 25 cm) and effective electrophoretic mobilities were obtained from apparent mobilities after subtraction of the respective electroosmotic mobility.

Capillary LC experiments were also performed on the Agilent electrophoresis system utilizing the external pressurization system implemented with a nitrogen gas bottle which enables applying pressures of up to 12 bar. The same monolithic silica capillary column as utilized for the CEC experiments was used for the pressure-driven chromatographic runs, and samples were injected electrokinetically in analogy to the CEC and CE experiments.

3.2 Materials and chemicals

The preparation of the enantioselective silica monolithic capillary columns (100 µm id) based on the chiral SO *trans*-(1*S*,2*S*)-2-(*N*-4-allyloxy-3,5-dichlorobenzoyl)aminocyclohexanesulfonic acid [48] (applied as quarternary tetrabutylammonia salt, *cf.* Fig. 1) was described previously [34]. The optimized monolithic column used throughout the study had, before SO bonding, a reactive sulfhydryl-loading of 56 µmol SH/25 cm, while after SO immobilization ~40% of the reactive sulfhydryls remained unmodified. In addition, a nonoptimized prototype column was prepared by a "flow-through immobilization" procedure leading to a thiol-monolith with a reactive sulfhydryl-loading of only 30 µmol SH/25 cm of which about 50% were still unmodified after SO immobilization (for more details see ref. [34]). Solvents (ACN and methanol) were of HPLC gradient grade from Merck (Darmstadt, Germany). (*R*,*S*)-2-Amino-1-butanol (AB) and formic acid (FA) were of analytical grade and purchased from Sigma–Aldrich (Steinheim, Germany). The chiral test substances mefloquine (erythro-α-2-piperidinyl-2,8-bis(trifluoromethyl)-4-quinolinemethanol), mefloquine-*O*-*tert*-butylcarbamate, and pronethalol have either been synthesized in-house or were gifts from various drug companies. Acetone has been used as an EOF-marker.

4 Results and discussion

4.1 Performance of sulfonic acid-based monolithic SCX (strong cation exchanger) capillary columns

Recently, we reported on the development of a siliceous monolithic stationary phase modified with a novel aminosulfonic acid-derived chiral SO (Fig. 1) [34]. The good performance in electrically driven stereoselective cation-exchange chromatography has prompted us to investigate more extensively the behavior of the silica-based monolithic capillary column under CEC but also under CLC conditions. In order to preclude in these CEC *versus* CLC comparisons bias originating from extra-column effects, the pressure-driven separations of the three test-analytes mefloquine, mefloquine-*O*-*tert*-butylcarbamate, and pronethalol (Fig. 2) were performed in the Agilent electrophoresis system, too. Throughout the following studies mobile phases composed of a mixture of ACN/methanol (80:20 v/v) containing FA and AB as electrolytes were used. The FA/AB ratio was always 2:1, which should ensure the complete protonation of the amine that acts as the counterion. Utilizing the available external pressurization assembly equipped with a nitrogen gas bottle, the application of pressures of up to 12 bar is possible resulting for the presently employed highly permeable monolithic capillary column in linear flow rates similar to those received by the application of electric fields (up to ~1.2 mm/s).

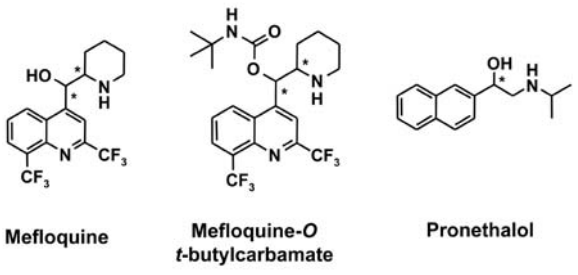

Figure 2. Structures of the basic test-solutes mefloquine, mefloquine-*O*-*tert*-butylcarbamate, and pronethalol.

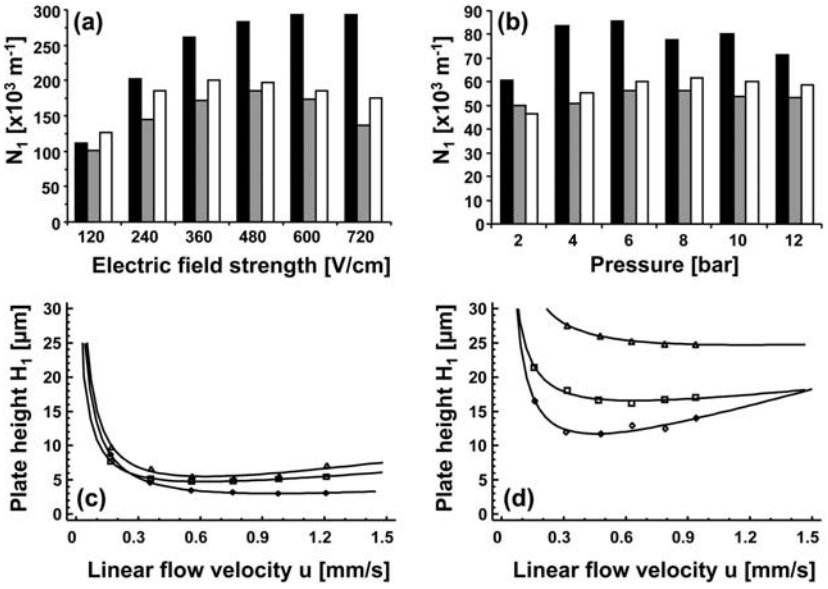

Figure 3. Dependence of the peak efficiencies, N/m, of the first eluted enantiomers of mefloquine (black bars), mefloquine-*O*-*tert*-butylcarbamate (gray bars), and pronethalol (white bars) in (a) enantioselective CEC on the applied electric field strength, and in (b) enantioselective CLC on the applied pressure as well as corresponding Van Deemter plots of mefloquine (♦), mefloquine-*O*-*tert*-butylcarbamate (▲), and pronethalol (■) in (c) CEC and (d) CLC. Experimental conditions: mobile phase, ACN/MeOH (80:20 v/v) containing FA and AB at an acid-to-base ratio of 2:1 with 25 mM FA and 12.5 mM AB. Electrokinetic injection at 10 kV for 10 s, capillary temperature, 20°C, UV detection at 216 nm.

The results of the comparative performance evaluation in CEC and CLC are illustrated in Fig. 3. The plate numbers for the three test compounds, but also other solutes, ranged from 100 000 to 300 000 m^{-1} in CEC (Fig. 3a) and 50 000 to 85 000 m^{-1} in CLC (Fig. 3b). This is remarkable for chiral separations and much better than with previously reported analogous SCX-type silica monolith capillary columns carrying a corresponding aminophosphonic acid SO moiety [33]. The analysis of the performance in terms of kinetic plots (van Deemter plots) (Figs. 3c and d) provides more information since it can be seen that in the investigated flow range the efficiency gain in CEC is mainly due to a greatly reduced A-term contribution to peak dispersion (about factor of 3). Since the covered flow range is not wide enough, it is not possible to derive any safe conclusions regarding the C-term contributions. It appears, however, that both in CEC and CLC a comparably efficient mass-transfer characteristics is proprietary to the present enantioselective SCX capillary column. From the initial slope of the C-term branch it becomes evident that in CEC also the C-term is slightly smaller, in particular for mefloquine, which is quite typical for CEC separations.

Representative chromatograms of CEC and CLC separations of the three test solutes monitored at the same linear bulk mobile phase flow velocities are given in Fig. 4. The improvement in terms of efficiencies of the CEC separations as compared to CLC conditions is striking. It is also quite eye-catching that the CEC separations are faster despite identical linear flow velocities. Not surprisingly this may be simply ascribed to the superimposed codirectional electrophoretic migration contribution. At first glance, it seems that this electrophoretic mobility increment is more significant for pronethalol than for the other two test solutes. To get an idea about the individual contributions of the various processes to be considered in CEC to the overall separation on a quantitative basis, we work out in the following the individual increments of electrokinetic and chromatographic processes.

4.2 Effect of electric field strength

The present monolithic silica exhibits a bimodal pore structure with a macropore diameter of ~2 µm and an average mesopore diameter of ~16 nm (which will be slightly reduced after surface modification) [33]. Hence, the occurrence of electrokinetic effects of the second kind caused by EDL overlap inside the mesopores is conceivable at low electrolyte concentrations [28]. This effect may be of significance at electrolyte concentrations significantly lower than 10 mM. For example, at an ionic strength of 25 mmol/L in an electrolyte system with a dielectric constant of about 35 which is similar to that of the BGE used herein, the Debye length κ^{-1} is around 1 nm and the value κr_{pore}, which denotes intense double layer overlaps if it approximates values around 1, is ~8, *i.e.*, double layer overlap is therefore largely absent. In comparison, for the BGE with 5 mM ionic strength the Debye length κ^{-1} is around 3 nm and the value κr_{pore} adopts a value of less than 3, which means that EDL overlap may become an issue. At this point it is noted that the cited work by Tallarek and coworkers [28] has employed aqueous eluents for which at the same ionic strength a slightly larger double layer thickness is obtained due to a higher dielectric constant (*e.g.*, around 2 and 4 nm at 25 and 5 mM). A more intense double layer overlap may result under such conditions.

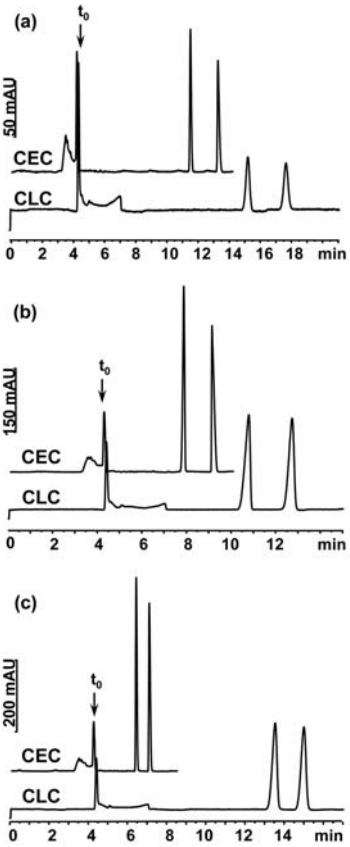

Figure 4. (Electro)chromatograms of the enantioselective separations of (a) mefloquine, (b) mefloquine-*O*-*tert*-butylcarbamate, and (c) pronethalol by CEC (upper traces) and CLC (lower traces). Experimental conditions: mobile phase, ACN/MeOH (80:20 v/v) containing 25 mM FA and 12.5 mM AB. Electrokinetic injection at 10 kV for 10 s, capillary temperature, 20°C, UV detection at 216 nm. Linear flow rates: CEC, 1.00 mm/s (580 V/cm, 20 kV) and CLC, 0.94 mm/s (12 bar).

In order to examine whether electrokinetic phenomena of the second kind are really of relevance under the conditions that we employ for stereoselective ion-exchange CEC experiments, the behavior of the EOF has been investigated in dependence of the applied electric field strength at three different concentrations of the electrolytes. If EDL overlap and CP are of any significance, a nonlinear increase in v_{eo} with electric field strength would be expected due to additionally induced EOF of second kind as outlined by Nischang and Tallarek [25]. As can be seen from Fig. 5, however, this is not the case because the EOF velocity changed linearly upon variation of the electric field strength from ~120 to 720 V/cm (4 – 24 kV applied voltage) even when counterionic strength was decreased from 25 mM over 12.5 to 5 mM AB.

It was reported by Nischang *et al.* [49] that in ion-exchange CEC on particulate stationary phase with narrow 8 nm-sized mesopores and a very high surface charge density (probably much higher than in the present work) ion-permselectivity could be discerned even with 40 mM ionic strength. As a consequence, retention factors of counterionic solutes strongly depended on the applied electric field strength under conditions at which CP was significant. The gradients in bulk electrolyte concentrations around a charge-selective particle that are formed due to EDL overlap and electric field-induced CP are a function of the applied electric field strength. Thus, when the field strength was increased, the counterionic solutes were more strongly retained, *i.e.* *k*-values increased with ε. In Fig. 6, the results regarding retention factors obtained in the present study for the enantioseparation of the three solutes by CEC in dependence on the applied electric field strength are depicted. It is striking that the observed electrochromatographic retention factors k_{CEC} were widely constant over the tested voltage range (Fig. 6a) even at a counterion concentration as low as 5 mmol/L AB (Fig. 6b). These trends confirm the absence of CP effects under the presently investigated ionic strength conditions.

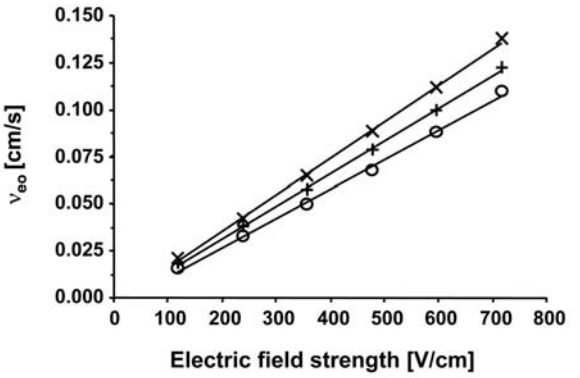

Figure 5. Influence of the applied electric field strength on the velocity of the EOF, v_{eo}, at varying eluent ionic strength. Experimental conditions: mobile phase, ACN/MeOH (80:20 v/v) containing FA and AB at an acid-to-base ratio of 2:1 with 5 mM (**x**), 12.5 mM (**+**), and 25 mM (**o**) AB. Electrokinetic injection at 10 kV for 10 s, capillary temperature, 20°C, UV detection at 216 nm.

It can therefore be concluded that no significant nonlinear electrokinetic effects occur under the herein utilized experimental conditions and that EDL overlap within intraskeletal pores which would cause ion-permselectivity resulting in CP and charge gradients is largely negligible.

4.3 Deconvolution of electrokinetic and chromatographic contributions

Since it was confirmed that at the presently employed high ionic strength conditions (*e.g.*, electrolyte systems

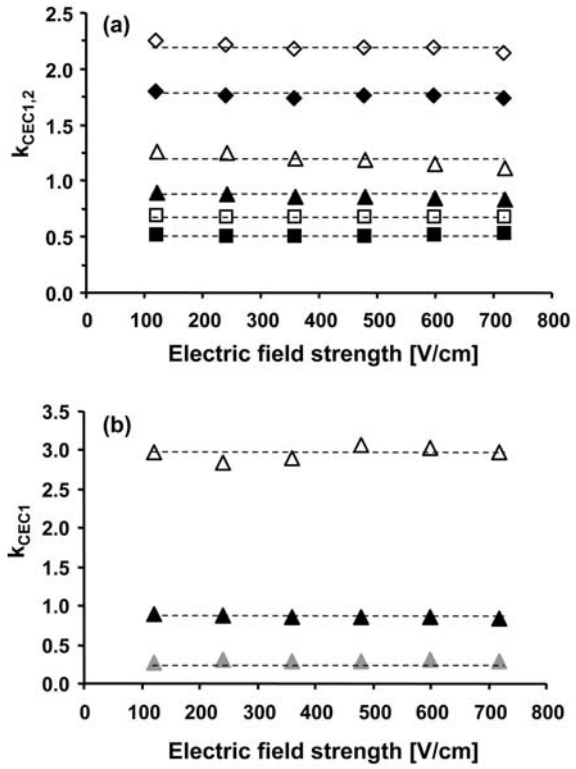

Figure 6. Dependence of the retention factors in CEC, k_{CEC}, (calculated by the chromatographic formalism, $k = (t_R - t_0)/t_0$) on the applied electric field strength at (a) constant and (b) varying ionic strength of the counterion. Markers: mefloquine (♦), mefloquine-*O*-*tert*-butylcarbamate (▲), and pronethalol (■). Closed symbols in (a) represent the first eluted enantiomer, open symbols the second eluted enantiomer. Experimental conditions: mobile phase, ACN/MeOH (80:20 v/v) containing FA and AB at an acid-to-base ratio of 2:1 with (a) 12.5 mM AB and (b) 5 mM (white triangles), 12.5 mM (black triangles), and 25 mM AB (gray triangles). Other conditions: same as in Fig. 3.

composed of 12.5 mM AB and 25 mM FA) CP and electrokinetic phenomena of the second kind were largely absent, Eqs. (1) and (2) should largely be obeyed and be applicable as a rough approximation to model migration in the present cation-exchange CEC system. In that case there should be a reasonable agreement between CEC mobilities calculated from the individual contributions μ^*_{eo}, $\mu_{ep,eff}$, and k_{CLC} with experimentally determined ones. The data for the three test solutes obtained with one BGE at distinct electrical field strengths are summarized in Table 1.

Mefloquine and mefloquine-*O*-*tert*-butylcarbamate have under given conditions a comparably low effective electrophoretic mobility of about 7.6 and 7.2×10^{-5} $cm^2 \cdot V^{-1} \cdot s^{-1}$, respectively. In contrast, the mobility of pronethalol is indeed higher (by a factor of about 3) (22.4×10^{-5} $cm^2 \cdot V^{-1} \cdot s^{-1}$) as already argued from the electrochromatogram of Fig. 4c. While the EOF contribution is of course the same for all three test solutes ($\mu^*_{eo} = 26.7 \times 10^{-5}$ $cm^2 \cdot V^{-1} \cdot s^{-1}$), the retention factors of the three solutes differ significantly. The retention factor in CLC for the first eluted enantiomer of mefloquine ($k_{CLC1} = 2.5$) is significantly higher than that of its *O*-*tert*-butylcarbamate ($k_{CLC1} = 1.5$). On contrary, k_{CLC1} of pronethalol is lying in-between ($k_{CLC1} = 1.9$). These values readily explain the relative migration times and mobilities, respectively, observed in CEC. For example, μ_{CEC1} as calculated from the individual contributions by Eq. (2) are 9.9, 13.8, and 17.2×10^{-5} $cm^2 \cdot V^{-1} \cdot s^{-1}$ for mefloquine, its *t*-butylcarbamate, and pronethalol, respectively. The corresponding mobilities for the second eluted enantiomers are calculated to be 8.5, 11.8, and 15.5×10^{-5} $cm^2 \cdot V^{-1} \cdot s^{-1}$ for mefloquine, its *tert*-butylcarbamate, and pronethalol, respectively. This means, for example, that the CEC mobilities of mefloquine are, despite a slightly higher electrophoretic mobility, much lower than that of its corresponding *O*-*tert*-butylcarbamate due to higher retention factors. On the other hand, the faster separation of pronethalol compared to mefloquine-*O*-*tert*-butylcarbamate can be easily explained by enhanced effective electrophoretic mobilities. Most importantly, the calculated values ($\mu^*_{CEC1,2,calc}$) agree reasonably well with the experimentally measured mobility values ($\mu^*_{CEC1,2}$) (see Table 1). In any case, the deviation between calculated and experimental values was always less than 2.9%. Such an agreement is good enough for a rough approximation of chromatographic and electrokinetic increments and its use for rationalizing their contribution to the overall CEC separation, and is again a strong indication for the absence of significant nonlinear electrokinetic effects under given experimental conditions. However, care must be taken upon transmission of the model to other conditions in particular eluents with low ionic strength and stationary phases with higher surface charge density as well as smaller pore sizes.

To elucidate under which conditions, *i.e.*, for which ionic strength range the framework of Eq. (2) is valid and practically applicable, the same model has been used to model migration in CEC as a function of the ionic strength. Thus, the concentration of the AB counterion was varied from 10 to 25 mM at a constant acid-to-base ratio of 2:1 and the μ^*_{eo}, $\mu_{ep,eff}$, and $k_{CLC1,2}$ as well as $\mu^*_{CEC1,2}$ were determined.

The results for μ^*_{eo}, $\mu_{ep,eff}$, and k_{CLC} as functions of the ionic strength are summarized in Table 2 along with the corresponding calculated and experimental CEC mobility data. Again there is a reasonable agreement between calculated and experimental μ^*_{CEC} values within the experimental error in the ionic strength range of about 10 mM and higher. The typical average error is 5% or less (note: corresponding calculations with apparent μ_{eo} and μ_{CEC} not considering the tortuosity of the flow channels gave always much larger errors, typically 10 – 30%). The

Table 1. Deconvolution of electrokinetic and chromatographic contributions to the separation of three test solutes by enantioselective cation-exchange CEC on a monolithic silica CSP in dependence on the applied electric field strength[a)]

Analyte	Field strength (V/cm)	$\mu_{ep,eff}$[b, c)]	μ^*_{eo}[b, c)]	k_{CLC1}[e, f)]	k_{CLC2}[e, f)]	μ^*_{CEC1}[b, g)]	$\mu^*_{CEC1,calc}$[b, h)]	μ^*_{CEC2}[b, g)]	$\mu^*_{CEC2,calc}$[b, h)]
		($\times 10^{-5}$ cm$^2 \cdot$ s$^{-1} \cdot$ V^{-1})					($\times 10^{-5}$ cm$^2 \cdot$ s$^{-1} \cdot$ V^{-1})		
Mefloquine	120 – 720[b)]	7.55 ± 0.08	26.7 ± 0.9	2.46 ± 0.03	3.02 ± 0.04	9.65 ± 0.37	9.88 ± 0.25	8.22 ± 0.28	8.51 ± 0.22
Mefloquine-*O*-*tert*-butyl-carbamate	120 – 720[b)]	7.22 ± 0.45	26.6 ± 1.0	1.45 ± 0.02	1.89 ± 0.02	14.2 ± 0.71	13.8 ± 0.24	11.8 ± 0.15	11.6 ± 0.57
Pronethalol	120 – 720[b)]	22.4 ± 0.55	26.9 ± 0.7	1.96 ± 0.02	2.28 ± 0.02	17.6 ± 0.39	17.2 ± 0.44	15.8 ± 0.30	15.5 ± 0.28

a) Experimental conditions: mobile phase, ACN/MeOH (80:20 v/v) containing 25 mM FA and 12.5 mM AB; electrokinetic injection at 10 kV/10 s; capillary temperature, 20°C; UV detection at 216 nm. Subscripts 1 and 2 indicate first and second eluted enantiomer.

b) Experiments carried out at six different field strengths between 120 and 720 V/cm. Given mobilities correspond to the statistical mean of these six experiments ± SD.

c) Effective electrophoretic mobilities of the solutes in achiral CE under identical experimental conditions.

d) Actual mobility of the EOF under CEC conditions, calculated by Eq. (3).

e) Retention factors (mean ± SD, $n = 3$) obtained in CLC under identical experimental conditions at a pressure of 12 bar ($\mu_{press} = 0.94$ mm/s).

f) $k = (t_R - t_0)/t_0$.

g) Experimental actual mobilities of the enantiomers under CEC conditions calculated according to Eq. (5).

h) Theoretical actual mobilities calculated from μ^*_{eo}, $\mu_{ep,eff}$, and k_{CLC} according to Eq. (2).

Table 2. Deconvolution of electrokinetic and chromatographic contributions to the separation of three test solutes by enantioselective cation-exchange CEC on a monolithic silica CSP in dependence on the ionic strength[a)]

Analyte	AB counter-ion concentration (mM)	$\mu_{ep,eff}$[b)]	μ^*_{eo}[c)]	k_{CLC1}[d)]	k_{CLC2}[d)]	μ^*_{CEC1}[e)]	$\mu^*_{CEC1,calc}$[f)]	μ^*_{CEC2}[e)]	$\mu^*_{CEC2,calc}$[f)]
		($\times 10^{-5}$ cm$^2 \cdot$ s$^{-1} \cdot$ V^{-1})					($\times 10^{-5}$ cm$^2 \cdot$ s$^{-1} \cdot$ V^{-1})		
Mefloquine	10	7.5	26.6	3.29	4.07	8.2	8.0	6.9	6.7
	15	5.9	24.3	1.85	2.27	10.7	10.6	9.3	9.2
	20	5.1	22.5	1.28	1.55	12.0	12.1	10.7	10.8
	25	4.3	20.4	0.93	1.09	12.5	12.8	11.4	11.8
Mefloquine-*O*-*tert*-butyl-carbamate	10	7.2	26.9	1.87	2.43	12.7	11.9	10.5	9.9
	15	6.3	24.3	1.13	1.48	14.5	14.3	12.3	12.3
	20	5.8	22.6	0.82	1.06	15.8	15.6	13.6	13.8
	25	5.3	21.0	0.61	0.77	16.4	16.3	14.4	14.8
Pronethalol	10	20.5	26.7	2.41	2.80	15.7	13.8	14.0	12.4
	15	18.3	23.9	1.45	1.68	18.5	17.2	17.0	15.7
	20	16.9	21.4	1.04	1.19	20.5	18.8	18.6	17.5
	25	15.4	19.9	0.78	0.89	20.6	19.9	19.9	18.7

a) Experimental conditions: mobile phase, ACN/MeOH (80:20 v/v) containing FA and AB in variable concentrations at a fixed molar ratio of 2:1; applied voltage, 8 kV; electrokinetic injection at 10 kV/10 s; capillary temperature, 20°C; UV detection at 216 nm. Subscript 1 and 2 indicate first and second eluted enantiomer.

b) Effective electrophoretic mobilities of the solutes in achiral CE under identical experimental conditions.

c) Actual mobilities of the EOF under CEC conditions, calculated by Eq. (3).

d) Retention factors obtained in CLC under identical experimental conditions at a pressure of 12 bar ($\mu_{press} = 0.94$ mm/s); $k = (t_R - t_0)/t_0$.

e) Experimental actual mobilities of the enantiomers under CEC conditions calculated according to Eq. (5).

f) Theoretical actual mobilities calculated from μ^*_{eo}, $\mu_{ep,eff}$, and k_{CLC} according to Eq. (2).

deviations in dependence on the electrical field strength at conditions as specified in Table 1 (data from Table 1) and in dependence on the ionic strength (data from Table 2) are depicted graphically in Figs. 7a and b, respectively. Figure 7a demonstrates the satisfactory agreement between modeled and experimental CEC mobility values (at an ionic strength >10 mM) for all three solutes over the entire investigated electrical field range. From Fig. 7b it can be seen that at ionic concentrations lower than 10 mM there is, in general, a tendency for a systematic deviation which could be due to increasing importance of CP and a gain of the relative contributions of nonlinear electrokinetic effects. Hence, under such conditions the present model should not be applied.

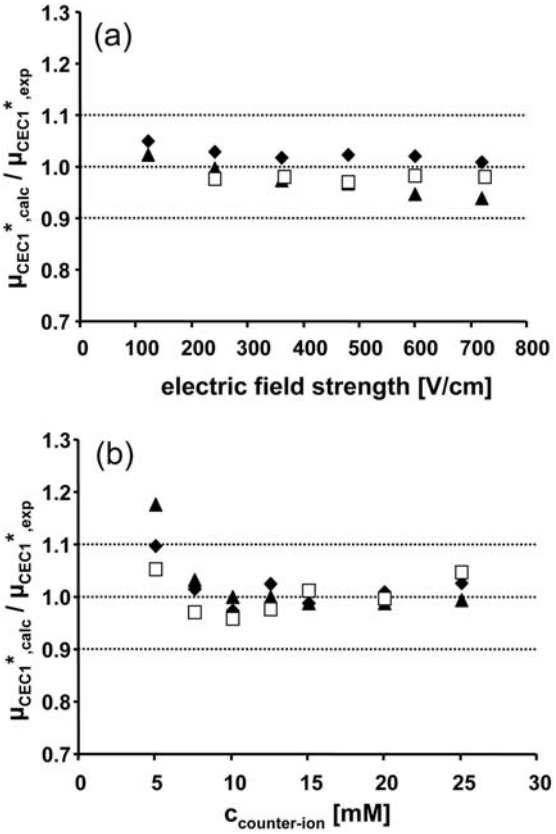

Figure 7. Comparison of experimental electrochromatographic mobilities $\mu^*_{CEC,exp}$ obtained in stereoselective CEC with theoretical values $\mu^*_{CEC,calc}$ of the first eluted enantiomers of mefloquine (♦), mefloquine-*O*-*tert*-butylcarbamate (▲), and pronethalol (□) in dependence on (a) the applied electric field strength and (b) the counterion concentration. Calculated by Eqs. (2) and (5), respectively, on the basis of actual mobilities. Experimental conditions: same as in Tables 1 (a) and 2 (b), respectively.

4.4 Practical implications

Knowledge of the individual contributions to CEC separations would certainly further the understanding of CEC separation processes. In view of this, it is worthwhile to deconvolute the increments as described above. Thereby, it may be sufficient, to perform solely the CE runs under identical conditions in addition to the CEC experiments, which minimizes the experimental workload and gives access to chromatographic retention factors even if for any reason no suitable CLC equipment is available. The chromatographic retention factors can then be straightforwardly obtained from the CEC and CE runs by rewriting Eq. (2) as follows

$$k_{CLC} = \frac{\mu^*_{eo} + \mu_{ep,eff}}{\mu_{CEC}} - 1 \qquad (11)$$

The knowledge of the individual migration contributions may also be valuable for the design of an adequate pressure-assisted CEC separation [50].

4.4.1 Advancement of the understanding of the separation mechanism in the course of mobile phase optimization

CEC separations are typically optimized by univariate strategies, varying one parameter while keeping the others constant and making phenomenological interpretations how to arrive at optimal conditions. The problem in CEC is that the complexity of the separation is not deconvoluted and the separation behavior in dependence on experimental variables thus becomes hardly predictable. Application of the above methodology in the course of optimization of enantiomer separations on current stereoselective ion-exchange CEC system, in contrast, would help to make optimization procedures in CEC more rational.

Herein, we adopted the methodology to have a closer look into the origin of nonlinearities of plots of log *k versus* log counterion concentration in CEC for some of the tested compounds (*e.g.*, pronethalol) while others adhered to linearity as predicted by the stoichiometric displacement model (Eq. 10) for ion-exchange chromatography systems (*e.g.*, mefloquine and its *tert*-butylcarbamate) (Fig. 8a).

The ionic strength of the BGE is a key parameter in ion-exchange CEC as it exerts strong influence on all individual separation processes, *i.e.*, EOF, electrophoretic migration of the solutes and ion-exchange processes as well. Figure 8b illustrates how the migration contributions develop as a function of the counterion concentration. According to the von Smoluchowsky equation, v_{eo} depends proportionally on the ζ-potential which in analogy to the Debye–Hückel theory [51] is a function of the EDL thickness δ and thus depends inversely proportional on the square root of the electrolyte concentration (Eq. 7). Indeed, the mobility and thus the linear velocity of the EOF v_{eo} in CEC decreased linearly with the square root of the ionic strength as theory predicts (Eq. 8) (Fig. 8b). While the flow in CEC is reduced with increase in electrolyte concentrations, this is of course not the case in CLC where the linear flow v_{press} remains constant because the influential factors, *i.e.*, applied pressure (here 4 bar), column permeability and length, and viscosity of the eluent do not change significantly with ionic strength (Fig. 8b). Figure 8b also shows that already an applied pressure of 4 bar allows to achieve a linear flow velocity comparable to the EOF that can be afforded at a high ionic strength (25 mM). Hence overall, with pressure driven flow a much faster separation may be accomplished even when the CE instrument with the external pressurization system is used as an HPLC system.

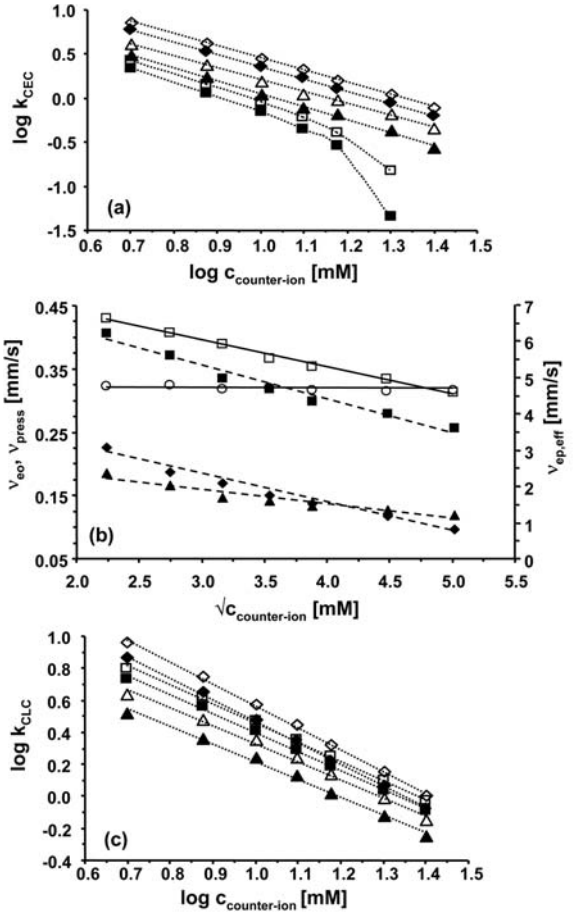

Figure 8. Effect of counterion concentration (AB concentration) on (a) CEC retention factors k_{CEC}, (b) EOF velocity in CEC, v_{eo} (open squares), linear flow velocities in CLC, v_{press} (open circles) (both left ordinate) as well as CE migration velocities $v_{ep,eff}$ of mefloquine (♦), its *t*-butylcarbamate (▲) and pronethalol (■) (right ordinate), and (c) on chromatographic retention factors k_{CLC}. Closed symbols in (a) and (c) stand for the first eluted enantiomer, open symbols for the second eluted enantiomer. Experimental conditions: mobile phase, ACN/MeOH (80:20 v/v) containing FA and AB at an acid-to-base ratio of 2:1. Electrokinetic injection at 10 kV for 10 s, capillary temperature, 20°C, UV detection at 216 nm. Applied electric field strength (CEC and CE), 240 V/cm (8 kV) and applied pressure (CLC), 4 bar.

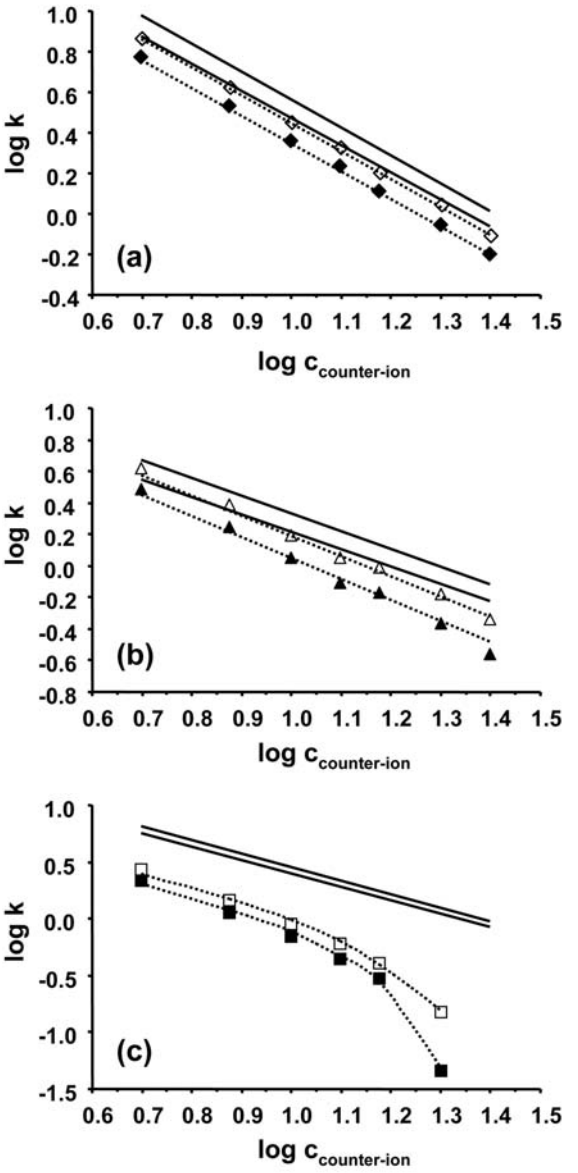

Figure 9. Retention factors *k* vs. counterion concentration. Experimental *k* values of CEC runs ($k_{CEC,exp}$) indicated by markers, k_{CEC} values as calculated by the individual increments marked by dotted lines ($k_{CEC,calc}$), and experimental chromatographic *k* values (k_{CLC}) denoted by solid line. Experimental conditions: see Fig. 8.

Effective electrophoretic mobilities, on the other hand, are strongly affected by the ionic strength as well and, in accordance with the theory of ion conductance in solution based on the Debye–Hückel–Onsager limiting law [45], dropped linearly with the square root of the ionic strength of the eluent (Fig. 8b). Mefloquine-*O*-*tert*-butylcarbamate, which has a lower mobility at infinite dilution and at low ionic strength conditions than the congeneric mefloquine, is less susceptible to the ionic strength effect as can be seen from a smaller Onsager slope. As a result, at high electrolyte concentrations it reaches higher electrophoretic mobilities than mefloquine.

The dependence of the chromatographic retention factors on mobile phase ionic strength is depicted in Fig. 8c. Typical behavior for ion-exchange systems is observed for all tested solutes with a linear drop of log *k* with log counterion concentration. The overall consequence is that the CEC separation process becomes faster at higher ionic strength conditions despite reduced EOF velocities

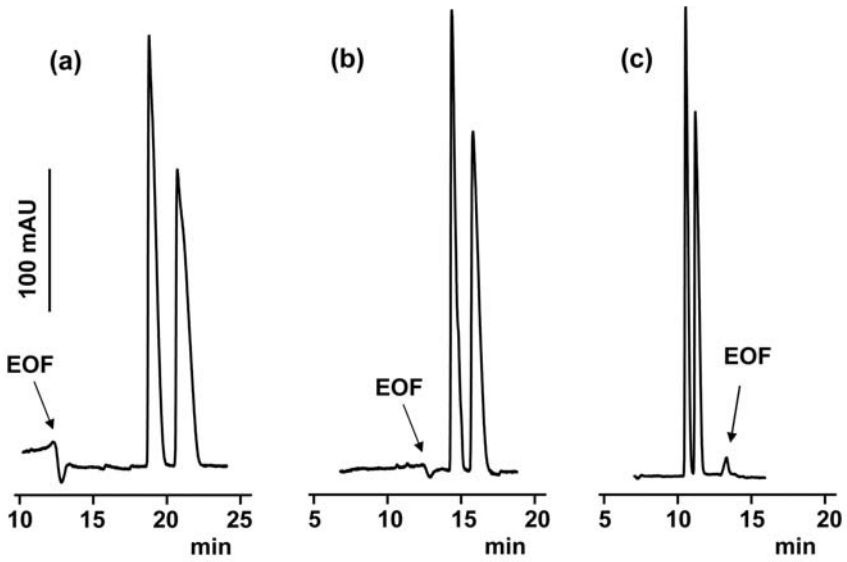

Figure 10. CEC separations of (a) mefloquine, (b) mefloquine-*O-tert*-butylcarbamate, and (c) pronethalol on a nonoptimized prototype of the SCX-type monolith column of Fig. 1. Experimental conditions (identical to those of Fig. 4): mobile phase, ACN/MeOH (80:20 v/v) containing 25 mM FA and 12.5 mM AB. Applied voltage: 20 kV (filed strength 580 V/cm). Electrokinetic injection at 10 kV for 10 s, capillary temperature, 20°C, UV detection at 216 nm.

and decelerated electrophoretic solute migration because the ion-exchange process is dominating and its reduced actual ion-exchange capacity at elevated ion concentrations more than compensates for the weakened mobility contributions.

Figure 9 illustrates the dependence of experimental k values from CEC runs ($k_{CEC,exp}$), of k_{CEC} values as calculated from individual increments ($k_{CEC,calc}$), and experimental chromatographic k values (k_{CLC}) on counterion concentration. From this representation of the data, the relative importance of electrophoretic migration to the CEC separation of the three model compounds, which appears to be different for the three test solutes, becomes readily visible. In case of mefloquine, the relative influence of electrophoretic migration is comparably low with an almost constant contribution over the investigated electrolyte concentration range which slightly reduces the k_{CEC} values as compared to k_{CLC}. Hence, due to dominance of the ion-exchange process, it is no surprise that the ionic strength dependence in CEC resembles that of CLC. The relative importance of electrophoretic migration is only marginally larger for mefloquine-*O-tert*-butylcarbamate, mainly because this derivative shows a reduced retention factor as compared to the parent mefloquine. A slight gain of the relative influence of the electrophoretic migration contribution at elevated ionic strength conditions is noticed, again because of the greatly reduced retention factors at such conditions. For pronethalol the situation changes; the electrophoretic mobility makes a significant contribution to k_{CEC} values and at high ionic strength conditions it becomes more dominating. In other words, the separation process turns to a more electrophoretically driven separation rather than a chromatographically driven one which is also reflected by the nonlinearities of the log k_{CEC} *versus* log counterion concentration plots.

In any case, the k_{CEC} values could be correctly predicted from the individual increments (k_{CLC}, μ^*_{eo}, $\mu_{ep,eff}$) as evident in Fig. 9 from overlap of the experimental k_{CEC} values (denoted by markers) with the calculated ones which are indicated by the dotted lines. In conclusion, the nonlinearities for pronethalol can be readily explained on the basis of the individual migration contributions and are not a result of secondary effects such as altered retention factors or EOF of the second kind originating from the influence of electric field.

4.4.2 Column development

The deciphering of the individual separation increments was also very valuable in the course of the development of the given SCX monolith columns and the optimization of the surface chemistry, in particular of the SO coverage. The separations of the test solutes (Fig. 2) obtained by a prototype SCX monolith that was prepared by a nonoptimized synthetic protocol are shown in Fig. 10. It is clearly evident that this first column fabrication attempt did not afford the optimal column both in terms of enantioselectivities and efficiencies. Comparing these separations with the ones on the optimized column of Fig. 4, it is eye-catching that the retentions are much lower. At the beginning of the study, with only the CEC runs in hand, it was, however, uncertain whether the low retention times in CEC were a result of low chromatographic retention factors or high electrophoretic mobilities. The determination of the individual increments has rapidly shed light on this issue.

The EOF (actual electroosmotic mobility μ^*_{eo}) was relatively weak reaching a value of about $8.91 \times 10^{-5}\,cm^2 \cdot$

Table 3. Determination of chromatographic enantioselectivity values from CEC and CE experiments[a)]

Analyte	Field strength (V/cm)	k_{CLC1}[c)]	$k_{CLC1,calc}$[b, d)]	k_{CLC2}[c)]	$k_{CLC2,calc}$[b, d)]	α_{CLC}[e, f)]	$\alpha^*_{CLC,calc}$[b, e, g)]
Mefloquine	120 – 720[b)]	2.46 ± 0.03	2.55 ± 0.05	3.02 ± 0.04	3.10 ± 0.08	1.23 ± 0.00	1.22 ± 0.01
Mefloquine-*O*-*tert*-butyl-carbamate	120 – 720[b)]	1.45 ± 0.02	1.39 ± 0.08	1.89 ± 0.02	1.81 ± 0.13	1.31 ± 0.01	1.32 ± 0.02
Pronethalol	120 – 720[b)]	1.96 ± 0.02	1.89 ± 0.05	2.28 ± 0.02	2.22 ± 0.01	1.16 ± 0.00	1.17 ± 0.01

a) Experimental conditions: mobile phase, ACN/MeOH (80:20 v/v) containing 25 mM FA and 12.5 mM AB; electrokinetic injection at 10 kV/10 s; capillary temperature, 20°C; UV detection at 216 nm. Subscripts 1 and 2 indicate first and second eluted enantiomer.

b) Theoretical k_{CLC} and α_{CLC} values are given as statistical mean (±SD) of six values derived from CE and CEC experiments which were carried out at six different field strengths between 120 and 720 V/cm.

c) Retention factors (mean ± SD, $n = 3$) obtained in CLC under identical experimental conditions at a pressure of 12 bar ($v_{press} = 0.94$ mm/s).

d) Theoretical values calculated by Eq. (11) from corresponding actual mobilities μ^*_{eo}, μ^*_{CEC}, and $\mu_{ep,eff}$, as given in Table 1.

e) $\alpha = k_2/k_1$.

f) As calculated from experimental k_{CLC} values (mean ± SD, $n = 3$).

g) As calculated from theoretical $k_{CLC,calc}$ values.

$V^{-1} \cdot s^{-1}$ only. Since the BGE and other conditions were identical as in Table 1, the effective electrophoretic mobilities were the same as specified in Table 1 (7.55, 7.22, and 22.4×10^{-5} $cm^2 \cdot V^{-1} \cdot s^{-1}$ for mefloquine, its *tert*-butylcarbamate and pronethalol, respectively). The chromatographic retention factors as calculated by Eq. (11) were thus 1.05 and 1.27 (for mefloquine), 0.60 and 0.75 (for mefloquine-*O*-*tert*-butylcarbamate), and 0.80 and 0.90 (for pronethalol) for first and second eluted enantiomers, respectively. Comparison of these retention factors to those obtained on the optimized column (see Table 1) shows that they are about 50% lower than the k_{CLC} values on the optimized column.

Hence, it became obvious that the main culprit for the worse separations with the nonoptimized prototype column was a low SO coverage. The low EOF strength lends additional support to this conclusion. The lower enantioselectivities may be the result of excessive nonenantioselective adsorption sites that were not covered with SO and negatively contributed to the overall separation that originates from the enantioselective sites at the SCX SO. The conclusion of these findings have paved the way for a dedicated optimization of the SO coverage [34] which finally yielded the optimal column described above with its remarkable enantioselectivities and efficiencies.

4.4.3 Screening of new CSPs

In our laboratory, we employ CEC as a miniaturized separation technology to test and evaluate new SOs and CSPs to be finally used for conventional HPLC enantiomer separation. Thereby, we used the above-described methodology for the determination of chromatographic retention factors and enantioselectivities from CEC experiments making use of Eq. (11). The basis for the validity and thus applicability of this procedure is that secondary effects which may alter chromatographic enantiorecognition are absent in the CEC runs (which was proven to be the case for the above specified range of experimental conditions). Moreover, it would not make much sense if there is not an agreement between α values calculated from the k values by means of Eq. (11) and experimentally determined chromatographic α values. This agreement is demonstrated in Table 3.

By calculation of the retention factors $k_{CLC,calc}$ from CEC and CE runs using μ^*_{eo}, μ^*_{CEC}, and $\mu_{ep,eff}$ given in Table 1 according to Eq. (11), corresponding chromatographic enantioselectivities $\alpha^*_{CLC,calc}$ of 1.22, 1.32, and 1.17 could be determined for mefloquine, mefloquine-*O*-*tert*-butylcarbamate, and pronethalol, respectively. The corresponding experimental α values from independent CLC experiments under comparable conditions of 1.23, 1.31, and 1.16 were a close match to the predictions from the individual increments, confirming the validity of the approach. The methodology is even applicable if the solutes elute before the EOF marker. Due to the reasonable agreement of $\alpha_{CLC,calc}$ derived from CEC experiments (with known electrophoretic mobility under the same BGE conditions) and experimental α_{CLC}, this methodology provides the basis for the estimation of chromatographic enantioselectivities in an extended microscale screening of novel chiral SOs by CEC.

5 Concluding remarks

In the present paper, we studied the behavior of a monolithic silica-based CSP functionalized with a SCX, *trans*-(1*S*,2*S*)-2-(*N*-4-allyloxy-3,5-dichlorobenzoyl)aminocyclohexanesulfonic acid, under electrically driven CEC and

pressure-driven CLC conditions for the enantioselective separation of basic test solutes. Upon variation of the applied electric field strength (in the range of 120 – 720 V/cm) and the pressure (2 – 12 bar), respectively, as well as the ionic strength in the mobile phase (concentration of the amine counterion between 5 and 25 mM, always at two-fold acid coion concentration), the contributions of electrokinetic and chromatographic processes were investigated. As under the herein tested experimental conditions the observed EOF changed straight proportionally with the electric field strength and retention factors of the counterionic solutes were independent of the electric field strength it could be concluded that nonlinear electrokinetic effects are negligible. The latter would arise in case of significant EDL overlap inside the mesopores of the monolithic material which leads to CP phenomena when a high voltage drop is applied to the capillary column due to the formation of charge-selective, *i.e.*, ion-permselective regions in the stationary phase. Such an electrokinetic phenomenon would affect not only the EOF but to a certain extent also the CEC retention factors of charged solutes. This opened up the possibility to model CEC migrations by a straightforward framework which is based on the simple combination of individual migration contributions (k_{CLC}, μ_{eo}^{*}, $\mu_{ep,eff}$). Reasonable agreement between CEC mobilities calculated from the individual increments and experimentally determined ones could be found with typical deviations of less than 5%. The deconvolution of the CEC separation contributions and determination of individual CEC migration/retention increments, respectively, has the power to shed light onto the complex dependencies in the course of the optimization of CEC separations. Moreover, it provides a framework building the basis for the promising approach of using CEC as a microscale tool in the screening of novel chromatographic chiral SOs and CSPs enabling a first assessment of their chromatographic enantioselectivities with only little material requirements.

The financial support by the Austrian Christian Doppler Research Society and the industry partners AstraZeneca (Mölndal, Sweden) and Merck KGaA (Darmstadt, Germany) is gratefully acknowledged.

The authors declared no conflict of interest.

6 References

[1] Deyl, Z., Svec, F. (Eds.), *Capillary Electrochromatography*, *J. Chromatogr. Libr., Vol. 62*, Elsevier, Amsterdam 2001.

[2] Breadmore, M. C., Hilder, E. F., Macka, M., Avdalovic, N., Haddad, P. R., *Electrophoresis* 2001, *22*, 503 – 510.

[3] Choudhary, G., Horvath, C., *J. Chromatogr. A* 1997, *781*, 161 – 183.

[4] Dittmann, M. M., Masuch, K., Rozing, G. P., *J. Chromatogr. A* 2000, *887*, 209 – 221.

[5] Henry, M. P., Ratnayake, C. K., *J. Chromatogr. A* 2005, *1079*, 69 – 76.

[6] Rathore, A. S., Horvath, C., *J. Chromatogr. A* 1996, *743*, 231 – 246.

[7] Rathore, A. S., Horvath, C., *J. Chromatogr. A* 1997, *781*, 185 – 195.

[8] Rathore, A. S., Horvath, C., *Anal. Chem.* 1998, *70*, 3069 – 3077.

[9] Rathore, A. S., Wen, E., Horvath, C., *Anal. Chem.* 1999, *71*, 2633 – 2641.

[10] Rathore, A. S., Horvath, C., *Electrophoresis* 2002, *23*, 1211 – 1216.

[11] Rathore, A. S., *Electrophoresis* 2002, *23*, 3827 – 3846.

[12] Rathore, A. S., McKeown, A. P., Euerby, M. R., *J. Chromatogr. A* 2003, *1010*, 105 – 111.

[13] Rathore, A. S., Li, Y., Wilkins, J., *J. Chromatogr. A* 2005, *1079*, 299 – 306.

[14] Stahlberg, J., *J. Chromatogr. A* 2000, *887*, 187 – 198.

[15] Stol, R., Poppe, H., Kok, W. T., *J. Chromatogr. A* 2000, *887*, 199 – 208.

[16] Vallano, P. T., Remcho, V. T., *Anal. Chem.* 2000, *72*, 4255 – 4265.

[17] Wen, E., Asiaie, R., Horvath, C., *J. Chromatogr. A* 1999, *855*, 349 – 366.

[18] Xiang, R., Horvath, C., *Anal. Chem.* 2002, *74*, 762 – 770.

[19] Wan, Q.-H., *J. Phys. Chem. B* 1997, *101*, 8449 – 8453.

[20] Walhagen, K., Huber, M. I., Hennessy, T. P., Hearn, M. T. W., *Biopolymers (Peptide Science)* 2003, *71*, 429 – 453.

[21] Eimer, T., Unger, K. K., van der Greef, J., *Trend Anal. Chem.* 1996, *15*, 463 – 468.

[22] Liu, Z., Otsuka, K., Terabe, S., *J. Chromatogr. A* 2002, *959*, 241 – 253.

[23] Deng, Y., Zhang, J., Tsuda, T., Yu, P. H., Boulton, A. A., Cassidy, R. M., *Anal. Chem.* 1998, *70*, 4586 – 4593.

[24] Yao, C., Tang, S., Gao, R., Jiang, C., Yan, C., *J. Sep. Sci.* 2004, *27*, 1109 – 1114.

[25] Nischang, I., Tallarek, U., *Electrophoresis* 2004, *25*, 2935 – 2945.

[26] Tallarek, U., Leinweber, F. C., Nischang, I., *Electrophoresis* 2005, *26*, 391 – 404.

[27] Leinweber, F. C., Pfafferodt, M., Seidel-Morgenstern, A., Tallarek, U., *Anal. Chem.* 2005, *77*, 5839 – 5850.

[28] Nischang, I., Chen, G., Tallarek, U., *J. Chromatogr. A* 2006, *1109*, 32 – 50.

[29] Nischang, I., Reichl, U., Seidel-Morgenstern, A., Tallarek, U., *Langmuir* 2007, *23*, 9271 – 9281.

[30] Tobler, E., Lämmerhofer, M., Wuggenig, F., Hammerschmidt, F., Lindner, W., *Electrophoresis* 2002, *23*, 462 – 476.

[31] Zarbl, E., Lämmerhofer, M., Woschek, A., Hammerschmidt, F., Parenti, C., Cannazza, G., Lindner, W., *J. Sep. Sci.* 2002, *25*, 1269 – 1283.

[32] Hebenstreit, D., Bicker, W., Lämmerhofer, M., Lindner, W., *Electrophoresis* 2004, *25*, 277 – 289.

[33] Preinerstorfer, B., Lubda, D., Lindner, W., Lämmerhofer, M., *J. Chromatogr. A* 2006, *1106*, 94 – 105.

[34] Preinerstorfer, B., Hoffmann, C. V., Lubda, D., Lämmerhofer, M., Lindner, W., *Electrophoresis* 2007, in press.

[35] Rathore, A. S., Horvath, C., in: Deyl, Z., Svec, F. (Eds.), *Capillary Electrochromatography*, *J. Chromatogr. Libr., Vol. 62*, Elsevier, Amsterdam 2001, pp. 1 – 38.

[36] Knox, J. H., *J. Chromatogr. A* 1994, *680*, 3 – 13.

[37] Rice, C. L., Whitehead, R., *J. Phys. Chem.* 1965, *69*, 4017 – 4024.

[38] Wan, Q.-H., *J. Chromatogr. A* 1997, *782*, 181 – 189.

[39] Wan, Q.-H., *Anal. Chem.* 1997, *69*, 361 – 363.

[40] Cikalo, M. G., Bartle, K. D., Myers, P., *J. Chromatogr. A* 1999, *836*, 35 – 51.

[41] Poppe, H., Stol, R., Kok, W. T., *J. Chromatogr. A* 2002, *965*, 75 – 82.

[42] Rifai, R. A., Demesmay, C., Cretier, G., Rocca, J. L., *Chromatographia* 2001, *53*, 691 – 696.

[43] Stol, R., Kok, W. T., in: Rathore, A. S., Guttman, A. (Eds.), *Electrokinetic Phenomena*, Marcel Dekker, New York, NY 2004, pp. 189 – 209.

[44] Tallarek, U., Paces, M., Rapp, E., *Electrophoresis* 2003, *24*, 4241 – 4253.

[45] Jouyban, A., Kenndler, E., *Electrophoresis* 2006, *27*, 992 – 1005.

[46] Stahlberg, J., *J. Chromatogr. A* 1999, *855*, 3 – 55.

[47] Okada, T., *Anal. Chem.* 1998, *70*, 1692 – 1700.

[48] Hoffmann, C. V., Lämmerhofer, M., Lindner, W., *J. Chromatogr. A* 2007, *1161*, 242 – 251.

[49] Nischang, I., Spannmann, K., Tallarek, U., *Anal. Chem.* 2006, *78*, 3601 – 3608.

[50] Eimer, T., Unger, K. K., Tsuda, T., *Fresenius' J. Anal. Chem.* 1995, *352*, 649 – 653.

[51] Schwer, C., Kenndler, E., *Anal. Chem.* 1991, *63*, 1801 – 1807.

Appendix #4

Manuscript Draft M-I

Separation of *Cinchona* Alkaloids on a novel Strong Cation Exchange type Chiral Stationary Phase – Comparison with commercially available Strong Cation Exchanger and Reversed-Phase Packing Materials

Christian V. Hoffmann, Michael Lämmerhofer, Wolfgang Lindner*

University of Vienna, Christian Doppler Laboratory for Molecular Recognition Materials, Department of Analytical Chemistry & Food Chemistry, Währinger Strasse 38, A-1090 Vienna, Austria

*corresponding author

e-mail: wolfgang.lindner@univie.ac.at

Tel: ++43-1-4277-52300

Fax: ++43-1-4277-9523

Abstract

A recently reported chiral strong cation exchanger (cSCX) type stationary phase was investigated for the LC separation of a series of *Cinchona* alkaloids and synthetic derivatives thereof to test its usefulness as alternative methodology for the separation of those important pharmaceuticals. The cSCX column packing material was qualitatively compared on the one hand against a commercially available nonenantioselective SCX-material, PolySULFOETHYL-A, and on the other hand against a modern C18 reversed-phase stationary phase which is commonly employed for *Cinchona* alkaloid analysis. Both SCX columns showed no pronounced peak tailing phenomena which typically hamper their RP analysis and require specific optimization. Thus, the cSCX-based assay provided

new feasibilities for the separation of the *Cinchona* alkaloids in polar organic mode as opposed to conventional reversed-phase methodologies. In particular, a method for the simultaneous determination of eight *Cinchona* alkaloids (quinine, quinidine, cinchonine, cinchonidine, and their corresponding dihydro analogs) using the cSCX column in HPLC has been developed and exemplarily applied to impurity profiling of a commercial alkaloid sample. Furthermore, both SCX materials allowed successful separation of C9-epi and 10,11-didehydro derivatives from their respective educts in an application in synthetic *Cinchona* alkaloid chemistry.

Keywords

Column liquid chromatography, *Cinchona* alkaloid, Reversed-phase, cation exchanger, packing materials, quinine, quinidine, cinchonine, cinchonidine, epiquinine, epiquinidine.

1 Introduction

Cinchona alkaloid bases and their derivatives play a variety of important roles ranging from use as pharmaceuticals like quinine and quinidine to serving as functional molecules in chemical technology as co-catalysts,[1] organocatalysts,[2-4] and selectors (SOs) of chiral stationary phases (CSPs).[5, 6] Hence, robust and simple chromatographic methodology for the purpose of their quantitative analysis, identification, purity control, and reaction monitoring of the preparations of latter *Cinchona* alkaloid derivatives as well as their preparative chromatographic purification is crucial. The use of reversed-phase (RP) liquid chromatographic assays for the determination of quinine and quinidine are not only recommended by pharmaceutical guidelines but are also generally reported as the prime technique for *Cinchona* alkaloid analysis in the literature,[7-9] also for synthetic

derivatives.[10] RP analysis of these strongly basic compounds potentially bears, however, the risk for severe peak tailing and excessive band broadening due to secondary cation exchange (CX)-type interactions with residual acidic silanol groups of unmodified patches on the silica-support surface which always remain as isles between the patches of lipid layer originating from derivatized silanols with alkyl strands. These interactions are superimposed upon the primarily intended hydrophobic interaction-related partitioning processes in RP analysis. Significant efforts have been made to reduce this phenomenon for basic species in general, both by mobile phase strategies [11-16] employing analysis at alkaline pH, the use of ion-pairing systems or amine-type additives, and by optimizing the surface chemistry to minimize the number of residual silanol groups, i.e. by end-capping concepts. Alternative interaction/separation principles like mixed-mode stationary phases as well as non-silica based solid supports have also been applied.[17] In the attempt to overcome this severe limitation of RP-materials, we elucidated the potential of a chiral SCX stationary phase fort the analysis of *Cinchona* alkaloid mixtures as alternative column packing material.

The sulfonic acid-based SCX-type CSP (cSCX) (Figure 1) was developed as a favourable representative of a series of CSPs based on low molecular mass chiral carboxylate-, phosphonate-, and sulfonate-containing SOs for the enantiomer separation of chiral basic compounds mainly driven by a cation-exchange process.[18] These packing materials were typically operated in mild, often MS-compatible polar organic eluents using isocratic elution and turned out to be very useful also for challenging non-enantioselective analytical separation problems of basic compounds. The investigated analyte set comprises the four major natural *Cinchona* alkaloids (quinine, quinidine, cinchonine, cinchonidine) as well as their dihydro derivatives, and in addition, four synthetic derivatives viz. C9-epi and 10,11-didehydro derivatives that are typically prepared directly from the natural congeners [1,19-21] (Scheme 1). These relevant natural and synthetic *Cinchona* species show only minor

structural or stereochemical differences and thus require stationary phases that not only provide appropriate peak performance but also high selectivity. Quinine and quindine as well as their corresponding derivatives are diastereomers (identical configurations in position 1,3,4 but opposite configurations at carbon 8 and 9). The same is valid for the cinchonine and cinchonidine series which lack the methoxy substituent of the quinoline ring. Thus, they can be separated by RP-HPLC. However, we believe that a chiral stationary phase such as the cSCX might be an interesting alternative for this application. To document this the performance of the cSCX column was compared with commercially available RP- and SCX packing materials. The latter was a PolySulfoethyl A which is based on poly(2-sulfoethylaspartamide) and has, in sharp contrast to the cSCX, non-enantioselective character owing to the racemic nature of the ligand. Furthermore, the applicability of the cSCX stationary phase was assessed for the separation of natural and synthetic alkaloid mixtures and for determination of low abundant impurities in commercial alkaloid samples.

<Figure 1: chemical structure of the cSCX stationary phase>

<Scheme 1: overview of the *Cinchona* alkaloids and derivatives>

2 Experimental

2.1 Materials

All stationary phases investigated herein were based on silica of 5 μm particle size. A Zorbax Eclipse XDB-C18 column was purchased from Agilent Technologies (Waldbronn,

Germany), was of 150 x 4.6 mm I.D. dimensions and based on silica with pore size of 80 Å. Racemic strong cation exchanger PolySulfoethyl-A (PSE-A) was obtained from PolyLC Inc. (Columbia, MD, USA), was of 150 x 4.6 mm I.D. dimensions and based on silica with pore size of 300 Å. The cSCX column (Figure 1) was prepared in house according to a published procedure[18] and had a loading of 229 μmol SO per gram CSP as was calculated from the nitrogen content of the modified silica (120 Å pore size) obtained by elemental analysis. It was slurry-packed into a stainless-steel column of the dimension 150 x 4 mm I.D. at VDS Optilab (Berlin, Germany). MeOH and acetonitrile (ACN) as organic solvents for HPLC were of HPLC-grade from Merck (Darmstadt, Germany) while water was purified by double distillation. Mobile phase additives acetic acid (HOAc), formic acid (FA), triflouroacetic acid (TFA), diethylamine (DEA), diemethylamine (DMA), triethylamine (TEA), tris(2-hydroxyethyl)amine, 2-amino-1-butanol, and ammonium acetate (NH_4OAc) were of analytical grade (Sigma-Aldrich). Commercially available *Cinchona* alkaloids quinine, quinidine, and 10,11-Dihydroquinine were from Buchler (Braunschweig, Germany) while 10,11-Dihydroquinidine, Cinchonine, and Cinchonidine were from Sigma-Aldrich (Vienna, Austria). 10,11-Dihydro analogues of Cinchonine and Cinchonidine were specified impurities of some of the before listed commercial alkaloids. 10,11-Didehydroquinine and –quinidine as well as C9-Epiquinine and C9-Epiquinidine were synthesized according to literature procedures.[10, 21]

2.2 HPLC Instrumentation and Chromatography.

Chromatographic measurements were performed on a 1100 Series HPLC system from Agilent Technologies (Waldbronn, Germany) consisting of a solvent degasser, a pump, an autosampler, a column thermostat and a multi-wavelength UV-Vis detector for detection at selected wavelengths between 230 and 280 nm. Data acquisition and analysis was carried

out with ChemStation chromatographic data software from Agilent Technologies. For the data presented herein, all separations were performed in isocratic mode at a mobile phase flow rate of 1.0 ml/min. The RP column was operated using an ACN-water mixture containing 0.1% (v/v) FA. For the ion exchanger stationary phases PSE-A and cSCX, polar organic mobile phases consisting of MeOH and/or ACN and acidic and basic additives were applied.[18, 22] The void volumes of the columns were determined by injecting a solution of acetone in MeOH with detection at 280 nm for the SCX columns and an aqueous solution of uracil for the RP column. Column temperature was 25° C. Sample concentrations were typically of 0.5 to 1.0 mg/ml with injection volumes between 1-10 µl if not otherwise stated.

3 Results and Discussion

3.1 Role of the packing material

Separation and analysis of *Cinchona* alkaloids has significant importance.[7] Like in various pharmacopeias, RP-HPLC is commonly employed for this purpose. Unfortunately, not seldom peaks tend to tail what is seen for other strong bases as well. Such strong peak tailing may have different origin. First, RP phases like any other bonded silica adsorbent has a heterogeneous surface with at least two distinct adsorption sites: hydrophobic interaction sites of the alkyl-ligands characterized by a fast adsorption-desorption kinetics and cation exchange sites stemming from residual silanols with usually slow kinetics. The resultant heterogeneous mass transfer kinetics for basic compounds may be source for significant peak tailing even under linear conditions i.e. with low sample masses under non-overload conditions.[23] This problem is hard to be overcome since virtually all common type-B RP-phases possess residual silanols (usually in relatively low density) and

therefore are principally susceptible for this effect. Mobile phase conditions that reduce silanol activity (e.g. addition of 0.1% TFA or FA for suppression of silanol dissociation) or adequate balance of the cation exchange process (through addition of bases to the eluent) may, at least partly, help to improve peak shape.

Peak tailing may also result from heterogeneous thermodynamics with overloading of one type of sites, i.e. the low density sites which are here the residual silanols and cation-exchange sites, respectively.[24] Such effects were also thoroughly studied experimentally by McCalley for a set of various bases on several RP-phases.[25, 26] It was found that peak shape (plate numbers and symmetry) deteriorated dramatically when the injected sample mass was increased above 0.5 µg (for a 250 x 0.46 mm ID column). Hence, one must take care not to overload the column. However, this is usually impossible if low quantities of impurities (e.g. < 0.1%) must be analyzed in pharmaceuticals such as *Cinchona* alkaloids (*vide infra*). Last but not least, most complex is the situation in which the two sources for peak tailing combine.[24]

In this paper, we test an alternative separation material namely an cSCX phase for its potential to overcome the problem of peak tailing. The cSCX itself retains basic solutes by virtue of a primary ion-exchange mechanism and has surface heterogeneity as well. However, the SCX sites are present in reasonable quantities (~ 0.76 µmol/m^2) and are supposed to be well accessible on the surface ending up in a reasonably high actual surface density. Since ion-exchange has exceptional loading capacity, overloading phenomena are observed only at much larger mass loads as compared to overloading of secondary cation-exchange sites of RP-materials. Moreover, hydrophobic interactions are effectively disrupted by the nonaqueous polar organic mobile phase conditions (i.e. with methanolic eluents) presumably leading eventually to more homogeneous mass transfer.

Furthermore, the cSCX may overcome another limitation. RP phases often reveal a lower diastereoselectivity (i.e. selectivity between diastereomers which are made up of identical

molecular lipophilicity increments) than chiral stationary phases (note the diastereomeric relationship of the congeners in left and right hand columns of Scheme 1). The hopefully enhanced diastereoselectivity of the cSCX could help in the analysis of complex samples and in purity determinations (which are under quest of overload conditions) as well. To illustrate the effect we compared the separations of six alkaloids Dh-QN, Dh-QD, QN, QD, Di-QN, and Di-QD, which differ in stereochemistry, basicity, and hydrophobicity, on cSCX with a typical RP separation employing a Zorbax Eclipse XDB-C18 column and a typical eluent (0.1% FA in ACN-water mixture) as well as the non-enantioselective SCX PSE-A (Fig. 2). The chromatographic parameters are summarized in Table 1.

<Figure 2: chromatographic comparison RP, PSE-A, cSCX>

<Table 1: data of chromatographic comparison RP, PSE-A, cSCX>

Similar elution orders were observed on all three columns regarding the degree of saturation of the group in 3-position according to the principal lipophilicity (increase from alkyne over alkene to alkane) and/or basicity of quinuclidine amine of the analytes (pK_b values of 9.9 for the dihydro-, 9.3 for vinyl, and 8.4 for the didehydro species were calculated using ACD/pKa DB 7.0 software from ACDLabs, Advanced Chemistry Development, Ontario, Canada). For example, in RP mode the more hydrophobic dihydro compounds eluted after the alkaloids with the vinyl group i.e. a double bond, thereby confirming the elution order typically reported for RP separations and the high separation power of RP for the degree of saturation.[7] Similarly, the stronger basic dihydro species were retained longer in CX mode. However, a switch in elution order among the pairs of diastereomers is noticed in the cation-exchange mode as compared to the RP mode (where the Quinidines eluted before the Quinines which obviously adopt an overall conformation

with a larger accessible hydrophobic surface area as compared to the diastereomeric Quinidines).

As speculated, the highest diastereoselectivities of all phases were indeed found for the cSCX CSP (see Table 1). This effect is certainly related to specific molecular recognition phenomena and the adequate binding site geometry and functionality of the cSCX for the *Cinchona* alkaloids rather than a simple non-specific cation-exchange process because the non-enantioselective SCX of the PSE-A yielded the lowest diastereoselectivities of all tested phases.

The separations obtained with the RP material suffered from pronounced peak tailing under the given elution conditions in accordance to the theory and reports presented above. In sharp contrast, both of the tested strong cation exchangers with sulfonic acid ion-exchange site did not at all experience such strong peak tailing phenomena. Overall best peak efficiencies were available on cSCX. Most remarkable is, however, that on both SCX phases peak symmetry is close to perfect of a Gaussian peak shape, at least in comparison to the RP separation. Obviously, heterogeneous mass transfer kinetics could be successfully dampened on the SCX phases. Hence, it may be concluded that both cation exchangers – and in particular the cSCX phase – conceptually represent useful complementary and alternative separation materials to the conventional RP approach in the analysis of basic compounds like *Cinchona* alkaloids.

3.2 Applications

3.2.1 Reaction monitoring of synthetic *Cinchona* alkaloid derivatives

TLC and flash chromatography using bare silica are typically used for purity control and purification purposes of synthetic *Cinchona* derivatives. Appropriate HPLC analysis methodologies, however, could allow detailed reaction monitoring including

quantification, ideally in conjunction with MS-detection. Already the above presented column comparison included such an exemplary case with the 10,11-Didehydro derivatives being important building blocks that are accessible via direct conversion of either QN or QD.[10, 20] In another example for synthetic modifications of *Cinchona* alkaloids that lead to minor structural changes only, both SCX packing materials were applied for the analysis of the C9-epimerization of QN and QD, one more common synthetic modification in *Cinchona* alkaloid chemistry that leads to eQN and eQD, respectively.[21]

Again, both cation exchangers provided enough selectivity for baseline separation of the diastereomers (in the present case of epimers), an important aspect when it comes to purity determination and identification (Figure 3). Other than before with Di-QN and Di-QD, no consistent elution behavior between PSE-A and cSCX columns for the epimerization species were observed although both packing materials are strong cation exchangers with similar sites for the ion exchange process, i.e. β-amidosulfonic acid scaffolds, and almost identical mobile phases (12.5 and 25mM NH_4OAc in MeOH) have been applied. Obviously, the strength of interaction between stationary phases and analytes and thus, retention, seems not only to depend on analyte basicity. Besides the prevailing ion pairing particular additional specific interactions – H-bonding, π-π-interactions etc. – are likely to take place that are expected to be different between PSE-A and cSCX stationary phases due to their overall distinct chemical ligand structures.

<Figure 3: HPLC analysis of epi-derivatives on cSCX and PSE-A>

3.2.2 Quality control of natural *Cinchona* alkaloids

3.2.2.1 Method development

Despite their extensive use as functional entities in different fields of chemistry the main applications of *Cinchona* alkaloids still are for pharmaceutical purposes, supplied by their

isolation from its natural source, *Cinchona* bark. Therefore, also the main chromatographic challenge in this context remains the analysis of the naturally found *Cinchona* alkaloids. There are about 35 bases ascribed to this class of natural products but typically the focus is on the four principal alkaloids (CN, CD, QN, QD) and their dihydro derivatives.[7] Since raw products may be accompanied by a variety of other alkaloids (esp. QN/QD by their corresponding 6'-demethoxy and 10,11-dihydro congeners), assay specificity is usually the critical factor. Thus, the HPLC method must provide sufficient selectivity to separate the main alkaloids and the dihydro-derivatives simultaneously in reasonable run time at low instrument costs. MS is typically not an available tool in routine analysis labs and hence UV or fluorescence detection are the detection schemes of first choice. Unfortunately, they impose higher demands on selectivity requirements for the chromatographic separations. Most published reports in the literature cannot separate simultaneously all four main alkaloids besides their dihydro-derivatives and in addition run times with common 5 µm-packed columns are typically excessive in the order of 30-60 min.[7] There was only one HPLC-UV and HPLC-fluorescence method, respectively, which enabled the separation of 7 of the 8 components mentioned above.[8] However, also this assay required a cycle time of about 50 min which is too long for nowadays demands of high throughput analyses in quality control laboratories.

Hence, we optimized the separation of a mixture of the eight major *Cinchona* alkaloids using standard conditions (25 °C, 1.0 ml/min) for a 150 x 4 mm size column and isocratic elution (which would eventually allow recycling and therefore economical use of the eluent) on the cSCX stationary phase. Mobile phase variables such as type and concentration of counter-ions (ammonium, dimethylammonium, diethylammonium, triethylammonium, tris(2-hydroxyethyl)ammonium and 1-hydroxy-2-butylammonium), type of co-ion (FA, AcOH, TFA), acid-base ratio, type and percentage of polar organic solvent (methanol, acetonitrile and mixtures thereof) have been thoroughly studied.

Finally, this chromatographic method development yielded elution conditions (25mM HOAc and 25 mM DEA in ACN-MeOH 1:1 v/v) that allowed the separation of all eight major *Cinchona* alkaloids within reasonable analysis time of 15 min using the cSCX column. The optimized separation in terms of critical resolution (i.e. maximal resolution for the critical peak pair) is shown in Figure 4. As can be seen CD and QN constitute the critical peak pair under the given conditions ($R_{S,crit}$ = 1.7). However, if a better resolution is required for this peak pair, a slight adjustment in the elution conditions may readily furnish this result (e.g. exchange of diethylammonium by ammonium as counter-ion and replacement of the MeOH-ACN mixture by methanol), at expense of the resolution for other peak pairs (usually either Dh-CN and/or Dh-CD with respective neighbouring peaks).

<Figure 4: HPLC separation of eight major alkaloids>

It is also quite clear that, if a mass spectrometer is available as detector, less selectivity demands are imposed on the chromatographic method because the detection selectivity compensates for the lack of chemoselectivity of the cSCX and/or of limited peak capacity under isocratic elution conditions. The herein propagated chromatographic methodology with the cSCX column has the advantage of optimal MS compatibility regarding elution conditions as exemplified by Figure 5. The employed polar organic eluent with ammonium acetate as counter- and co-ion additives is fully volatile and should offer due to its low surface tension enhanced ionization efficiency for the ESI-interface as compared to highly aqueous eluents adopted for RP-separation of *Cinchona* alkaloids.[27] The slightly altered elution conditions compared to the optimized separation in Figure 4 do not significantly influence the peak performance. The appealing peak shape persists under these conditions. In contrast, eluents optimized with regards to peak shape in RP-HPLC (employing acid or

base additives or triethylammonium phosphate buffer) are less favourable in terms of ESI-MS sensitivity or are completely incompatible.[8]

<Figure 5: LC-MS>

3.2.2.2 Validation

In order to assess the applicability of the above HPLC-UV method with the cSCX column for the simultaneous analysis of the eight component mixture, a preliminary validation was performed according to the ICH guidelines for pharmaceutical assays comprising parameters such as assay specificity, linearity, LOQ, LOD as well as intra-assay precision and accuracy. The results for the calibration, linearity and sensitivity are given in Table 2 and for precision and accuracy in Table 3.

Assay specificity as a prerequisite for obtaining an accurate and reliable method has already been extensively discussed above. All realistic isomers and structural analogs are resolved from each other. For the calibration a series of standard solutions of different concentrations of the respective alkaloids in the mixture were applied to analysis using the same optimized elution conditions as specified in Figure 4. Linear relationships between UV absorbance and sample concentration were observed in the ranges given in Table 2, i.e. about 0.2 µg/mL – 1 mg/mL (CD, QN, QD) and 1 µg/mL – 1 mg/mL (CN, Dh-QN, Dh-QD). Since no individual standards were available from Dh-CD and Dh-CN, it was not possible to validate the full linearity range for these two side alkaloids of CD and CN, respectively. It may, however, be assumed that the linear range is about the same as for the latter. LOD and LOQ were assessed at a signal-to-noise ratio of S/N = 3:1 and 10:1, respectively, and the corresponding values can be found in Table 2. LOQs ranged between 0.2 to 1 µg/mL for the distinct alkaloids at an injection volume of 10 µL.

Intra-assay precision and accuracy were assessed at three distinct levels from quadruplicate injections of separately prepared quality control standards of alkaloid mixtures. As can be seen from Table 3, intra-assay precision is excellent in the middle and high concentration range (< 1% RSD), and still acceptable in the low concentration range (typically < 15% at LOQ). Also accuracy was found to be adequate at all measured concentration levels (within ±5% from the true value).

Overall it may be concluded that the given assay for simultaneous analysis of *Cinchona* alkaloids in pharmaceutical drug substances could be reliably implemented in quality control protocols.

<Table 2>

<Table 3>

3.2.2.3 Application to Impurity Profiling

A chromatographic method for the simultaneous determination of all major *Cinchona* alkaloids represents the basis for analysis and quantification of these compounds in e.g. plant extracts, pharmaceutical and cosmetics formulations, and commercial bulk chemicals. In order to test the applicability of the cSCX column and the above described analytical procedure determination and quantification of the *Cinchona* alkaloid composition of a commercially available major *Cinchona* alkaloid were exemplarily exercised.

A commercial sample of ~85 % CN was dissolved in methanol at a concentration of 4.9 mg/mL and an aliquot of 10 µL was injected onto the cSCX column employing the optimized conditions (see Figure 6). It is seen in Figure 6 that the nice peak performance is maintained even when higher masses of the base are injected in order to be able to detect

minor amounts of impurities. This is a crucial requirement for impurity profiling when impurity peaks elute after the main component. It seems that a cation-exchange separation system such as the present cSCX has some advantages in terms of loading capacity without loss of peak performance and resolution over RP separation systems.[28]

As specified by the supplier, the sample was found to contain several impurities in the range of 0.08% to 13.5% (w/w). Besides the expected Dh-CN (13.5%) also minor amounts of QN (0.08%), QD (0.8%) and Dh-QD (0.2%) were detected in this commercial sample.

<Figure 6: Impurity analysis of CN>

4 Conclusions

A SCX type CSP, initially designed for the enantiomer separation of chiral basic compounds, has exemplarily been applied to the chromatographic separation of strongly basic natural *Cinchona* alkaloids and synthetic derivatives thereof. The chiral SCX packing material conceptually circumvents the intrinsic drawback of analysis of strongly basic compounds in RP mode, that is peak tailing and band broadening due to interactions of the basic analytes with residual acidic silanol groups of the stationary phase, and thus provided excellent peak efficiencies. In combination with enhanced diastereoselectivities for the corresponding *Cinchona* alkaloid diastereomers as opposed to RP-HPLC, this facilitates the simultaneous determination of eight major *Cinchona* alkaloids in complex mixtures as well as in impurity profiling. A good mass loading capacity of the chiral SCX phase appears to be further helpful together with the better peak symmetries when impurities of les than 0.1% must be analysed besides a major component and the impurities are eluted

after the main peak. It was also demonstrated that the method is compatible with ESI-MS detection thereby reducing the demands on the selectivity of the chromatographic method. After preliminary validation, the applicability of the method was demonstrated for the impurity determination of a commercial CN sample.

Supported also by a qualitative comparison with commercially available RP and SCX packing materials, the chiral SCX stationary phase turned out as a successful alternative to conventional RP analysis, with complementary separation properties for the HPLC analysis of basic compounds, and could potentially serve as a material especially for a secondary independent analytical method.

Acknowledgements

The financial support of this research project by the Austrian Christian Doppler Research Society and the industrial partners AstraZeneca (Mölndal, Sweden) and Merck (Darmstadt, Germany) is gratefully acknowledged. The authors thank in particular Dr. Karol Kacprzak for providing us with samples of synthetic *Cinchona* alkaloid derivatives eQN, eQD, Di-QN, and Di-QD.

References

[1] K. Kacprzak, J. Gawronski, *Synthesis* **2001**, 961.

[2] J. Seayad, B. List, *Org. Biomol. Chem.* **2005**, *3*, 719.

[3] P. I. Dalko, L. Moisan, *Ang. Chem. Int. Ed.* **2004**, *43*, 5138.

[4] S. K. Tian, Y. G. Chen, J. F. Hang, L. Tang, P. McDaid, L. Deng, *Acc. Chem. Res.* **2004**, *37*, 621.

[5] M. Lämmerhofer, W. Lindner, in *Advances in Chromatography, Vol. 46* (Eds.: E. Grushka, N. Grinberg), CRC Ress, Taylor & Francis Group, Boca Raton, **2008**, pp. 1.

[6] M. Lämmerhofer, W. Lindner, *J. Chromatogr. A* **1996**, *741*, 33.

[7] D. V. McCalley, *J. Chromatogr. A* **2002**, *967*, 1.

[8] R. Gatti, M. G. Gioia, V. Cavrini, *Analyt. Chim. Acta* **2004**, *512*, 85.

[9] C. Giroud, T. Vanderleer, R. Vanderheijden, R. Verpoorte, C. E. M. Heeremans, W. M. A. Niessen, J. Vandergreef, *Planta Medica* **1991**, *57*, 142.

[10] K. M. Kacprzak, W. Lindner, N. M. Maier, *Chirality* **2008**, *20*, 441.

[11] D. V. McCalley, *Analyst* **1990**, *115*, 1355.

[12] D. V. McCalley, *J. Chromatogr.* **1983**, *260*, 184.

[13] D. V. McCalley, *Chromatographia* **1983**, *17*, 264.

[14] D. V. McCalley, *J. Chromatogr.* **1986**, *357*, 221.

[15] D. V. McCalley, *J. Chromatogr. A* **1996**, *738*, 169.

[16] D. V. McCalley, *J. Sep. Sci.* **2003**, *26*, 187.

[17] G. Theodoridis, I. Papadoyannis, A. Hermanslokkerbol, R. Verpoorte, *Chromatographia* **1995**, *41*, 153.

[18] C. V. Hoffmann, M. Lammerhofer, W. Lindner, *J. Chromatogr. A* **2007**, *1161*, 242.

[19] J. Suszko, F. Szelag, *Bull. Int. Acad. Pol. Sci. Cl. Sci. Math.* **1936**, *SerA*, 403.

[20] W. M. Braje, J. Frackenpohl, O. Schrake, R. Wartchow, W. Beil, H. M. R. Hoffmann, *Helv. Chim. Acta* **2000**, *83*, 777.

[21] N. M. Maier, L. Nicoletti, M. Lammerhofer, W. Lindner, *Chirality* **1999**, *11*, 522.

[22] K. Gyimesi-Forrás, K. Akasaka, M. Lämmerhofer, N. M. Maier, T. Fujita, M. Watanabe, N. Harada, W. Lindner, *Chirality* **2005**, *17*, S134.

[23] T. Fornstedt, G. Zhong, G. Guiochon, *J. Chromatogr. A* **1996**, *741*, 1.

[24] T. Fornstedt, G. Zhong, G. Guiochon, *J. Chromatogr. A* **1996**, *742*, 55.

[25] D. V. McCalley, R. G. Brereton, *J. Chromatogr. A* **1998**, *828*, 407.

[26] D. V. McCalley, *J. Chromatogr. A* **1998**, *793*, 31.

[27] H. P. Nguyen, K. A. Schug, *J. Sep. Sci.* **2008**, 31, 1465.

[28] W. Bicker, D. Hebenstreit, M. Lämmerhofer, W. Lindner, *Electrophoresis* **2003**, *24*, 2532.

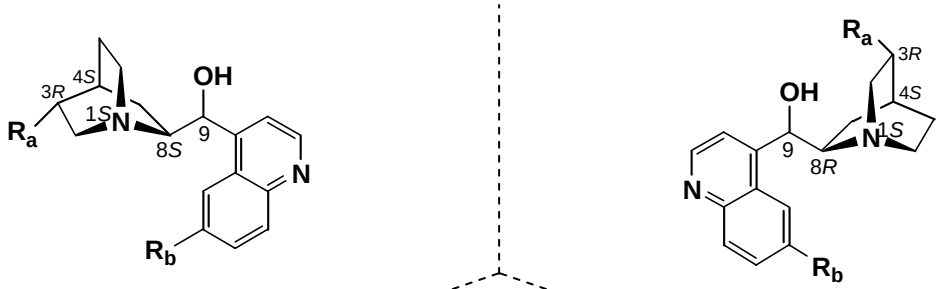

name	*availability*	*abs. config. (C9)*	R_a	R_b	*abs. config. (C9)*	*availability*	*name*
Dihydro-QN **Dh-QN**	natural	(9*R*)		OCH_3	(9*S*)	natural	Dihydro-QD **Dh-QD**
Quinine **QN**	natural	(9*R*)		OCH_3	(9*S*)	natural	Quinidine **QD**
Didehydro-QN **Di-QN**	synthetic	(9*R*)		OCH_3	(9*S*)	synthetic	Didehydro-QD **Di-QD**
Cinchonidine **CD**	natural	(9*R*)		H	(9*S*)	natural	Cinchonine **CN**
epi-Quinine **eQN**	synthetic	(9*S*)		OCH_3	(9*R*)	synthetic	epi-Quinidine **eQD**
Dihydro-CD **Dh-CD**	natural	(9*R*)		H	(9*S*)	natural	Dihydro-CN **Dh-CN**

Scheme 1.

Chemical structures of the *Cinchona* alkaloids and derivatives thereof tested (Note: compunds in the left and in the right columns are diastereomeric to each other).

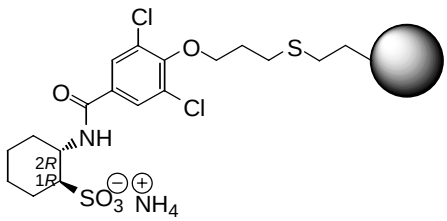

Figure 1.

Chemical structure of the self-made cSCX stationary phase.

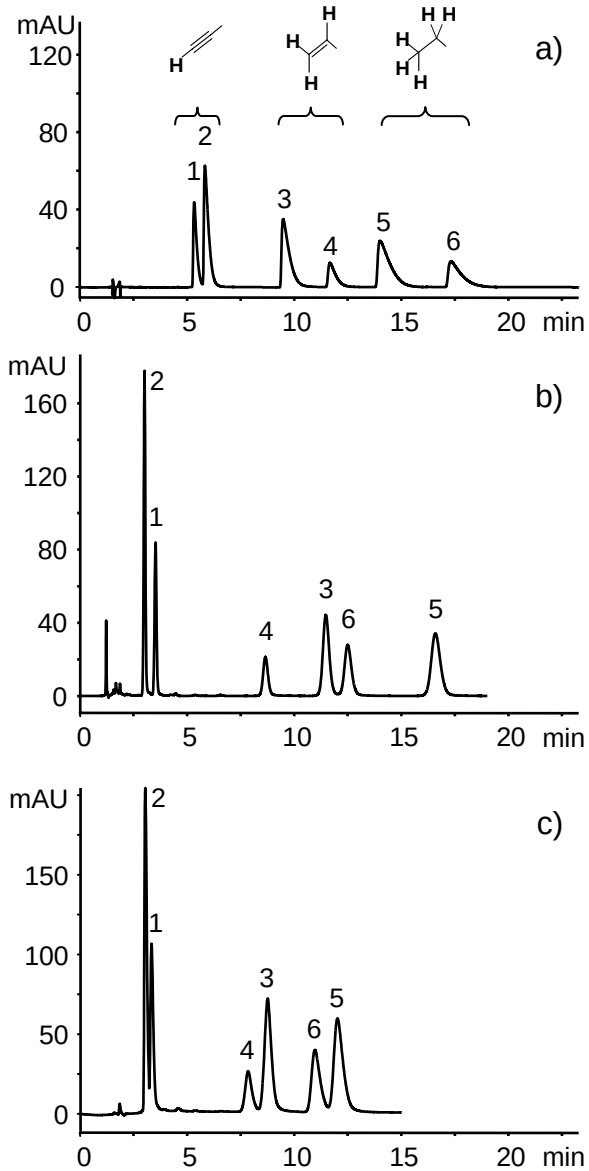

Figure 2.

Chromatograms of HPLC separations of Quinines and Quinidines on different stationary phases: a) RP, b) cSCX, c) PSE-A. Di-QD (1), Di-QN (2), QD (3), QN (4), Dh-QD (5), Dh-QN (6). Eluents: 5% ACN in water, 0.1% FA (RP), 37.5 mM NH_4OAc in MeOH (cSCX), 12.5 mM NH_4OAc in MeOH (PSE-A). UV detection at 254 nm.

Peak	*k*			*Symm.*			*N [column^{-1}]*			*Peak*	R_S			α		
	RP	**cSCX**	**PSE-A**	**RP**	**cSCX**	**PSE-A**	**RP**	**cSCX**	**PSE-A**		**RP**	**cSCX**	**PSE-A**	**RP**	**cSCX**	**PSE-A**
1	1.15	1.37	0.80	0.33	0.99	0.53	5456	7173	2851							
2	1.35	1.03	0.64	0.27	0.98	0.62	3895	7319	2989	**1-2**	1.5	3.3	1.2	1.17	1.34	1.24
3	2.82	6.74	3.75	0.24	0.84	0.80	3608	6883	3527							
4	3.71	4.84	3.25	0.29	0.85	0.76	5821	6891	2937	**3-4**	3.5	5.8	1.6	1.31	1.39	1.15
5	4.65	10.2	5.52	0.22	0.80	0.62	3199	7133	3640							
6	5.99	7.43	4.96	0.26	0.82	0.64	4236	6976	3570	**5-6**	3.2	5.9	1.4	1.29	1.37	1.11

Table 1.

Chromatographic data of HPLC separations of Quinines and Quinidines on RP, cSCX, and PSE-A type stationary phases. Peak numbering and other conditions as in Fig. 2.

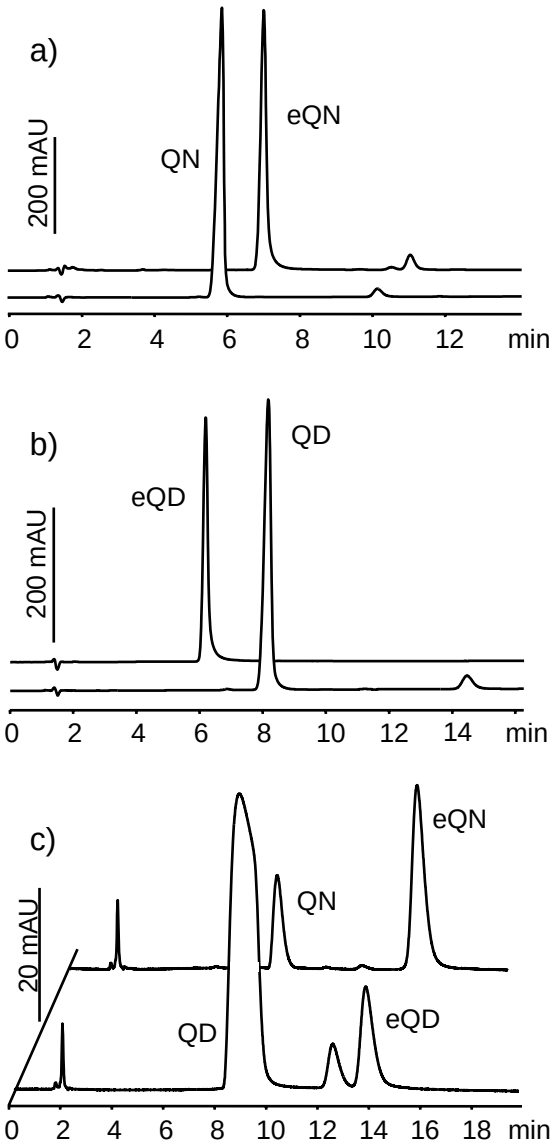

Figure 3.

HPLC chromatograms of QN and QD and their C9-epimers on a), b) cSCX and c) PSE-A. Additional peaks correspond to respective Dihydro derivatives. Eluents: HOAc & DEA (25 mM each) in ACN/MeOH 1:1 (v/v) (cSCX), 12.5 mM NH_4OAc in MeOH (PSE-A). UV detection at 254 nm.

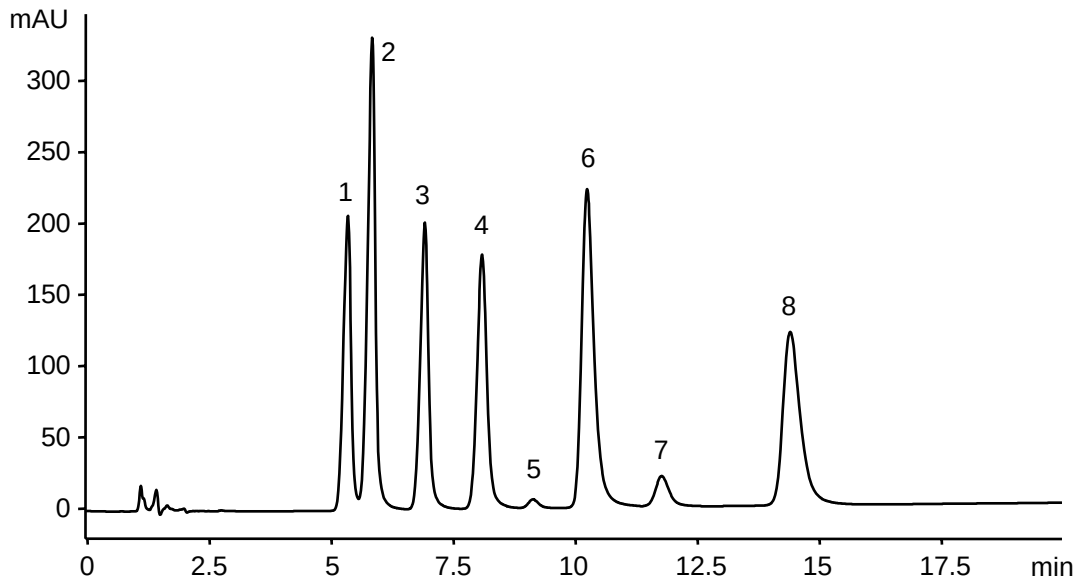

Figure 4.

Chromatogram of the HPLC separation of major *Cinchona* alkaloids on the cSCX column. CD (1), QN (2), CN (3), QD (4), Dh-CD (5), Dh-QN (6), Dh-CN (7), Dh-QD (8). Eluent: HOAc & DEA (25 mM each) in ACN/MeOH 1:1 (v/v). UV detection at 254 nm.

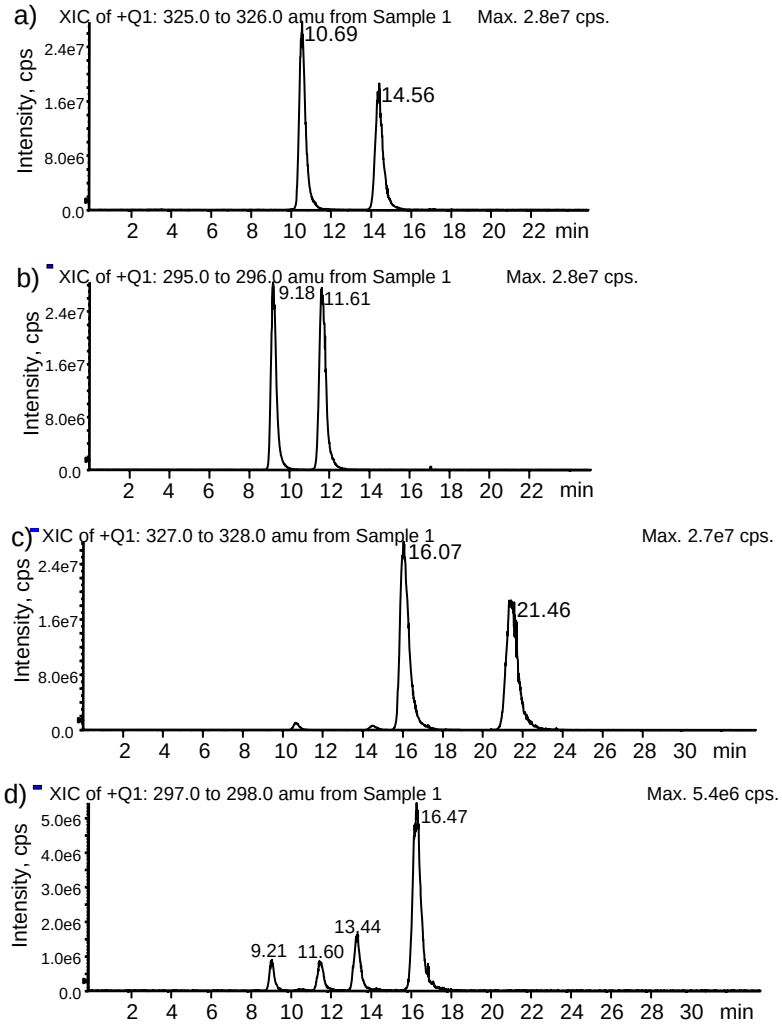

Figure 5.

Extracted ion-count LC-MS spectra of the separation of eight Cinchona alkaloids on the cSCX column. a) m/z 325-236 for QN and QD, b) m/z 295-296 for CD and CN, c) m/z 327-328 for DH-QN and DH-QD, and d) m/z 297-298 for DH-CD and DH-CN. Eluent: 30mM NH_4OAc in ACN/MeOH 25:75 (v/v)

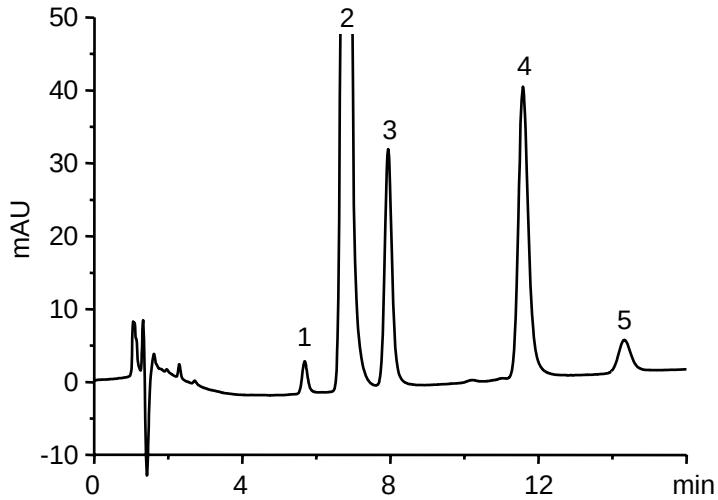

Figure 6.

HPLC impurity profiling and quantification of a commercially available sample of CN on the cSCX column. QN (1) 0.08 %, CN (2) 85.43 %, QD (3) 0.82 %, Dh-CN (4) 13.47 %, Dh-QD (5) 0.2 % (w/w). Eluent: HOAc & DEA (25 mM each) in ACN/MeOH 1:1 (v/v). UV detection at 240 nm. Sample conc.: 4.9 mg/mL, inj.vol. 10 μL.

Table 2: Calibration data, linearity and sensitivity

Sample	UV-Det.[a)]	Conc. Range[b)]	Slope	Intercept	r^2	LOD[c)]	LOQ[d)]
CD	254	0,00019-0,96	5469,4	26,2	0,9988	0,00001	0,00019
QN	254	0,00019-0,94	6669,7	36,0	0,9986	0,00001	0,00019
CN	254	0,00087-0,87	4434,7	17,8	0,9987	0,00017	0,00087
QD	254	0,00020-0,99	6411,7	37,0	0,9987	0,00001	0,00020
Dh-CD	240	0,00080-0,04	6371,7	-0,8	0,9976	0,00040	0,00080
Dh-QN	254	0,00100-1,01	4775,1	28,0	0,9986	0,00020	0,00100
Dh-CN	240	0,00150-0,15	5640,8	3,8	0,9988	0,00030	0,00150
Dh-QD	254	0,00100-1,00	5419,8	29,0	0,9986	0,00020	0,00100

a) [nm]

b) [g/L]

c) according to S:N 3:1

d) according to S:N 10:1

Table 3: Precision and accuracy

	Prescision (n=4)			Accuracy
Sample	**RSD (%)** 1:5000[c)]	**RSD (%)** 1:70[c)]	**RSD (%)** 1:5[c)]	**(%)**
CD[a)]	10,9499	0,3873	0,1142	99,22
QN[a)]	4,3030	0,3895	0,2463	99,06
CN[a)]	8,0000	0,8392	0,1806	99,19
QD[a)]	7,1908	0,8075	0,1526	98,30
DH-CD[b)]	< LOQ	4,5660	2,7029	99,50
DH-QN[a)]	14,4088	0,8072	0,2060	99,26
DH-CN[b)]	< LOQ	5,5566	0,2904	99,32
DH-QD[a)]	18,1818	1,9470	0,3048	104,66

a) UV detection at 254 nm

b) UV detection at 240 nm

c) dilutions from a 1.0 g/L stock solution

Appendix #5

Publication P-IV

Anal. Chem. **XXXX,** *xxx,* 000–000

Synergistic Effects on Enantioselectivity of Zwitterionic Chiral Stationary Phases for Separations of Chiral Acids, Bases, and Amino Acids by HPLC

Christian V. Hoffmann, Reinhard Pell, Michael Lämmerhofer, and Wolfgang Lindner*

Christian Doppler Laboratory for Molecular Recognition Materials, Department of Analytical Chemistry & Food Chemistry, University of Vienna, Währinger Strasse 38, A-1090 Vienna, Austria

In an attempt to overcome the limited applicability scope of earlier proposed *Cinchona* alkaloid-based chiral weak anion exchangers (WAX) and recently reported amino-sulfonic acid-based chiral strong cation exchangers (SCX), which are conceptionally restricted to oppositely charged solutes, their individual chiral selector (SO) subunits have been fused in a combinatorial synthesis approach into single, now zwitterionic, chiral SO motifs. The corresponding zwitterionic ion-exchange-type chiral stationary phases (CSPs) in fact combined the applicability spectra of the parent chiral ion exchangers allowing for enantioseparations of chiral acids and amine-type solutes in liquid chromatography using polar organic mode with largely rivaling separation factors as compared to the parent WAX and SCX CSPs. Furthermore, the application spectrum could be remarkably expanded to various zwitterionic analytes such as α- and *β*-amino acids and peptides. A set of structurally related yet different CSPs consisting of either a quinine or quinidine alkaloid moiety as anion-exchange subunit and various chiral or achiral amino acids as cation-exchange subunits enabled us to derive structure−enantioselectivity relationships, which clearly provided strong unequivocal evidence for synergistic effects of the two oppositely charged ion-exchange subunits being involved in molecular recognition of zwitterionic analytes by zwitterionic SOs driven by double ionic coordination.

The basis of enantioselective chromatography is the transient formation of noncovalent diastereomeric complexes between chiral solute and chiral stationary phase (CSP). Typically, these binding events are caused and mediated by various electrostatic and hydrophobic intermolecular interactions, among which long-range ion-pairing forces are ideally suited for bringing an ionizable chiral analyte in close contact with the CSP's oppositely charged chiral binding site. An ion-pairing-type enantioselective molecular recognition process could principally occur on every CSP that contains ionizable groups within its chiral selector (SO) moieties, regardless of whether they are part of separation materials based on small SO molecules or glycopeptide-type selectors or protein-type selectors.[1−5] CSPs that are based on immobilized derivatives of *Cinchona* alkaloid bases as low molecular mass chiral SOs specifically employ the ion-pairing process as the primary interaction between SOs and acidic analytes. Figure 1 shows the SO structure of a quinine-type representative of this thoroughly investigated class of chiral weak anion exchangers (AX; WAX) CSPs providing excellent enantioseparation capabilities for a broad range of chiral acids.[6,7]

Complementary to AX-type CSPs, also separation materials based on fully synthetic low molecular mass weak and strong cation exchanger (CX; WCX and SCX) SOs (Figure 1) have been developed by our group for chiral basic analytes.[8−14] Along this line only very recently, a more complex boronic acid-based chiral CX SO derived from the macrodiolide boromycin was also reported[15] indicating the potential of ion exchangers in enantioselective chromatography.

However, chiral cation and anion exchangers encounter the limitation of only addressing analytes that carry a charge of opposite sign. Furthermore, the large group of chiral amphoteric compounds typically cannot be readily analyzed with CSPs of pure AX or CX character although these analytes seem very well

* To whom correspondence should be addressed. E-mail: Wolfgang.Lindner@univie.ac.at. Tel.: ++43-1-4277-52300. Fax: ++43-1-4277-9523.

(1) Maier, N. M.; Franco, P.; Lindner, W. *J. Chromatogr., A* **2001**, *906*, 3–33.
(2) Ilisz, I.; Berkecz, R.; Peter, A. *J. Sep. Sci.* **2006**, *29*, 1305–1321.
(3) Haginaka, J. *J. Chromatogr., A* **2001**, *906*, 253–273.
(4) Franco, E. J.; Hofstetter, H.; Hofstetter, O. *J. Sep. Sci.* **2006**, *29*, 1458–1469.
(5) Armstrong, D. W.; Tang, Y.; Chen, S.; Zhou, Y.; Bagwill, C.; Chen, J.-R. *Anal. Chem.* **1994**, *66*, 1473–1484.
(6) Lämmerhofer, M., Lindner, W. In *Advances in Chromatography*; Grushka, E., Grinberg, N., Eds.; CRC Ress, Taylor & Francis Group: Boca Raton, FL, 2008; Vol. 46, pp 1−109.
(7) Lämmerhofer, M.; Lindner, W. *J. Chromatogr., A* **1996**, *741*, 33–48.
(8) Constantin, S.; Bicker, W.; Zarbl, E.; Lammerhofer, M.; Lindner, W. *Electrophoresis* **2003**, *24*, 1668–1679.
(9) Hebenstreit, D.; Bicker, W.; Lammerhofer, M.; Lindner, W. *Electrophoresis* **2004**, *25*, 277–289.
(10) Zarbl, E.; Lämmerhofer, M.; Woschek, A.; Hammerschmidt, F.; Parenti, C.; Cannazza, G.; Lindner, W. *J. Sep. Sci.* **2002**, *25*, 1269–1283.
(11) Tobler, E.; Lämmerhofer, M.; Wuggenig, F.; Hammerschmidt, F.; Lindner, W. *Electrophoresis* **2002**, *23*, 462–476.
(12) Preinerstorfer, B.; Lubda, D.; Lindner, W.; Lammerhofer, M. *J. Chromatogr., A* **2006**, *1106*, 94–105.
(13) Preinerstorfer, B.; Lindner, W.; Lammerhofer, M. *Electrophoresis* **2005**, *26*, 2005–2018.
(14) Hoffmann, C. V.; Lammerhofer, M.; Lindner, W. *J. Chromatogr., A* **2007**, *1161*, 242–251.
(15) Wang, C. L.; Armstrong, D. W.; Risley, D. S. *Anal. Chem.* **2007**, *79*, 8125–8135.

10.1021/ac801384f CCC: $40.75

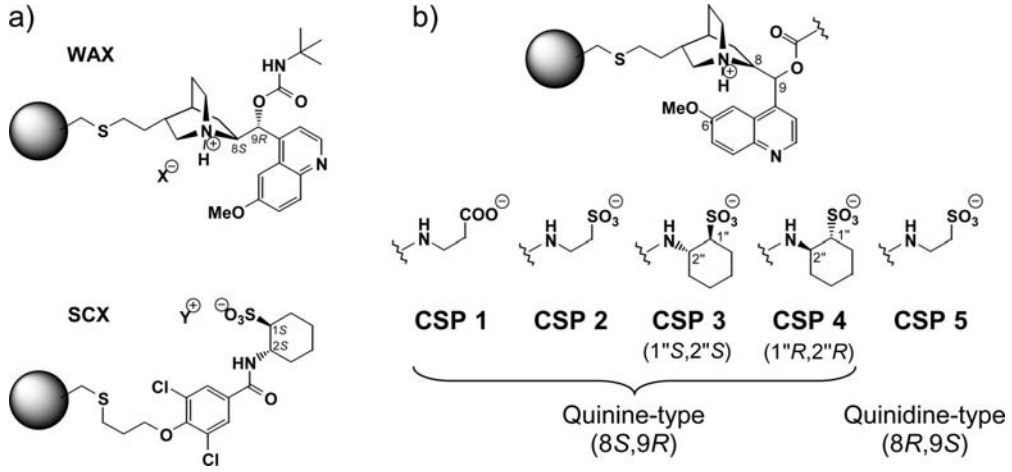

Figure 1. Chemical structures of (a) previously reported weak anion exchanger QN-AX (WAX) and strong cation exchanger (SCX) CSPs that represent lead structures for (b) newly prepared zwitterionic **CSPs 1**−**5**.

susceptible to the concept of ion exchangers due to their ionic nature. This current status quo on ion-exchanger-based CSPs prompted us to develop in a combinatorial approach novel low molecular mass chiral SOs that incorporate both CX and AX entities derived from SCX and WAX SOs (Figure 1) to yield well-defined zwitterionic SO structures that address the enantiomer separation not only of chiral acids and chiral bases but also of chiral amphoteric compounds, altogether with one single CSP.

Direct amino acid enantioseparations have already been reported for glycopeptide-,[16−23] crown ether-,[24−28] protein-,[3,4] these small-molecule-, and ligand-exchange-type CSPs,[29,30] (mostly driven by molecular interaction principles other than classical ion exchange, such as multiple hydrogen bonding and metal chelation). Few enantiomer separations of amino acids have also been described for a chiral anion exchanger.[31,32] Nevertheless, chromatographic enantiomer separations of chiral amino acids still remains a challenging task where the zwitterionic SO approach could provide a novel and promising perspective.

Principally, stationary phases containing complementary charged groups have already been described in the literature[33−37] and were applied mainly for the separation of inorganic cations and anions. Systems employing chiral zwitterionic moieties have also been reported previously[38−42] but were not systematically envisioned for enantiomer separations.

Hence, we report herein de novo design and synthesis of novel zwitterionic SOs and their corresponding brush-type **CSPs 1**−**5** (Figure 1) as well as their successful evaluation in HPLC for enantioseparation capabilities not only toward chiral acids and chiral amines but also for chiral zwitterionic analytes like amino acids and dipeptides using polar organic mobile-phase conditions. In particular, zwitterionic **CSPs 3** and **4** (Figure 1, see also Supporting Information) illustrate the concept of merging cation- and anion-exchanger moieties in one single SO by incorporating key chiral motifs of the well-known WAX and SCX congeners with the alkaloid base and the *trans*-2-aminocyclohexanesulfonic acid. Comprehensive investigations on *Cinchona*-type receptors in enantioseparation techniques suggested the C9-position of the alkaloid scaffold (see Figure 1) for introducing the aminosulfonic acid via carbamate linkage if enantioselective properties toward acid analytes should remain largely unaltered. For more detailed examinations of the enantioselective ionic interaction processes, achiral carboxylic and sulfonic acids with amino groups in β-position were incorporated in **CSPs 1**, **2**, and **5**. In **CSP 5**, the

(16) Berthod, A.; Chen, X. H.; Kullman, J. P.; Armstrong, D. W.; Gasparrini, F.; D'Acquarica, I.; Villani, C.; Carotti, A. *Anal. Chem.* **2000**, *72*, 1767–1780.
(17) Berthod, A.; Yu, T.; Kullman, J. P.; Armstrong, D. W.; Gasparrini, F.; D'Acquarica, I.; Misiti, D.; Carotti, A. *J. Chromatogr., A* **2000**, *897*, 113–129.
(18) D'Acquarica, H.; Gasparrini, F.; Misiti, D.; Zappia, G.; Cimarelli, C.; Palmieri, G.; Carotti, A.; Cellamare, S.; Villani, C. *Tetrahedron: Asymmetry* **2000**, *11*, 2375–2385.
(19) Cavazzini, A.; Nadalini, G.; Dondi, F.; Gasparrini, F.; Ciogli, A.; Villani, C. *J. Chromatogr., A* **2004**, *1031*, 143–158.
(20) Staroverov, S. M.; Kuznetsov, M. A.; Nesterenko, P. N.; Vasiarov, G. G.; Katrukha, G. S.; Fedorova, G. B. *J. Chromatogr., A* **2006**, *1108*, 263–267.
(21) Sztojkov-Ivanov, A.; Lazar, L.; Fulop, F.; Armstrong, D. W.; Peter, A. *Chromatographia* **2006**, *64*, 89–94.
(22) Peter, A.; Berkecz, R.; Fulop, F. *J. Pept. Sci.* **2006**, *12*, 234–234.
(23) Berkecz, R.; Torok, R.; Ilisz, I.; Forro, E.; Fulop, F.; Armstrong, D. W.; Peter, A. *Chromatographia* **2006**, *63*, S37−S43.
(24) Berkecz, R.; Ilisz, I.; Fulop, F.; Pataj, Z.; Hyun, M. H.; Peter, A. *J. Chromatogr. A* **2008**, *1189*, 285–291.
(25) Berkecz, R.; Sztojkov-Ivanov, A.; Ilisz, I.; Forro, E.; Fulop, F.; Hyun, M. H.; Peter, A. *J. Chromatogr., A* **2006**, *1125*, 138–143.
(26) Hyun, M. H. *J. Sep. Sci.* **2003**, *26*, 242–250.
(27) Hyun, M. H.; Cho, Y. J.; Song, Y.; Choi, H. J.; Kang, B. S. *Chirality* **2007**, *19*, 74–81.
(28) Hyun, M. H.; Jin, J. S.; Lee, W. J. *J. Chromatogr., A* **1998**, *822*, 155–161.
(29) Davankov, V. A.; Bochkov, A. S.; Kurganov, A. A.; Roumeliotis, P.; Unger, K. K. *Chromatographia* **1980**, *13*, 677–685.
(30) Davankov, V. A. *J. Chromatogr., A* **1994**, *666*, 55–76.
(31) Gika, H.; Lämmerhofer, M.; Papadoyannis, I.; Lindner, W. *J. Chromatogr., B* **2004**, *800*, 193–201.
(32) Sardella, R.; Lämmerhofer, M.; Natalini, B.; Lindner, W. *Chirality* **2008**, *20*, 571–576.
(33) Nesterenko, P. N.; Haddad, P. R. *Anal. Sci.* **2000**, *16*, 565–574.
(34) Hu, W. Z.; Haddad, P. R. *Trends Anal. Chem.* **1998**, *17*, 73–79.
(35) Hu, W. Z.; Haraguchi, H. *Anal. Chem.* **1994**, *66*, 765–767.
(36) Hu, W. Z.; Tao, H.; Haraguchi, H. *Anal. Chem.* **1994**, *66*, 2514–2520.
(37) Hu, W. Z.; Takeuchi, T.; Haraguchi, H. *Anal. Chem.* **1993**, *65*, 2204–2208.
(38) Yu, L. W.; Hartwick, R. A. *J. Chromatogr. Sci.* **1989**, *27*, 176–185.
(39) Yu, L. W.; Floyd, T. R.; Hartwick, R. A. *J. Chromatogr. Sci.* **1986**, *24*, 177–182.
(40) Nesterenko, P. N.; Elefterov, A. I.; Tarasenko, D. A.; Shpigun, O. A. *J. Chromatogr., A* **1995**, *706*, 59–68.
(41) Viklund, C.; Sjogren, A.; Irgum, K.; Nes, I. *Anal. Chem.* **2001**, *73*, 444–452.
(42) Jiang, W.; Fischer, G.; Girmay, Y.; Irgum, K. *J. Chromatogr., A* **2006**, *1127*, 82–91.

alkaloid base quinine was, in addition, replaced by its pseudoenantiomer quinidine, which was expected to affect elution order upon enantioseparation and thereby could to shed more light on the underlying molecular recognition process. Extensive chromatographic data obtained from both a large and a diverse set of chiral analytes and also the group of CSPs with systematically varied SO structures provided insights into the working principles of novel zwitterionic CSPs and the establishment of a new enantioseparation concept for chiral zwitterionic analytes that relies on simultaneous double ion pairing.

EXPERIMENTAL SECTION

General Information and Materials. The preparation of the chiral SCX CSP (Figure 1) was reported previously.[14] The WAX-type CSP of Figure 1 is commercially available from Chiral Technologies (Illkirch, France). All aspects concerning the preparation of **CSPs 1−5** (Figure 1) are described in detail in the Supporting Information (see also Figure S-1). The basis of the assignments of **CSP 3** (1″*S*,2″*S*) and **CSP 4** (1″*R*,2″*R*) are preliminary X-ray crystallographic data on the SO of **CSP 3** (data not shown). The SO loadings of **CSPs 1−5** ranged between 196 and 229 μmol/g CSP as was calculated from the nitrogen content of the modified silica obtained by elemental analysis. Due to these relatively uniform SO loadings of **CSPs 1−5**, the influences of SO coverage on the chromatographic behavior can be neglected and the observed differences in their chromatographic behaviors can be largely ascribed to the SO structure variations. All CSPs were packed into stainless steel columns of dimensions 150 × 4 mm i.d.

MeOH and acetonitrile (ACN) as solvents for HPLC were of HPLC-grade from Merck (Darmstadt, Germany). Mobile-phase additives acetic acid (HOAc), formic acid (FA), diethylamine (DEA), and ammonium acetate were of analytical grade (Sigma-Aldrich). The chiral basic and zwitterionic analytes used in this study were either commercially available or were kind gifts from research partners. N-Blocked amino acids as acidic analytes were either commercially available or synthesized according to literature procedures.[43]

HPLC Instrumentation and Chromatography. Chromatographic measurements were performed on a 1100 Series HPLC system from Agilent Technologies (Waldbronn, Germany) consisting of a solvent degasser, a pump, an autosampler, a column thermostat, and a multiwavelength UV−vis detector for detection of analytes containing a chromophore sufficient for UV detection. For analytes with weak UV absorbance properties, a Corona charged aerosol detector (CAD) from ESA Biosciences, Inc. was used instead as specifically stated in the figure captions and tables. Data acquisition and analysis was carried out with ChemStation chromatographic data software from Agilent Technologies. Elution orders of selected solute enantiomers were assessed by injection of either single enantiomers of known absolute configuration or specifically enantioenriched samples or by using an online OR-990 optical rotation detector from Jasco (Gross-Umstadt, Germany). Polar organic mobile phases consisting of MeOH and ACN with acidic and basic additives that act as co- and counterions and modulate the ionic interactions between charged SOs and solutes were applied in these investigations since they have been successfully and extensively used for the parent, purely anionic or cationic ion-exchanger CSPs.[14,44] Elution was performed in isocratic mode at a mobile-phase flow rate of 1.0 mL/min. If not otherwise stated, column temperature was 25 °C. UV detection was accomplished at selected wavelengths between 230 and 280 nm. The void volumes of the columns were determined by injecting a solution of acetone in MeOH with detection at 280 nm. All analytes were applied as methanolic solutions of 0.5−1.0 mg/mL.

RESULTS AND DISCUSSION

Due to the large set of data stemming from 64 chiral analytes and five zwitterionic CSPs that have been evaluated, the results are broken down and discussed in separate sections related to different ion-exchange modes, i.e. anion, cation, and zwitterion exchange and no mobile-phase optimizations of key variables for enantioselectivity[7,14,43,44] such as pH in aqueous or proton activity in nonaqueous eluent systems, character of the bulk solvents, and the acidic and basic additives, and were carried out for the herein presented studies on zwitterionic CSPs.

Enantioseparation of Chiral Acids. In a series of experiments, **CSPs 1−5** were tested regarding enantioseparations of different chiral acids in order to assess whether the main property of the *Cinchona*-type WAX CSPs—namely, enantiorecognition ability for chiral acidic analytes—could principally be conserved in the novel zwitterionic CSPs. For this purpose, a small but representative set of eight chiral acidic analytes was selected comprising various N-derivatized amino acids, which were among typical model analytes that have been previously employed in a series of investigations of *Cinchona* alkaloid-type WAX CSPs, in particular toward describing their molecular recognition principles and for characterization of novel CSP derivatives thereof.[6,7,43,45−47] Both structures of the analytes as well as chromatographic results are listed in Table 1.

Clearly, enantiorecognition properties that allow for enantiomer separation of acidic analytes are still present in all five zwitterionic CSPs (see also Figure 2a). With only a few exceptions, all analytes were baseline separated on all CSPs. The α-values measured on the zwitterionic CSPs are subject to only slight variances in comparison to the parent chiral WAX CSP. The effect of the type of protecting group on chiral recognition and enantioselectivity on *Cinchona*-type CSPs has previously been described in detail[43,48] and can be confirmed also with **CSPs 1−5**: the 3,5-dinitrobenzoyl (DNB) amides truly yield excellent enantioseparations (α-values up to 15 with resolutions >20), the Fmoc, DNP, and acetyl groups give good separations followed by the Z-group; the DNP group leads to a reversal of the elution order compared to the other N-protection groups.

SOs of **CSP 1** and **CSP 2** are structural homologues, which differ only in the type of their acid function, carboxylic versus

(43) Czerwenka, C.; Lammerhofer, M.; Lindner, W. *J. Sep. Sci.* **2003**, *26*, 1499–1508.
(44) Gyimesi-Forrás, K.; Akasaka, K.; Lämmerhofer, M.; Maier, N. M.; Fujita, T.; Watanabe, M.; Harada, N.; Lindner, W. *Chirality* **2005**, *17*, S134−S142.
(45) Krawinkler, K. H.; Maier, N. M.; Sajovic, E.; Lindner, W. *J. Chromatogr., A* **2004**, *1053*, 119–131.
(46) Maier, N. M.; Schefzick, S.; Lombardo, G. M.; Feliz, M.; Rissanen, K.; Lindner, W.; Lipkowitz, K. B. *J. Am. Chem. Soc.* **2002**, *124*, 8611–8629.
(47) Tobler, E.; Lammerhofer, M.; Lindner, W. *J. Chromatogr., A* **2000**, *875*, 341–352.
(48) Mandl, A.; Nicoletti, L.; Lämmerhofer, M.; Lindner, W. *J. Chromatogr., A* **1999**, *858*, 1–11.

Table 1. HPLC Enantiomer Separation of Various Chiral Acidic Analytes on CSP 1-5[a]

Analyte		k_1	α	R_S	EO
Ac-Phe	**CSP 1**	1.04	**1.43**	**3.75**	**D**
	CSP 2	0.29	**1.50**	**1.80**	**D**
	CSP 3	0.24	**1.62**	**2.29**	**D**
	CSP 4	0.41	**1.40**	**1.88**	**D**
	CSP 5	0.14	**1.55**	**1.02**	**L**
Z-Phe	**CSP 1**	1.92	**1.19**	**2.15**	**D**
	CSP 2	0.63	**1.17**	**0.78**	**D**
	CSP 3	0.55	**1.24**	**1.63**	**D**
	CSP 4	0.95	**1.13**	**1.12**	**D**
	CSP 5	0.33	**1.19**	**0.65**	**L**
Fmoc-Phe	**CSP 1**	2.95	**1.37**	**4.05**	**D**
	CSP 2	1.03	**1.35**	**1.80**	**D**
	CSP 3	0.94	**1.52**	**3.35**	**D**
	CSP 4	1.51	**1.27**	**2.30**	**D**
	CSP 5	0.59	**1.30**	**1.26**	**L**
DNB-Phe	**CSP 1**	3.18	**6.38**	**21.93**	**D**
	CSP 2	1.01	**7.22**	**10.92**	**D**
	CSP 3	0.97	**15.03**	**22.43**	**D**
	CSP 4	0.43	**5.00**	**17.55**	**D**
	CSP 5	0.65	**5.00**	**13.08**	**L**
Ac-Trp	**CSP 1**	1.72	**1.83**	**7.24**	**D**
	CSP 2	0.77	**1.93**	**4.24**	**D**
	CSP 3	0.80	**3.01**	**10.74**	**D**
	CSP 4	1.00	**1.54**	**4.25**	**D**
	CSP 5	0.36	**1.95**	**3.46**	**L**
DNP-Phe	**CSP 1**	6,28	**1.42**	**3.47**	**L**
	CSP 2	2.13	**1.53**	**2.94**	**L**
	CSP 3	2.06	**1.48**	**4.63**	**L**
	CSP 4	3.48	**1.77**	**7.77**	**L**
	CSP 5	1.49	**1.30**	**2.46**	**D**
Fmoc-Leu	**CSP 1**	1.34	**1.33**	**3.10**	**n.d.**
	CSP 2	0.47	**1.27**	**1.12**	**n.d.**
	CSP 3	0.43	**1.43**	**2.35**	**n.d.**
	CSP 4	0.67	**1.32**	**2.25**	**n.d.**
	CSP 5	0.28	**1.18**	**0.52**	**n.d.**
DNB-Glu	**CSP 1**	6.53	**3.96**	**16.37**	**n.d.**
	CSP 2	1.54	**4.40**	**8.91**	**n.d.**
	CSP 3	1.48	**5.82**	**17.71**	**n.d.**
	CSP 4	2.16	**3.08**	**13.14**	**n.d.**
	CSP 5	0.80	**3.36**	**9.25**	**n.d.**

[a] Conditions: stationary phase, column dimension 150 × 4 mm i.d.; mobile phase, 50 mM formic acid and 25 mM diethylamine in MeOH; flow 1.0 mL/min; T 25 °C; t_0 = 1.49 min. EO, elution order (conuration of the first eluted enantiomer); n.d., not determined.

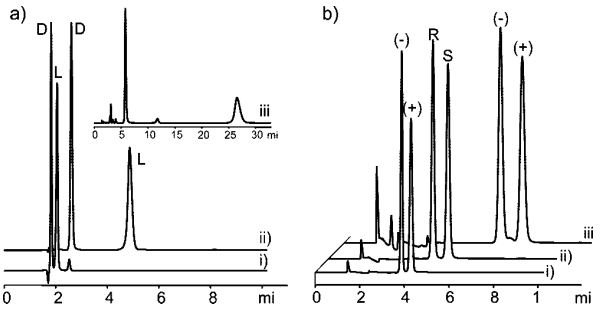

Figure 2. HPLC enantiomer separations on **CSP 3** of (a) acidic analytes (i) Ac-Phe, (ii) Ac-Trp, and (iii) DNB-Asp (see Table 1) and (b) basic analytes (i) butoxamine, (ii) celiprolol, and (iii) isoxsuprine (see Table 2). Mobile phase: 50 mM FA and 25 mM DEA in MeOH (acidic analytes) and ACN/MeOH (9/1 v/v; basic analytes).

sulfonic acid. Since both of the CSPs have almost identical SO loadings, the marked difference in retention between **CSP 1** and **CSP 2** can therefore be readily explained with acid strength: The stronger sulfonic acid in **CSP 2** is a more dominant intramolecular counterion compared to the weaker carboxylic acid in **CSP 1** and, consequently, leads to shorter retention times at similar acid concentrations in the mobile phase. Hence, retention factors on carboxylic acid-based **CSP 1** are up to 4-fold higher (e.g., for diacidic DNB-Glu) than on sulfonic acid-based **CSP 2**. At this point it should be noted that the effect of an intrinsic or intramolecular counterion on ion-exchanger-based enantioselective chromatography will be the topic of another detailed study that is currently in preparation. The partly significant differences in enantioselectivity and retention between sulfonic acid type **CSPs 3** and **4** at similar SO loadings reflect the diastereomeric relationship of these SOs relative to each other leading possibly to altered molecular recognition processes of the analytes.

Elution orders of analyte enantiomers may become a critical factor in practical applications and the ability to switch elution orders can be an instrumental tool, for instance, when it comes to impurity profiling and preparative enantioseparation.[49] In general, synthetic low molecular weight SOs and corresponding CSPs can offer the advantage that they allow a switch in the elution order by a change to the CSP of opposite configuration. For both parent CSPs of the herein presented zwitterionic CSPs

(49) Bicker, W.; Hebenstreit, D.; Lämmerhofer, M.; Lindner, W. *Electrophoresis* **2003**, *24*, 2532–2542.

Table 2. HPLC Enantiomer Separation of Various Chiral Basic Analytes on CSP 1-5[a]

Analyte [b]		k'_1	α	R_S	EO
1,1-Diphenylprolinol	CSP 1	1.24	**1.00**	**0.00**	
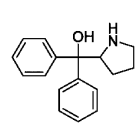	CSP 2	2.91	**1.00**	**0.00**	
1	CSP 3	2.89	**1.18**	**2.77**	-
	CSP 4	3.20	**1.08**	**1.26**	+
	CSP 5	1.88	**1.00**	**0.00**	
Bamethan	CSP 1	2.21	**1.00**	**0.00**	
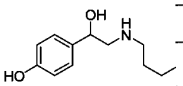	CSP 2	6.20	**1.00**	**0.00**	
2	CSP 3	6.51	**1.17**	**2.93**	-
	CSP 4	5.60	**1.00**	**0.00**	
	CSP 5	3.14	**1.00**	**0.00**	
Butoxamine	CSP 1	0.83	**1.13**	**0.56**	+
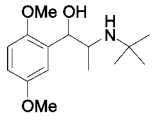	CSP 2	1.94	**1.12**	**1.57**	+
3	CSP 3	1.59	**1.17**	**2.34**	-
	CSP 4	1.69	**1.15**	**2.24**	+
	CSP 5	1.18	**1.12**	**1.10**	-
Mefloquine [c), d)]	CSP 1	1.06	**1.86**	**1.49**	+
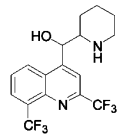	CSP 2	1.97	**1.31**	**3.28**	+
4	CSP 3	1.17	**15.17**	**11.97**	+
	CSP 4	1.89	**1.63**	**3.80**	+
	CSP 5	0. 91	**1.84**	**3.77**	-
Pseudo-Ephedrine	CSP 1	1.02	**1.00**	**0.00**	
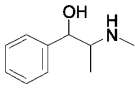	CSP 2	3.14	**1.00**	**0.00**	
5	CSP 3	2.83	**1.16**	**2.38**	-
	CSP 4	2.40	**1.00**	**0.00**	
	CSP 5	1.90	**1.00**	**0.00**	
Lorazepam [c)]	CSP 1	0.44	**1.00**	**0.00**	
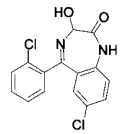	CSP 2	0.51	**1.00**	**0.00**	
6	CSP 3	0.46	**1.32**	**2.09**	n.d.
	CSP 4	0.38	**1.10**	**0.59**	n.d.
	CSP 5	0.38	**1.13**	**0.59**	n.d.

Analyte		k'_1	α	R_S	EO
Flecainid	CSP 1	0.65	**1.00**	**0.00**	
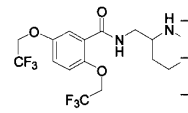	CSP 2	2.03	**1.00**	**0.00**	
7	CSP 3	2.21	**1.15**	**2.06**	+
	CSP 4	1.93	**1.16**	**2.22**	-
	CSP 5	1.16	**1.00**	**0.00**	
Isoxsuprine	CSP 1	1.51	**1.00**	**0.00**	
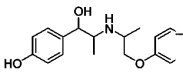	CSP 2	3.49	**1.03**	**0.20**	+
8	CSP 3	3.68	**1.18**	**2.81**	-
	CSP 4	3.43	**1.25**	**3.74**	+
	CSP 5	1.87	**1.00**	**0.00**	
O-*t*Bu-carbamoyl-Mefloquine [d)]	CSP 1	0.83	**1.00**	**0.00**	
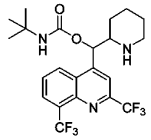	CSP 2	2.04	**1.09**	**1.08**	+
9	CSP 3	2.27	**1.16**	**2.11**	-
	CSP 4	2.00	**2.55**	**12.88**	+
	CSP 5	1.19	**1.00**	**0.00**	
Isopenbutolol	CSP 1	0.83	**1.00**	**0.00**	
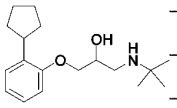	CSP 2	2.37	**1.04**	**0.54**	+(R)
10	CSP 3	2.21	**1.20**	**2.87**	+(R)
	CSP 4	2.10	**1.05**	**0.67**	+(R)
	CSP 5	1.41	**1.00**	**0.00**	
Bunitrolol	CSP 1	0.87	**1.00**	**0.00**	
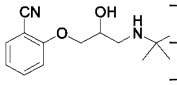	CSP 2	2.16	**1.06**	**0.58**	+
11	CSP 3	1.85	**1.18**	**2.51**	+
	CSP 4	1.79	**1.04**	**0.56**	+
	CSP 5	1.34	**1.00**	**0.00**	
Celiprolol	CSP 1	0.99	**1.00**	**0.00**	
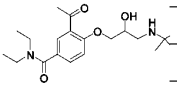	CSP 2	2.71	**1.05**	**0.56**	
12	CSP 3	2.13	**1.21**	**2.81**	
	CSP 4	2.03	**1.04**	**0.56**	
	CSP 5	1.42	**1.00**	**0.00**	

[a] Conditions: column dimension 150 × 4 mm i.d.; mobile phase, 50 mM formic acid and 25 mM diethylamine in acetonitrile/MeOH (9/1, v/v); flow 1.0 mL/min; T 25 °C; t_0 = 1.49 min. UV detection at 254 nm. n.d., not determined. EO, elution order (first eluted enantiomer). [b] Analyte description: name, entry number, structural forumula. [c] Mobile phase: 50 mM formic acid and 25 mM diethylamine in MeOH. [d] Mefloquine: *erythro*-α-2-piperidinyl-2,8-bis(trifluoromethyl)-4-quinolinemethanol.

(see Figure 1), this kind of elution order reversal has been shown previously,[14,43,48] e.g., for the quinine-based weak anion-exchanger CSP and its pseudoenantiomeric quinidine-based CSP. **CSPs 1−5** show similar behavior (Table 1). The elution order of chiral acidic analytes upon enantioseparation is always the same on zwitterionic **CSPs 1−4**, which are all quinine-based, and matches that reported in the literature for the parent, pure anion-exchanger-type quinine-based (WAX) CSP. By contrast, **CSP 5**, which employs pseudoenantiomeric quinidine as WAX part of the zwitterionic SO, leads to a reversal of the elution order compared to **CSPs 1−4**. These findings strongly suggest that the novel zwitterionic CSPs exhibit a *Cinchona* base dominated chiral recognition mechanism toward acidic analytes, which is very similar to the conventional quinine- and quinidine-type CSPs. Consequently, the acidic groups that have been introduced at the C9-position of the alkaloid moiety do not fundamentally alter this molecular recognition scenario, but mostly act as intramolecular counterions leading to reduced run times as compared to parent anion exchangers (see Figure 3a).

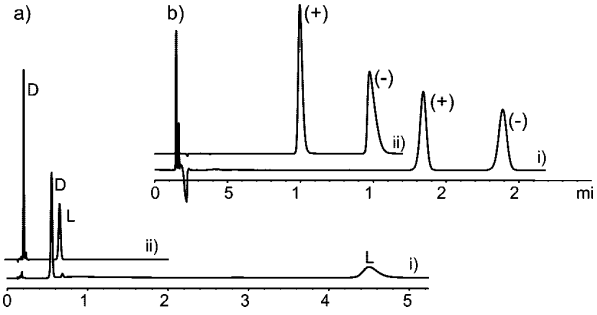

Figure 3. HPLC enantiomer separations of (a) DNB-Phe (see Table 1) on (i) **QN-AX** and (ii) **CSP 4** and (b) Mefloquine (see Table 2) on (i) SCX and (ii) **CSP 4**. Mobile phase: 50 mM HOAc and 25 mM NH_3 in MeOH.

Enantioseparation of Chiral Amines. After confirmation of enantioselectivity toward chiral acidic analytes due to their *Cinchona* base motif, the zwitterionic CSPs were investigated regarding their separation potential toward chiral amine enantiomers on the basis of their cation-exchanger site. It was particularly interesting to assess whether enantioselectivity could be transferred by incorporation of the *trans*-2-aminocyclohexanesulfonic acid moiety from the SCX CSP into the novel zwitterionic SOs or whether even an achiral acidic side chain in conjunction with the alkaloid structure could provide enantioselectivity for chiral amine solutes. For that purpose, a set of 12 chiral bases was studied that contained mainly amino alcohol-type pharmaceuticals such as β-blockers, β-sympathomimetics, and other drugs (see Table 2) as these analytes were typically well recognized by the parent pure SCX CSPs[14] and, thus, should support the characterization of novel zwitterionic CSPs in view of the parent SCX materials. The results are summarized in Table 2.

Overall, there are two distinct observations that correlate with the chirality of the acidic SO subunit. Both zwitterionic **CSPs 3** and **4**—that have chiral acidic moieties—show enantioselectivity toward the selected analytes similar to the parent SCX CSP in the range of $\alpha = 1.05-2.00$ (see also Figure 2b) but with reduced retention due to the intramolecular counterion activity of the *Cinchona* moiety (see Figure 3b). Thereby, **CSP 3** clearly provides a broad application range by baseline separating all of the 12 analytes. The diastereomeric **CSP 4,** however, shows less pronounced enantioselectivity by separating only one analyte better than **CSP 3** (entry 8 in Table 2) and five solutes in total. In contrast, **CSPs 1**, **2**, and **5**—each with acidic but achiral side chains—show negligible enantioselectivity toward the chosen set of analytes, with the exception of the antimalarial drug mefloquine (entry 4), which can be baseline separated with any of the five zwitterionic CSPs. This leads to the conclusion that the chiral *trans*-2-aminocyclohexanesulfonic acid moiety in **CSP 3** and **4** is truly beneficial but not essential for the observed enantioselective properties of the discussed zwitterionic CSPs toward chiral amines.

The measured elution orders do not show a general trend. When operating **CSPs 3** and **4**, which rely on diastereomeric chiral SOs but with opposite configuration of only their acid subunits, reversal of elution order was found for five solutes (entries 1, 3, 7, 8, and 9) while for four other analytes, elution order remained unchanged (entries 4, 10, 11, and 12), which is a clear indication that the chiral subunits of the fused zwitterionic entity do not act entirely independently from each other. Furthermore, comparison of elution orders on pseudoenantiomeric **CSPs 2** and **5**, which are reversed upon exchange of quinine by pseudoenantiomeric quinidine (entries 3 and 4), points toward a directing influence of the alkaloid motif. Obviously, it seems as if besides the crucial role of the chiral β-aminocyclohexanesulfonic acid moieties the "chiral environment" of the alkaloid substructure is also to some extent involved in an overall chiral recognition process toward the herein selected amine analytes. For instance, the very high enantioselectivity for mefloquine ($\alpha > 15$ on **CSP 3**) suggests that in this specific case the quinine motif is crucial and, in combination with the chiral acid subunit, enables an almost "ideal fit" of the well0bound mefloquine enantiomer.

The above-mentioned results on enantioseparations of chiral acids and chiral amines truly state that the "combinatorial concept" of combining both anion and cation exchangers in one SO motif has succeeded. Especially with **CSPs 3** and **4**, the chiral acidic and basic subunits that have been selected from the parent SCX and WAX CSPs (see Figure 1) maintain their individual enantiomer distinction capabilities when fused together in one single SO. Consequently, novel zwitterionic materials like **CSPs 3** and **4** now allow enantiomer separations of chiral acids and chiral bases with one single but zwitterionic ion-exchanger-type CSP.

Enantioseparation of Chiral Zwitterionic Analytes. Direct chromatographic enantiomer separation of zwitterionic analytes like unprotected amino acids using mild elution conditions and without problematic mobile-phase additives still remains a challenging task in the field of chiral separations. CSPs based on zwitterionic SOs could in this regard open up new applications for present enantioselective ion exchangers. First, it was of interest whether this can be accomplished and if so whether this phenomenon could be of broad scope. Second, the experiments were also designed to gain insights into such peculiar interaction mechanisms of chiral zwitterionic ion exchangers. For these purposes, a rather large, diverse set of zwitterionic analytes was compiled (Table 3), which included cyclic and acyclic, natural and nonnatural α- and β-amino acids with one and two chiral centers, with primary and secondary amino groups, with carboxylic and sulfonic acids, and with aliphatic, aromatic, and functional group-containing side chains as well as several dipeptides.

Chromatographic conditions that have been applied for enantioseparations of chiral acids and chiral amines on zwitterionic CSPs, according to conditions established for SCX and WAX CSPs (see sections above), proved to be directly applicable also for enantioseparation of zwitterionic analytes on zwitterionic **CSPs 1**−**5**.

Chromatographic results and solute structures are both summarized in Table 3. Prior to discussing these data in detail, some additional information should be provided: In a control experiment, both parent types of CSPs (see Figure 1) were tested for their enantiomer separation capabilities for nontarget solutes—quinine-based WAX toward basic and zwitterionic solutes and 2-aminocyclohexanesulfonic acid-based SCX toward acidic and zwitterionic analytes (see Tables 1−3). Basic analytes injected onto the WAX-type CSP eluted just before the void volume of the column and were not enantioseparated. Acidic solutes injected onto the SCX-type CSP showed similar behavior. These findings can be explained by the fact that, if SO and solute both carry a charge of the same sign, dominantly an electrostatic repulsion occurs and

Table 3. HPLC Enantiomer Separation of Various Chiral Zwitterionic Analytes on CSP 1-5[a]

Analyte[b]		k'_1	α	R_S	EO
Leucine	CSP 1	0.32	**1.00**	**0.00**	-
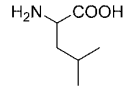	CSP 2	0.58	**1.00**	**0.00**	-
1	CSP 3	0.94	**1.25**	**1.47**	L
	CSP 4	0.54	**1.00**	**0.00**	-
	CSP 5	0.37	**1.00**	**0.00**	-
Isoleucine	CSP 1	0.31	**1.00**	**0.00**	-
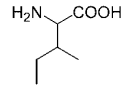	CSP 2	0.56	**1.00**	**0.00**	-
2	CSP 3	0.89	**1.28**	**1.94**	n.d.
	CSP 4	0.56	**1.14**	**0.62**	n.d.
	CSP 5	0.35	**1.00**	**0.00**	-
Norleucine	CSP 1	0.32	**1.00**	**0.00**	-
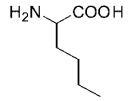	CSP 2	0.57	**1.00**	**0.00**	-
3	CSP 3	0.90	**1.28**	**1.94**	n.d.
	CSP 4	0.61	**1.05**	**0.35**	n.d.
	CSP 5	0.36	**1.00**	**0.00**	-
Neopentylglycine	CSP 1	0.37	**1.00**	**0.00**	-
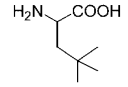	CSP 2	0.60	**1.08**	**0.42**	n.d.
4	CSP 3	1.08	**1.41**	**3.21**	n.d.
	CSP 4	0.67	**1.14**	**0.80**	n.d.
	CSP 5	0.42	**1.00**	**0.00**	-
Phenylglycine	CSP 1	0.52	**1.00**	**0.00**	-
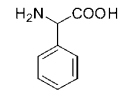	CSP 2	0.88	**1.00**	**0.00**	-
5	CSP 3	1.47	**1.03**	**0.37**	L
	CSP 4	0.73	**1.17**	**1.22**	D
	CSP 5	0.51	**1.13**	**0.58**	
β-Phenylalanine	CSP 1	0.63	**1.00**	**0.00**	-
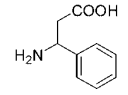	CSP 2	1.47	**1.00**	**0.00**	-
6	CSP 3	3.92	**1.11**	**1.45**	S
	CSP 4	1.05	**1.16**	**1.41**	S
	CSP 5	0.94	**1.12**	**0.64**	
Threonine	CSP 1	0.43	**1.00**	**0.00**	-
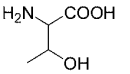	CSP 2	0.74	**1.00**	**0.00**	-
7	CSP 3	1.21	**1.26**	**1.94**	L
	CSP 4	0.68	**1.00**	**0.00**	-
	CSP 5	0.46	**1.00**	**0.00**	-
Eflornithine	CSP 1	0.90	**1.00**	**0.00**	-
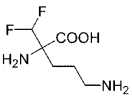	CSP 2	4.14	**1.26**	**0.59**	n.d.
8	CSP 3	9.65	**1.28**	**1.09**	n.d.
	CSP 4	2.53	**1.36**	**1.10**	n.d.
	CSP 5	1.96	**1.20**	**0.67**	n.d.
threo-Ritalinic acid	CSP 1				
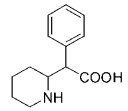	CSP 2				
17	CSP 3	3.21	**1.80**	**7.45**	n.d.
	CSP 4				
	CSP 5				
Tyrosine	CSP 1	0.64	**1.08**	**0.19**	D
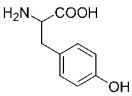	CSP 2	1.06	**1.07**	**0.38**	n.d.
18	CSP 3	1.65	**1.10**	**0.79**	n.d.
	CSP 4	0.97	**1.00**	**0.00**	-
	CSP 5	0.53	**1.04**	**0.26**	n.d.
meta-Tyrosine	CSP 1	0.83	**1.00**	**0.00**	-
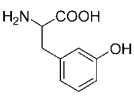	CSP 2	1.18	**1.07**	**0.48**	
19	CSP 3	1.86	**1.00**	**0.00**	-
	CSP 4	1.24	**1.00**	**0.00**	-
	CSP 5	0.76	**1.00**	**0.00**	-

Analyte		k'_1	α	R_S	EO
α-Methyl-Leucine	CSP 1	0.24	**1.00**	**0.00**	-
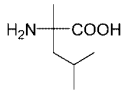	CSP 2	0.41	**1.11**	**0.54**	n.d.
9	CSP 3	0.52	**1.00**	**0.00**	-
	CSP 4	0.33	**1.47**	**1.67**	n.d.
	CSP 5	0.26	**1.00**	**0.00**	-
N-Methyl-Leucine	CSP 1	0.26	**1.00**	**0.00**	-
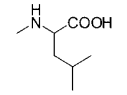	CSP 2	0.45	**1.00**	**0.00**	-
10	CSP 3	0.53	**1.12**	**0.60**	n.d.
	CSP 4	0.43	**1.00**	**0.00**	-
	CSP 5	0.28	**1.00**	**0.00**	-
tBu-Glycine	CSP 1	0.28	**1.00**	**0.00**	-
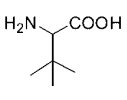	CSP 2	0.53	**1.00**	**0.00**	-
11	CSP 3	0.80	**1.48**	**3.38**	L
	CSP 4	0.54	**1.08**	**0.50**	L
	CSP 5	0.36	**1.00**	**0.00**	-
β-Neopentylglycine	CSP 1	0.33	**1.00**	**0.00**	-
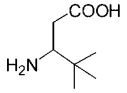	CSP 2	0.86	**1.10**	**0.67**	n.d.
12	CSP 3	2.04	**1.32**	**3.41**	n.d.
	CSP 4	0.57	**1.00**	**0.00**	-
	CSP 5	0.63	**1.15**	**0.75**	n.d.
Phenylalanine	CSP 1	0.51	**1.00**	**0.00**	-
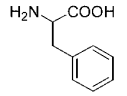	CSP 2	0.77	**1.06**	**0.45**	D
13	CSP 3	1.16	**1.17**	**1.50**	L
	CSP 4	0.73	**1.00**	**0.00**	-
	CSP 5	0.46	**1.00**	**0.00**	-
α-Methyl-	CSP 1	0.39	**1.29**	**0.75**	D
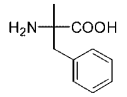	CSP 2	0.65	**1.28**	**1.99**	D
14	CSP 3	0.75	**1.17**	**1.38**	D
	CSP 4	0.60	**1.44**	**2.72**	D
	CSP 5	0.38	**1.25**	**1.38**	
Glutamate	CSP 1	1.53	**1.00**	**0.00**	-
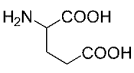	CSP 2	1.21	**1.00**	**0.00**	-
15	CSP 3	2.17	**1.06**	**0.56**	L
	CSP 4	1.23	**1.00**	**0.00**	-
	CSP 5	0.63	**1.00**	**0.00**	-
Cysteic acid	CSP 1				
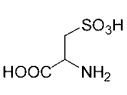	CSP 2	1.23	**1.00**	**0.00**	-
16	CSP 3	3.93	**1.15**	**1.24**	D
	CSP 4	1.84	**1.07**	**0.53**	n.d.
	CSP 5	0.76	**1.00**	**0.00**	-
erythro-Ritalinic	CSP 1				
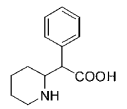	CSP 2				
25	CSP 3	1.82	**1.45**	**4.94**	n.d.
	CSP 4				
	CSP 5				
α-Methyl-Tyrosine	CSP 1	0.46	**1.35**	**0.87**	
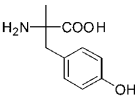	CSP 2	0.61	**1.37**	**2.63**	
26	CSP 3	0.97	**1.21**	**1.76**	D
	CSP 4	0.74	**1.44**	**2.89**	D
	CSP 5	0.51	**1.28**	**1.18**	L
α-Methyl-meta-Tyr	CSP 1	0.53	**1.43**	**1.24**	n.d.
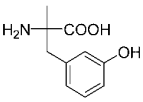	CSP 2	0.82	**1.34**	**1.72**	
27	CSP 3	1.00	**1.48**	**3.90**	n.d.
	CSP 4	0.87	**1.50**	**3.58**	n.d.
	CSP 5	0.55	**1.40**	**1.92**	n.d.

Table 3. Continued

Analyte		k'_1	α	R_S	EO
DOPA	**CSP 1**	1.25	**1.00**	**0.00**	-
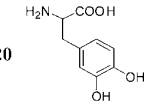	**CSP 2**	1.40	**1.09**	**0.29**	
20	**CSP 3**	2.26	**1.07**	**0.51**	
	CSP 4	1.26	**1.12**	**0.68**	
	CSP 5	0.81	**1.00**	**0.00**	-
Acetidine carboxylic	**CSP 1**	0.47	**1.00**	**0.00**	-
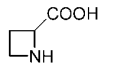	**CSP 2**	0.83	**1.00**	**0.00**	-
21	**CSP 3**	1.35	**1.35**	**2.93**	**n.d.**
	CSP 4	1.07	**1.00**	**0.00**	-
	CSP 5	0.48	**1.19**	**0.76**	**n.d.**
3,4-Dehydroproline	**CSP 1**	0.43	**1.00**	**0.00**	-
	**CSP 2**	0.65	**1.18**	**0.83**	**n.d.**
22	**CSP 3**	0.94	**1.95**	**5.18**	**n.d.**
	CSP 4	0.67	**1.29**	**1.30**	**n.d.**
	CSP 5	0.42	**1.23**	**0.63**	**n.d.**
Pipecolinic acid	**CSP 1**	0.33	**1.00**	**0.00**	-
	**CSP 2**	0.64	**1.00**	**0.00**	-
23	**CSP 3**	0.78	**1.13**	**0.87**	**L**
	CSP 4	0.57	**1.00**	**0.00**	-
	CSP 5	0.42	**1.12**	**0.50**	**D**
Nipecotic acid	**CSP 1**	0.55	**1.00**	**0.00**	-
	**CSP 2**	1.52	**1.12**	**0.73**	**R**
24	**CSP 3**	2.21	**1.95**	**7.12**	**R**
	CSP 4	1.42	**1.25**	**1.71**	**R**
	CSP 5	0.91	**1.20**	**1.14**	**S**
CHSA [d]	**CSP 1**	1.63	**1.00**	**0.00**	-
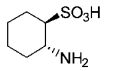	**CSP 2**	0.76	**1.00**	**0.00**	-
33	**CSP 3**	3.34	**1.08**	**0.90**	-
	CSP 4	0.90	**1.00**	**0.00**	-
	CSP 5	0.51	**1.00**	**0.00**	-
2-	**CSP 1**	0.36	**1.00**	**0.00**	-
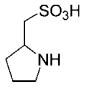	**CSP 2**	0.73	**1.14**	**1.12**	**R**
34	**CSP 3**	2.21	**1.22**	**2.59**	**R**
	CSP 4	0.77	**1.20**	**1.49**	**R**
	CSP 5	0.49	**1.09**	**0.51**	**n.d.**
Tryptophane	**CSP 1**	0.79	**1.49**	**1.02**	
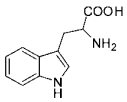	**CSP 2**	1.50	**1.61**	**5.13**	**D**
35	**CSP 3**	2.48	**1.66**	**6.12**	**D**
	CSP 4	1.48	**1.52**	**4.11**	**D**
	CSP 5	0.93	**1.41**	**2.42**	**L**
erythro-β-Methyl-	**CSP 1**	0.83	**1.85**	**2.03**	-
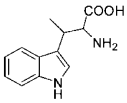	**CSP 2**	1.23	**2.15**	**9.26**	-
36	**CSP 3**	2.87	**2.25**	**9.98**	-
	CSP 4	1.54	**1.93**	**7.26**	-
	CSP 5	1.02	**1.90**	**4.29**	-
Gly-Phe	**CSP 1**	0.78	**1.39**	**0.82**	**n.d.**
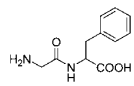	**CSP 2**	1.96	**1.34**	**3.09**	**n.d.**
37	**CSP 3**	2.69	**1.00**	**0.00**	-
	CSP 4	1.42	**1.29**	**2.60**	**n.d.**
	CSP 5	0.88	**1.75**	**3.75**	**n.d.**
Leu-Leu (D,D)/(L,L)	**CSP 1**	0.27	**2.00**	**1.63**	**n.d.**
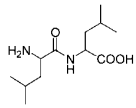	**CSP 2**	0.95	**1.55**	**3.67**	**n.d.**
38	**CSP 3**	1.15	**1.45**	**2.56**	**n.d.**
	CSP 4	0.69	**1.32**	**1.11**	**n.d.**
	CSP 5	0.41	**1.99**	**3.33**	**n.d.**

Analyte		k'_1	α	R_S	EO
α-Methyl-DOPA	**CSP 1**	0.74	**1.46**	**0.44**	**D**
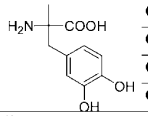	**CSP 2**	1.15	**1.49**	**3.57**	
28	**CSP 3**	1.35	**1.51**	**3.83**	**D**
	CSP 4	1.06	**1.54**	**3.48**	**D**
	CSP 5	0.68	**1.38**	**1.81**	**L**
Proline	**CSP 1**	0.42	**1.00**	**0.00**	-
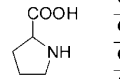	**CSP 2**	0.70	**1.13**	**0.66**	**L**
29	**CSP 3**	1.00	**1.64**	**4.30**	**L**
	CSP 4	0.64	**1.21**	**0.87**	**L**
	CSP 5	0.46	**1.26**	**1.00**	**D**
α-Methyl-Proline	**CSP 1**	0.33	**1.00**	**0.00**	-
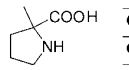	**CSP 2**	0.55	**1.11**	**0.65**	-
30	**CSP 3**	0.61	**1.79**	**4.65**	-
	CSP 4	0.48	**1.14**	**0.62**	-
	CSP 5	0.37	**1.20**	**0.66**	-
α-Benzyl-Proline	**CSP 1**	0.44	**1.38**	**0.84**	**n.d.**
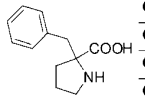	**CSP 2**	0.70	**1.44**	**2.74**	**n.d.**
31	**CSP 3**	0.56	**1.81**	**4.16**	**n.d.**
	CSP 4	0.64	**1.93**	**4.18**	**n.d.**
	CSP 5	0.50	**1.53**	**2.17**	**n.d.**
Tic [c]	**CSP 1**	0.52	**1.00**	**0.00**	-
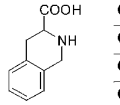	**CSP 2**	0.84	**1.10**	**0.78**	**S**
32	**CSP 3**	1.21	**1.33**	**3.07**	**S**
	CSP 4	0.84	**1.15**	**1.11**	**S**
	CSP 5	0.60	**1.11**	**0.57**	**R**
1,2-Dimethyl	**CSP 1**	0.23	**1.00**	**0.00**	-
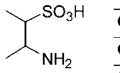	**CSP 2**	0.45	**1.00**	**0.00**	-
39	**CSP 3**	0.75	**1.82**	**6.02**	**n.d.**
	CSP 4	0.44	**1.14**	**0.67**	**n.d.**
	CSP 5	0.26	**1.00**	**0.00**	-
2-Amino-3,3-	**CSP 1**	0.27	**1.00**	**0.00**	-
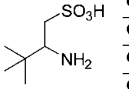	**CSP 2**	0.45	**1.69**	**3.41**	**D**
40	**CSP 3**	1.29	**2.60**	**10.70**	**D**
	CSP 4	0.53	**1.10**	**0.58**	**D**
	CSP 5	0.32	**1.60**	**1.99**	**L**
α-Methyl-Trp	**CSP 1**	0.73	**2.34**	**3.73**	**n.d.**
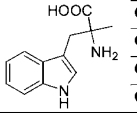	**CSP 2**	1.40	**2.66**	**11.41**	**n.d.**
41	**CSP 3**	1.70	**3.69**	**15.38**	**n.d.**
	CSP 4	1.39	**2.61**	**10.28**	**n.d.**
	CSP 5	0.88	**2.33**	**6.77**	**n.d.**
1-Methyl-Trp	**CSP 1**	0.85	**1.29**	**0.64**	
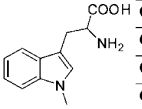	**CSP 2**	1.44	**1.33**	**2.02**	**D**
42	**CSP 3**	2.29	**1.38**	**3.66**	**D**
	CSP 4	1.34	**1.59**	**4.11**	**D**
	CSP 5	0.95	**1.19**	**1.18**	**L**
Ala-Phe (D,D)/(L,L)	**CSP 1**	0.58	**1.90**	**1.97**	**n.d.**
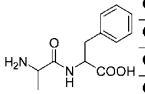	**CSP 2**	1.56	**1.59**	**5.89**	**n.d.**
43	**CSP 3**	1.57	**1.33**	**2.85**	**n.d.**
	CSP 4	1.19	**1.68**	**5.44**	**n.d.**
	CSP 5	0.70	**2.48**	**5.97**	**n.d.**
Pro-Phe (D,D)/(L,L)	**CSP 1**	0.93	**1.58**	**1.43**	**DD**
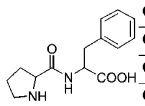	**CSP 2**	1.92	**1.91**	**6.42**	**DD**
44	**CSP 3**	1.64	**1.44**	**2.92**	**DD**
	CSP 4	1.94	**1.96**	**4.58**	**DD**
	CSP 5	0.94	**2.56**	**6.35**	**LL**

[a] Conditions: column dimension 150 × 4 mm i.d.; mobile phase, 50 mM formic acid and 25 mM diethylamine in MeOH; flow 1.0 mL/min; *T* 25 °C; t_0 = 1.50 min. EO, elution order (conuration of the first eluted enantiomer). n.d., not determined. [b] Analyte description: name, entry number, structural formula. [c] Tic: 1,2,3,4-tetrahydroisoquinoline-3-carboxylic acid. [d] CHSA: *trans*-2-aminocyclohexanesulfonic acid (1*S*,2*S*)/(1*R*,2*R*).

the solutes are excluded rather than retained by the CSP. For zwitterionic analytes under the given, weakly acidic mobile-phase conditions, only very weak retentions and no enantioseparations were observed on both SCX and WAX CSPs (corresponding data not shown). In sharp contrast, zwitterionic analytes (viz. chiral amino acids) could be readily resolved into enantiomers on the novel zwitterionic **CSPs 1**−**5**. Moreover, *β*-amino acid enantiomers were typically stronger retained and partly better enantioseparated than related α-amino acids (i.e., see entries 23 and 24 in Table 3). These findings lead to the conclusion that both charged sites of the zwitterionic solute, the protonated amine and the dissociated acid, are recognized more or less simultaneously by the likewise doubly ionized zwitterionic SOs of **CSPs 1**−**5** and that this double ionic interaction is fundamental for the observed enantioseparation of zwitterionic analytes on zwitterionic **CSPs 1**−**5**.

For all compounds shown in Table 3, baseline separation or at least partial separation could be achieved with one of the five zwitterionic CSPs. Since the set of analytes is quite diverse, a broad scope of applicability regarding enantiomer separations of chiral zwitterionic analytes could be attributed for the novel zwitterionic CSPs. Of course, column performance is not equally distributed among the different CSPs and toward each of the analytes. Regarding the trends among the analyte structures, for instance, the group of tryptophan and its derivatives could be very well separated while for other amino acids that contain aromatic groups like the phenylalanines and the tyrosines enantioselectivities were lower and a full baseline separation was not always possible with the given nonoptimized eluent. Moreover, cyclic amino acids having a secondary amine group were slightly better separated than acyclic aliphatic amino acids of the leucine and glycine type, which might be due to their more rigid structure. On the other hand, it is surprising that no separation was accomplished for the *trans*-2-aminocyclohexanesulfonic acid (entry 33), a moiety that is an essential part of the SOs of **CSP 3** and **4**, while for 1,2-dimethyltaurine (entry 39), the acyclic counterpart, decent enantioselectivity could be obtained. A more general observation was that for α-alkyl-substituted α-amino acids' enantioselectivity was clearly increased compared to the nonsubstituted compounds as can be seen, for example, for phenylalanine (entries 13 and 14) or tyrosine (entries 18 and 26). Exemplary chromatograms of enantiomer separations of cyclic as well as acyclic α- and *β*-amino acids using **CSP 3** are shown in Figure 4 to also illustrate the typically observed appealing separation efficiencies and peak symmetries in the zwitterion exchange mode.

However, for some particular solutes, separation suffered from peak tailing so that no full baseline separations could be obtained under given conditions despite reasonable enantioselectivities, such as for eflornithine and other amino acids that carry additional functional groups. Such phenomena, which may originate from a slow desorption kinetics or heterogeneous mass-transfer characteristics, point toward improper counterion strength or type. Optimal adjustment of the mobile phase and its pH or proton activity is expected to reduce such phenomena but was not further investigated in this study.

Besides the expected solute-specific structure−enantioselectivity relationships that can be derived from the data shown in Table 3, SO structure variations also exert profound consequences on the enantioseparation abilities of the zwitterionic CSPs.

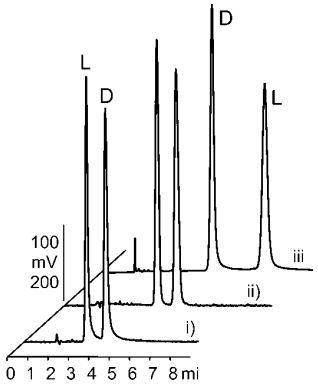

Figure 4. HPLC enantiomer separations of amino acids (i) DL-proline, (ii) dl-*β*-neopentylglycine, and (iii) DL-tryptophan on zwitterionic **CSP 3** (see also Table 3). Mobile phase: 50 mM FA and 25 mM DEA in MeOH. Detection: CAD or UV at 254 nm.

As mentioned above, **CSPs 1** and **2**, which are structural homologues that differ only in the type of their acidic function, have been designed and synthesized for the purpose of comparing the carboxylic and sulfonic acid function within a zwitterionic SO. Despite close structural similarity, results from Table 3 indicate marked differences on their separation performances for amino acids. Retention factors for amphoteric solutes are always lower on the carboxylic acid-based **CSP 1** than on the sulfonic acid-based **CSP 2**. In contrast to acidic solutes, a stronger acid moiety in the SO leads to a stronger ionic interaction with basic groups of the zwitterionic analytes at the active cation-exchange site under the given mobile-phase conditions. Furthermore, **CSP 2** provides better peak efficiency yielding noticeably improved resolution even if enantioselectivity is similar (see entry 28 of Table 3). Dedicated mobile-phase optimizations might possibly level out this effect. However, it appears that the sulfonic acid function is better suited for making an easy-to-use zwitterionic CSP.

CSPs 3 and **4** both rely on quinine- and *trans*-2-aminocyclohexanesulfonic acid-based SOs and are diastereomeric to each other due to opposite configurations within the amino acid part, i.e., the cation-exchange subunit, only. Despite entirely identical structural increments, differences in their enantioselectivity profiles toward zwitterionic analytes may be expected due to their diastereomeric relationship. This is indeed corroborated by the fact that **CSP 3** shows larger retention factors for all but one analyte from Table 3 (entry 31). Apparently, the configurational ensemble of **CSP 3** is associated with a conformational arrangement being more favorable in terms of spatial orientations of the primary cation−anion-exchange sites for simultaneous solute−selector contacts through double ionic interactions with the zwitterionic analytes. Hence, an overall tighter binding of amino acids and peptides is observed as compared to **CSP 4**. In principle, though, stronger binding does not necessarily mean higher enantioselectivity. However, roughly 75% of all analytes are also better separated on **CSP 3** than on **CSP 4**.

In summary, **CSP 3** provides both a broader scope of applicability and higher separation factors among all zwitterionic CSPs presented in this study. It clearly illustrates the inherent potential of the combinatorial concept of synthetic low molecular

mass chiral selectors, which is readily capable for dedicated synthetic SO structure optimizations. As a beneficial side effect of this approach, valuable information on molecular recognition events is provided and ideas how to rationally design new, even more potent CSPs are given.

Elution order is a piece of information that must not be left out of consideration in the course of elucidations of chiral recognition mechanisms. In the present cases, elution orders should help to attribute enantioselective interactions to the different acidic and basic active subunits of the SOs in the series of **CSPs 1**−**5**. Therefore, the elution orders of several analytes from Table 3 were determined, when individual enantiomers were available.

At first, the influence of the acid subunit is to be regarded since the acidic moieties (i.e., the cation-exchange subunits) of zwitterionic **CSPs 3** and **4** are of opposite configuration and could potentially influence elution order. In other words, the elution order should be reversed if this substructure alone is the dominating and exclusively directing center of chiral recognition. Still, no change in elution order for amphoteric amino acid analytes is observed between the two diastereomeric cyclohexanesulfonic acid-based materials, indicating that the chiral acidic moieties are important but not exclusively dominant in the enantiodistinction process of zwitterionic solutes. Furthermore, also **CSPs 1** and **2**, which contain achiral acidic moieties, show elution orders identical to **CSPs 3** and **4**. In other words, all four CSPs that employ the quinine motif provide the same elution order. Only with **CSP 5**, which is based on quinidine and is pseudoenantiomeric to **CSP 2**, elution orders of zwitterionic solutes are inverted. Altogether, these findings are strong empirical evidence that the alkaloid moiety is of central importance in the chiral recognition process and plays with its particular configurational arrangement a directing role for the relative enantiomer affinities and elution orders, not only for chiral acidic analytes but also for chiral zwitterionic and amphoteric compounds likewise. Consequently, also in zwitterion-exchange mode, elution order can principally be reversed simply by changing to the (pseudo)enantiomeric form of the zwitterionic CSP, a valuable feature of such synthetic low molecular mass-type SOs and corresponding CSPs that comparably versatile CSPs from the natural chiral pool (e.g., antibiotics-based CSPs) do not offer so easily.

CONCLUSION

Novel ion-exchanger-type CSPs based on zwitterionic selectors have been prepared and evaluated for the enantiomer separation of chiral acids, amines, and amino acids in HPLC. The presented SOs combine in a combinatorial approach key cation- and anion-exchanger SO motifs in one single chiral compound resulting zwitterionic CSPs using straightforward synthesis and mainly conventional commercially available starting materials. Chromatographic evaluation showed that, especially with **CSPs 3** and **4**, packing materials were generated with essentially combined enantioseparation capabilities of the parent WAX and SCX CSPs toward chiral acidic and basic analytes. Additionally, this conceptual SO combination provided powerful CSPs that enable also enantioseparations of zwitterionic analytes via a double ion-pairing process. Baseline separation or at least partial separation of 40 amino acids of various types and structures as well as dipeptides could be achieved with novel zwitterionic **CSPs 1**−**5** without dedicated mobile-phase optimizations, with **CSP 3** providing the broadest scope of applicability. The above structure−enantioselectivity relationship studies clearly unveiled that for the latter class of compounds the individual charge centers of the new zwitterionic ion exchangers act in a synergistic way through double ion-pairing (ion-exchange)-mediated processes. The pronounced differences in enantioselectivity in-between structurally different but closely related **CSPs 1**−**5** also in the zwitterion exchange mode indicate the potential of SO structure-based optimization of selectivity available with low molecular mass chiral SOs, in particular when expanding the herein employed combinatorial synthetic approach using various cation- and anion-exchanger building blocks for their preparation. Subsequently, further improvement of overall enantioselectivity by means of SO structure optimization as well as target-oriented SO design for a preparative separation challenge seem possible.

From a practical point of view, the current zwitterionic CSPs should have considerable impact for enantiomer separations of amino acids. Mild elution conditions, preclusion of problematic additives from the mobile phase, ability to systematically reverse elution orders, and the potential of elevated sample loadabilities are characteristic benefits over state-of-the-art technology, which could make these zwitterionic chiral ion exchangers appealing for practical applications of enantiomer separations of amino acid and other polar analytes.

ACKNOWLEDGMENT

The financial support of this research project by the Austrian Christian Doppler Research Society and the industrial partners AstraZeneca (Mölndal, Sweden) and Merck (Darmstadt, Germany) is gratefully acknowledged. The authors thank in particular Dr. Antál Péter for providing us with a sample of *erythro*-β-methyl tryptophan.

SUPPORTING INFORMATION AVAILABLE

Results and Discussion on preparation of **CSPs 1**−**5**, Figure S-1 on CSP synthesis, general information and materials for synthesis, synthetic procedures for the preparation of **CSPs 1**−**5** including characterization data, Figures S-2 and S-3 on supplementary HPLC chromatograms of enantioseparations on zwitterionic CSPs, references. This material is available free of charge via the Internet at http://pubs.acs.org.

Received for review July 4, 2008. Accepted August 29, 2008.

AC801384F

Table 3. HPLC enantiomer separation of various chiral zwitterionic analytes on CSP 1-5[a)]

Analyte [b)]		k'_1	α	R_S	EO
Leucine	**CSP 1**	0.32	**1.00**	**0.00**	-
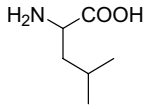	**CSP 2**	0.58	**1.00**	**0.00**	-
	CSP 3	0.94	**1.25**	**1.47**	L
1	**CSP 4**	0.54	**1.00**	**0.00**	-
	CSP 5	0.37	**1.00**	**0.00**	-
Isoleucine	**CSP 1**	0.31	**1.00**	**0.00**	-
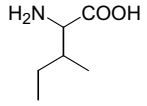	**CSP 2**	0.56	**1.00**	**0.00**	-
	CSP 3	0.89	**1.28**	**1.94**	**n.d.**
2	**CSP 4**	0.56	**1.14**	**0.62**	**n.d.**
	CSP 5	0.35	**1.00**	**0.00**	-
Norleucine	**CSP 1**	0.32	**1.00**	**0.00**	-
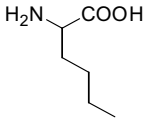	**CSP 2**	0.57	**1.00**	**0.00**	-
	CSP 3	0.90	**1.28**	**1.94**	**n.d.**
3	**CSP 4**	0.61	**1.05**	**0.35**	**n.d.**
	CSP 5	0.36	**1.00**	**0.00**	-
Neopentylglycine	**CSP 1**	0.37	**1.00**	**0.00**	-
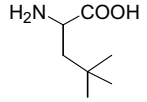	**CSP 2**	0.60	**1.08**	**0.42**	**n.d.**
	CSP 3	1.08	**1.41**	**3.21**	**n.d.**
4	**CSP 4**	0.67	**1.14**	**0.80**	**n.d.**
	CSP 5	0.42	**1.00**	**0.00**	-
Phenylglycine	**CSP 1**	0.52	**1.00**	**0.00**	-
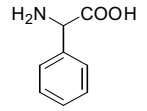	**CSP 2**	0.88	**1.00**	**0.00**	-
	CSP 3	1.47	**1.03**	**0.37**	**L**
5	**CSP 4**	0.73	**1.17**	**1.22**	**D**
	CSP 5	0.51	**1.13**	**0.58**	**D**
β-Phenylalanine	**CSP 1**	0.63	**1.00**	**0.00**	-
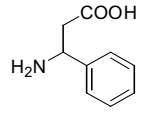	**CSP 2**	1.47	**1.00**	**0.00**	-
	CSP 3	3.92	**1.11**	**1.45**	**S**
6	**CSP 4**	1.05	**1.16**	**1.41**	**S**
	CSP 5	0.94	**1.12**	**0.64**	**R**
Threonine	**CSP 1**	0.43	**1.00**	**0.00**	-
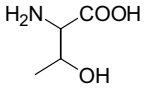	**CSP 2**	0.74	**1.00**	**0.00**	-
	CSP 3	1.21	**1.26**	**1.94**	**L**
7	**CSP 4**	0.68	**1.00**	**0.00**	-
	CSP 5	0.46	**1.00**	**0.00**	-
Eflornithine	**CSP 1**	0.90	**1.00**	**0.00**	-
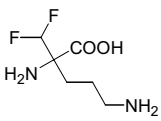	**CSP 2**	4.14	**1.26**	**0.59**	**n.d.**
	CSP 3	9.65	**1.28**	**1.09**	**n.d.**
8	**CSP 4**	2.53	**1.36**	**1.10**	**n.d.**
	CSP 5	1.96	**1.20**	**0.67**	**n.d.**

Analyte		k'_1	α	R_S	EO
α-Methyl-Leucine	**CSP 1**	0.24	**1.00**	**0.00**	-
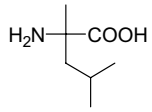	**CSP 2**	0.41	**1.11**	**0.54**	**n.d.**
	CSP 3	0.52	**1.00**	**0.00**	-
9	**CSP 4**	0.33	**1.47**	**1.67**	**n.d.**
	CSP 5	0.26	**1.00**	**0.00**	-
N-Methyl-Leucine	**CSP 1**	0.26	**1.00**	**0.00**	-
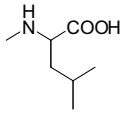	**CSP 2**	0.45	**1.00**	**0.00**	-
	CSP 3	0.53	**1.12**	**0.60**	**n.d.**
10	**CSP 4**	0.43	**1.00**	**0.00**	-
	CSP 5	0.28	**1.00**	**0.00**	-
tBu-Glycine	**CSP 1**	0.28	**1.00**	**0.00**	-
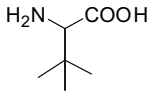	**CSP 2**	0.53	**1.00**	**0.00**	-
	CSP 3	0.80	**1.48**	**3.38**	**L**
11	**CSP 4**	0.54	**1.08**	**0.50**	**L**
	CSP 5	0.36	**1.00**	**0.00**	-
β-Neopentylglycine	**CSP 1**	0.33	**1.00**	**0.00**	-
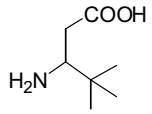	**CSP 2**	0.86	**1.10**	**0.67**	**n.d.**
	CSP 3	2.04	**1.32**	**3.41**	**n.d.**
12	**CSP 4**	0.57	**1.00**	**0.00**	-
	CSP 5	0.63	**1.15**	**0.75**	**n.d.**
Phenylalanine	**CSP 1**	0.51	**1.00**	**0.00**	-
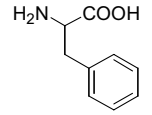	**CSP 2**	0.77	**1.06**	**0.45**	**D**
	CSP 3	1.16	**1.17**	**1.50**	**L**
13	**CSP 4**	0.73	**1.00**	**0.00**	-
	CSP 5	0.46	**1.00**	**0.00**	-
α-Methyl-Phenylalanine	**CSP 1**	0.39	**1.29**	**0.75**	**D**
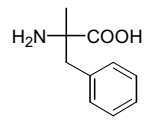	**CSP 2**	0.65	**1.28**	**1.99**	**D**
	CSP 3	0.75	**1.17**	**1.38**	**D**
14	**CSP 4**	0.60	**1.44**	**2.72**	**D**
	CSP 5	0.38	**1.25**	**1.38**	**L**
Glutamate	**CSP 1**	1.53	**1.00**	**0.00**	-
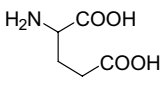	**CSP 2**	1.21	**1.00**	**0.00**	-
	CSP 3	2.17	**1.06**	**0.56**	**L**
15	**CSP 4**	1.23	**1.00**	**0.00**	-
	CSP 5	0.63	**1.00**	**0.00**	-
Cysteic acid	**CSP 1**				
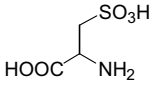	**CSP 2**	1.23	**1.00**	**0.00**	-
	CSP 3	3.93	**1.15**	**1.24**	**D**
16	**CSP 4**	1.84	**1.07**	**0.53**	**n.d.**
	CSP 5	0.76	**1.00**	**0.00**	-

Analyte		k'_1	α	R_S	EO
threo-Ritalinic acid	**CSP 1**				
	CSP 2				
	CSP 3	3.21	**1.80**	**7.45**	**n.d.**
17 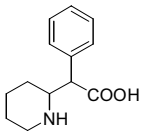	**CSP 4**				
	CSP 5				
Tyrosine	**CSP 1**	0.64	**1.08**	**0.19**	**D**
	CSP 2	1.06	**1.07**	**0.38**	**n.d.**
	CSP 3	1.65	**1.10**	**0.79**	**n.d.**
18 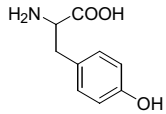	**CSP 4**	0.97	**1.00**	**0.00**	**-**
	CSP 5	0.53	**1.04**	**0.26**	**n.d.**
meta-Tyrosine	**CSP 1**	0.83	**1.00**	**0.00**	**-**
	CSP 2	1.18	**1.07**	**0.48**	**n.d.**
	CSP 3	1.86	**1.00**	**0.00**	**-**
19 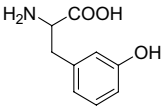	**CSP 4**	1.24	**1.00**	**0.00**	**-**
	CSP 5	0.76	**1.00**	**0.00**	**-**
DOPA	**CSP 1**	1.25	**1.00**	**0.00**	**-**
	CSP 2	1.40	**1.09**	**0.29**	**n.d.**
	CSP 3	2.26	**1.07**	**0.51**	**n.d.**
20 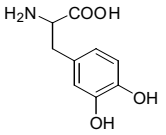	**CSP 4**	1.26	**1.12**	**0.68**	**n.d.**
	CSP 5	0.81	**1.00**	**0.00**	**-**
Acetidine carboxylic acid	**CSP 1**	0.47	**1.00**	**0.00**	**-**
	CSP 2	0.83	**1.00**	**0.00**	**-**
	CSP 3	1.35	**1.35**	**2.93**	**n.d.**
21 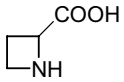	**CSP 4**	1.07	**1.00**	**0.00**	**-**
	CSP 5	0.48	**1.19**	**0.76**	**n.d.**
3,4-Dehydroproline	**CSP 1**	0.43	**1.00**	**0.00**	**-**
	CSP 2	0.65	**1.18**	**0.83**	**n.d.**
	CSP 3	0.94	**1.95**	**5.18**	**n.d.**
22 	**CSP 4**	0.67	**1.29**	**1.30**	**n.d.**
	CSP 5	0.42	**1.23**	**0.63**	**n.d.**
Pipecolinic acid	**CSP 1**	0.33	**1.00**	**0.00**	**-**
	CSP 2	0.64	**1.00**	**0.00**	**-**
	CSP 3	0.78	**1.13**	**0.87**	**L**
23 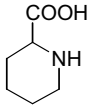	**CSP 4**	0.57	**1.00**	**0.00**	**-**
	CSP 5	0.42	**1.12**	**0.50**	**D**
Nipecotic acid	**CSP 1**	0.55	**1.00**	**0.00**	**-**
	CSP 2	1.52	**1.12**	**0.73**	**R**
	CSP 3	2.21	**1.95**	**7.12**	**R**
24 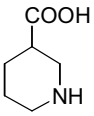	**CSP 4**	1.42	**1.25**	**1.71**	**R**
	CSP 5	0.91	**1.20**	**1.14**	**S**

Analyte		k'_1	α	R_S	EO
erythro-Ritalinic acid	**CSP 1**				
	CSP 2				
	CSP 3	1.82	**1.45**	**4.94**	**n.d.**
25 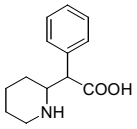	**CSP 4**				
	CSP 5				
α-Methyl-Tyrosine	**CSP 1**	0.46	**1.35**	**0.87**	**D**
	CSP 2	0.61	**1.37**	**2.63**	**D**
	CSP 3	0.97	**1.21**	**1.76**	**D**
26 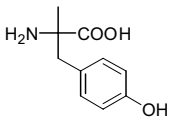	**CSP 4**	0.74	**1.44**	**2.89**	**D**
	CSP 5	0.51	**1.28**	**1.18**	**L**
α-Methyl-meta-Tyr	**CSP 1**	0.53	**1.43**	**1.24**	**n.d.**
	CSP 2	0.82	**1.34**	**1.72**	**n.d.**
	CSP 3	1.00	**1.48**	**3.90**	**n.d.**
27 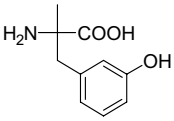	**CSP 4**	0.87	**1.50**	**3.58**	**n.d.**
	CSP 5	0.55	**1.40**	**1.92**	**n.d.**
α-Methyl-DOPA	**CSP 1**	0.74	**1.46**	**0.44**	**D**
	CSP 2	1.15	**1.49**	**3.57**	**D**
	CSP 3	1.35	**1.51**	**3.83**	**D**
28 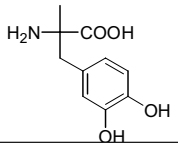	**CSP 4**	1.06	**1.54**	**3.48**	**D**
	CSP 5	0.68	**1.38**	**1.81**	**L**
Proline	**CSP 1**	0.42	**1.00**	**0.00**	**-**
	CSP 2	0.70	**1.13**	**0.66**	**L**
	CSP 3	1.00	**1.64**	**4.30**	**L**
29 	**CSP 4**	0.64	**1.21**	**0.87**	**L**
	CSP 5	0.46	**1.26**	**1.00**	**D**
α-Methyl-Proline	**CSP 1**	0.33	**1.00**	**0.00**	**-**
	CSP 2	0.55	**1.11**	**0.65**	**-**
	CSP 3	0.61	**1.79**	**4.65**	**-**
30 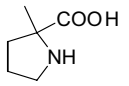	**CSP 4**	0.48	**1.14**	**0.62**	**-**
	CSP 5	0.37	**1.20**	**0.66**	**-**
α-Benzyl-Proline	**CSP 1**	0.44	**1.38**	**0.84**	**n.d.**
	CSP 2	0.70	**1.44**	**2.74**	**n.d.**
	CSP 3	0.56	**1.81**	**4.16**	**n.d.**
31 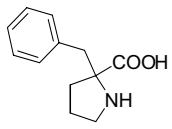	**CSP 4**	0.64	**1.93**	**4.18**	**n.d.**
	CSP 5	0.50	**1.53**	**2.17**	**n.d.**
Tic [c)]	**CSP 1**	0.52	**1.00**	**0.00**	**-**
	CSP 2	0.84	**1.10**	**0.78**	**S**
	CSP 3	1.21	**1.33**	**3.07**	**S**
32 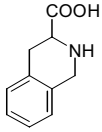	**CSP 4**	0.84	**1.15**	**1.11**	**S**
	CSP 5	0.60	**1.11**	**0.57**	**R**

Analyte		k'_1	α	R_S	EO
CHSA [d]	**CSP 1**	1.63	**1.00**	**0.00**	**-**
	CSP 2	0.76	**1.00**	**0.00**	**-**
33 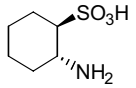	**CSP 3**	3.34	**1.08**	**0.90**	**-**
	CSP 4	0.90	**1.00**	**0.00**	**-**
	CSP 5	0.51	**1.00**	**0.00**	**-**
2-Pyrrolidinemethane-sulfonic acid	**CSP 1**	0.36	**1.00**	**0.00**	**-**
	CSP 2	0.73	**1.14**	**1.12**	**R**
34 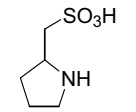	**CSP 3**	2.21	**1.22**	**2.59**	**R**
	CSP 4	0.77	**1.20**	**1.49**	**R**
	CSP 5	0.49	**1.09**	**0.51**	**n.d.**
Tryptophane	**CSP 1**	0.79	**1.49**	**1.02**	**D**
	CSP 2	1.50	**1.61**	**5.13**	**D**
35 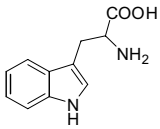	**CSP 3**	2.48	**1.66**	**6.12**	**D**
	CSP 4	1.48	**1.52**	**4.11**	**D**
	CSP 5	0.93	**1.41**	**2.42**	**L**
erythro-β-Methyl-Trp	**CSP 1**	0.83	**1.85**	**2.03**	**-**
	CSP 2	1.23	**2.15**	**9.26**	**-**
36 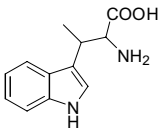	**CSP 3**	2.87	**2.25**	**9.98**	**-**
	CSP 4	1.54	**1.93**	**7.26**	**-**
	CSP 5	1.02	**1.90**	**4.29**	**-**
Gly-Phe	**CSP 1**	0.78	**1.39**	**0.82**	**n.d.**
	CSP 2	1.96	**1.34**	**3.09**	**n.d.**
37 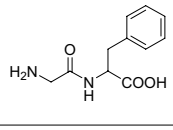	**CSP 3**	2.69	**1.00**	**0.00**	**-**
	CSP 4	1.42	**1.29**	**2.60**	**n.d.**
	CSP 5	0.88	**1.75**	**3.75**	**n.d.**
Leu-Leu (D,D)/(L,L)	**CSP 1**	0.27	**2.00**	**1.63**	**n.d.**
	CSP 2	0.95	**1.55**	**3.67**	**n.d.**
38 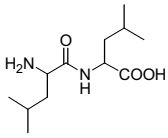	**CSP 3**	1.15	**1.45**	**2.56**	**n.d.**
	CSP 4	0.69	**1.32**	**1.11**	**n.d.**
	CSP 5	0.41	**1.99**	**3.33**	**n.d.**

Analyte		k'_1	α	R_S	EO
1,2-Dimethyl Taurine (S,R)/(R,S)	**CSP 1**	0.23	**1.00**	**0.00**	**-**
	CSP 2	0.45	**1.00**	**0.00**	**-**
39 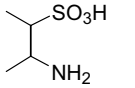	**CSP 3**	0.75	**1.82**	**6.02**	**n.d.**
	CSP 4	0.44	**1.14**	**0.67**	**n.d.**
	CSP 5	0.26	**1.00**	**0.00**	**-**
2-Amino-3,3-dimethyl-1-butanesulfonic acid	**CSP 1**	0.27	**1.00**	**0.00**	**-**
	CSP 2	0.45	**1.69**	**3.41**	**D**
40 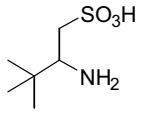	**CSP 3**	1.29	**2.60**	**10.70**	**D**
	CSP 4	0.53	**1.10**	**0.58**	**D**
	CSP 5	0.32	**1.60**	**1.99**	**L**
α-Methyl-Trp	**CSP 1**	0.73	**2.34**	**3.73**	**n.d.**
	CSP 2	1.40	**2.66**	**11.41**	**n.d.**
41 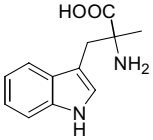	**CSP 3**	1.70	**3.69**	**15.38**	**n.d.**
	CSP 4	1.39	**2.61**	**10.28**	**n.d.**
	CSP 5	0.88	**2.33**	**6.77**	**n.d.**
1-Methyl-Trp	**CSP 1**	0.85	**1.29**	**0.64**	**D**
	CSP 2	1.44	**1.33**	**2.02**	**D**
42 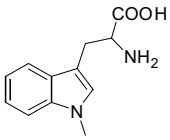	**CSP 3**	2.29	**1.38**	**3.66**	**D**
	CSP 4	1.34	**1.59**	**4.11**	**D**
	CSP 5	0.95	**1.19**	**1.18**	**L**
Ala-Phe (D,D)/(L,L)	**CSP 1**	0.58	**1.90**	**1.97**	**n.d.**
	CSP 2	1.56	**1.59**	**5.89**	**n.d.**
43 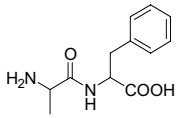	**CSP 3**	1.57	**1.33**	**2.85**	**n.d.**
	CSP 4	1.19	**1.68**	**5.44**	**n.d.**
	CSP 5	0.70	**2.48**	**5.97**	**n.d.**
Pro-Phe (D,D)/(L,L)	**CSP 1**	0.93	**1.58**	**1.43**	**DD**
	CSP 2	1.92	**1.91**	**6.42**	**DD**
44 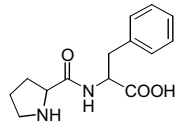	**CSP 3**	1.64	**1.44**	**2.92**	**DD**
	CSP 4	1.94	**1.96**	**4.58**	**DD**
	CSP 5	0.94	**2.56**	**6.35**	**LL**

[a] Conditions: column dimension 150 x 4 mm I.D.; mobile phase: 50 mM formic acid and 25mM diethylamine in MeOH; flow 1.0 ml/min; T 25° C; t_0 = 1.50 min. EO = elution order (configuration of the first eluted enantiomer). n.d. = not determined.

[b] Analyte description: name, entry number, structural formula.

[c] Tic: 1,2,3,4-tetrahydroisoquinoline-3-carboxylic acid

[d] CHSA: trans-2-aminocyclohexanesulfonic acid (1*S*,2*S*)/(1*R*,2*R*)

Supporting Information:

Synergistic Effects on Enantioselectivity of Novel Zwitterionic Chiral Stationary Phases for Separations of Chiral Acids, Bases, and Amino Acids by HPLC

*Christian V. Hoffmann, Reinhard Pell, Michael Lämmerhofer, Wolfgang Lindner**

Christian Doppler Laboratory for Molecular Recognition Materials, Department of Analytical Chemistry & Food Chemistry, University of Vienna, Währinger Strasse 38, A-1090 Vienna, Austria.

*Author for correspondence:
e-mail: Wolfgang.Lindner@univie.ac.at
Tel.: ++43-1-4277-52300
Fax: ++43-1-4277-9523

Table of Contents

Results and Discussion on the Preparation of CSP 1-5.

For carbamate-type derivatization with amino acids at the C9-position, quinine **1a** and quinidine **1b**, respectively, were activated by reaction with 4-nitrophenyl chloroformate[1] whereupon hydrochloride salts **2a** and **2b** precipitated from the reaction solution and could

be collected by filtration (Figure S-1). The achiral β-amino acids to be coupled were commercially available compounds like taurine and β-alanine while the chiral trans-2-aminocyclohexanesulfonic acid building block was prepared as a racemate according to published procedures.[2, 3]

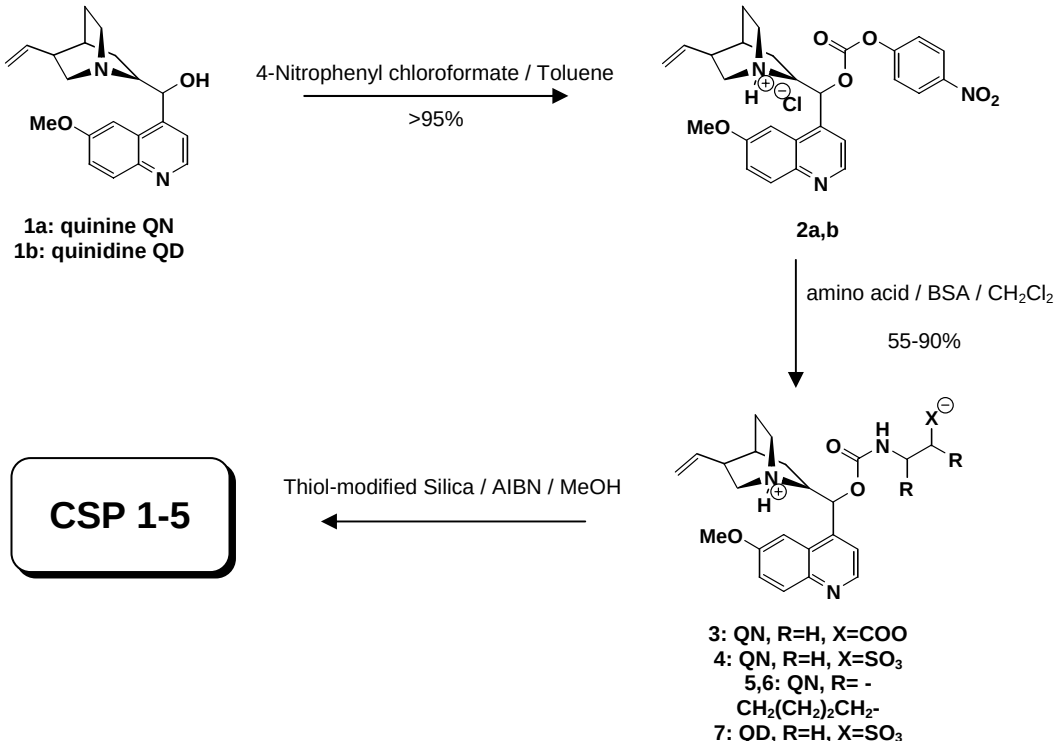

Figure S-1. Synthesis scheme for the preparation of **CSPs 1-5**.

In order to circumvent solubility problems, the different amino acids where converted into their trimethylsilyl esters with *N*,*O*-bis(trimethylsilyl)acetamide[4] prior to reacting with nitrophenylesters **2a** and **2b**. Zwitterionic SOs **3-7** could thereby be quickly prepared in acceptable to good yields. Covalent immobilization of the SOs onto thiol-modified silica gel was accomplished via radical addition reaction[5] and produced novel **CSPs 1-5** with SO loadings of 196-229 μmol per gram CSP. In the case of **CSPs 3** and **4**, preparative separation of their diastereomeric SOs prior to immobilization was necessary in order to guarantee for high purity of SO stereoisomers. While both standard reversed-phase (RP) and WAX-type chromatography did not allow feasible separations of the ampholytic compounds **5** and **6**, the employment of novel **CSP 1**, the β-alanine-quinine based zwitterionic material, gave a sufficient separation (analytical run: $\alpha = 2.24$, $R_S = 8.9$) and a

high loading capacity (up to 10 mg of sample injected onto a 150 x 4 mm column) while using an easily removable mobile phase consisting of 0.14% acetic acid in MeOH (data not shown). Although being a separation of diastereomers it indicates the potential of these novel chiral zwitterionic stationary phases also for the application of preparative separation and purification of ampholytic compounds.

General Information and Materials for Synthesis.

All chemical reactions were carried out under anhydrous conditions using nitrogen atmosphere and oven-dried glassware unless otherwise stated. ^{1}H and ^{13}C NMR spectra were acquired on a Bruker DRX 400 MHz spectrometer. The chemical shifts (δ) are given in parts per million (ppm) using tetramethylsilane as internal standard. Mass spectrometry was performed on a PESciex API 365 triple quadrupole mass spectrometer (Applied Biosystems/MDS Sciex, Concord, Canada) equipped with a standard electrospray source. Elemental analysis was carried out with an EA 1108 CHNS-O from Carlo Erba. Flash chromatography was carried out using Silica 60 (0.040-0.063 mm particle size) from Merck (Darmstadt, Germany).

Thiol-modified silica gel as support for the CSPs was prepared from spherical silica gel (Daisogel 120-5, pore size 120 Å, particle size 5 μm, from Daiso Chemical Co., Ltd., Japan), similar to a previously published procedure.[5] Thiol-group grafting level of 940 μmol/g was assessed by a spectrophotometric assay employing 2,2´-dithiodipyridine.[6] Trans-2-aminocyclohexane-sulfonic acid was prepared according to published procedures.[2, 3] All chemicals used for synthesis were of reagent grade quality or higher, purchased from Sigma-Aldrich (Vienna, Austria) and were used without further purification except the following: CH_2Cl_2 (Sigma-Aldrich) was distilled over calcium hydride prior to use, and quinine and quinidine were purchased from Buchler (Braunschweig, Germany).

Synthesis of zwitterionic, *Cinchona*-based CSPs 1-5 (Figure S-1).

General procedure for *Cinchona* activation.[1]

Typically, *Cinchona* alkaloid **1** (8.0 g, 24.66 mmol) was dissolved in toluene (300 ml) and the solution was dried azeotropically using a Dean-Stark apparatus. After cooling to

ambient temperature, 4-nitrophenyl chloroformate (5.0 g, 25 mmol) was added portionwise. The resulting mixture was stirred overnight. A pale yellow precipitate formed which was collected by filtration. Washing with n-hexane (3 x 50 ml) and drying under reduced pressure yielded **2** as a pale yellow solid (almost quantiative yield) that was used in the next step without further purification.

***O9-(4-Nitrophenyl)oxycarbonyl quinine hydrochloride* 2a**. MS (ESI, positive): 490.5 $[M+H]^+$, 979.5 $[2M+H]^+$.

***O9-(4-Nitrophenyl)oxycarbonyl quinidine hydrochloride* 2b**. MS (ESI, positive): 490.5 $[M+H]^+$, 979.5 $[2M+H]^+$.

General procedure for the preparation of zwitterionic SOs 3-7.

Typically, *N,O*-bis(trimethylsilyl)acetamide BSA (3.0 ml, 12 mmol) was added portionwise to a suspension of finely grounded amino acid (4.0 mmol) in dry CH_2Cl_2 (100 ml). The resulting mixture was stirred and heated under reflux until a clear solution was formed (up to 36 h). After cooling to ambient temperature, activated *Cinchona* alkaloid **2** (2.1 g, 4.0 mmol) was added portionwise and the solution was stirred overnight while becoming slightly yellow. After quenching with MeOH (2 ml), the reaction mixture was directly transferred to a bed of silica gel (150 g) which was preequilibrated with CH_2Cl_2. Purification by flash chromatography (CH_2Cl_2/MeOH 20/1 to 5/1) yielded the zwitterionic SO. Separation of the diastereomers **5** and **6** was carried out chromatographically by HPLC (details are given below).

***N-[[[(8S,9R)-6'-methoxycinchonan-9-yl]oxy]carbonyl]-β-alanine* 3**: 91%, pale brown solid. ^{1}H NMR [CD_3OD]: δ = 8.68 (d, 1H), 7.97 (d, 1H), 7.55 (d, 1H), 7.53 (d, 1H), 7.45 (dd, 1H), 6.93 (d, 1H), 5.75 (m, 1H), 5.09 (d, 1H), 5.01 (d, 1H), 4.02 (s, 3H), 3.75 (m, 1H), 3.64 (m, 1H), 3.53 (m, 1H), 3.48-3.33 (m, 2H), 3.27-3.14 (m, 2H), 2.73 (m, 1H), 2.47 (m, 2H), 2.21-2.08 (m, 2H), 2.03 (m, 1H), 1.84 (m, 1H), 1.71 (m, 1H). ^{13}C NMR: δ = 176.6 (COOH), 160.4 (C_{ar}), 156.2 (C=O), 148.1 (C_{ar}H), 145.0 (C_{ar}), 143.6 (C_{ar}), 139.4 (CH=), 131.8 (C_{ar}H), 127.4 (C_{ar}), 123.9 (C_{ar}H), 119.7 (C_{ar}H), 117.1 (CH_2=), 102.5 (C_{ar}H), 71.4 (CH), 59.8 (CH), 57.1 (OMe), 55.7 (CH_2), 44.8 (CH_2), 38.6 (CH), 38.5 (CH_2), 36.1 (CH_2), 28.3 (CH), 25.2 (CH_2), 20.9 (CH_2). MS (ESI, positive): 440.4 $[M+H]^+$, 462.4 $[M+Na]^+$, 879.6 $[2M+H]^+$, 901.5 $[2M+Na]^+$.

***N-[[[(8S,9R)-6'-methoxycinchonan-9-yl]oxy]carbonyl]-taurine* 4**: 55%, pale yellow solid. ^{1}H NMR [CD_3OD]: δ = 8.73 (d, 1H), 8.00 (d, 1H), 7.64 (d, 1H), 7.50 (s, 1H), 7.48 (d, 1H), 6.94 (s, 1H), 5.78 (m, 1H), 5.14 (d, 1H), 5.05 (d, 1H), 4.05 (s, 3H), 3.87-3.74 (m, 2H),

3.65 (m, 2H), 3.50 (m, 1H), 3.37 (m, 2H), 3.01 (m, 2H), 2.84 (m, 1H), 2.30-2.19 (m, 2H), 2.13 (m, 1H), 1.99 (m, 1H), 1.75 (m, 1H). ^{13}C NMR: δ = 160.5 (C_{ar}), 155.9 (C=O), 147.8 (C_{ar}H), 144.4 (C_{ar}), 143.6 (C_{ar}), 138.9 (CH=), 131.4 (C_{ar}H), 127.4 (C_{ar}H), 124.3 (C_{ar}H), 119.5 (C_{ar}H), 117.4 (CH_2=), 102.3 (C_{ar}H), 71.1 (CH), 60.0 (CH), 57.1 (OMe), 55.8 (CH_2), 51.5 (CH_2), 45.5 (CH_2), 38.4 (CH_2), 38.3 (CH), 28.2 (CH), 25.0 (CH_2), 20.7 (CH_2). MS (ESI, positive): 476.4 $[M+H]^+$, 498.4 $[M+Na]^+$. MS (ESI, negative): 474.2 $[M-H]^-$.

***trans-(1''S,2''S)-N-[[[(8S,9R)-6'-methoxycinchonan-9-yl]oxy]carbonyl]-2''-aminocyclohexanesulfonic acid* 5**: 64%, off white crystals. ^{1}H NMR [CD_3OD]: δ = 8.70 (d, 1H), 7.95 (d, 1H), 7.60 (d, 1H), 7.40 (dd, 1H), 7.30 (d, 1H), 6.85 (s, 1H), 5.77 (m, 1H), 5.23 (d, 1H), 5.04 (d, 1H), 4.03 (m, 1H), 3.92 (s, 3H), 3.81 (m, 1H), 3.73 (m, 2H), 3.38 (m, 1H), 2.85 (s, 1H), 2.70 (m, 1H), 2.39 (m, 1H), 2.31 (m, 1H), 2.21 (m, 1H), 2.12 (s, 1H), 1.95 (m, 2H), 1.85-1.68 (m, 3H), 1.52 (m, 1H), 1.30 (m, 4H). ^{13}C NMR: δ = 160.3 (C_{ar}), 155.6 (C=O), 148.2 (C_{ar}H), 145.0 (C_{ar}), 143.1 (C_{ar}), 139.2 (CH=), 131.9 (C_{ar}H), 127.1 (C_{ar}), 123.6 (C_{ar}H), 119.9 (C_{ar}H), 117.3 (CH_2=), 102.2 (C_{ar}H), 71.0 (CH), 63.6 (CH), 60.0 (CH), 56.5 (OMe), 56.0 (CH_2), 53.2 (CH), 46.1 (CH_2), 38.5 (CH), 35.0 (CH_2), 29.4 (CH_2), 28.2 (CH), 26.1 (2xCH_2), 25.3 (CH_2), 20.8 (CH_2). MS (ESI, positive): 530.5 $[M+H]^+$, 552.3 $[M+Na]^+$, 1059.7 $[2M+H]^+$, 1081.7 $[2M+Na]^+$.

***trans-(1''R,2''R)-N-[[[(8S,9R)-6'-methoxycinchonan-9-yl]oxy]carbonyl]-2''-aminocyclohexanesulfonic acid* 6**: 55%, off white solid. ^{1}H NMR [CD_3OD]: δ = 8.77 (d, 1H), 8.05 (d, 1H), 7.71 (d, 1H), 7.54 (d, 1H), 7.41 (s, 1H), 6.76 (s, 1H), 5.75 (m, 1H), 5.12 (d, 1H), 5.06 (d, 1H), 4.03 (s, 3H), 3.88 (m, 2H), 3.71 (m, 1H), 3.65 (m, 1H), 3.44 (m, 1H), 3.38 (m, 1H), 3.08 (m, 1H), 2.85 (s, 1H), 2.40-2.05 (m, 5H), 1.95 (m, 2H), 1.75 (m, 1H), 1.66 (m, 1H), 1.58 (m, 1H), 1.48 (m, 1H), 1.40-1.19 (m, 2H). ^{13}C NMR: δ = 160.0 (C_{ar}), 155.3 (C=O), 148.4 (C_{ar}H), 144.4 (C_{ar}), 142.7 (C_{ar}), 138.7 (CH=), 131.8 (C_{ar}H), 126.8 (C_{ar}), 123.7 (C_{ar}H), 120.2 (C_{ar}H), 117.2 (CH_2=), 101.9 (C_{ar}H), 71.1 (CH), 61.5 (CH), 59.8 (CH), 57.0 (OMe), 55.6 (CH_2), 53.4 (CH), 45.4 (CH_2), 37.7 (CH), 33.4 (CH_2), 29.0 (CH_2), 27.5 (CH), 25.8 (CH_2), 25.7 (CH_2), 24.8 (CH_2), 20.7 (CH_2). MS (ESI, positive): 530.3 $[M+H]^+$, 552.4 $[M+Na]^+$, 1059.7 $[2M+H]^+$, 1081.7 $[2M+Na]^+$.

***N-[[[(8R,9S)-6'-methoxycinchonan-9-yl]oxy]carbonyl]-taurine* 7**: 90%, yellow crystals. ^{1}H NMR [CD_3OD]: δ = 8.79 (d, 1H), 7.96 (d, 1H), 7.78 (d, 1H), 7.56-7.50 (m, 2H), 7.11 (s, 1H), 6.14 (m, 1H), 5.33-5.24 (m, 2H), 4.01 (s, 3H), 3.87 (m, 1H), 3.65-3.51 (m, 5H), 3.37 (m, 1H), 3.02 (m, 2H), 2.77 (m, 1H), 2.42 (m, 1H), 2.06 (m, 1H), 2.02-1.83 (m, 2H), 1.47 (m, 1H). ^{13}C NMR: δ = 161.2 (C_{ar}), 155.7 (C=O), 146.8 (C_{ar}), 145.8 (C_{ar}H), 141.2 (C_{ar}), 137.9 (CH=), 128.8 (C_{ar}H), 127.9 (C_{ar}), 126.1 (C_{ar}H), 120.1 (C_{ar}H), 118.4 (CH_2=),

102.6 ($C_{ar}H$), 71.4 (CH), 59.8 (CH), 57.4 (OMe), 51.5 (CH_2), 51.0 (CH_2), 50.1 (CH_2), 38.5 (CH_2), 38.2 (CH), 28.7 (CH), 23.7 (CH_2), 20.4 (CH_2). MS (ESI, positive): 476.2 $[M+H]^+$, 498.2 $[M+Na]^+$, 951.4 $[2M+H]^+$, 973.4 $[2M+Na]^+$.

HPLC Semipreparative Diastereomer Separation of SO 5 and 6

Isocratic semipreparative chromatographic resolution of diastereomers **5** and **6** was performed with the standard analytical HPLC system described in the Experimental section of the main articel in combination with a 12/13-switching valve from Agilent Technologies, which was connected to the flow path just behind the UV detector, for automated fraction collection. The employed stationary phase was β-alanine-based **CSP 1** that was packed in house into a stainless steel column (150 x 4 mm I.D). As mobile phase 25 mM (0.142%, v/v) HOAc in MeOH was used, the flow was set to 1.0 ml/min, and the column temperature was 25 °C. The diastereomeric mixture of amino acids **5** and **6** were dissolved in MeOH at a concentration of 100 mg/ml and were distributed to standard HPLC vials. Sample amounts injected onto the column were 85 µl or 8.5 mg, respectively. In a series of injections, the diastereomers were separated and collected in two fractions, which were concentrated in vacuo. The purity of the collected diastereomers was assessed analytically using similar conditions (**CSP 1**; 25 mM HOAc in MeOH). The first eluted diastereomer **5** was assigned the (1"*S*,2"*S*)-configuration in the cyclohexanesulfonic acid subunit, and accordingly, the second eluted diastereomer **6** the (1"*R*,2"*R*)-configuration. Basis of these assignments are preliminary X-ray crystallographic data on **5** (data not shown).

SO Immobilization and Column Packing

General procedure for the preparation of zwitterionic SO-based CSPs.

Typically, oven-dried thiol-modified silica gel (2.20 g) was suspended in MeOH (10 ml). SO (0.89 mmol) and azobisisobutyronitrile AIBN (30 mg, 0.18 mmol), each dissolved in MeOH (5 ml and 1 ml, respectively) were added. The suspension was stirred under reflux for 6 h. After cooling and filtration, the silica gel was washed with MeOH (3 x 20 ml), diethylether (2 x 20 ml), and dried in vacuo at 60 °C to yield the new CSP.

SO coverages were calculated from the nitrogen content obtained by elemental analysis: **CSP 1** (based on SO **3**): w-% C 10.60, w-% H 1.85, w-% N 0.825, w-% S 2.56; 196 µmol

SO per g CSP. **CSP 2** (based on SO **4**): w-% C 10.48, w-% H 1.85, w-% N 0.863, w-% S 3.26; 205 μmol SO per g CSP. **CSP 3** (based on SO **5**): w-% C 11.53, w-% H 1.96, w-% N 0.905, w-% S 3,19; 215 μmol SO per g CSP. **CSP 4** (based on SO **6**): w-% C 11.83, w-% H 1.92, w-% N 0.961, w-% S 3.19; 229 μmol SO per g CSP. **CSP 5** (based on SO **7**): w-% C 10.14, w-% H 1.78, w-% N 0.881, w-% S 3.15; 210 μmol SO per g CSP. **CSP 1**-**5** were slurry packed into stainless steel columns (150 x 4 mm I.D.) either in house or at VDS Optilab GmbH (Berlin, Germany).

Supplementary Chromatograms of HPLC Enantiomer Separations

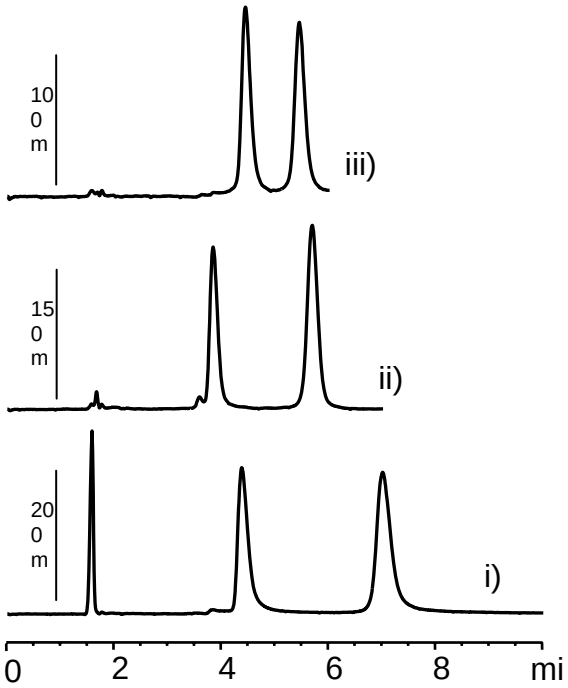

Figure S-2. HPLC enantiomer separations of a series of Phe-containing dipeptides on **CSP 2** (i) Gly-Phe, ii) Ala-Phe (DD/LL), iii) Pro-Phe (DD/LL), (samples are nonracemic, see also Table 3). Mobile phase: 50mM FA and 25mM DEA in MeOH. Detection: CAD or UV at 254 nm.

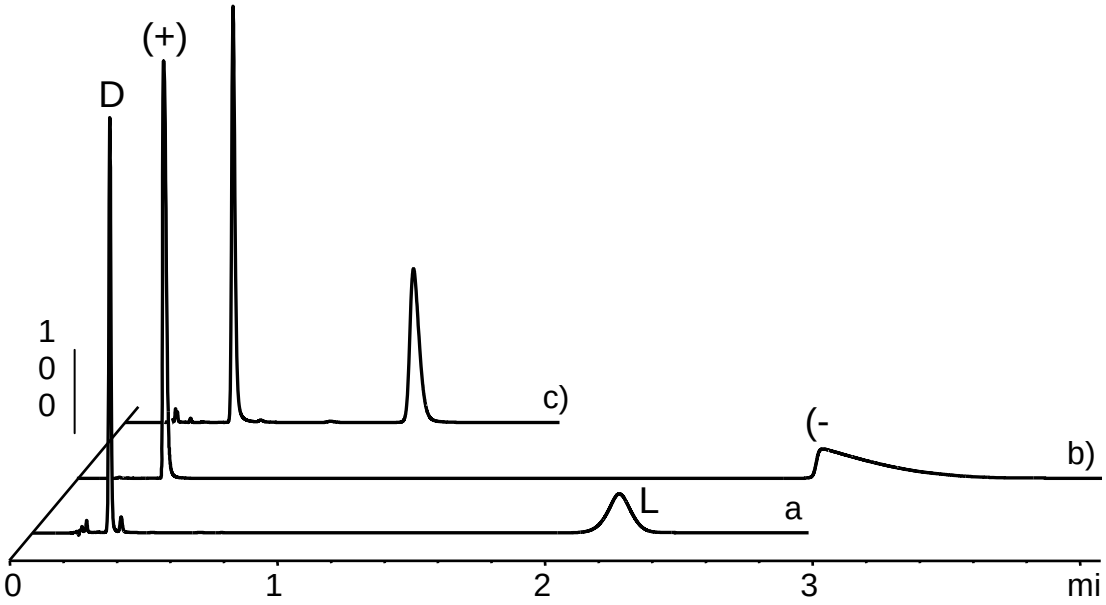

Figure S-3. HPLC enantiomer separations of a) DNB-Phe (see Table 1), b) Mefloquine (see Table 2), and c) DL-α-Methyl-Tryptophane (see Table 3) on **CSP 3**. Mobile phase: 50mM FA and 25mM DEA in MeOH.

References:

(1) Franco, P.; Lammerhofer, M.; Klaus, P. M.; Lindner, W. *Journal of Chromatogr. A* **2000**, *869*, 111-127.
(2) Cordero, F. M.; Cacciarini, M.; Machetti, F.; de Sarlo, F. *Eur. J. Org. Chem.* **2002**, 1407-1411.
(3) Hoffmann, C. V.; Lammerhofer, M.; Lindner, W. *Journal of Chromatogr. A* **2007**, *1161*, 242-251.
(4) Kricheldorf, H. R. *Liebigs Annalen der Chemie* **1972**, *763*, 17-38.
(5) Mandl, A.; Nicoletti, L.; Lämmerhofer, M.; Lindner, W. *J. Chromatogr. A* **1999**, *858*, 1-11.
(6) Nogueira, R.; Lammerhofer, M.; Maier, N. M.; Lindner, W. *Ana. Chim. Acta* **2005**, *533*, 179-183.

Appendix #6

Manuscript Draft M-II

Stationary Phase-related Investigations of Quinine-based Zwitterionic Chiral Stationary Phases operated in Anion, Cation, and Zwitterion Exchange Processes

Christian Hoffmann, Roland Reischl, Norbert M. Maier, Michael Lämmerhofer, Wolfgang Lindner*

Christian Doppler Laboratory for Molecular Recognition Materials, Department of Analytical Chemistry & Food Chemistry, University of Vienna, Währinger Strasse 38, A-1090 Vienna, Austria.

*Author for correspondence:
e-mail: Wolfgang.Lindner@univie.ac.at
Tel.: ++43-1-4277-52300
Fax: ++43-1-4277-9523

Abstract

The concept of recently introduced *Cinchona* alkaloid-type zwitterionic chiral stationary phases (CSPs) is based on fusing key cation and anion exchanger (CX, AX) moieties in one single low-molecular mass chiral selector (SO) with the resulting CSPs allowing enantiomer separations of a wide range of chiral ionizable analytes comprising acids, bases, and zwitterionic compounds. Herein, we report principal, systematic investigations of the ion exchange-type retention mechanisms available with the novel zwitterionic CSPs in nonaqueous polar organic mode. Typical CX and AX processes, corresponding to the parent single ion exchangers, are confirmed also for zwitterionic CSPs. The mechanism leading to recognition and retention of zwitterions was also found to be ion exchange mediated in a zwitterion exchange (ZX) mode. In both AX and CX mode the additional ionizable group within the SO besides the site responsible for the respective ion exchange process could be characterized as an intramolecular counterion (IMCI) that effectively participates in the ion exchange equilibria and thus, contributes to solute elution. In ZX mode both oppositely charged groups of the zwitterionic SO were found not only to be the sites for simultaneous ion pairing with the analyte but also functioned as IMCIs in the same time. The main practical consequences of the IMCI feature were significant reduction of the amounts and even elimination of acidic and basic additives required in the eluent systems to afford analyte elution while still providing faster analysis than the parent single ion exchanger-type CSPs. The set of ten structurally different zwitterionic CSPs employed in this study also allowed correlations between chromatographic behavior of the CSPs with

particular SO elements, thereby supporting the understanding of the working principles of these novel packing materials on a molecular level.

Keywords: Chiral stationary phase; Anion exchanger; Cation exchanger; Zwitterion; Liquid chromatography; Retention mechanism; Chiral acids; Amino acids; Chiral amines; Zwitterionic surface.

Introduction

Novel ion exchanger type chiral stationary phases (CSPs) with remarkably broad applicability based on zwitterionic selectors (SOs) have recently been reported for HPLC [1]. For their low molecular mass chiral SOs, both cation exchanger (CX) and anion exchanger (AX) moieties from already established parent single ion exchanger CSPs have been fused to afford defined, zwitterionic chiral SOs [2,3]. Consequently, these novel chiral separation materials exhibit enantioselectivity for a wide spectrum of chiral ionizable analytes (selectants, SAs) ranging from chiral acids over chiral amines to chiral amino acids and peptides. When these zwitterionic CSPs were being operated for the separation of chiral amines or chiral acids, respectively, significantly reduced analysis times were observed compared to corresponding parent CX or AX CSPs. This particular behavior has been ascribed to the intramolecularly present, oppositely charged ion exchanger moieties that seemed to act as intramolecular counterions (IMCIs) in the respective ion exchange processes. A similar concept has been described earlier in a series of publications on the analysis of inorganic anions and cations in electrostatic ion chromatography (EIC) using reversed phase (RP) columns coated with zwitterionic compounds as stationary phases where operation was even possible with pure water as eluent [4-9]. Here, separation and elution had been ascribed to electrostatic attraction and repulsion between analyte ion pairs and zwitterionic stationary phase where one charge of the stationary phase acted as ion exchange site and the other as electrostatic provider. These observations point for the novel zwitterionic CSPs towards a chiral ion exchanger that lacks a typical drawback of conventional ion exchanger-based CSPs, that is, the need of additional counterions in the mobile phase to let analysis take place in reasonable time frames. Reduction of amounts of mobile phase additives could become especially relevant for preparative applications where subsequent removal of residual additives from the single

enantiomers after enantioseparation represents an additional step. Hence, the IMCI feature of zwitterionic CSPs was of particular interest.

Following the detailed study on the enantioselective properties of *Cinchona* alkaloid-based zwitterionic CSPs [1] we report here principal investigations of the ion exchange modes – anion, cation, and zwitterion exchange (AX, CX, and ZX) mode – available with these packing materials. The examination of the retention mechanisms of acidic, basic, and amino acid analytes on zwitterionic CSPs was carried out in polar organic mode, partly in comparison to conventional, pure AX and CX CSPs. Thereby, the characterization of effects related to the intramolecular counterion (IMCI) feature plays a central role while also the consequences of different SO structures on the analytes' stereoselective retention behavior will be discussed. Since the first investigations of *Cinchona* alkaloid-based zwitterionic CSPs have shown that the alkaloid AX-part dominates overall enantioselective molecular recognition not only of chiral acidic and amino acid analytes but also partly of chiral basic solutes [1] we herein focused on the CX-parts of the zwitterionic CSPs with regard to retention behavior and enantioselectivity. For a better comparison and to give the presented studies a sound basis, an extended set of zwitterionic CSPs exclusively based on quinine as the AX moiety, but with different CX-parts was employed (see Fig. 1) comprising previously reported **CSPs 1-4** [1] as well as six novel zwitterionic CSPs (**CSPs 5-10**). **CSPs 5-7** structurally follow the known **CSPs 1-4** and carry their CX moieties as carbamates at the C9-position of the quinine alkaloid. Among **CSPs 8-10**, which represent a novel subtype of zwitterionic CSPs, the CX groups were introduced via ether linkage at the quinoline C6'-phenoxy group. Thus, the O9-*tert*butyl carbamoyl motif, identified earlier to be important for the enantioselective properties of the parent **QN-AX** CSP [10], remains conserved. However, the particular arrangement of AX- and CX-sites in the zwitterionic SOs of **CSPs 8-10** could potentially lead to an altered mode of zwitterionic recognition of chiral amphoteric compounds compared to the known C9-modified CSPs (see Fig. 1). Among the latter packing materials **CSP 5** mimics the O9-*tert*butyl carbamoyl motif by carrying a branched CX subunit. Both different linkage sites of the CX part within the alkaloid motif and various spacer lengths lead to zwitterionic SOs with CX moieties of different range and flexibility with respect to the relatively rigid quinine AX-scaffold. In combination with varied acid strength (weak and strong CX, WCX and SCX) of the CX subunits a series of CSPs resulted that are likely to exhibit divers ion exchange properties useful for the present study. All structural variations could help deriving structure-

separation relationships and thereby gaining more detailed insights into the working principles of the presented zwitterionic CSPs.

< Figure 1>

Experimental Section

Materials and Instrumentation for Chromatography.

QN-AX CSP (150 x 4 mm I.D., 120 Å, 5 μm) was from Bischoff (Leonberg, Germany) while **CSP 1-4** were identical to the recently reported zwitterionic CSPs [1]. SO coverages of these five CSPs are given in Table 1. Methanol (MeOH) and acetonitrile (ACN) as solvents for HPLC were of HPLC-grade from Merck (Darmstadt, Germany). Mobile phase additives acetic acid (HOAc) and ammonium acetate (NH_4OAc) were of analytical grade (Sigma-Aldrich, Austria). The chiral analytes employed in this study were either commercially available, synthesized according to literature procedures, or were kind gifts from research partners. All chromatographic measurements were performed on 1100 Series HPLC systems from Agilent Technologies (Waldbronn, Germany) consisting of a solvent degasser, a pump, an autosampler, a column thermostat and a UV-Vis detector (either a multi-wavelength or a diode array) for detection between 230 and 280 nm. Data acquisition and analysis was carried out with ChemStation chromatographic data software from Agilent Technologies. Elution was performed in isocratic mode at a mobile phase flow rate of 1.0 ml/min and at a column temperature of 25 °C. The void volumes of the columns were determined by injecting a methanolic solution of acetone with detection at 280 nm. All analytes were applied as methanolic solutions of 0.5-2.0 mg/ml.

Materials and General Information on CSP Preparation.

All chemical manipulations were carried out using nitrogen atmosphere and oven-dried glassware unless otherwise stated to assure anhydrous conditions. All chemicals used for synthesis were of reagent grade quality or higher, purchased from Sigma-Aldrich (Vienna, Austria) except quinine, which was bought from Buchler (Braunschweig, Germany), and were used without further purification. From Merck (Darmstadt, Germany) were Silica 60 (0.040-0.063 mm particle size) for flash chromatography and TLC aluminum sheets silica

gel 60 F_{254} for thin-layer chromatography. ^{1}H and ^{13}C NMR spectra were acquired on a Bruker DRX 400 MHz spectrometer. The chemical shifts (δ) are given in parts per million (ppm) using the solvent signal as internal reference. Mass spectrometry was performed on a PESciex API 365 triple quadrupole mass spectrometer (Applied Biosystems/MDS Sciex, Concord, Canada) equipped with a standard electrospray source. Spherical silica gel Daisogel 120-5 (pore size 120 Å, particle size 5 μm) as solid support for the CSPs was from Daiso Chemical Co., Ltd., Japan. SO coverages of the CSPs were calculated from the nitrogen content obtained by elemental analysis which was carried out with an EA 1108 CHNS-O from Carlo Erba. The CSPs were slurry packed into stainless steel columns (150 x 4 mm I.D.) either in house or at VDS Optilab GmbH (Berlin, Germany).

Preparation of zwitterionic CSPs 5-10 (Fig. 2).

Preparation of chiral SOs of **CSPs 5-7** [1,11] as well as the immobilization of zwitterionic SOs onto thiol-functionalized silica gel [12] in general were carried out according to published procedures, therefore only general protocols are provided.

Preparation of C9-type zwitterionic SOs

General procedure for the preparation of SOs of CSPs 5-7.

Briefly, to solution of quinine (8.0 g, 24.66 mmol) in dry toluene (300 ml) was added 4-nitrophenyl chloroformate (5.0 g, 25 mmol). After stirring the reaction mixture overnight a precipitate formed that was collected by filtration, washed with n-hexane (3 x 50 ml) and dried under reduced pressure to afford the desired activated quinine ester hydrochloride as a pale yellow solid (almost quantiative yield) which was used in the next step without further purification. In dry CH_2Cl_2 (100 ml) the corresponding amino acid (4.0 mmol; 3-amino-3-methylbutyric acid: 469 mg; 4-aminobutyric acid: 413 mg; 6-aminohexanoic acid: 525 mg) was suspended and *N,O*-bis(trimethylsilyl)acetamide BSA (3.0 ml, 12 mmol) was added. The resulting mixture was stirred and heated under reflux for up to 24 h until a clear solution formed to which, after cooling to ambient temperature, activated quinine ester hydrochloride (2.1 g, 4.0 mmol) was added and allowed to react overnight. The mixture was quenched with MeOH (2 ml), directly transferred to a pre-equilibrated (CH_2Cl_2) bed of silica gel (150 g) and purified by flash chromatography (CH_2Cl_2/MeOH 20/1 to 5/1) to afford the zwitterionic SOs.

SO of *CSP 5, N-[[[(8S,9R)-6'-methoxycinchonan-9-yl]oxy]carbonyl]-3-amino-3-methylbutyric acid*: 64%, off white crystals. ^{1}H NMR [CD_3OD]: δ = 8.68 (d, 1H), 7.98 (d,

1H), 7.61 (d, 1H), 7.54 (d, 1H), 7.48 (dd, 1H), 6.92 (d, 1H), 5.78 (m, 1H), 5.12 (d, 1H), 5.03 (d, 1H), 4.05 (s, 3H), 3.82-3.71 (m, 2H), 3.62 (m, 2H), 3.30-3.26 (m, 1H), 2.80 (m, 1H), 2.75 (d, 1H), 2.53 (d, 1H), 2.36-2.20 (m, 2H), 2.11 (m, 1H), 1.96 (m, 1H), 1.75 (m, 1H), 1.37 (s, 3H), 1.35 (s, 3H). ^{13}C NMR: δ = 174.9 (COOH), 160.5 (C_{ar}), 154.3 (C=O), 148.1 (C_{ar}H), 145.0 (C_{ar}), 143.5 (C_{ar}), 139.1 (CH=), 131.8 (C_{ar}H), 127.3 (C_{ar}), 124.0 (C_{ar}H), 119.9 (C_{ar}H), 117.3 (CH_2=), 102.4 (C_{ar}H), 70.3 (CH), 60.0 (CH), 57.2 (OMe), 55.7 (CH_2), 52.5 (CH_2), 45.0 (CH_2), 44.4 (C), 38.5 (CH), 28.3 (CH), 27.8 (CH_3), 27.7 (CH_3), 25.0 (CH_2), 20.6 (CH_2). MS (ESI, positive): 530.5 $[M+H]^+$, 552.3 $[M+Na]^+$, 1059.7 $[2M+H]^+$, 1081.7 $[2M+Na]^+$.

SO of CSP 6, ***N-[[[(8S,9R)-6'-methoxycinchonan-9-yl]oxy]carbonyl]-4-aminobutyric acid***: 55%, off white solid. ^{1}H NMR [CD_3OD]: δ = 8.70 (d, 1H), 7.98 (d, 1H), 7.58 (d, 1H), 7.54 (d, 1H), 7.47 (dd, 1H), 6.90 (d, 1H), 5.78 (m, 1H), 5.12 (d, 1H), 5.04 (d, 1H), 4.04 (s, 3H), 3.80 (m, 1H), 3.70 (m, 1H), 3.59 (m, 1H), 3.29-3.23 (m, 1H), 3.15 (m, 2H), 2.79 (m, 1H), 2.33-2.17 (m, 4H), 2.12 (m, 1H), 1.98 (m, 2H), 1.84-1.72 (m, 3H). ^{13}C NMR: δ = 177.3 (COOH), 160.5 (C_{ar}), 156.2 (C=O), 148.1 (C_{ar}H), 145.0 (C_{ar}), 143.5 (C_{ar}), 139.2 (CH=), 131.8 (C_{ar}H), 127.4 (C_{ar}), 124.0 (C_{ar}H), 119.7 (C_{ar}H), 117.3 (CH_2=), 102.4 (C_{ar}H), 71.3 (CH), 59.9 (CH), 57.2 (OMe), 55.8 (CH_2), 45.0 (CH_2), 41.5 (CH_2), 38.5 (CH), 32.3 (CH_2), 28.3 (CH), 26.2 (CH_2), 25.0 (CH_2), 20.6 (CH_2). MS (ESI, positive): 530.3 $[M+H]^+$, 552.4 $[M+Na]^+$, 1059.7 $[2M+H]^+$, 1081.7 $[2M+Na]^+$.

SO of CSP 7, ***N-[[[(8S,9R)-6'-methoxycinchonan-9-yl]oxy]carbonyl]-6-aminohexanoic acid***: 90%, yellow crystals. ^{1}H NMR [CD_3OD]: δ = 8.71 (d, 1H), 8.00 (d, 1H), 7.57 (d, 1H), 7.52-7.48 (m, 2H), 6.80 (d, 1H), 5.80 (m, 1H), 5.13 (d, 1H), 5.05 (d, 1H), 4.04 (s, 3H), 3.79 (m, 1H), 3.71-3.61 (m, 1H), 3.57 (m, 1H), 3.32-3.20 (m, 1H), 3.11 (m, 2H), 2.78 (m, 1H), 2.32-2.10 (m, 4H), 2.04-1.95 (m, 1H), 1.82 (m, 1H), 1.64-1.45 (m, 5H), 1.38-1.28 (m, 2H).

^{13}C NMR: δ = 160.5 (C_{ar}), 156.3 (C=O), 148.2 (C_{ar}H), 145.1 (C_{ar}), 143.5 (C_{ar}), 139.3 (CH=), 131.9 (C_{ar}H), 127.4 (C_{ar}), 123.8 (C_{ar}H), 119.8 (C_{ar}H), 117.2 (CH_2=), 102.4 (C_{ar}H), 71.5 (CH), 60.1 (CH), 56.9 (OMe), 56.0 (CH_2), 45.0 (CH_2), 41.8 (CH_2), 38.7 (CH), 34.9 (CH_2), 30.4 (CH_2), 28.3 (CH), 27.3 (CH_2), 25.7 (CH_2), 25.4 (CH_2), 21.2 (CH_2). MS (ESI, positive): 476.2 $[M+H]^+$, 498.2 $[M+Na]^+$, 951.4 $[2M+H]^+$, 973.4 $[2M+Na]^+$.

Preparation of C6'-type zwitterionic SOs

Cupreine-9O-tert.-butylcarbamate.

To a stirred suspension of 3.10 g (10.0 mmol) of dry cupreine [13,14] in 100 ml THF was added a solution of butyl lithium in hexane (6.9 ml, 11.0 mmol) via syringe over a period of 15 min. The resultant yellow solution was stirred at 0 °C for further 20 min. Then a solution of pivaloyl chloride (1.36 ml, 1.33 g, 11.0 mmol) in 10 ml THF was added over a period of 10 min. The cooling bath was removed and the mixture allowed to stir at ambient temperature. After 1 h the reaction mixture was quenched by addition of MeOH (2.0 ml) and concentrated under reduced pressure. The resultant yellowish oil was taken into 30 ml of dry toluene. Tert.-butylisocyanate (1.49 g, 15.0 mmol) and dibutyltin dilaurate (0.10 g, 0.16 mmol) were added and the heterogeneous mixture was heated to 60 °C for 10 h. After removal of the volatiles under reduced pressure, the residual oil was taken into MeOH (50 ml). Potassium carbonate (4.15 g, 30.0 mmol) was added and the suspension was stirred for 5 h at ambient temperature. The reaction mixture was concentrated under reduced pressure. The solid was suspended in 200 ml water and carefully (foaming!) acidified with 2 M hydrochloric acid to pH 2. The acidic solution was adjusted to pH 12 with concentrated aqueous ammonia and the formed precipitate was extracted with CH_2Cl_2 (3 x 50 ml). After drying ($MgSO_4$), the organic extracts were concentrated under reduced pressure to furnish a yellowish oil. Purification via gradient silica gel chromatography (CH_2Cl_2-MeOH. 10/0 to 7/3) gave 1.95 g (4.67 mmol, 47 %) of an off-white solid. MS (ESI, positive): 410.5 $[M-H]^+$.

Ester-type intermediates: 6'-[(4-ethoxycarbony)butyl)-cupreine-O9-tert.-butylcarbamate; 6'-[(6-methoxycarbonyl)hexyl)-cupreine-O9-tert.-butylcarbamate; 6'-[(4-methoxycarbonyl)undencenyl)-cupreine-O9-tert.-butylcarbamate.

To a solution of cupreine-O9-tert.-butylcarbamate (2.05 g, 5.0 mmol) in 20 ml DMF were added finely powdered cesium carbonate (2.44 g, 7.5 mmol) and the corresponding bromoalkyl ester (4.0 mmol; ethyl 4-bromobutyrate: 780 mg; methyl 6-bromohexanoate: 836 mg; methyl 11-bromoundecanoate: 1.12 g). The suspension was stirred for 20 h at ambient temperature. The volatiles were removed under high vacuum (0.1 mbar, bath temperature < 50 °C). The oily residue was taken into CH_2Cl_2 and washed with 2 M aqueous sodium hydroxide solution (3 x 100 ml) to remove excess cupreine 9O-tert.-butylcarbamate. The organic phase was dried ($MgSO_4$) and concentrated to yield a dark brown oil. The crude product was purified via gradient chromatography on silica gel (CH_2Cl_2-MeOH 10/0 to 9/1).

6'-[(4-ethoxycarbony)butyl)-cupreine-O9-tert.-butylcarbamate: 1.70 g (3.25 mmol, 65%). MS (ESI, positive): 524.6 $[M-H]^+$.

6'-[(6-methoxycarbonyl)hexyl)-cupreine-O9-tert.-butylcarbamate: 1.96 g (3.65 mmol, 73%). MS (ESI, positive): 538.5 $[M-H]^+$.

6'-[(4-methoxycarbony)undencenyl)-cupreine-O9-tert.-butylcarbamate: 1.82 g (3.00 mmol, 60%). MS (ESI, positive): 608.6 $[M-H]^+$.

Zwitterionic SOs: 4-[(O9-tert.-butylcarbamoyl)-cuprein-6'-yl]-butyric acid; 6-[(O9-tert.-butylcarbamoyl)-cuprein-6'-yl]-hexanoic acid; 11-[(O9-tert.-butylcarbamoyl)-cuprein-6'-yl]-undanoic acid.

The respective ester intermediate (5.0 mmol) was dissolved in MeOH (20 ml), and 7.5 ml of a 2 M NaOH in MeOH and 0.5 ml water were added. The mixture was stirred at ambient temperature and the progress of the hydrolysis of the esters was monitored via TLC (CH_2Cl_2-MeOH 4/1). After complete conversion (3 to 5 h depending on derivative) the reaction mixture was quenched with a stoichiometric amount (7.5 ml) of 2 M methanolic HCl. The volatiles were carefully removed under reduced pressure (vigorous foaming!). The sticky residue consisting of sodium chloride and the target compound was repeatedly re-suspended in dry toluene and evaporated to remove traces of water. The resultant material was treated with 50 ml CH_2Cl_2, filtered, mixed with 25 g silica gel and evaporated. The so pre-adsorbed material was loaded onto glass columns containing 60 g silica gel pre-equilibrated with CH_2Cl_2. Gradient elution (CH_2Cl_2-MeOH 10/0 to 9/1) followed by drying in high vacuum furnished the pure zwitterionic SOs as colorless glassy solids.

SO of CSP 8: 4-[(O9-tert.-butylcarbamoyl)-cuprein-6'-yl]-butyric acid: 1.53 g (3.10 mmol, 62%). ^{1}H NMR [$CDCl_3$]: δ = 9.15 (s, 1H), 8.70 (d, 1H), 8.03 (d, 1H), 8.00 (d, 1H), 7.35 (dd, 1H), 7.28 (d, 1H), 6.89 (s, 1H), 5.65 (m, 1H), 5.06-4.97 (m, 3H), 4.42-4.31 (m, 1H), 4.28-4.16 (m, 1H), 3.64-3.54 (m, 1H), 3.44-3.35 (m, 1H), 3.35-3.27 (m, 1H), 3.15-3.03 (m, 1H), 2.77-2.69 (m, 1H), 2.63-2.45 (m, 3H), 2.27-2.17 (m, 1H), 2.10-1.90 (m, 4H), 1.88-1.76 (m, 1H), 1.70-1.58 (m, 1H), 1.32 (s, 9H). ^{13}C NMR: δ = 177.6 (COOH), 158.4 (C_{ar}), 152.2 (C=O), 146.9 (C_{ar}H), 144.4 (C_{ar}), 142.9 (C_{ar}), 138.6 (CH=), 131.6 (C_{ar}H), 126.1 (C_{ar}), 123.4 (C_{ar}H), 116.8 (C_{ar}H), 116.4 (CH_2=), 101.4 (C_{ar}H), 70.3 (CH), 69.2 (OCH_2), 58.0 (CH), 54.6 (CH_2), 51.1 (C-NH), 41.7 (CH_2), 37.8 (CH), 31.8 (CH_2), 28.9 (CH_3), 27.3 (CH), 25.6 (CH_2), 23.7 (CH_2), 19.4 (CH_2). MS (ESI, positive): 496.5 $[M-H]^+$.

SO of CSP 9: 6-[(O9-tert.-butylcarbamoyl)-cuprein-6'-yl]-hexanoic acid 1.71g (3.25 mmol, 65%). ^{1}H NMR [$CDCl_3$]: δ = 8.71 (d, 1H), 8.50 (s, 1H), 8.02 (d, 1H), 7.49 (d, 1H), 7.39 (dd, 1H), 7.30 (d, 1H), 6.69 (s, 1H), 5.66 (m, 1H), 5.02-4.93 (m, 2H), 4.92 (s, 1H), 4.31-4.16 (m, 2H), 3.44-3.34 (m, 1H), 3.34-3.25 (m, 1H), 3.25-3.16 (m, 1H), 3.05-2.93 (m, 1H), 2.76-2.66 (m, 1H), 2.50-2.34 (m, 3H), 2.00-1.49 (m, 11H), 1.31 (s, 9H). ^{13}C NMR: δ = 177.1 (COOH), 158.2 (C_{ar}), 152.5 (C=O), 146.9 ($C_{ar}H$), 144.5 (C_{ar}), 143.5 (C_{ar}), 139.8 (CH=), 131.5 ($C_{ar}H$), 126.1 (C_{ar}), 122.8 ($C_{ar}H$), 117.1 ($C_{ar}H$), 115.6 (CH_2=), 102.6 ($C_{ar}H$), 71.4 (CH), 69.4 (OCH_2), 57.9 (CH), 54.8 (CH_2), 51.0 (C-NH), 41.8 (CH_2), 38.4 (CH), 35.1 (CH_2), 28.9 (CH_3), 28.5 (CH_2), 27.6 (CH), 26.3 (CH_2), 25.9 (CH_2), 24.5 (CH_2), 20.4 (CH_2). MS (ESI, positive): 524.4 $[M-H]^+$.

SO of CSP 10: 11-[(O9-tert.-butylcarbamoyl)-cuprein-6'-yl]-undanoic acid: 1.60 g (2.70 mmol, 54%). ^{1}H NMR [$CDCl_3$]: δ = 8.71 (d, 1H), 8.02 (d, 1H), 7.44 (s, 1H), 7.38 (dd, 1H), 7.32 (d, 1H), 6.63 (d, 1H), 6.54 (s, 1H), 5.69 (m, 1H), 5.04-4.93 (m, 2H), 4.87 (s, 1H), 4.24-4.11 (m, 2H), 3.33-3.20 (m, 3H), 2.99-2.87 (m, 1H), 2.75-2.66 (m, 1H), 2.54-2.36 (m, 1H), 2.32-2.24 (m, 2H), 1.93-1.75 (m, 5H), 1.72-1.49 (m, 6H), 1.45-1.32 (m, 10H), 1.30 (s, 9H). ^{13}C NMR: δ = 177.9 (COOH), 158.0 (C_{ar}), 151.1 (C=O), 146.8 ($C_{ar}H$), 144.3 (C_{ar}), 143.6 (C_{ar}), 140.4 (CH=), 131.3 ($C_{ar}H$), 126.5 (C_{ar}), 122.5 ($C_{ar}H$), 117.6 ($C_{ar}H$), 115.3 (CH_2=), 101.8 ($C_{ar}H$), 71.8 (CH), 68.6 (OCH_2), 58.0 (CH), 55.2 (CH_2), 50.9 (C-NH), 42.0 (CH_2), 38.8 (CH), 34.9 (CH_2), 29.2 (CH_2), 28.9 (CH_3), 28.9 (CH_2), 28.9 (CH_2), 28.8 (CH_2), 28.7 (CH_2), 28.6 (CH_2), 27.6 (CH), 26.7 (CH_2), 25.9 (CH_2), 25.0 (CH_2), 21.5 (CH_2). MS (ESI, positive): 594.7 $[M-H]^+$.

General procedure for imobilization of zwitterionic SOs to afford CSPs 5-10 [12].

To a mechanically stirred suspension of thiol-modified silica gel [10] (3.0 g) in MeOH (15 ml) the corresponding zwitterionic SO (0.75 – 0.89 mmol for **CSPs 5-7**, 0.66 – 0.76 mmol for **CSPs 8-10**) and 30 mg (0.18 mmol) AIBN, each dissolved in MeOH (5 and 1 ml, respectively), were added. The suspension was heated to reflux for 5 h. After cooling, the modified silicas were isolated by filtration, washed with hot MeOH (5 x 40 mL), then with CH_2Cl_2 (3x 30 mL) and diethylether (3 x 30 mL). Drying at 60 °C under reduced pressure for 12 h provided corresponding **CSPs 5-10**. SO coverages of the CSPs were calculated from the nitrogen content obtained by elemental analysis (see Table 1).

Results and Discussion

Selector and CSP Synthesis.

Generally, CSP preparation (Fig. 2) was carried out using published procedures or standard protocols whereby for C9-modification, quinine was reacted with 4-nitrophenyl chloroformate to form an activated intermediate that allowed introduction of CX units via carbamate coupling of amino acids [1,11]. For C6′-type zwitterionic SOs, at first the tert.-butyl-carbamate was regioselectively introduced at the C9-hydroxyl group of cupreine. Alkylation at the remaining C6'-hydroxyl group with bromo-carboxylic acid esters and their subsequent alkaline hydrolysis furnished zwitterionic SOs. Covalent SO immobilization onto thiol-modified silica support via radical addition reaction [12] yielded corresponding zwitterionic **CSPs 1-10**. The SO loadings of the prepared CSPs is given in Table 1. SO coverage plays an important role in the discussion of column performance and comparison, especially of retention behavior, as it can be expected for the investigated ion exchanger CSPs, and a given appropriate eluent system, that the ionizable analyte will exhibit certain interactions with the SO being a significant part of the stationary phase. In order to effectively correlate differences in chromatographic behavior with a particular SO structure, SO coverages of the compared CSPs should ideally be the same [15]. For eight out of ten zwitterionic CSPs investigated herein (see Table 1) a relatively narrow range of SO loadings could be achieved (average: 206 ± 14 μmol SO/g CSP) that allowes to largely attribute differences in chromatographic performance to structural differences among the zwitterionic SOs. However, the values for **CSPs 6** and **7** (256 and 160 μmol/g, respectively) and also for the pure anion exchanger CSP, **QN-AX** (about 350 μmol/g), deviated considerably from the above average, therefore only general comparison of these latter CSP and their characteristics will be possible in the following section.

<Figure 2>

<Table 1>

General Aspects of the Chromatographic Evaluation of CSPs 1-10

Besides aqueous reversed-phase (RP) and nonpolar normal-phase (NP) eluents nonaqueous polar organic conditions represent common operation modes in enantioselective HPLC, which became particularly popular for macrocyclic antibiotics-based CSPs and the analysis of polar chiral analytes in general. Such polar organic elution conditions have also been successfully used for both AX- and CX-type CSPs as well as for the zwitterionic CSPs reported so far. Thereby, acidic and basic ionizable additives in the eluent could serve as co- and counterions for the respective mode of ion exchange [16,17]. For the investigations presented herein, polar organic mobile phases were applied which consisted of MeOH as bulk solvent and, where necessary, of acetic acid and ammonia in concentrations ranging from 0.5 to 500 mM. The chiral acidic, basic, and zwitterionic test analytes are depicted in Fig. 3. Both consistent mobile phase compositions and a limited set of analytes account for comparison of the investigated CSPs and the observed chromatographic effects. Detailed studies on the mobile phase composition itself and its influences on the performance of zwitterionic CSPs are topic of a subsequent publication. For the benefit of clarity, only exemplary data are shown in order to illustrate overall trends and typical CSP behaviors. In the following sections, detailed investigations of the ion exchange processes of firstly amino acids, then basic, and finally acidic chiral solutes on zwitterionic CSPs will be presented and discussed. Qualitative comparison of the CSPs with regard to their structural differences and the assessment of the intramolecular counterion (IMCI), especially in the AX mode as compared to a **QN-AX** type CSP that lacks this feature, will also be included.

<Figure 3>

Zwitterionic Analytes on Zwitterionic CSPs

For both pure AX- and CX-type CSPs operated in polar organic eluent systems an ion exchange-driven retention mechanism has been confirmed where analyte retention could be conveniently adjusted by varying the concentration and thereby the competitive effect of the salt forming counterions in the mobile phase [3,17-19]. However, enantioseparation of chiral zwitterions is typically not possible on AX- and CX-type CSPs, as only two particular applications have been reported for **QN-AX** so far [20,21]. This capability, in contrast, has been demonstrated to be a main characteristic of the novel zwitterionic CSPs [1]. Simultaneous double ion pairing has been proposed as central molecular recognition

mechanism of zwitterionic SO and solute. On the other hand, structural pecularities of both CX- and AX-parts within the zwitterionic SO had significant influence on the CSPs' enantioselective properties [1]. In order to get deeper insights into the retention mechanism, the influence of the counterion concentration on the retention of zwitterionic solutes on zwitterionic CSPs in support of an underlying ion exchange process was assessed. For that purpose, zwitterionic CSPs were operated in mobile phases of relatively broad range of additive concentrations (from 1-100 mM HOAc and 0.5-50 mM ammonia, respectively, in a constant ratio of acid to base of 2:1), and representative results are depicted in Fig. 4.

<Figure 4>

Similar to single ion exchanger CSPs, also retention of the zwitterionic analytes on zwitterionic CSPs decreased with increasing concentration of counterions in the mobile phase. A logarithmic plot of the retention factors versus counterion concentration, obtained for three **CSPs 1**, **2**, and **8** (with both SCX- and WCX-type subunits as well as CX subunits at C9- and C6′-position) and one α- and one β-amino acid (see Fig. 4a), revealed linear dependencies that clearly indicate according to a stoichiometric displacement model [22,23] an ion exchange dominated retention mechanism on all three zwitterionic CSPs. The slopes of the curves which are proportional to the effective charges involved in the ion exchange process, however, are very small with values of -0.1 to -0.2. Therefore, the system of both zwitterionic solutes and CSPs has – in terms of retention – a quite low sensitivity for competitive effects of counterions in the mobile phase. For the investigated CSPs and the zwitterionic retention mechanism in general, a decrease in additive concentration of a 100-fold was found to lead to an increase of retention by a factor of <3. These findings mark a significant difference to the parent ion exchanger CSPs: For a pure CX-type CSP for example, only a 4-fold decrease in counterion concentration was reported to lead to an increase of retention by a factor of 3.6 (the SO loading was comparable to that of the zwitterionic CSPs studied herein) [3]. As a practical consequence, retention times of zwitterionic solutes on **CSPs 1-10** can be adjusted by variation of counterion concentration only in a limited range. This effect is illustrated for the case of tryptophane and **CSP 2** in Fig. 4b, which also shows that the data for a mobile phase of pure MeOH with no additives at all is in line with the discussed behavior by affording the longest retention times. Even if CSP operation with additive-free eluents is not recommended for routine analysis since the

sample amount on column had to be carefully adjusted to avoid phenomena like peak distortion and splitting, these simple conditions indicate that the effect from intramolecularly present counterions within the zwitterionic SO – represented by its AX- and CX-parts – alone is sufficient to enable elution and thereby dominate the ion exchange equilibria during ZX mode.

The intercepts of the curves in Fig. 4a are directly proportional to the binding constants of the SO-SA association. Hence, the three CSPs shown principally differ in their ability to bind zwitterionic solutes as C6′-WCX-type **CSP 8** yielded the lowest intercepts (-0.70), and consequently, retention factors, while among the C9-modified structural homologues, SCX-type **CSP 2** gave higher intercepts (+0.26) than WCX-type **CSP 1** (-0.05). When comparing the two C9-modified CSPs (see Fig. 1), the contribution of the SCX-part within the zwitterionic SO of **CSP 2** to ion pairing interaction with the protonated amine of the amino acid solute is apparently stronger than that of the WCX-part of **CSP 1** - despite the simultaneously active IMCI effects of the same CX-parts on solute displacement (a SCX-type IMCI is expected to exhibit higher elution strength than a WCX-type IMCI). Oppositely, the reduced retention for WCX-type **CSP 8** seems to stem from its different arrangement of CX- and AX-parts within the chiral SO which rather favours an enhanced IMCI activity of the CX-part with respect to the AX moiety than a double ionic coordination. Hence, decreased retention of zwitterionic solutes result as compared to C9-modified **CSPs 1** and **2**. The principal differences in ion pairing-mediated binding of zwitterionic analytes among the three types of zwitterionic CSPs in the order C9-SCX > C9-WCX >> C6′-WCX are confirmed on a broader structural basis by Fig. 5, in which the retention behavior of all ten zwitterionic CSPs, each with a different CX-part, is illustrated for three representative amino acid analytes using one common mobile phase. Although data of only three analytes are shown for the benefit of clarity, Fig. 5 adequately depicts our overall observations. Furthermore, the enantioseparation capabilities of **CSPs 1-10** with respect to their structural variations generally follow the trend of retention (data not shown). The different achiral acidic subunits of the novel **CSPs 5-10** yield no overall improvements of enantioselective molecular recognition of zwitterionic solutes compared to the earlier reported **CSPs 1-4**. In particular, the C6′-type zwitterionic **CSPs 8-10** allow only minute retention and limited enantioselectivity, and are therefore less suited for the enantioseparation of chiral amino acids via a zwitterion exchange process than the C9-CX-type CSPs. Finally, the partly significant differences within the group of zwitterionic **CSPs 2-4** with SCX subunits indicate that not only the strength of the ion exchanger sites in the

SO but also their spacial arrangement plays a major role for molecular recognition of the zwitterionic analyte.

<Figure 5>

Basic Analytes on Zwitterionic CSPs

The zwitterionic CSPs in an earlier study were reported to allow enantioselective cation and anion exchange besides enantiomer separations of zwitterionic analytes in ZX mode [1]. For probing if an expected CX process is involved in amine retention on zwitterionic packing materials, **CSPs 1-10** were subjected to analysis of basic analytes using polar organic eluents containing a range of concentrations of counterions (5-50 mM ammonia in MeOH, with HOAc at a acid-to-base ratio of 2:1). Representative data obtained with **CSP 1** and **2** for three chiral drugs or drug-like amines, that is, Mefloquine, N-deisopropyl-Disopyramide, and Tocainide are shown in Fig. 6.

<Figure 6>

In the double logarithmic plots of retention versus counterion concentration, linear relationships can be observed. Therefore, also zwitterionic CSPs function as typical cation exchangers upon analysis of basic compounds due to their CX motifs. Not surprisingly, SCX-type **CSP 2** shows stronger retention than WCX-type **CSP 1** under identical elution conditions. The slopes of the curves lie in the range of -0.5 to -0.8 and are slightly lower than for pure CX-type CSPs which was attributed to a contribution of an IMCI effect to analyte elution, additionally to the counterions in the eluent system. For the exemplary data shown in Fig. 6, it should be noted that with **CSPs 1** and **2**, only Mefloquine enantiomers could be base-line separated while the two other chiral bases were eluted as single peaks. Generally, the studies presented herein indicate that, among zwitterionic CSPs, only **CSPs 3** and **4** offer enantioselectivity towards a substantial range of chiral basic compounds while the remaining **CSPs 1** and **2** as well as novel **CSPs 5-10** are not suited for enantiomer separation of chiral amines, thereby confirming earlier findings [1]. These observations can be mainly attributed to the fact that the CX subunits of **CSPs 1**, **2**, and **5-**

10, which represent the primary interaction sites, are relatively far away from the next chiral center and that their linkage moieties are rather flexible.

Acidic Analytes on Zwitterionic CSPs

Besides the above discussed CX and ZX mode, zwitterionic CSPs provide with anion exchange a third mode of enantioselective ion exchange which is associated with the basic alkaloid motif. For zwitterionic **CSPs 1-4**, an enantioselective AX mechanism was stated to be still in place that is largely unchanged compared to the parent **QN-AX**-type CSPs [2,10] in terms of enantioseparation capabilities [1]. However, a marked difference in overall retention behavior between **QN-AX** and zwitterionic CSPs was observed that lead to significantly faster elution. Besides potential differences in SO coverage of the packing materials, this effect was correlated with the intramolecularly present CX groups acting as counterions in the AX process. The zwitterionic CSPs in this study incorporate distinct CX-parts of different acid strength, flexibility, and areas of influence within the SO and with respect to the AX-site. Therefore, the present set of CSPs (see Fig. 1), in combination with variations of the counterion concentration in the mobile phase, was expected to be an insightful tool to investigate the particularities of AX mode in a zwitterionic SO environment and to characterize the IMCI feature. Following a detailed study on the AX properties of **QN-AX**-type CSPs [17] elution conditions consisting of MeOH and solely acid additives (50-400 mM HOAc in MeOH, viz. 0.286-2.287% v/v) have been applied during enantioseparations of a series of chiral acidic analytes on five zwitterionic CSPs and, for a qualitative comparison also on a **QN-AX** CSP. Representative data are shown in Fig. 7a as double logarithmic plots of retention factors versus counterion concentrations.

<Figure 7>

Generally, on all investigated CSPs retention of chiral acidic analytes decreased with increasing counterion concentration in the eluent, again confirming ion exchange as primary retention mechanism. As expected, **QN-AX** showed the largest intercept and a linear relationship between log k and log c over the entire investigated concentration range (slope about -0.6), thereby reproducing the literature findings [17,24,25]. A linear dependency was also observed for sulfonate-based **CSP 2**, although with both significantly smaller values of intercept and slope (-0.1 to -0.2). Among the four carboxylate-containing

zwitterionic CSPs shown intercepts were relatively similar and closer to the parent AX-type CSP **QN-AX** than to the zwitterionic **CSP 2**. The different slopes corroborate the stoichiometric displacement model which states the slope as the ratio of effective charges of solute and counterion, and that decreasing slopes for a given analyte indicate increasing effective charges of the – here intramolecular – counterions being fundamental to a stronger competitive strength in the ion exchange process [22-24].

The relationship between retention and counterion concentration on **CSPs 1**,**6**,**7**, and **10**, however, was not linear over the whole concentration range. Here, it seems that retention responded stronger on counterion concentration changes at higher (> 150 mM) than at lower (< 150 mM) concentrations while dependencies within the two concentration regimes tended to be linear (see Fig. 7a). This bilinear dependency is exemplified with **CSP 6** and data on several acidic analytes in Fig. 7b. At lower counterion concentrations WCX-type zwitterionic CSPs afforded slopes of -0.2 to -0.3 while at higher concentrations slopes approached values very similar to those observed for **QN-AX** (around -0.5). These findings of a conceptually bilinear dependency of log k on log c suggest that for zwitterionic **CSPs 1**,**6**,**7**, and **10** under the given elution conditions their IMCI is outnumbered by higher concentrations of HOAc (an acid of comparable strength to the carboxylic CX functions within the SOs). In this concentration regime the zwitterionic CSPs resemble a **QN-AX**-type CSP with a different C9-substituent. In the low counterion concentration regime, however, the IMCI effect is of major relevance and becomes a dominant factor for the actual retention and AX capacity.

For **CSP 2**, though, the IMCI effect cannot be simply set off by the eluent ionic strength in the given concentration range because the intramolecular sulfonic acid is a significantly stronger competitor for analyte binding to the AX-site than HOAc in the mobile phase even at higher concentrations. Consequently, **CSP 2** exhibited overall weakest sensitivity to changes of the counterion concentration, showed no bilinear dependency under the applied mobile phase conditions, and afforded overall shortest retention times under the given elution conditions (see Figs. 7a and c). Nevertheless, AX between SO and SA is still the dominating process of analyte retention on **CSP 2**, despite the low slopes of -0.1 to -0.2 [8]. Among the WCX-type zwitterionic CSPs the C6'-modified ones accounted for the most effective IMCI properties while among the various C9-modifications only minor differences in retention could be observed as Fig. 7c also illustrates. In other words, the IMCI feature of the herein presented zwitterionic CSPs offers significantly faster analysis times as compared to a parent AX-type CSP while principally requiring smaller amounts of

additives in the mobile phase to be successfully operated, yet still allowing excellent enantioselectivity towards chiral acidic solutes.

The above employed conditions were different from those used for the zwitterionic and basic solutes reported earlier herein. We also investigated how zwitterionic CSPs could be operated for all three confirmed ion exchange modes with one common type of polar organic mobile phase. Upon employing MeOH and different concentrations of HOAc and ammonia at a constant ratio of 2:1 in MeOH during analysis of chiral acidic analytes as well on **CSPs 1-10** a particular unexpected retention behavior was observed that is illustrated in Fig. 8.

<Figure 8>

Starting from pure MeOH retention of chiral acidic solutes at first increased with steadily increasing additive concentrations, opposite to the typical dependency of retention on counterion concentration in ion exchange-based chromatograpy. At certain additive concentration levels, finally, the dependencies changed to the typical behavior of decreasing retention with increasing counterion concentration. The maximum retention, i.e. the turning point was observed at 50 mM for sulfonic acid-based **CSP 2** and at 10 mM for carboxylic acid-based **CSPs 1** and **6**. We believe that this for ion exchanger-type CSPs uncommon retention behavior is related to the zwitterionic surface character of the zwitterionic CSPs which in turn is associated with some pecularities in ion distributions and electrostatic surface potentials. In the following, some tentative mechanistic explanations will therefore be proposed.

In pure, additive-free MeOH the surface potential of the current zwitterionic CSPs seems to be negative and therefore the anionic analytes typically eluted due to electrostatic repulsion before the void volume of the CSP leading to ion exclusion rather than retention (in case of successful enantioseparations at least the first eluted enantiomer, see Fig. 8; data on further analytes not shown). A possible rationale for a net negative surface charge could be the fact that in the present zwitterionic CSPs the cationic AX sites are closer to the surface (where they could in addition interact with residual silanol groups) due to attachment via the quinuclidine moiety. Hence, they represent the inner charges while the anionic CX sites are more located towards the bulk mobile phase. By introducing acidic and basic additives and steadily increasing their concentrations the negative surface potential of the zwitterionic CSPs is first gradually decreased to zero and then increased to

positive values which corresponds to the regime of generally increasing retention above void volume, as depicted in Fig 8. Note at this point that the acid-to-base ratio of the additives of 2:1 leads to acid excess in the eluent. Finally, when the additive concentrations reach a critical level and as the thickness of the diffusive double layer on the surface significantly shrinks with increasing ionic strength in the liquid phase the surface charge goes through an extremum and then decays but stays at positive values. That is when the typical ion exchange-related dependency between counterion concentration and retention comes into play. As SCX-type **CSP 2** incorporates a sulfonate anion being the origin of a more pronounced net negative charge it now becomes evident why it requires more additives than WCX-type **CSPs 1** and **6** to show the typical behavior of an AX process in polar organic mobile phase conditions. A feasible theoretical model partly supporting these initial explanations of retention phenomena shown in Fig. 8 can be found in the literature [26] where an extended Gouy-Chapman-Stern theory had been employed to evaluate ion binding to phosphatidylchloline-based zwitterionic membranes and vesicles. Also the chromatographic retention of anions on zwitterionic surfaces has been shown to exhibit bell-shaped dependencies like found herein [27]. However, substantial further work like the determination of the effective net charges of the zwitterionic SOs by capillary electrophoresis (CE) as well as the measurement of the true surface potentials of the CSP particles in the corresponding liquid phase conditions will be necessary to fully clarify the electrostatic properties of the herein investigated zwitterionic CSPs.

At this point it should be noted that the present zwitterionic CSPs enabled enantioseparation and elution of chiral analytes in pure, additive-free MeOH on an analytical level not only in ZX mode (see Fig. 4b) but also in single ion exchange like AX mode (see Fig. 8) due to the IMCI [4]. However, only CSPs consisting of a WAX-site and a SCX-site like **CSP 2** were found to be principally suited for operation in pure MeOH. On weak/weak type zwitterionic CSPs like **CSP 6** retention times were not stable alongside several injections because the intramolecular carboxylate counterion could not effectively displace the analyte from the SO's AX-site within reasonable equilibration times. Overall, even for SCX-based zwitterionic CSPs capacity in pure MeOH turned out to be limited with respect to sample amount, thus preparative enantioseparations using additive-free conditions were not possible (data not shown). From a practical point of view polar organic mobile phase conditions that contain both acidic and basic additives to afford weakly acidic conditions turned out to be universally applicable in AX, CX, and ZX modes for successful enantioseparations in HPLC.

A final aspect of the investigations of zwitterionic CSPs in AX mode was a qualitative comparison of **CSPs 1-10** and the pure AX-type CSP, **QN-AX**, for their overall enantioseparation performance towards a small set of chiral acidic analytes that are typical model compounds in AX-type CSP characterization [2,28] while applying the standard mobile phase of MeOH and 50 mM HOAc/25 mM ammonia that was used so far in the studies presented herein. The aim of this comparison was the illustration of 1) the general effect of the IMCI on column performance, and 2) of the chromatographic consequences of the structural differences among the zwitterionic CSPs. The substantially higher retention factors on **QN-AX** compared to zwitterionic **CSPs 1-10** (see Fig. 9a) reflect – besides **QN-AX**'s higher SO loading – the findings on acidic analyte retention and the IMCI feature described at the beginning of this section (see Fig. 7). The data for the zwitterionic CSPs themselves confirm the earlier findings, too: SCX-based C9-modified CSPs are stronger eluting for acids than WCX-based C9-modified CSPs, whereas more detailed structural differences like length or steric demand of the CX tether have only minor consequences on retention. The C6'-WCX modification provides more effective IMCIs than the C9-WCX modification, however, if the tether between C6'-CX-part and alkaloid motif is not long enough analyte binding via ion pairing is almost completely denied (see Fig. 9, **CSP 8**). Since comparison of enantioselectivities at very short retention times easily becomes questionable, resolution R_S was selected as a chromatographic parameter to assess enantioselective column properties (see Fig. 9b). Here, the very low retentions on **CSP 8** lead to poor enantiomer resolutions, thereby indicating that quinine's molecular recognition properties were drastically altered by the introduction of the short chain CX motif. More gemerally speaking, small structural changes on the chiral SO can have strong effects on the overall enantioselectivity as well. **QN-AX** CSP turned out to be still most successful for the studied set of analytes which is mainly due to excellent resolutions even at lower enantioselectivities ($\alpha < 2.0$). The remaining zwitterionic CSPs showed overall similar resolutions. A proper balance of effectiveness of the IMCI on the one hand and enantioselective molecular recognition on the other hand is realized best with a long chain C6'-modified zwitterionic CSP like **CSP 10** where the IMCI almost acts as "independently" as a counterion in the mobile phase by leading to short retention times while keeping the enantioselectivity of the quinine tert.-butyl-carbamate scaffold roughly fully available.

<Figure 9>

The practical benefits of a zwitterionic SO in enantioselective AX mode are illustrated best for chiral acidic analytes that either are well enantioseparated on **QN-AX**-type CSPs with $\alpha > 2.0$ (e.g. DNB-Phe in Fig. 10a, b) and the second eluting enantiomer being strongly bound by the chiral SO, or principally show very strong interactions with the stationary phase like bisacidic compounds (DNB-Glu in Fig. 10c). In both cases retention times were effectively shortened using a zwitterionic *Cinchona* alkaloid-based CSP (from 50 min to <20 min for DNB-Phe and from >120 min to 25 min for DNB-Glu) using mild elution conditions that are well suited for MS analysis while enantioselectivity and resolution were still more than sufficient.

<Figure 10>

Conclusions

The herein presented systematic chromatographic investigation of a series of novel enantioselective zwitterionic CSPs in polar organic mode and qualitatively comparing them to the parent **QN-AX** CSP resulted in at a better understanding of the working principles of the three ion exchange modes that these materials offer – cation, anion, and zwitterion exchange. In addition, a more detailed correlation between SO structure and chromatographic behavior could be provided. Thus, ion pairing and ion exchange was confirmed for all three operational modes as the process being mainly responsible for analyte retention. Furthermore, the two intramolecularly present ionizable functional groups – namely AX- and CX-sites – were found to mutually act as counterions in all investigated ion exchange processes. Practical consequences for AX and CX mode were the significant shortening of analysis times and the reduction of amounts of ionizable additives in the mobile phase usually required for successful CSP operation. In ZX mode not only the analytes are coordinated via double ion pairing, both intramolecular counterions (IMCIs) also contribute to analyte elution. Therefore, retention in ZX mode is only weakly sensitive to changes of the counterion concentration in the eluent anymore. C6'-long chain modified **CSPs 9** and **10** turned out to be well suited for being operated in the AX mode which is in contrast to their limited applicability in ZX mode.

The distinct arrangement of chiral AX- and especially sulfonate-type CX-sites via the C9-position of the alkaloid was confirmed to be essential for effective enantioselective

zwitterion recognition. Enantioselective CX for the resolution of a broader range of basic chiral analytes was found to be not available with achiral CX moieties within the zwitterionic SO and remains restricted to packing materials employing chiral acidic subunits like **CSP 3** and **4**. The set of ten zwitterionic CSPs investigated in this study effectively showed how systematic synthetic variations of SO structure elements can generate new chromatographic properties and enable a better understanding of the working principles of – in this particular case – zwitterionic CSPs. However, the more this novel class of CSPs is studied the more particular facets and properties arise that need to be investigated. Still, the various aspects connected to mobile phase composition and its influences on AX, CX, and ZX modes on zwitterionic CSPs are not described yet but will be presented in a subsequent article. Since the IMCI property facilitates the elution of analytes from zwitterionic CSPs these packing materials can be expected to be promising also in SFC. Finally, the potential of zwitterionic CSPs in preparative enantiomer separations especially of zwitterionic analytes, but also in AX and CX modes remain to be elucidated, thereby studying the influence of the IMCI on CSP capacity.

Acknowledgements

The financial support of this research project by the Austrian Christian Doppler Research Society and the industrial partners AstraZeneca (Mölndal, Sweden) and Merck (Darmstadt, Germany) is gratefully acknowledged.

References

[1] C.V. Hoffmann, R. Pell, M. Lammerhofer, W. Lindner, in press (2008).

[2] M. Lämmerhofer, W. Lindner, J. Chromatogr. A 741 (1996) 33.

[3] C.V. Hoffmann, M. Lammerhofer, W. Lindner, J. Chromatogr. A 1161 (2007) 242.

[4] W.Z. Hu, T. Takeuchi, H. Haraguchi, Anal. Chem. 65 (1993) 2204.

[5] W.Z. Hu, H. Tao, H. Haraguchi, Anal. Chem. 66 (1994) 2514.

[6] W.Z. Hu, H. Haraguchi, Anal. Chem. 66 (1994) 765.

[7] W.Z. Hu, P.R. Haddad, Trends Anal. Chem. 17 (1998) 73.

[8] H.A. Cook, W.Z. Hu, J.S. Fritz, P.R. Haddad, Analytical Chemistry 73 (2001) 3022.

[9] H.A. Cook, G.W. Dicinoski, P.R. Haddad, J. Chromatogr. A 997 (2003) 13.

[10] A. Mandl, L. Nicoletti, M. Lämmerhofer, W. Lindner, J. Chromatogr. A 858 (1999) 1.

[11] P. Franco, M. Lammerhofer, P.M. Klaus, W. Lindner, J. Chromatogr. A 869 (2000) 111.

[12] N.M. Maier, L. Nicoletti, M. Lammerhofer, W. Lindner, Chirality 11 (1999) 522.

[13] L.D. Small, H. Rosenberg, P. Nwangwu, T.L. Holcslaw, S.J. Stohs, J. Med. Chem. 22 (1979) 1014.

[14] H. Li, Y. Wang, L. Tang, L. Deng, J. Am. Chem. Soc 126 (2004) 9906.

[15] D. Lubda, Diploma thesis (2003).

[16] M. Lämmerhofer, N.M. Maier, W. Lindner, American Laboratory 30 (1998) 71.

[17] K. Gyimesi-Forrás, K. Akasaka, M. Lämmerhofer, N.M. Maier, T. Fujita, M. Watanabe, N. Harada, W. Lindner, Chirality 17 (2005) S134.

[18] E. Tobler, M. Lammerhofer, W. Lindner, J. Chromatogr. A 875 (2000) 341.

[19] E. Zarbl, M. Lämmerhofer, A. Woschek, F. Hammerschmidt, C. Parenti, G. Cannazza, W. Lindner, J. Sep. Sci. 25 (2002) 1269.

[20] H. Gika, M. Lämmerhofer, I. Papadoyannis, W. Lindner, J. Chromatogr. B 800 (2004) 193.

[21] R. Sardella, M. Lämmerhofer, B. Natalini, W. Lindner, Chirality 20 (2008) 571.

[22] W. Kopaciewicz, M.A. Rounds, J. Fausnaugh, F.E. Regnier, J. Chromatogr. 266 (1983) 3.

[23] B. Sellergren, K.J. Shea, J. Chromatogr. A 654 (1993) 17.

[24] M. Lämmerhofer, W. Lindner, in N. Grinberg, E. Grushka (Editors), Advances in Chromatography, CRC Press LLC, Boca Raton, FL, USA, 2007.

[25] M. Lämmerhofer, W. Lindner, in E. Grushka, N. Grinberg (Editors), Advances in Chromatography, CRC Ress, Taylor & Francis Group, Boca Raton, 2008, p. 1.

[26] S.A. Tatulian, J. Phys. Chem. 98 (1994) 4963.

[27] T. Okada, J.M. Patil, Langmuir 14 (1998) 6241.

[28] C. Czerwenka, M. Lammerhofer, W. Lindner, J. Sep. Sci. 26 (2003) 1499.

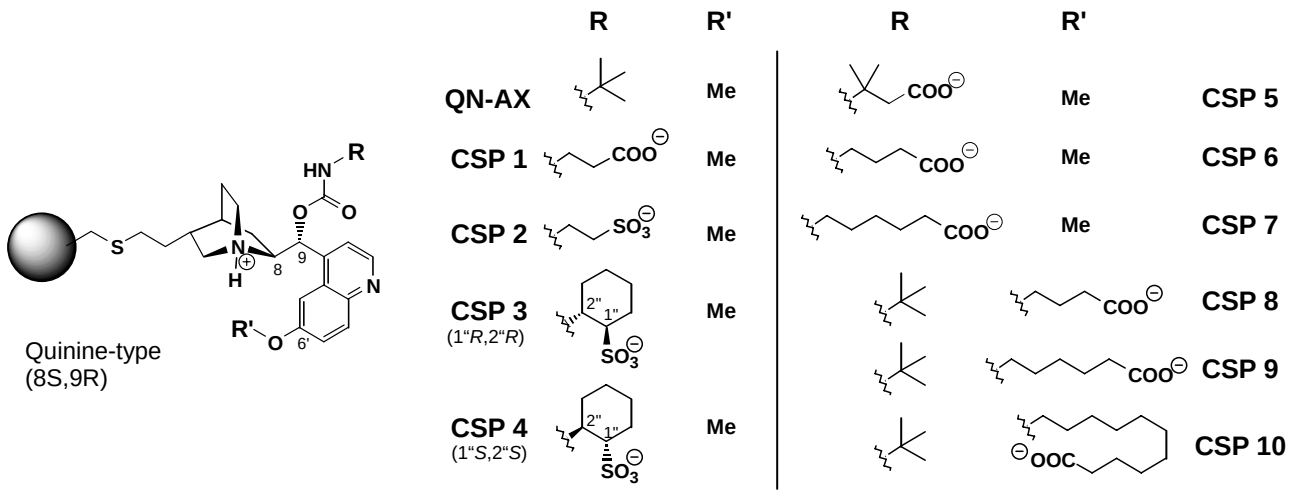

Figure 1.

Chemical structures of the investigated CSPs: commercially available chiral weak anion exchanger **QN-AX** besides chiral zwitterionic CSPs that have been reported previously (**CSP 1**-**4**) and that have been newly prepared for this study (**CSPs 5**-**10**).

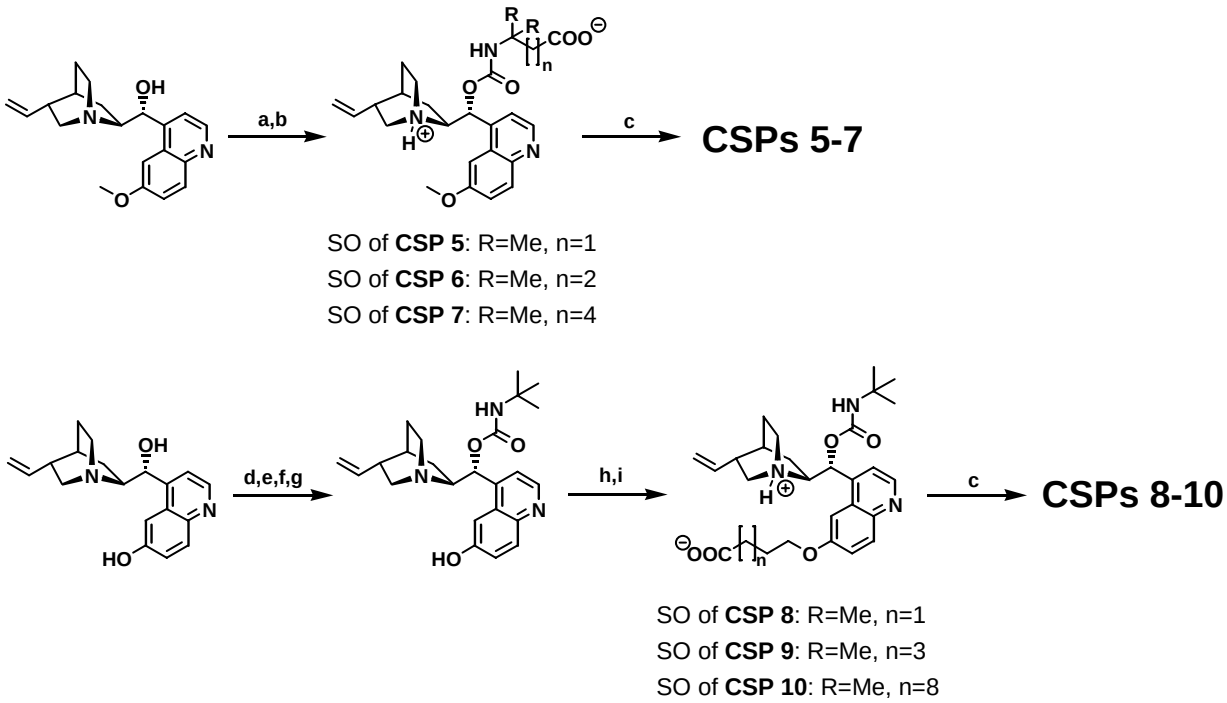

Figure 2.

Synthesis of zwitterionic CSPs. a) 4-nitrophenyl chloroformate / toluene, b) amino acid / BSA / CH_2Cl_2, c) thiol-modified silica / AIBN / MeOH, d) BuLi / THF, e) tBuCOCl, f) tBuNCO / toluene, g) K_2CO_3 / MeOH, h) Br-$(CH_2)_n$-COOEt / Cs_2CO_3 / DMF, i) NaOH / MeOH / H_2O.

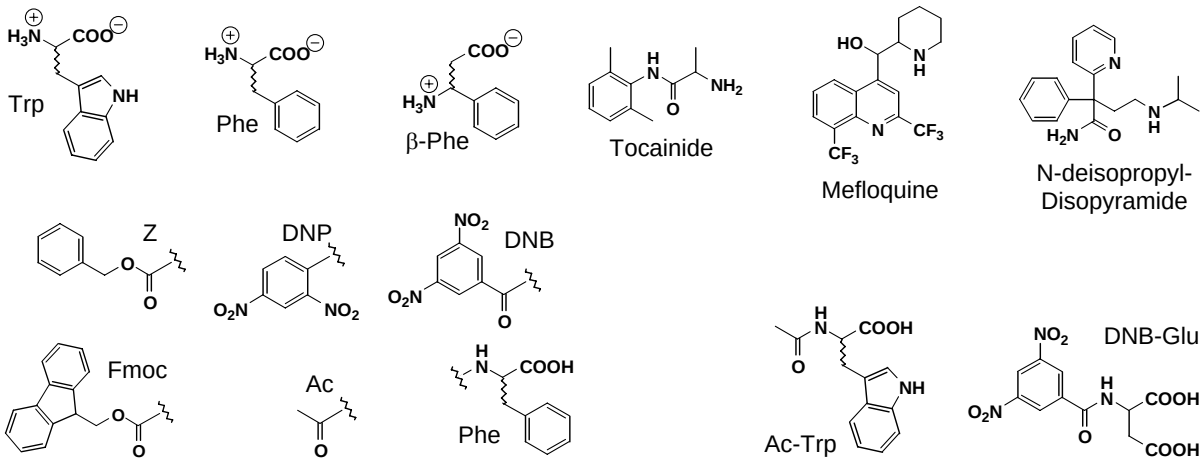

Figure 3.

Chemical structures of chiral amino acid, basic, and acidic analytes that were employed in the present study on zwitterionic CSPs.

Table 1. SO coverages* in μmol SO per g CSP of the herein investigated CSPs

CSP 1	196	**CSP 2**	205	**CSP 3**	215
CSP 4	229	**CSP 5**	223	**CSP 6**	256
CSP 7	160	**CSP 8**	195	**CSP 9**	202
CSP 10	185	**QN-AX**	350		

*) calculated from the N content obtained from elemental analysis

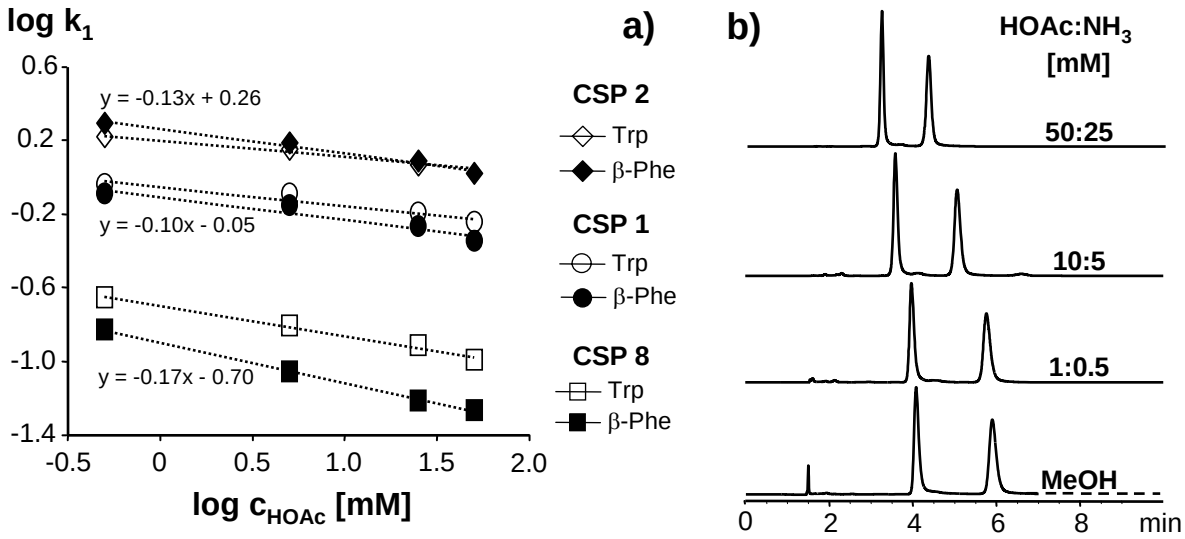

Figure 4.

Zwitterionic CSPs in the ZX mode. Effect of the counterion concentration (various concentrations of HOAc and NH_3 at a constant acid-to-base ratio of 2:1 ranging from 1:0.5 - 100:50 mM in MeOH) in the mobile phase on the retention of a) Trp and β-Phe as representative chiral analytes on three different zwitterionic CSPs. b) Chromatograms of HPLC enantiomer separations of Trp on **CSP 2** using mobile phases of pure MeOH and various concentrations of HOAc and NH_3 in mM in MeOH.

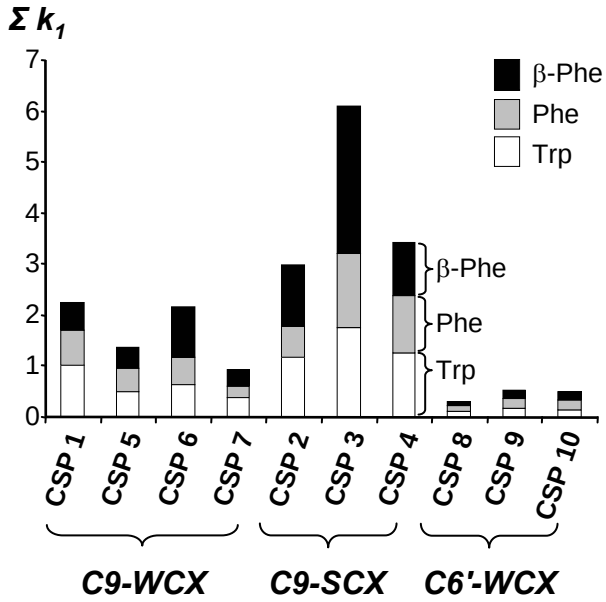

Figure 5.

Zwitterionic CSPs in the ZX mode. Qualitative comparison of the retention behavior of all investigated zwitterionic CSPs. Data are shown for three amino acids in additive manner; mobile phase: 50 mM HOAc and 25 mM NH_3 in MeOH.

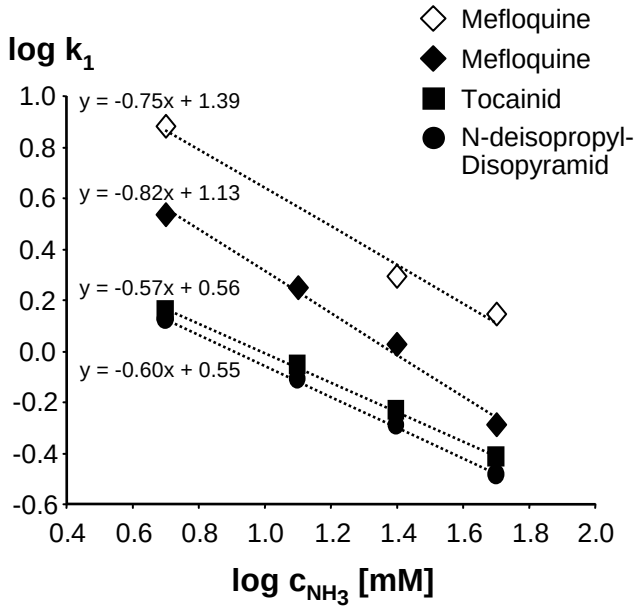

Figure 6.

Zwitterionic CSPs in the CX mode. Effect of the counterion concentration (various concentrations of NH_3 ranging from 5 - 50 mM in MeOH, together with HOAc at a constant acid-to-base ratio of 2:1) in the mobile phase on the retention of chiral basic analytes on **CSP 1** (filles symbols) and **CSP 2** (empty symbols).

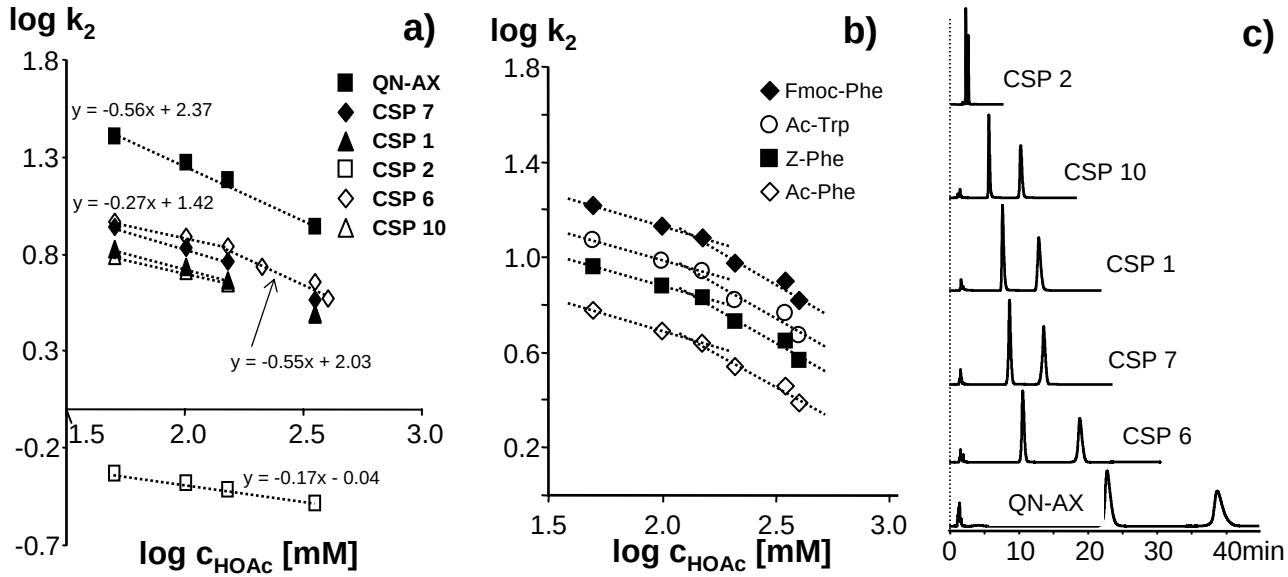

Figure 7.

Zwitterionic CSPs in the AX mode. Effect of the concentration of HOAc (50 - 400 mM, 0.286 - 2.287% v/v) as counterion in the mobile phase on the retention of chiral acidic analytes: a) comparison of five different zwitterionic CSPs against a **QN-AX** CSP for a representative analyte Z-Phe; b) data of a series of four different analytes on **CSP 6**; c) Chromatograms of HPLC enantioseparations of Ac-Trp on five different zwitterionic CSPs and a **QN-AX** CSP (mobile phase: 50 mM or 0.286% v/v HOAc in MeOH).

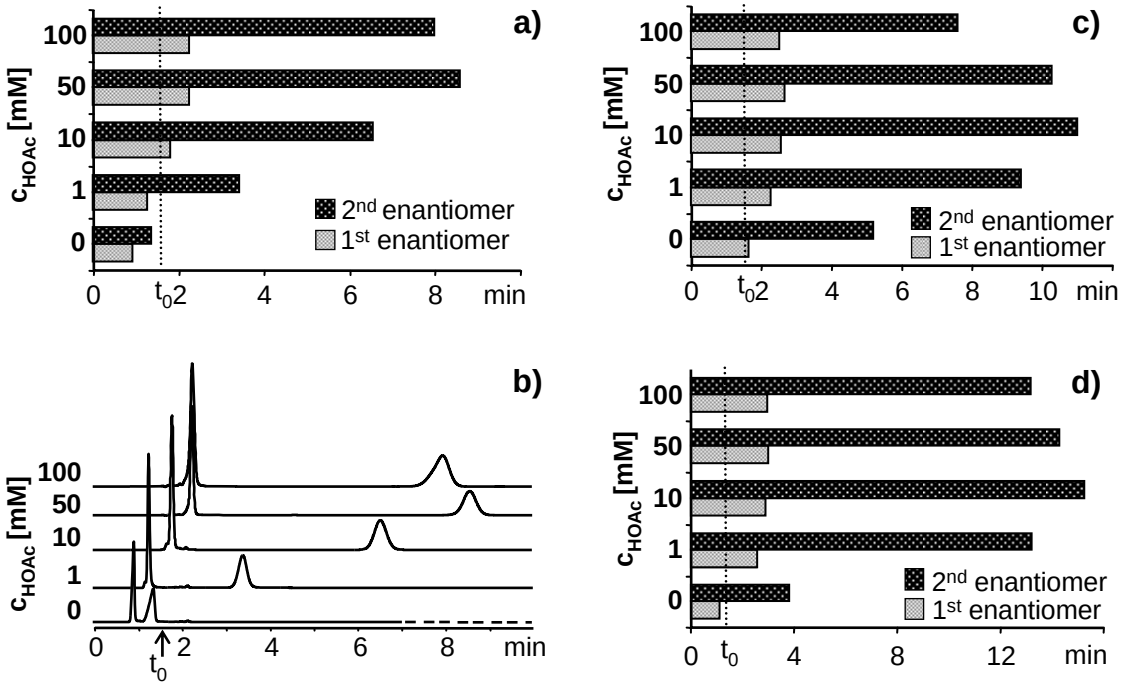

Figure 8.

Nonlinear dependency of retention of chiral acidic analyte DNB-Phe on additive concentration in mobile phases containing both basic co- and acidic counterions (no additives as well as various concentrations of HOAc and NH_3 at a constant acid-to-base ratio of 2:1 ranging from 1:0.5 - 100:50 mM in MeOH): a) and b) on SCX-type zwitterionic **CSP 2**, c) on WCX-type zwitterionic **CSP 1**, and d) on WCX-type zwitterionic **CSP 6**.

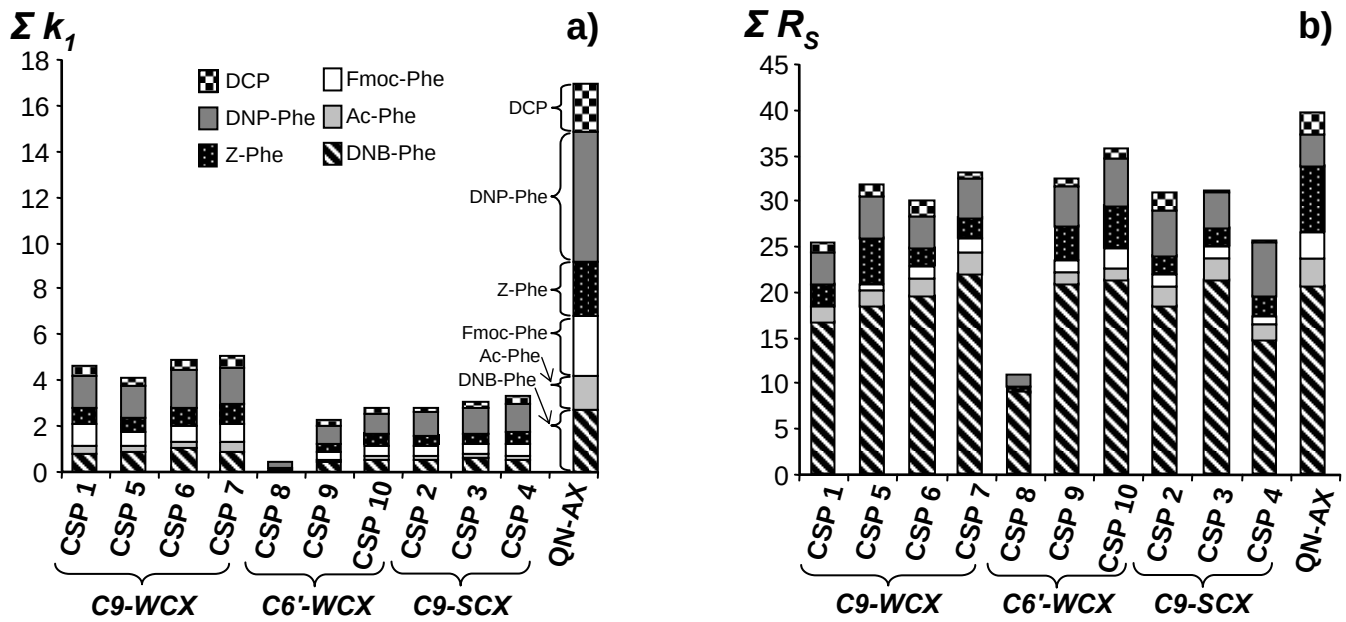

Figure 9.

Qualitative comparison of the eleven investigated CSPs towards chiral acidic analytes: a) retention of the first eluted enantiomer, and b) resolution of the respective enantiomer separations. Data shown in additive manner for six representative analytes. Mobile phase: 50 mM HOAc and 25 mM NH_3 in MeOH.

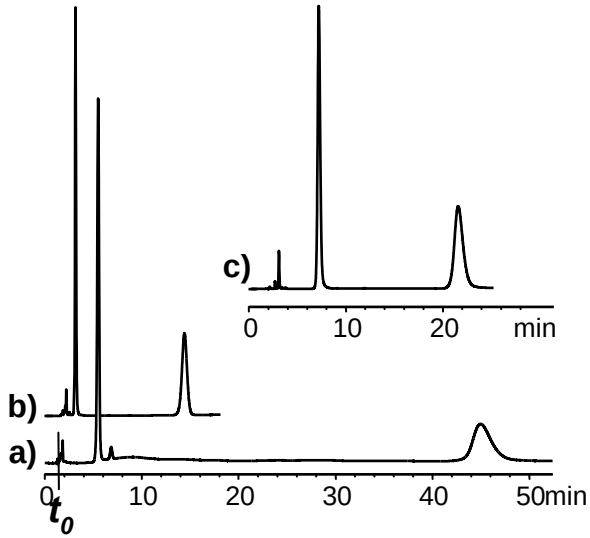

Figure 10.

HPLC enantiomer separations of DNB-Phe on a) **QN-AX** CSP, and b) on zwitterionic **CSP 6** as well as bisacidic DNB-Glu on c) **CSP 6**. Mobile phase: 50 mM HOAc and 25 mM NH_3 in MeOH. DNB-Glu did not elute from **QN-AX** within 120 min under the given mobile phase conditions (chromatogram not shown).

Appendix #7

Manuscript Draft M-III

Investigations of Mobile Phase Contributions to Enantioselective Anion and Zwitterion Exchange Modes on Quinine-based Zwitterionic Chiral Stationary Phases

Christian Hoffmann, Roland Reischl, Norbert M. Maier, Michael Lämmerhofer, Wolfgang Lindner*

University of Vienna, Christian Doppler Laboratory for Molecular Recognition Materials, Department of Analytical Chemistry & Food Chemistry, Währinger Strasse 38, A-1090 Vienna, Austria.

*Author for correspondence:
e-mail: Wolfgang.Lindner@univie.ac.at
Tel.: ++43-1-4277-52300
Fax: ++43-1-4277-9523

Abstract

Novel chiral stationary phases (CSPs) based on zwitterionic *Cinchona* alkaloid-type low-molecular mass chiral selectors (SOs), as they have been reported recently, were principally investigated in HPLC towards effects on their chromatographic behavior by mobile phase composition. Mobile phase characteristics like acid-to-base ratio and type of acidic and basic additives as well as effect of type of bulk solvents in nonaqueous polar organic and aqueous reversed-phase (RP) eluent systems were varied in order to illustrate the variability and applicability of zwitterionic CSPs with regard to mobile phase aspects. Chiral SOs of the five zwitterionic CSPs investigated herein contained weak and strong cation exchanger (WCX, SCX) sites at C9- and C6'-position of the *Cinchona* alkaloid scaffold which itself accomodated the weak anion exchanger (WAX) site. The study focused on zwitterion exchange (ZX) operational mode and chiral amino acids as target analytes. Besides, also the anion exchange (AX) mode for chiral N-blocked amino acid analytes was considered, because of the intramolecular counterion (IMCI) property available in AX mode. Overall, most general and successful conditions in ZX mode were found to be weakly acidic methanolic mobile phases. In aqueous eluents RP contributions to retention came into play but only at low organic modifier content because of the highly polar character of zwitterionic analytes. At higher acetonitrile content HILIC-related retention phenomena were observed. When using weakly basic eluent system in AX mode remarkably fast enantiomer separations involving exclusion phenomena were possible with one enantiomer eluting before and the other after void volume.

Keywords: Chiral stationary phase; Ion exchange; Zwitterion; Liquid chromatography; Mobile phase composition; Polar organic mode.

Introduction

In liquid chromatography (LC) and also in enantioselective LC using chiral stationary phases (CSPs) the mobile phase composition triggers the retention and selectivity characteristics of a system and thus represents an essential part in method development and an important tool to optimize not only enantioselectivity but also other critical parameters for optimal overall column performance like peak efficiency and analysis time. *Cinchona* alkaloid-based zwitterionic CSPs have been introduced only recently to the field of enantioselective chromatography and provide a number of benefits [1]. Due to their zwitterionic nature the employed low molecular mass chiral selectors (SOs) principally enable enantiomer separations of a remarkably broad range of ionizable chiral analytes ranging from acidic over basic to zwitterionic compounds. Hence, anion, cation, and zwitterion exchange (AX, CX, ZX) processes have been confirmed to be dominantly involved in SO-SA interaction and analyte retention [1,2]. However, aspects of mobile phase composition have not been considered systematically on a broader basis so far for *Cinchona* alkaloid-based zwitterionic CSPs as a possibility to affect chromatographic performance. Nonetheless, it is evident that variations of mobile phase parameters are a powerful tool to optimize column performance and to provide chromatographic insights for a better understanding of the working principles and the applicability of these packing materials. This has earlier been illustrated for nonenantioselective zwitterionic stationary phases in achiral applications [3] and for AX- and CX type CSPs in enantioselective chromatograpy [4,5].

In the present study the effects of mobile phase composition on the chromatographic behavior of quinine (QN)-derived zwitterionic CSPs (Fig. 1) for enantioseparations in ZX and AX operational modes in HPLC were evaluated. For that purpose, systematic studies were carried out to elucidate the contribution of 1) the ratio of acidic to basic additives (as a measure for proton activity in the eluent system), 2) the type of acidic and basic additive to the mobile phase, and 3) of aprotic (acetonitrile) and protic (methanol) bulk solvent content in nonaqueous and aqueous eluent systems. In ZX mode the presented mobile phase investigations particularly focused on retention and enantioselective recognition

phenomena for chiral zwitterionic analytes. Operation of **CSPs 2-4**, and **6** for the enantioseparation of chiral acidic solutes in AX mode aimed at describing an additional feature of zwitterionic CSPs, i.e. the intramolecular counterion (IMCI), as opposed to the parent QN-derived AX-type CSPs.

<Figure 1>

Experimental Section

General Information on the investigated CSPs.

CSPs 2, **3**, **4**, **6**, and **10** were available from previous investigations [1,2]. Principally, their SOs are synthetically accessible following published procedures [1,2] and were covalently immobilized onto thiol-modified spherical silica gel [6] as solid support which initially was bare Daisogel 120-5 from Daiso Chemical Co., Ltd., Japan (pore size 120 Å, particle size 5 µm). The CSPs were slurry packed into stainless steel columns (150 x 4 mm I.D.) either in house or at VDS Optilab GmbH (Berlin, Germany). SO coverages of the CSPs were calculated from the nitrogen content obtained by elemental analysis. **CSP 2**, **3**, **4**, **6**, and **10** were identical to the recently reported zwitterionic CSPs [1,2] and had a SO coverage of 205, 215, 229, 256, and 185 µmol per g CSP, respectively.

Materials and Instrumentation for Chromatography.

HPLC-grade methanol (MeOH) and acetonitrile (ACN) were from Merck (Darmstadt, Germany) while deionised water was purified by double-distillation. Water-containing eluent systems were degassed by ultrasonication prior to use. Mobile phase additives acetic like acid (HOAc), formic acid (FA), trifluoroacetic acid (TFA), 2-amino-1-butanol (AB), diethylamine (DEA), triethylamine (TEA), ammonium acetate (NH_4OAc), ammonium formate, and ammonium trifluoroacetate were of analytical grade (Sigma-Aldrich, Austria). The chiral analytes employed in this study were either commercially available, synthesized according to literature procedures, or were kind gifts from research partners.

All chromatographic measurements were performed on 1100 Series HPLC systems from Agilent Technologies (Waldbronn, Germany) consisting of a solvent degasser, a pump, an

autosampler, a column thermostat and a UV-Vis detector (either a multi-wavelength or a diode array) for detection of analytes between 230 and 280 nm. Data acquisition and analysis was carried out with ChemStation chromatographic data software from Agilent Technologies. Elution was performed in isocratic mode at a mobile phase flow rate of 1.0 ml/min and at a column temperature of 25 °C. The void volumes of the columns were determined by injecting a methanolic solution of acetone with detection at 280 nm. All analytes were applied as methanolic solutions of 0.5-2.0 mg/ml.

Results and Discussion

General Aspects

The set of novel zwitterionic **CSPs 2-4**, **6**, and **10** (see Fig. 1) that has been investigated with respect to mobile phase contributions herein had been introduced previously [1,2]. Generally, the CSPs consisted of a QN alkaloid moiety with its tertiary quinuclidine amine serving as the WAX-site and a SCX or WCX-site introduced to the alkaloid scaffold either at the C9-position featuring a carbamate or at C6'-position via ether linkage (see Fig.1). CSPs with the CX-part in C9-position typically were most effective in ZX mode for enantioseparations of chiral amino acids while CSPs with the carboxylate group in C6'-position were largely competitive in terms of enantioselectivity in AX mode for enantioseparations of chiral acidic analytes [6,7]. Therefore, C9-type **CSPs 2-4**, and **6** were selected for investigations of mobile phase aspects in the ZX mode and the C6'-type **CSP 10** served as a test system for the AX mode for which the IMCI feature for single ion exchange modes was exemplarily investigated. As chiral test analytes (selectants, SA) both zwitterions and acids were selected for which generally enantioselectivity was observed in previous studies (see Fig. 2).

<Figure 2 >

In the following sections results of the various mobile phase investigations will be presented and discussed. For the benefit of clarity the figures in these sections typically illustrate overall, general observations that are shown for representative CSPs and analytes. In the study on bulk solvent effects only experiments in ZX mode will be presented since the results obtained so far for AX mode do not indicate major differences to the already well described parent AX-type *Cinchona* alkaloid based CSPs.

Effect of the Acid-to-Base Ratio in the Mobile Phase

Chromatographic enantiomer separation based on ion exchange requires SO and SA to have ionizable functionalities of opposite charge like anionic acid groups and cationic basic amines, thereby facilitating long range ionic interactions that bring the two species in close contact where additional, also enantioselective intermolecular interactions can come into play. Not surprisingly, the ion exchange process is highly dependent on the ionization states of SO and SA which are in turn correlated with proton activity of the mobile phase media. Crucial to the proton activity of the eluent system are acidic and basic additives to the mobile phase and their acid-base equilibria which are superimposed to the ion exchange equilibria according to a stoichiometric displacement model where the additives act as co- and counterions [8,9]. As expected, it was found for AX-type CSPs like *Cinchona* carbamate-based packing materials to exhibit pH dependent retention and enantioselectivity towards chiral acidic analytes with optimal operation conditions at weakly acidic conditions [7,10]. Under these conditions the amine-type SO is mainly protonated and the solute is fully dissociated, therefore ion pairing is maximised. Due to the reciprocity principle in the ion exchange process, for corresponding CX-type CSPs principally similar optimal eluent conditions have been described [5]. Also for other zwitterionic separation materials reported so far, retention of zwitterionic analytes was found to be dependent on the mobile phase pH, affording retention maxima at maximum overlap of the pI values of the involved zwitterionic species [11-15].

Novel zwitterionic CSPs (see Fig. 1) enable a defined enantioselective ZX mode of operation where molecular recognition is mediated via simultaneous double ion pairing between zwitterionic SOs on the one hand and zwitterionic SAs like amino acids and peptides on the other [1]. Furthermore, these zwitterionic CSPs provide the unique feature of an intramolecular counterion (IMCI) which was found very recently to have particular effects on overall retention characteristics [2]. It was therefore of main interest herein to study the effects of the ratio of acidic and basic additives to the mobile phase (as an alternative measure of proton activity in nonaqueous polar organic eluents) on the chromatographic performance of zwitterionic CSPs. For that purpose, methanolic mobile phases containing 25 mM of an organic base additive and varying amounts of organic acid additive affording net acid-to-base ratios of 4:1 to 0.5:1 (i.e. from acid to base excess) have been used as eluent systems. Furthermore, additive concentrations have been selected to

assure that the IMCI property will be active in the AX mode since a previous study showed that higher counterion concentrations (above ~150 mM for HOAc) diminish the IMCI effect. C9-modified **CSPs 3** and **6** have been investigated in the ZX mode and will be considered first (see Fig. 3a), followed by **CSPs 6** and **10** in the AX mode (see Fig. 3b).

<Figure 3>

The chromatographic parameters (retention k_1, enantioselectivity α, and resolution R_S) show similar dependencies on the acid-to-base ratio in the eluent for a representative amino acid analyte Trp (Fig. 3a). Although not pronounced, maxima can be observed at slight acid excess (2:1) while at larger excess of acidic additive (2:1 to 4:1) minor decreases of the three parameters occurred. At equimolar (1:1) and especially at base excess (0.5:1) conditions, however, a significant decrease of retention (and also α and R_S) could be seen. Obviously, on the way to base excess conditions (1:1 to 0.5:1) both amines of SO and SA become increasingly unprotonated. As a consequence, the double ionic interaction as the fundamental process in enantioselective ZX mode is no longer favorable and, besides a decrease of retention, loss of enantioselectivity occurs simultaneously. At acid excess conditions, on the other hand, the ionization states of both SO and SA seem to be sufficient to let the enantioselective ion exchange process remain in function. The slight decrease in retention at increasing acid excess can be attributed an effect of increasing counterion concentration with regard to the AX-part of the SO. The findings on effects of acid-to-base ratio in the mobile phase on ZX mode therefore support the proposed interaction mechanism and principally correspond to the behavior of other zwitterionic packing materials reported in the literature [3,11,12,16-20].

Findings for the chromatographic parameters k_1, k_2, and R_S on the variation of the acid-to-base ratio of the eluent system while operating zwitterionic CSPs in the AX mode for one representative acidic analyte (DNB-Phe) are depicted in Fig. 3b. Other than before in the ZX mode, retention steadily decreased alongside gradually changing the acid-to-base ratio from acid to base excess conditions. Resolution roughly followed the same trend. In particular, at base excess conditions analytes finally eluted before the void volume of the column, meaning that they were excluded instead of retained by the CSP. This particular exclusion behavior seems to be correlated with the zwitterionic nature of the chiral SOs involved since on pure AX-type *Cinchona* alkaloid CSPs acidic analytes at weakly basic mobile phase conditions are typically eluted with void volume or with little retention [10].

This at first glance surprising behavior could be caused by the fact that the acidic analyte is expected to be fully dissociated and therefore negatively charged at base excess conditions. Similarly, the CX-site of the zwitterionic SO will also be in the dissociated state while the amine-type AX-site within the same molecule is not fully protonated anymore. Hence, also the SO is net negatively charged. This leads to an electrostatic repulsion between SO and SA rather than attraction which is manifested by a partial exclusion of the SA from the pores of the negatively charged ZWIX-CSP. However, when taking a closer look at chromatograms obtained at base excess conditions very particular enantiomer separations were in parts observable (see Fig. 4a). Despite the short analysis times (at a void volume of about 1.45 min), the first, "weakly bound" but actually repelled enantiomer was clearly eluted before the void volume according to the above described exclusion mechanism while the stronger bound enantiomer was retained to elute shortly or even substantially after the void volume. This indicates, however, that the force of the electrostatic repulsion is overcompensated by a set of favorable, attractive intermolecular interactions between the enantioselectively strongly bound SA and the chiral SO. These remarkable and fast enantiomer separations were typically observed for chiral acidic analytes which were well separated (roughly $\alpha > 2$) under acid excess mobile phase conditions on the same, zwitterionic CSPs. Oppositely, other analytes that were less effectively enantioseparated using acid excess conditions (roughly $\alpha < 2$) eluted before the void volume only partially separated or even as single peaks when applying base excess conditions (see Ac-Phe in Fig. 4a).

<Figure 4>

Similar exclusion/retention phenomena of acidic analytes were reported earlier in a detailed study on the molecular recognition mechanism of a teicoplanin-based CSP [21] where the unfavoured enantiomer was often eluted before the void volume due to a claimed electrostatic repulsion from the carboxylate-containing SO whereas the favoured enantiomer was properly retained. This remarkable enantioselectivity had been attributed to the fact that the second eluted enantiomer could enter the SO's cavity to exhibited multiple hydrogen bond interactions that overcame the ionic repulsion.

In a comparable manner and as envisioned before, also exclusion/retention-type enantioseparation on zwitterionic CSPs can be rationalized. Principally, ion pairing on zwitterionic CSPs is one possible SO-SA interaction which however can not solely account

for enantioselective molecular recognition upon formation of diastereomeric SO-SA complexes. In fact, also other types of intermolecular interactions must be involved at least for one enantiomer to let enantioseparation take place. Detailed investigations revealed that the molecular recognition mechanism of *Cinchona* carbamate-based AX-type CSPs relies on additional intermolecular SO-SA interactions besides the dominating ion pairing process like H-bonding due to the SO's carbamate group, π-π interactions employing the quinoline motif, and hydrophobic interactions evolving from the alkyl parts of C9- and C6'-modifications [6,10,22]. These additional interactions are typically restricted to one enantiomer only because of the geometrical and conformational appearance of the chiral SO at the given mobile phase conditions and can have significant energetical contributions to SA-binding. If these secondary interactions are reasonably strong they could be expected to be fundamental for the characteristic retention behavior of the second eluted enantiomers in Fig. 4a. The IMCI property, which is responsible for excluding the weaker bound enantiomer, in concert with non-ionic interactions exclusive for the stronger binding enantiomer are therefore proposed to be the basis of retention mechanisms that underlie chromatograms as shown in Fig. 4a. This suggestion is supported by preliminary loading studies where the enantioseparation proved to be stable also at increasing sample size on column (see Fig. 4b). This could certainly lead to favorable situations for preparative applications, especially in combination with rather short run times. Furthermore, the repulsion/retention behaviors of acidic analytes on zwitterionic CSPs are strikingly similar to the elution of related acidic analytes on zwitterionic CSPs in pure, additive-free MeOH (and very low additive concentrations) reported earlier [2]. Thereby, and in view of the herein proposed explanations on solute repulsion, the concept of a zwitterionic CSP with negative surface potential in pure MeOH is clearly supported.

In summary, variation of the acid-to-base ratio of polar organic mobile phases during operation of zwitterionic CSPs in AX and ZX mode provided informations to better understand the working principles of zwitterionic CSPs. For ZX mode acid excess elution conditions were confirmed as a useful starting point when applying zwitterionic CSPs. The investigations on the AX mode using base excess mobile phase conditions presented herein opened up an additional mode of operation of zwitterionic CSPs. Further detailed studies in this direction are needed to explore the full potential, particularly for preparative enantiomer separation.

Effect of Type of Base and Acid as Mobile Phase Additive

Besides variations of the acid-to-base ratio employment of various types of acid and base additives to the mobile phase represent another parameter to adjust the overvall properties of the eluent system. Simultaneously, also the ion exchange processes will potentially be affected due to the different competitive strengths of the particular additives as they also act as co- and counterions in analyte displacement. Since in ZX mode both CX and AX occur both acidic and basic additives play the role of both co- and counterion. Hence, it is expected from these studies to gain further insight into the zwitterion exchange mechanism and the possibilities to affect it. On the other hand, testing of different types of acidic additives in the AX mode aimed at assessing the potential of the IMCI – due to its proximity to the AX-site within the SO – to diminish acid additive effects. Scheme 1 generally summarizes the findings on variations of types of additives and retention for pure AX- and CX-type CSPs regarding retention behavior as they are reported in the literature so far [4,5,23] and was considered as a general guideline when setting up the experiments and discussing the results on the type of acidic and basic additive on zwitterionic CSPs.

<Scheme 1>

An acid-to-base ratio of 2:1, which was confirmed for successful CSP operation in the previous section, was principally applied upon testing different types of additives. Identical molar concentrations of 50 mM for acidic and 25 mM for basic additives assured comparability and featured the additives' elution characteristics. Solvent properties of the acidic and basic additives that could affect chromatography have been neglected due to their low concentrations in the bulk solvent MeOH. Observations in ZX and AX modes will be presented first with regard to basic additives and then to acidic additives.

As of the amine component three organic amine-type bases NH_3, DEA, and TEA were selected as they differ in their degree of alkyl substitution. Acid excess in the mobile phase assured that the bases are present in their ammonium forms.

A previous study testing different bases in enantioselective AX mode using a QN-AX type CSP showed that no effect on enantioselectivity and resolution but increasing elution strength in the order NH_3 < DEA < TEA occurred which was attributed to the co-ion character of the basic additives [23]. Just the opposite trend was found for enantioselective CX-type CSPs (increasing elution strength in the order DIEA < DEA < NH_3) [10], where the basic additive served as the counterion that enabled analyte elution (Scheme 1) [5].

Alongside increasing elution strength, resolution and enantioselectivity simultaneously improved, too.

<Figure 5>

When operating zwitterionic CSPs in the ZX mode for the enantioseparation of chiral amino acids the type of basic additive in the mobile phase turned out to have almost no effect at all on overall column performance (Fig. 5a). This observation is surprising since enantioselective molecular recognition in the ZX mode requires both AX- and CX-site within the chiral SO for defined analyte coordination, and therefore, at least minor influence of the type of basic additive on chromatographic behavior had been expected. Considering the literature findings described above shortly, however, the effects of the type of base on retention were of opposite direction on AX- and CX-type CSPs, depending on their role as co- or counterion. Now in ZX mode on zwitterionic CSPs the effects due to the type of basic additive possibly balance each other.
In the AX mode (acidic solutes) on zwitterionic **CSPs 2-4**, **6**, and **10** enantioselectivity and resolution also remained unaffected by changes of the type of basic co-ion (Fig. 5b). This is in accordance with the behavior reported for pure AX-type CSPs, thereby confirming a principal characteristic of the recognition process for chiral acidic solutes on QN-AX type CSPs also for *Cinchona* alkaloid-type zwitterionic CSPs. However, also retention in AX mode on zwitterionic CSPs is barely influenced by the type of basic co-ion (compare Scheme 1), and it seems as if the intramolecular counterion within the zwitterionic SO compensated for the different elution strength of the co-ions. Generally, it can be concluded that from a practical point of view the type of basic additive has minor impact on column performance of zwitterionic CSPs operated in both AX and ZX modes.

According to a detailed report on the competitive effects of ten different mono-, di-, and trivalent acidic counterions using ten different pure AX-type CSPs based on *Cinchona* alkaloid derivatives in polar organic mode (see Scheme 1) [4], the type of acidic additive strongly influences retention and also enantioselectivity, thereby indicating that the choice of the right counterion is important for successful operation of ion exchanger-type CSPs. In enantioselective CX, however, no marked influence of acidic additives was observable as a result of their co-ion role in this type of ion exchange (Scheme 1). In order to study the particularities of chiral zwitterionic packing materials regarding acidic additives three organic acids commonly used in HPLC were selected, namely TFA, FA, and HOAc. The

main aspect when comparing their competitive effects is acid strength since all of them are monovalent carboxylic acids with similar steric demand. TFA is the strongest acid with a calculated pK_a of 0.53 (pK_a values in aqueous solution calculated by ACD Labs/pK_a DB 7.0 software), followed by FA (3.74) and HOAc (4.79).

<Figure 6>

Fig. 6a illustrates our observations in ZX mode for three exemplary chiral amino acid analytes on **CSP 4**. Both FA and HOAc allowed reasonable retention and also enantioselectivity, however, differences were not very pronounced. Typically, FA yielded better results whereas analyte specific effects were also common. These weak responses to a particular type of acidic additive at the given additive concentration indicate that both CX- and AX-sites within the zwitterionic SO are strongly involved not only in analyte binding but – due to proximity – also in analyte elution while the contribution from the mobile phase components is reduced. This description seems appropriate as long as the additive to the mobile phase is not a noticeably stronger acid than the acidic CX-group within the chiral SO which is the case for FA and HOAc. However, with TFA retention almost vanished. Here, the lack of retention can be correlated with the acidity of TFA which is stronger than the acid functions of both the analytes and also the CX-site within the zwitterionic SO. Thus, TFA leads to formation of stable ion pairs between the amines of both SO and SA and TFA while possibly also reducing the degree of dissociation of the acid functions of SO and SA at the given additive concentration. Consequently, ionic interactions between SO and SA are suppressed, and alongside retention and enantioselectivity are strongly reduced.

The masking effect of TFA was also observable in the AX mode on zwitterionic CSPs where the IMCI contribution was investigated for chiral acidic analytes upon variation of the type of acidic counterion (Fig. 6b). Using TFA lead to hardly any retention and no enantioselectivity at all, according to the above described mechanism. On the contrary, the weakest acid in this set, HOAc, also afforded very short retention times, though, in combination with the highest enantioselectivities. Other than TFA, HOAc obviously supports the dissociation states necessary for ionic interaction and enables proper ion pairing of SO and SA. Hence, the typical *Cinchona* carbamate-type enantioselective molecular recognition process becomes possible. The short retention times can be

attributed to an effective contribution of the IMCI group under the given elution conditions. FA showed the highest retention factors in this comparison which indicates a transition state in terms of retention where the zwitterionic CSP is beginning to adopt the characteristics of the pure AX-type CSP and the IMCI and its effects are increasingly set off. Due to the short retention times enantioselectivities were higher with HOAc than with FA but on the other hand resolution was generally found to be best using FA. The influence of the type of acidic counterion in the AX mode on zwitterionic CSPs turned out to be not as straight forward as for the parent AX-type *Cinchona* alkaloid CSPs [4] but testing acidic additives in combination with variation of the proton activity can be a useful tool to adjust column performance e.g. to fast analysis of improved resolution.

Overall, the type of acidic additive had more pronounced effect on chromatographic behavior of zwitterionic CSPs than the type of basic additive. This could be regarded as a sign of the AX-type interaction being more involved in the retention mechanism of zwitterions on zwitterionic packing materials like **CSPs 2-4**, **6**, and **10** than the CX-type interaction which is nevertheless essential for enantioselective molecular recognition in ZX mode.

Influence of Bulk Solvents of the Mobile Phase

Among the various possibilities to principally tune chromatographic behavior of CSPs by means of mobile phase composition it remains the important parameter of the bulk solvents of the eluent system to be studied. In this context our investigations aimed at mapping the effects of protic MeOH and aprotic ACN, at first in nonaqueous and afterwards in aqueous polar organic elution modes.

A study on a CX-type CSP in nonaqueous conditions showed marked influence of ACN in enhancing enantioselectivity while overall retention was affected rather analyte-specific [5,24]. It was also found that a certain amount of protic MeOH (not less than 5% v/v) is essential for good peak performance which had been ascribed to sufficient solvation of the ionized species involved in ion exchange equilibria. A systematic study on mobile phase effects on AX-type CSPs also compared MeOH and ACN for enantioseparations of a model analyte. However, solely the pure solvents and no mixtures were employed. Thus, no general conclusion regarding the type of bulk solvent could safely be drawn on a broader basis [4]. For *Cinchona* alkaloid-based AX-type CSPs, however, there are several examples in the literature where ACN-MeOH mixtures have been used to successfully

optimize particular enantioseparation challenges [25,26]. For testing the ZX mode for bulk solvent dependencies, eluent systems of increasing ACN content in MeOH were used that also contained constant amounts of additives at an acid-to-base ratio of 2:1. Thereby weakly acidic conditions were guaranteed throughout the measurements since upon changing the bulk solvent composition acid-base equilibria are shifted and therefore proton activity may change. Fig. 7 exemplarily depicts the overall pronounced effects of protic and aprotic solvents on the chromatographic behavior of zwitterionic CSPs in ZX mode for the enantiomer separation of chiral amino acids.

<Figure 7>

Clearly, a type of hydrophilic interaction liquid chromatography (HILIC) operational mode with protic MeOH being stronger eluting than aprotic ACN is present in ZX mode on zwitterionic CSPs which becomes activated at relatively low (around 50%) ACN content or even less. It is characterized by increasing retention with higher ACN percentage [3,27,28]. However, the presence of higher ACN contents did not enhance the enantioselective properties of the present zwitterionic CSPs as can be derived from the subsequent decrease of enantioselectivity and resolution with increasing ACN percentage (see Fig. 7). Furthermore, a substantial drop of peak efficiency alongside increase of the aprotic character of the eluent was observable. Thereby, base-line separations initially present in ACN-deficient eluent systems were often lost upon application of higher ACN percentages. Hence, ZX mode on zwitterionic CSPs seems to require – more than single ion exchangers – protic solvents for adequate solvation of the highly polar zwitterionic SO and SA and for a balanced double ionic retention/elution process. Protic solvents are especially important in ZX mode when considering the increased local charge density in zwitterionic species compared to single charged compounds in pure AX or CX. It seems that with increasing ACN content adsorption/desorption kinetics become slower and lead to diminished peak efficiencies. Overall, best column performance in ZX mode in terms of short analysis time, peak efficiency, and enantioselectivity is observed with MeOH only or low volume fraction of ACN in MeOH as bulk solvents in the mobile phase system. However, the pronounced influence of aprotic solvents like ACN in ZX mode allow adjustments of retention times in a wide range which also suggests that the potential in varying protic and aprotic bulk solvents using the present zwitterionic CSPs rather holds in chemoselective than enantioselective applications.

If protic bulk solvents and solvation of the ionic components involved play an important role in ZX mode, extension of the investigations to the aqueous ond/or hydroorganic eluent conditions were a logical consequence. When operated in reversed-phase (RP) conditions the present zwitterionic CSPs can be considered as mixed mode RP/ion exchanger type stationary phases due to their various hydrophobic molecular increments as depicted in Fig. 1. Consequently, there are two principal scenarios possible in RP mode: Increasing water content can introduce nonspecific hydrophobic interactions between the chiral analyte and the hydrophobic parts of the CSP leading to increased retention possibly accompanied by a lower enantioselectivity. On the other hand, it was interesting to elucidate whether in aqueous eluent systems dedicated hydrophobic interactions, e.g. between nonpolar groups of the chiral analyte and the SO, are involved in enantioselective molecular recognition besides the simultaneous double ion pairing process. The mobile phase systems for assessing the effects of water as a bulk solvent in ZX mode consisted of methanolic solutions of increasing water content while weakly acidic conditions were assured by adding acidic and basic additives. Exemplary observations are depicted in Fig. 8 for **CSP 2** and three chiral amino acid analytes that contain aromatic side chains of different hydrophobicity – 3,4-dihydroxyphenyl (α-Me-DOPA), 3-hydroxyphenyl (α-Me-m-Tyr), and indole (Trp) – to potentially provide sufficient but different RP-response.

<Figure 8>

By introducing water to the MeOH-type eluent system retention of the polar amino acid solutes slightly decreased. Depending on the hydrophobicity of the solutes only at high water contents RP-like retention increments came into play. Thus, at 80% (v/v) water in MeOH the most hydrophobic solute in this comparison, Trp, showed a marked increase of retention whereas the monohydroxylated Tyr derivative was just as strongly retained as in water-free eluent and α-Me-DOPA still decreased in retention. This behavior was also typical for even less hydrophobic, aliphatic and polar functional group containing amino acids. Obviously, the strength of the ionic interactions between SO and analyte is reduced by the strong solvation of SO and SA, and as desolvation is energetically unfavorable SO-SA interactions are essentially weakened. Hence, in the process of double ion pairing and diastereomeric SO-SA complex formation further, nonionic intermolecular contacts are probably less accessible as a result of the strong solvation of the zwitterionic SO and SA

by the water network. This might explain why enantioselectivity did not benefit from increasing amounts of water in the eluent (see Fig. 8). Resolution and peak efficiency (data not shown) were similarly affected which can be correlated also with the commonly observed slower diffusive mass transfer into the intraparticulate pores in aqueous eluent systems.

When working with aqueous solutions measuring the apparent pH (pH_a) as an indicator of proton activity becomes appropriate. The mobile phases initially prepared in this section contained constant amounts of additives (75mM HOAc, 25mM NH_3). However, when measuring the pH_a values of these hydroorganic eluents an increase of the eluents' acidity was observed [29,30] (0% v/v water in MeOH: pH_a 6.50; 20% water in MeOH: pH_a 6.15; 80% water in MeOH: pH_a 4.65). In order to examine whether the superimposed pH_a change was responsible for the loss of selectivity, a further mobile phase with comparable pH_a composed of 80% (v/v) water in MeOH and pH_a 6.15 (from 26.5 mM HOAc, 25 mM NH_3) was prepared and tested as well. There were hardly any differences observable to the other, more acidic mobile phase of 80% water in MeOH (pH_a 4.65), thus ruling out that the observed effects were pH_a-related rather than a solvent effect.

Fig. 9 somewhat summarizes and extends the overall bulk solvent effects observed in ZX mode by displaying retention and resolution of exemplary enantioseparations of chiral amino acids on one WCX- and one SCX-based zwitterionic CSP. ACN had lower elution strength than MeOH (ACN:H_2O versus MeOH:H_2O), and with decreasing protic character of the eluent solvent mixture retention increased. Thereby, the stronger binding SCX-based CSP is more affected than the WCX-type congener. Evidently, HILIC-supported ion exchange is the predominant mode of operation present on zwitterionic CSPs and the balanced, but not too strong protic character of the mobile phase is of central importance for the double ion pairing process that is mainly responsible for analyte retention and enantioselectivity.

<Figure 9>

Also the investigations on water-containing mobile phases for zwitterionic CSPs in ZX mode lead to the conclusion that overall best chromatographic performance regarding all relevant parameters like retention, enantioselectivity, resolution, and peak efficiency, is again achieved in nonaqueous methanolic eluents. However, it should be noted that the employment of low volume fractions of water in MeOH-based eluent systems may be

appropriate for certain applications because the solubility of zwitterionic analytes in water containing eluents is often dramatically increased compared to nonaqueous mobile phases. In particular for preparative enantioseparations enhanced solubility of the chiral analyte can compensate for slight decreases in separation efficiency in regard of the final productivity.

Conclusion

The present study reports on the effects of mobile phase composition on chromatographic performance of novel zwitterionic CSPs in HPLC enantiomer separations of chiral acidic and amino acid analytes. For that purpose, typical mobile phase parameters like proton activity, type of additives, and type of bulk solvents in aqueous and nonaqueous eluent systems were tested on representative zwitterionic CSPs in anion and zwitterion exchange mode. With zwitterionic CSPs and their operation in ZX mode, enantioselectivity seems to be – more than ever before with single CX- and AX-type CSPs – determined by the particular SO structure. By changes in the mobile phase system mainly the not necessarily enantioselective ion exchange processes themselves and the superimposed acid-base equilibria are affected. Therefore, peak efficiency and retention could be adjusted and optimized considerably while this was not the case for enantioselectivity. Overall, weakly acidic methanolic mobile phases were found as promising starting points when operating zwitterionic CSPs in both AX and ZX mode. Aprotic solvents like ACN introduced HILIC-related retention phenomena which mainly determined the enantioseparation capabilities in ZX mode. On the other hand, applications in HILIC mode as a novel packing material for nonchiral separation challenges could represent an interesting perspective of the present zwitterionic CSPs. While RP interactions in ZX mode required high water content in the eluent to contribute to retention because of the very polar nature of the zwitterionic analytes these interactions turned out to be nonspecific and not particularly involved in the enantioselective molecular recognition of chiral zwitterionic solutes. Nevertheless, the possibility to operate zwitterionic CSPs under RP conditions – at least with high organic modifier content – is important for preparative applications in ZX mode where the solubility of highly polar analytes becomes increasingly relevant. However, the potential of zwitterionic CSPs for preparative enantioseparations of amino acids still remains to be properly assessed although preliminary studies that were carried out so far seem promising. In AX mode zwitterionic CSPs enabled remarkable and very

fast enantiomer separations of chiral acids in the void volume time frame under weakly basic conditions due to the zwitterionic nature of the involved chiral SOs. Here again, further investigations of the preparative potential seem relevant, in particular in comparison with the parent QN-AX CSP. Finally, the findings on aprotic solvents in ZX mode can provide helpful information for the adaptation of zwitterionic CSPs for SFC mode where aprotic CO_2 represents the main eluent component.

Acknowledgements

The financial support of this research project by the Austrian Christian Doppler Research Society and the industrial partners AstraZeneca (Mölndal, Sweden) and Merck (Darmstadt, Germany) is gratefully acknowledged. The authors like to thank in particular Dr. Antál Péter for providing us with a sample of *erythro*-β-methyl-Tic.

References

[1] C.V. Hoffmann, R. Pell, M. Lammerhofer, W. Lindner, in press (2008).

[2] C.V. Hoffmann, R. Reischl, N.M. Maier, M. Lammerhofer, W. Lindner, in preparation (2008).

[3] W. Jiang, G. Fischer, Y. Girmay, K. Irgum, J. Chromatogr. A 1127 (2006) 82.

[4] K. Gyimesi-Forrás, K. Akasaka, M. Lämmerhofer, N.M. Maier, T. Fujita, M. Watanabe, N. Harada, W. Lindner, Chirality 17 (2005) S134.

[5] C.V. Hoffmann, M. Lammerhofer, W. Lindner, J. Chromatogr. A 1161 (2007) 242.

[6] A. Mandl, L. Nicoletti, M. Lämmerhofer, W. Lindner, J. Chromatogr. A 858 (1999) 1.

[7] M. Lämmerhofer, W. Lindner, J. Chromatogr. A 741 (1996) 33.

[8] W. Kopaciewicz, M.A. Rounds, J. Fausnaugh, F.E. Regnier, J. Chromatogr. 266 (1983) 3.

[9] B. Sellergren, K.J. Shea, J. Chromatogr. A 654 (1993) 17.

[10] M. Lämmerhofer, W. Lindner, in N. Grinberg, E. Grushka (Editors), Advances in Chromatography, CRC Press LLC, Boca Raton, FL, USA, 2007.

[11] L.W. Yu, R.A. Hartwick, J. Chromatogr. Sci. 27 (1989) 176.

[12] P.N. Nesterenko, A.I. Elefterov, D.A. Tarasenko, O.A. Shpigun, J. Chromatogr. A 706 (1995) 59.
[13] J.H. Knox, J. Jurand, J. Chromatogr. 203 (1981) 85.
[14] J.H. Knox, J. Jurand, J. Chromatogr. 218 (1981) 341.
[15] J.H. Knox, J. Jurand, J. Chromatogr. 218 (1981) 355.
[16] W. Jiang, K. Irgum, Anal. Chem. 71 (1999) 333.
[17] W. Jiang, K. Irgum, Anal. Chem. 73 (2001) 1993.
[18] C. Viklund, A. Sjogren, K. Irgum, I. Nes, Anal. Chem. 73 (2001) 444.
[19] W. Jiang, K. Irgum, Anal. Chem. 74 (2002) 4682.
[20] P. Appelblad, T. Jonsson, W. Jiang, K. Irgum, J. Sep. Sci. 31 (2008) 1529.
[21] A. Cavazzini, G. Nadalini, F. Dondi, F. Gasparrini, A. Ciogli, C. Villani, J. Chromatogr. A 1031 (2004) 143.
[22] N.M. Maier, L. Nicoletti, M. Lämmerhofer, W. Lindner, Chirality 11 (1999) 522.
[23] X. Xiong, W.R.G. Baeyens, H.Y. Aboul-Enein, J.R. Delanghe, T. Tu, J. Ounyang, Talanta 71 (2007) 573.
[24] E. Tobler, M. Lämmerhofer, F. Wuggenig, F. Hammerschmidt, W. Lindner, Electrophoresis 23 (2002) 462.
[25] M. Lammerhofer, O. Gyllenhaal, W. Lindner, J. Pharm. Biomed. Anal. 35 (2004) 259.
[26] E. Tobler, M. Lammerhofer, W. Lindner, J. Chromatogr. A 875 (2000) 341.
[27] T. Ikegami, K. Tomomatsu, H. Takubo, K. Horie, N. Tanaka, J. Chromatogr. A 1184 (2008) 474.
[28] P. Hemstrom, K. Irgum, J. Sep. Sci. 29 (2006) 1784.
[29] K. Sarmini, E. Kenndler, J. Biochem. Biophys. Methods 38 (1999) 123.
[30] S.P. Porras, E. Kenndler, J. Chromatogr. A 1037 (2004) 455.

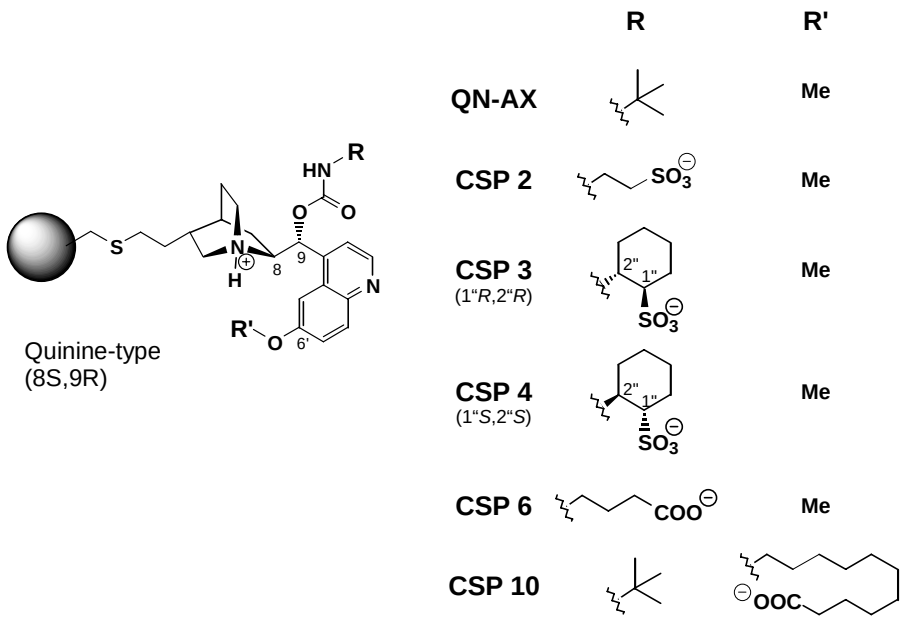

Figure 1.

Chemical structures of the commercially available chiral weak anion exchanger **QN-AX** and chiral zwitterionic CSPs that have been investigated in this study (**CSPs 2-4, 6, 10**).

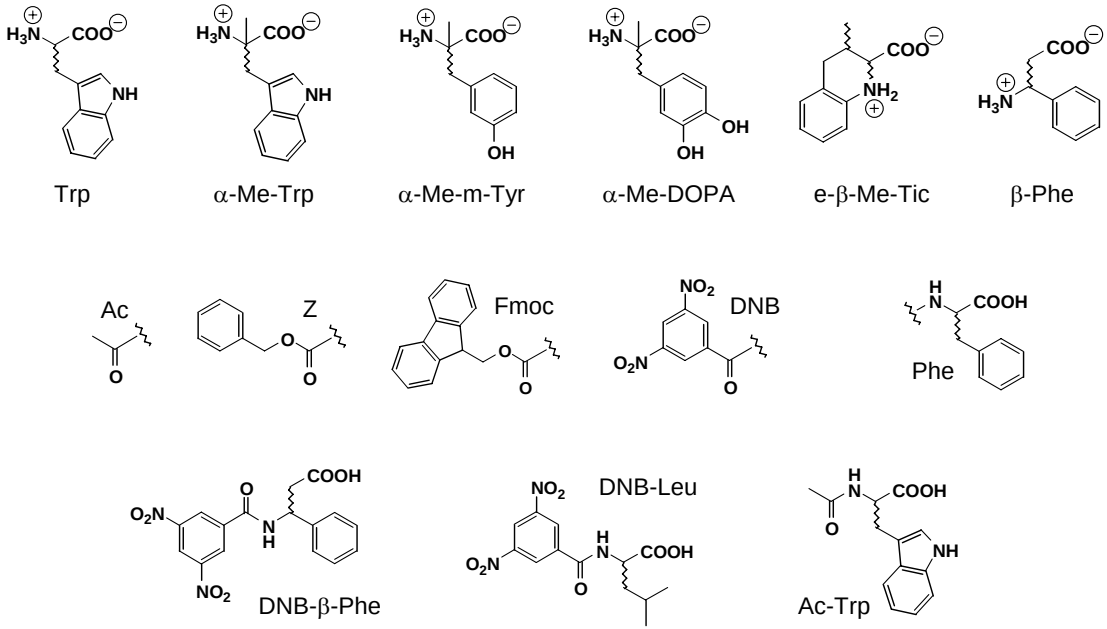

Figure 2.

Chemical structures of the chiral analytes that were used in the present study on zwitterionic CSPs.

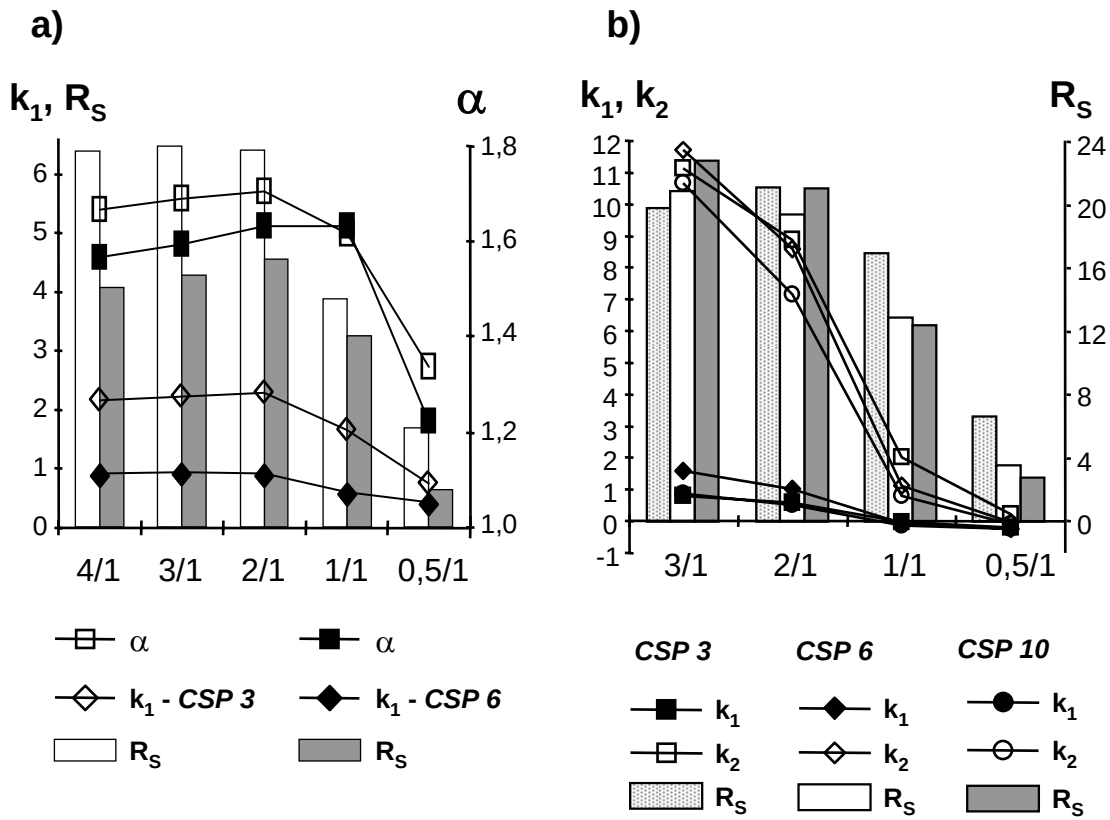

Figure 3.

Effect of the acid-to-base ratio in the mobile phase on the chromatographic behavior of zwitterionic CSPs. a) Retention, enantioselectivity, and resolution for analyte Trp on **CSP 3** and **CSP 6**. b) Retention and resolution for analyte DNB-Phe on **CSP 3**, **6**, and **10**. Mobile phases: combinations 25 mM NH_3 and 100, 75, 50, and 25 mM HOAc, respectively, in MeOH, to afford acid-to-base ratios of 4:1, 3:1, 2:1, and 1:1. Acid-to-base ratio of 0.5:1 was prepared by adding 12.5 mM AB to 12.5 mM NH_4OAc in MeOH.

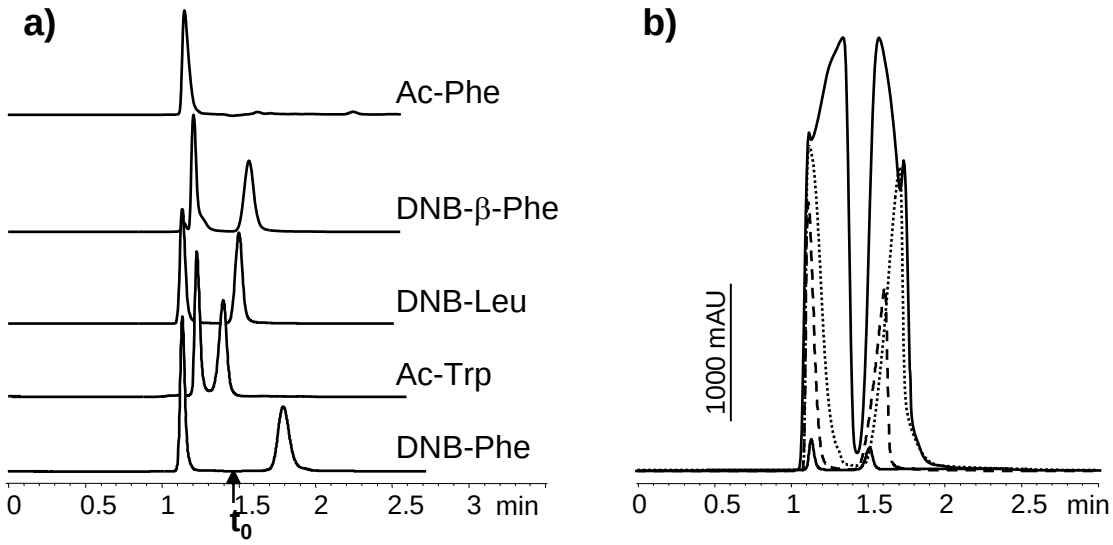

Figure 4.

HPLC enantioseparations on zwitterionic **CSP 3** using base excess mobile phase conditions (12.5 mM AB and 12.5 mM NH_4OAc in MeOH) of a) N-derivatized amino acids, and b) DNB-Leu with increasing sample loading (10, 150, 500, and 800 μg on column, UV detection at 320 nm).

		increasing elution strength →		
AX *type CSP*	*counter-ion*	**HOAc**	**FA**	**TFA**
	co-ion[a)]	**NH_3**	**DEA**	**TEA**
CX *type CSP*	*counter-ion*	**DIEA**[b)]	**DEA**	**NH_3**
	co-ion[a)]	**HOAc**	**FA**	**TFA**

[a)]principally, effect of co-ion substantially smaller than effect of counter-ion

[b)]diisopropylethylamine

Scheme 1.

Elution strength of type of co- and counter-ion additives on retention on single ion exchanger type CSPs, according to findings reported in the literature [4,5,23].

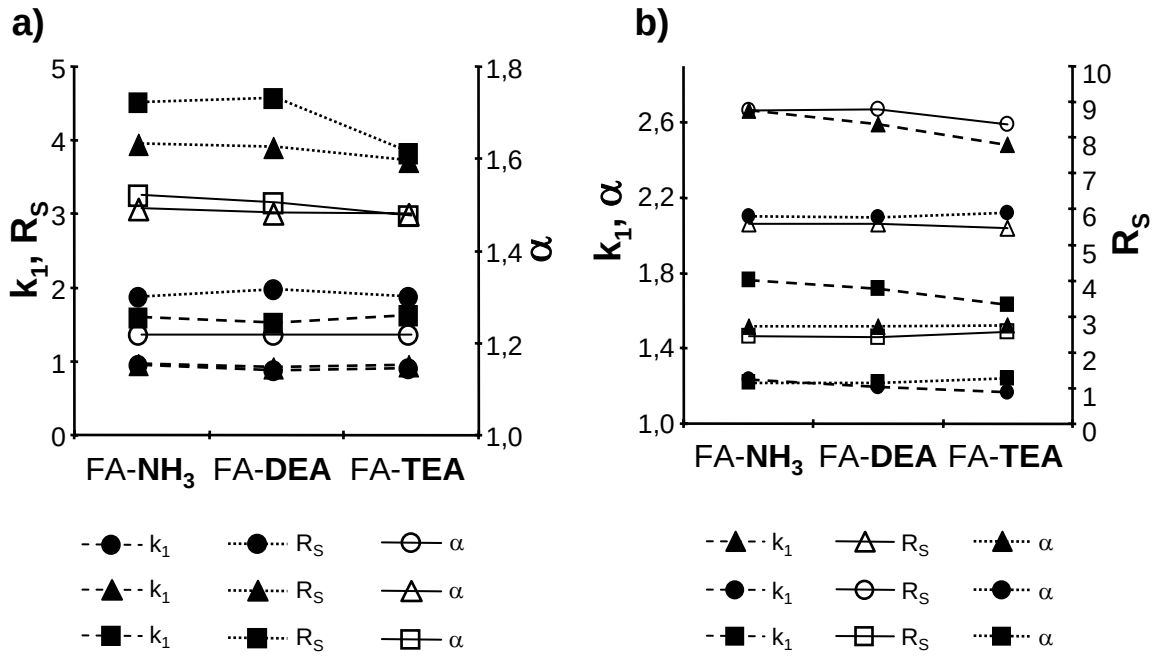

Figure 5.

Influence of the type of basic additive in the mobile phase on retention, resolution, and enantioselectivity on zwitterionic CSPs. a) Data for three amino acid analytes α-Me-m-Tyr (triangle symbols), erythro-β-Me-Tic (round symbols), and Trp (square symbols) on **CSP 4**. b) Data for three acidic analytes Fmoc-Phe (triangle symbols), Ac-Trp (round symbols), and Z-Phe (square symbols). Mobile phases: 50 mM formic acid (FA) and 25 mM base (either NH_3, diethylamine DEA, or triethylamine TEA) in MeOH.

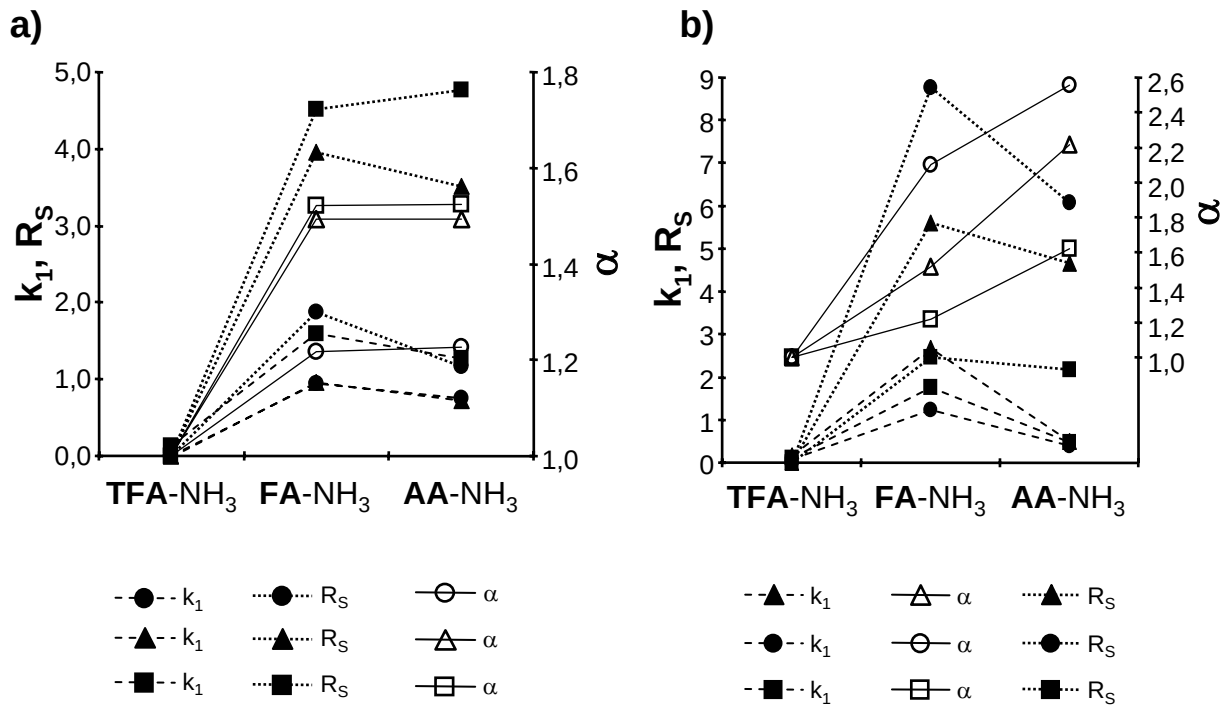

Figure 6.

Influence of the type of acidic additive in the mobile phase on retention, enantioselectivity, and resolution on zwitterionic CSPs. a) Representative data are shown for amino acid analytes α-Me-m-Tyr (triangle symbols), *erythro*-β-Me-Tic (round symbols), and Trp (square symbols) on **CSP 4**. b) Representative data are shown for acidic analytes Fmoc-Phe (triangle symbols), Ac-Trp (round symbols), and Z-Phe (square symbols) on **CSP 4**. Mobile phases: 50 mM acid (either TFA, formic acid FA, or acetic acid AA) and 25 mM NH_3 in MeOH.

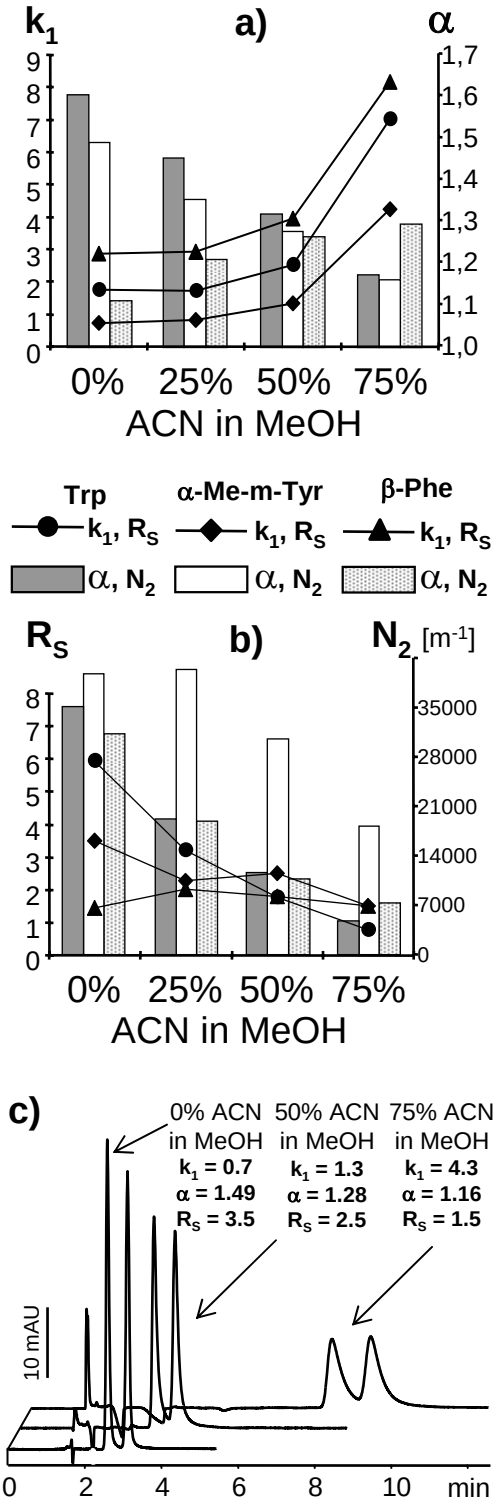

Figure 7.

Influence of ACN and MeOH as bulk eluent solvents in ZX mode for amino acid analytes α-Me-m-Tyr, β-Phe, and Trp on zwitterionic **CSP 3**. a) Data on enantioselectivity and retention and b) data on resolution and plate numbers are shown. c) HPLC enantiomer seprations of α-Me-m-Tyr using methanolic eluent systems of different ACN content. Mobile phases consisted of 50 mM AA and 25 mM NH_3 in ACN-MeOH mixtures (v/v).

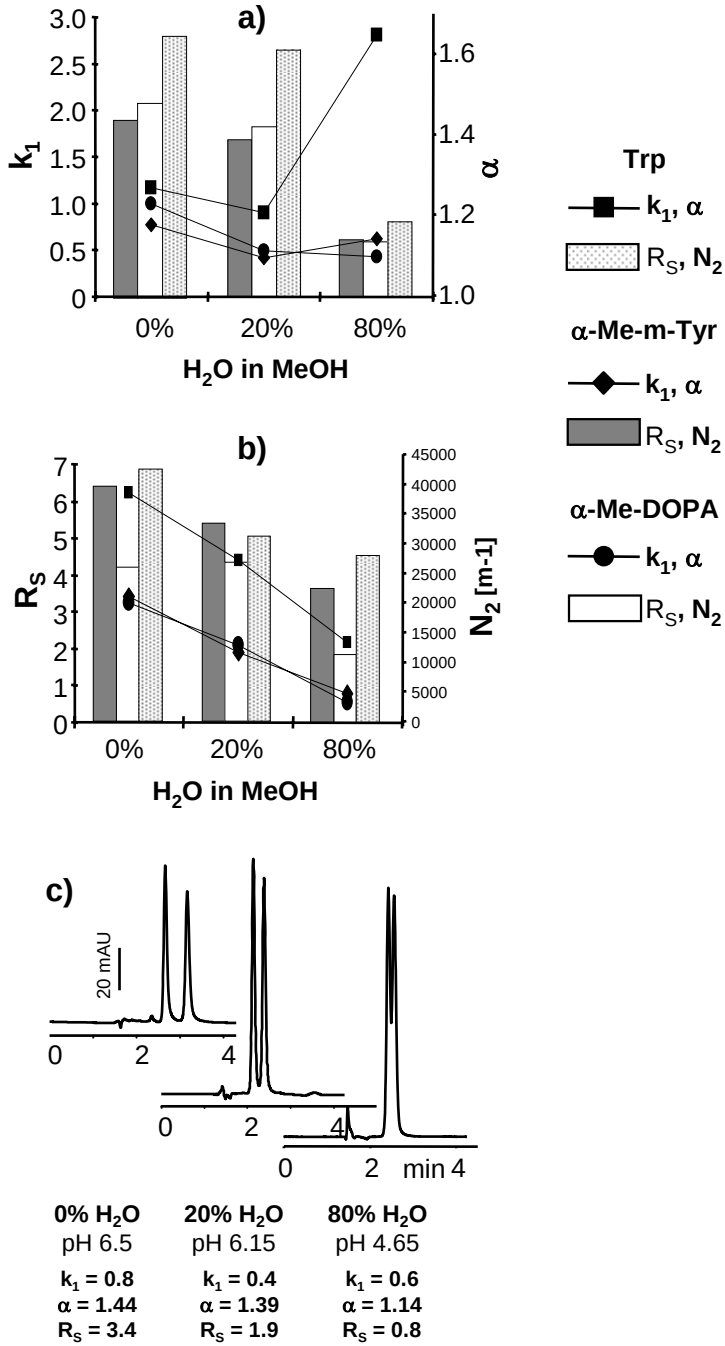

Figure 8.

Influence of H_2O and MeOH as bulk eluent solvents in ZX mode for amino acid analytes α-Me-m-Tyr , Trp, and α-Me-DOPA on zwitterionic **CSP 2**. a) Data on enantioselectivity and retention and b) data on resolution and plate numbers are shown. c) Representative HPLC enantiomer separations of α-Me-m-Tyr using methanolic eluent systems of different H_2O content. Mobile phases: 75 mM HOAc and 25 mM NH_3 in MeOH-H_2O mixtures (v/v).

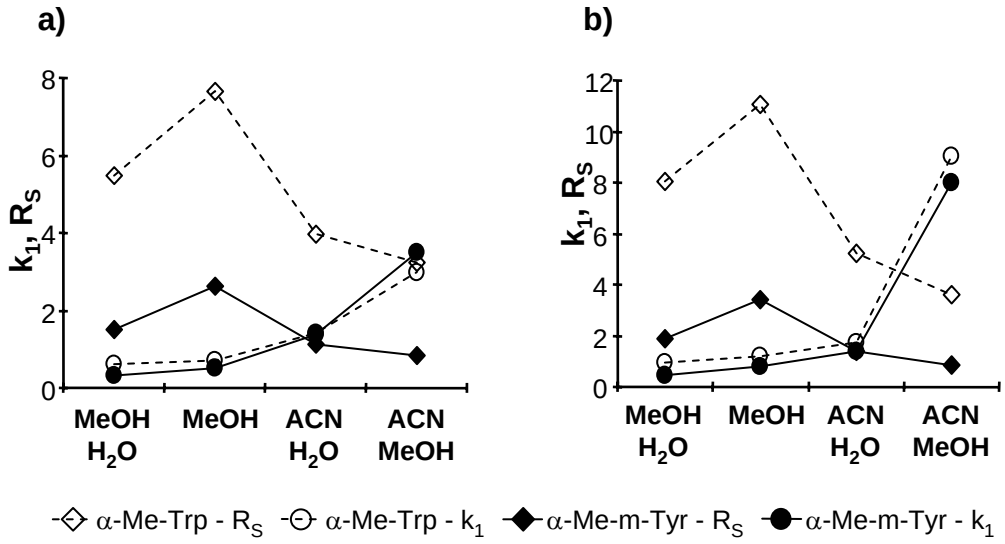

Figure 9.

Influence of protic/aprotic character of the eluent system in ZX mode on retention and resolution for amino acid analytes α-Me-Trp, and α-Me-m-Tyr on a) WCX-type zwitterionic **CSP 6** and b) SCX-type zwitterionic **CSP 2**. Mobile phases: 50 mM HOAc and 25 mM NH_3 in MeOH or MeOH-H_2O, ACN-H_2O, and ACN-MeOH mixtures (80/20 v/v).

Appendix #8

Experimental Section on SO-SA Complex Crystallization

Experimental for SO-SA Complex Crystallization

General Aspects

The basic tert.-butyl carbamoyl quinidine (tBuQD) was prepared according to A. Mandl et.al., *J. Chromatogr. A* **1999**, *858*, 1-11. All experimental conditions and materials for preparing the acidic DNB-homologue **2** of **SO 1** were as described in C. Hoffmann et.al., *J. Chromatogr. A* **2007**, *1161*, 242-251, except the following procedure.

Synthesis of trans-2-(*N*-3,5-dinitrobenzoyl)aminocyclohexanesulfonic acid 2:

A solution of trans-2-aminocyclohexanesulfonic acid (180 mg, 1.0 mmol) and DIPEA (500 µl, 3.0 mmol) in DMF (8 ml) was stirred a 5° C while 3,5-dinitrobenzoyl chloride (345 mg, 1.5 mmol) was added in portions. The resulting suspension was allowed to warm up to 25° C and stirr overnight. Concentration in vacuo afforded a dark brown oil that was dissolved in dichloromethane (30 ml) and extracted once with aqueous NaOH (5 ml, 0.3 M). The aqueous phase was concentrated in vacuo to afford crude racemic **2** as a pale yellow solid. This residue was directely submitted to semipreparative enantiomer separation which yielded virtually enantiopure sulfonic acids **2a** and **b** as their ammonium salts (combined 250 mg, 64 %). $[\alpha]^{20}_{D}$ = - 45.0° (MeOH, 1.0 g/100 ml, first eluted enantiomer). ^{1}H NMR [CD_3OD]: δ = 9.10-9.02 (s, 3H), 4.24-4.12 (m, 1H), 2.99-2.90 (m, 1H), 2.45-2.35 (m, 1H), 2.22-2.12 (m, 1H), 1.88-1.76 (m, 2H), 1.66-1.52 (m, 1H), 1.48-1.32 (m, 3H). ^{13}C NMR: δ = 164.4 (C=O), 149.9 (C), 139.8 (C), 128.7 (CH), 121.6 (CH), 62.5 (CH), 52.7 (CH_2), 33.9 (CH_2), 29.2 (CH_2), 26.2 (CH_2), 25.9 (CH_2). MS (ESI, negative): 372.1 $[M-H]^-$, 745.3 $[2M-H]^-$, 767.3 $[2M-H+Na]^-$.

Crystallization

Sulfonic acid **2a** as its ammonium salt (30.0 mg)**,** obtained as the first eluted enantiomer by semipreparative enantioseparation on a tBuQN-CSP (QN-AX), was combined with an equimolar amount of tBuQD (32.5 mg) which is expected to be the stronger binding stereoisomer for **2a** compared tBuQN. Dissolving of the combined compounds in MeOH, thorough mixing and evaporation to dryness unter high vacuum and 60° C was repeated serveral times in order to remove the ammonia and to form the desired ion pair between the sulfonic acid and the quinidine derivative. Then, the residue was dissolved in CH_2Cl_2 (1 ml) followed by dropwise addition of heptane just until the solution became cloudy. More CH_2Cl_2

was added to give again a clear solution and the vessel was covered with filter paper and let stand for 7 days at ambient temperature when crystals suitable for X-ray analysis had formed.

X-Ray Analysis Data

Identifier	CHHO002
Formula	$C_{42}H_{62}N_6O_{13}S$
Space group	P 2_1
Cell length	**a** 12.7575(6) **b** 20.9405(10) **c** 18.7286(8)
Cell Angles	α 90.00 β 90.047(2) γ 90.00
Cell Volume	5003.31
Z,Z'	**Z**: 4 **Z'**: 0
R-factor (%)	5.8

Number	Label	Charge	SybylType	Xfrac	Yfrac	Zfrac	Symm. op.
1	S1	0	S.o2	0.0019	0.7419	0.3293	x,y,z
2	O1	0	O.2	-0.0586	0.7994	0.3194	x,y,z
3	O2	0	O.2	0.0891	0.7395	0.2779	x,y,z
4	O3	0	O.2	0.0360	0.7309	0.4018	x,y,z
5	O4	0	O.2	0.1615	0.5505	0.3475	x,y,z
6	O5	0	O.2	0.1575	0.5686	0.0161	x,y,z
7	O6	0	O.2	0.3203	0.5502	-0.0103	x,y,z
8	O7	0	O.2	0.5832	0.5565	0.1743	x,y,z
9	O8	0	O.2	0.5359	0.5521	0.2849	x,y,z
10	C1	0	C.3	-0.0321	0.6113	0.3204	x,y,z
11	H1	0	H	-0.0041	0.6097	0.3703	x,y,z
12	C2	0	C.3	-0.0841	0.6769	0.3081	x,y,z
13	H2	0	H	-0.1043	0.6802	0.2566	x,y,z
14	C3	0	C.3	-0.1830	0.6840	0.3536	x,y,z
15	H3A	0	H	-0.1627	0.6853	0.4047	x,y,z
16	H3B	0	H	-0.2174	0.7250	0.3419	x,y,z
17	C4	0	C.3	-0.2608	0.6298	0.3422	x,y,z
18	H4A	0	H	-0.3218	0.6356	0.3742	x,y,z
19	H4B	0	H	-0.2863	0.6305	0.2923	x,y,z
20	C5	0	C.3	-0.2088	0.5659	0.3577	x,y,z
21	H5A	0	H	-0.1882	0.5638	0.4086	x,y,z
22	H5B	0	H	-0.2590	0.5308	0.3482	x,y,z
23	C6	0	C.3	-0.1127	0.5577	0.3109	x,y,z
24	H6A	0	H	-0.1349	0.5563	0.2602	x,y,z
25	H6B	0	H	-0.0790	0.5163	0.3223	x,y,z
26	C7	0	C.2	0.1441	0.5729	0.2889	x,y,z
27	C8	0	C.2	0.2244	0.5699	0.2304	x,y,z
28	C9	0	C.2	0.1983	0.5674	0.1589	x,y,z
29	H9	0	H	0.1271	0.5694	0.1442	x,y,z
30	C10	0	C.2	0.2783	0.5620	0.1085	x,y,z
31	C11	0	C.2	0.3812	0.5581	0.1266	x,y,z
32	H11	0	H	0.4345	0.5536	0.0916	x,y,z
33	C12	0	C.2	0.4044	0.5611	0.1988	x,y,z
34	C13	0	C.2	0.3298	0.5650	0.2511	x,y,z
35	H13	0	H	0.3488	0.5645	0.3002	x,y,z
36	N1	0	N.am	0.0546	0.6028	0.2705	x,y,z
37	H1A	0	H	0.0481	0.6177	0.2267	x,y,z
38	N2	0	N.3	0.2493	0.5594	0.0329	x,y,z
39	N3	0	N.3	0.5154	0.5560	0.2212	x,y,z
40	S01	0	S.o2	0.0598	0.2417	0.1686	x,y,z
41	O01	0	O.2	-0.0022	0.1833	0.1751	x,y,z
42	O02	0	O.2	0.1454	0.2425	0.2214	x,y,z
43	O03	0	O.2	0.0963	0.2548	0.0967	x,y,z
44	O04	0	O.2	0.2339	0.4150	0.1587	x,y,z
45	O05	0	O.2	0.1970	0.4198	0.4915	x,y,z
46	O06	0	O.2	0.3540	0.4439	0.5218	x,y,z
47	O07	0	O.2	0.6342	0.4178	0.3523	x,y,z
48	O08	0	O.2	0.5954	0.4124	0.2394	x,y,z
49	N01	0	N.am	0.1083	0.3799	0.2350	x,y,z
50	H01	0	H	0.0945	0.3713	0.2800	x,y,z
51	C01	0	C.3	0.0241	0.3715	0.1832	x,y,z
52	H01A	0	H	0.0537	0.3755	0.1340	x,y,z
53	C02	0	C.3	-0.0289	0.3052	0.1909	x,y,z
54	H02	0	H	-0.0504	0.2998	0.2419	x,y,z
55	C03	0	C.3	-0.1258	0.2984	0.1447	x,y,z
56	H03A	0	H	-0.1595	0.2567	0.1545	x,y,z
57	H03B	0	H	-0.1050	0.2991	0.0938	x,y,z
58	C04	0	C.3	-0.2048	0.3524	0.1588	x,y,z
59	H04A	0	H	-0.2659	0.3473	0.1267	x,y,z
60	H04B	0	H	-0.2301	0.3495	0.2087	x,y,z
61	C05	0	C.3	-0.1562	0.4164	0.1469	x,y,z

62	H05A	0	H	-0.2076	0.4503	0.1583	x,y,z
63	H05B	0	H	-0.1361	0.4208	0.0961	x,y,z
64	C06	0	C.3	-0.0591	0.4239	0.1942	x,y,z
65	H06A	0	H	-0.0814	0.4235	0.2448	x,y,z
66	H06B	0	H	-0.0268	0.4659	0.1844	x,y,z
67	C07	0	C.2	0.2049	0.3999	0.2190	x,y,z
68	C08	0	C.2	0.2807	0.4056	0.2806	x,y,z
69	C09	0	C.2	0.2485	0.4129	0.3516	x,y,z
70	H09	0	H	0.1761	0.4131	0.3635	x,y,z
71	C010	0	C.2	0.3243	0.4197	0.4040	x,y,z
72	C011	0	C.2	0.4301	0.4194	0.3904	x,y,z
73	H011	0	H	0.4804	0.4238	0.4276	x,y,z
74	C012	0	C.2	0.4592	0.4124	0.3207	x,y,z
75	C013	0	C.2	0.3865	0.4056	0.2644	x,y,z
76	H013	0	H	0.4097	0.4011	0.2165	x,y,z
77	N02	0	N.3	0.2889	0.4284	0.4780	x,y,z
78	N03	0	N.3	0.5705	0.4142	0.3032	x,y,z
79	O10	0	O.3	0.0806	0.7309	0.0573	x,y,z
80	O9	0	O.3	0.4178	0.7321	0.3276	x,y,z
81	O11	0	O.2	0.0049	0.6625	0.1352	x,y,z
82	N4	0	N.4	0.0637	0.8343	0.1814	x,y,z
83	H4	0	H	0.0638	0.8028	0.2164	x,y,z
84	N5	0	N.2	0.4730	0.7125	0.0361	x,y,z
85	N6	0	N.am	-0.0487	0.6688	0.0203	x,y,z
86	H6	0	H	-0.0340	0.6869	-0.0209	x,y,z
87	C14	0	C.3	-0.0425	0.8368	0.1479	x,y,z
88	H14A	0	H	-0.0967	0.8395	0.1855	x,y,z
89	H14B	0	H	-0.0549	0.7973	0.1200	x,y,z
90	C15	0	C.3	-0.0503	0.8952	0.0986	x,y,z
91	H15	0	H	-0.0897	0.9294	0.1245	x,y,z
92	C16	0	C.3	0.0632	0.9191	0.0863	x,y,z
93	H16	0	H	0.0634	0.9529	0.0485	x,y,z
94	C17	0	C.3	0.1050	0.9472	0.1570	x,y,z
95	H17A	0	H	0.1806	0.9569	0.1526	x,y,z
96	H17B	0	H	0.0673	0.9872	0.1686	x,y,z
97	C18	0	C.3	0.0873	0.8976	0.2158	x,y,z
98	H18A	0	H	0.1507	0.8940	0.2460	x,y,z
99	H18B	0	H	0.0280	0.9107	0.2464	x,y,z
100	C19	0	C.3	0.1336	0.8640	0.0636	x,y,z
101	H19A	0	H	0.2019	0.8807	0.0468	x,y,z
102	H19B	0	H	0.1005	0.8402	0.0239	x,y,z
103	C20	0	C.3	0.1499	0.8197	0.1280	x,y,z
104	H20	0	H	0.2179	0.8319	0.1508	x,y,z
105	C21	0	C.2	-0.1101	0.8789	0.0311	x,y,z
106	H21	0	H	-0.0801	0.8484	-0.0004	x,y,z
107	C22	0	C.2	-0.1976	0.9034	0.0138	x,y,z
108	H22A	0	H	-0.2297	0.9341	0.0441	x,y,z
109	H22B	0	H	-0.2310	0.8911	-0.0294	x,y,z
110	C23	0	C.3	0.1554	0.7479	0.1113	x,y,z
111	H23	0	H	0.1409	0.7229	0.1557	x,y,z
112	C24	0	C.2	0.2652	0.7332	0.0850	x,y,z
113	C26	0	C.2	0.3357	0.7322	0.2103	x,y,z
114	H26	0	H	0.2673	0.7370	0.2295	x,y,z
115	C27	0	C.2	0.4199	0.7287	0.2549	x,y,z
116	C28	0	C.2	0.5234	0.7195	0.2267	x,y,z
117	H28	0	H	0.5818	0.7165	0.2580	x,y,z
118	C29	0	C.2	0.5374	0.7152	0.1555	x,y,z
119	H29	0	H	0.6064	0.7097	0.1374	x,y,z
120	C30	0	C.2	0.4527	0.7187	0.1070	x,y,z
121	C31	0	C.2	0.3914	0.7155	-0.0075	x,y,z
122	H31	0	H	0.4041	0.7100	-0.0571	x,y,z
123	C32	0	C.2	0.2867	0.7263	0.0143	x,y,z

124	H32	0	H	0.2320	0.7287	-0.0200	x,y,z
125	C33	0	C.3	0.3172	0.7365	0.3606	x,y,z
126	H33A	0	H	0.3259	0.7387	0.4126	x,y,z
127	H33B	0	H	0.2755	0.6988	0.3482	x,y,z
128	H33C	0	H	0.2814	0.7751	0.3438	x,y,z
129	C34	0	C.2	0.0095	0.6843	0.0753	x,y,z
130	C35	0	C.3	-0.1379	0.6230	0.0221	x,y,z
131	C36	0	C.3	-0.1056	0.5605	0.0583	x,y,z
132	H36A	0	H	-0.0444	0.5427	0.0338	x,y,z
133	H36B	0	H	-0.1637	0.5300	0.0558	x,y,z
134	H36C	0	H	-0.0880	0.5688	0.1084	x,y,z
135	C37	0	C.3	-0.1616	0.6067	-0.0572	x,y,z
136	H37A	0	H	-0.0995	0.5874	-0.0790	x,y,z
137	H37B	0	H	-0.1801	0.6459	-0.0829	x,y,z
138	H37C	0	H	-0.2203	0.5766	-0.0595	x,y,z
139	C38	0	C.3	-0.2289	0.6520	0.0582	x,y,z
140	H38A	0	H	-0.2483	0.6917	0.0338	x,y,z
141	H38B	0	H	-0.2109	0.6613	0.1079	x,y,z
142	H38C	0	H	-0.2882	0.6222	0.0567	x,y,z
143	C25	0	C.2	0.3494	0.7288	0.1355	x,y,z
144	O09	0	O.3	0.4738	0.2395	0.1814	x,y,z
145	O010	0	O.3	0.1251	0.2550	0.4459	x,y,z
146	O011	0	O.2	0.0461	0.3203	0.3655	x,y,z
147	N04	0	N.4	0.1054	0.1513	0.3202	x,y,z
148	H04	0	H	0.1110	0.1821	0.2846	x,y,z
149	N05	0	N.2	0.5143	0.2652	0.4736	x,y,z
150	N06	0	N.am	-0.0021	0.3190	0.4835	x,y,z
151	H06	0	H	0.0156	0.3034	0.5254	x,y,z
152	C028	0	C.2	0.5739	0.2511	0.2848	x,y,z
153	H028	0	H	0.6341	0.2512	0.2551	x,y,z
154	C029	0	C.2	0.5855	0.2573	0.3561	x,y,z
155	H029	0	H	0.6537	0.2619	0.3759	x,y,z
156	C030	0	C.2	0.4969	0.2571	0.4018	x,y,z
157	C031	0	C.2	0.4329	0.2656	0.5151	x,y,z
158	H031	0	H	0.4439	0.2717	0.5648	x,y,z
159	C032	0	C.2	0.3280	0.2575	0.4905	x,y,z
160	H032	0	H	0.2713	0.2585	0.5234	x,y,z
161	C033	0	C.3	0.3756	0.2352	0.1460	x,y,z
162	H03C	0	H	0.3869	0.2319	0.0944	x,y,z
163	H03D	0	H	0.3340	0.2734	0.1565	x,y,z
164	H03E	0	H	0.3380	0.1973	0.1629	x,y,z
165	C034	0	C.2	0.0545	0.3013	0.4265	x,y,z
166	C035	0	C.3	-0.0922	0.3631	0.4801	x,y,z
167	C036	0	C.3	-0.0646	0.4244	0.4400	x,y,z
168	H03F	0	H	-0.0476	0.4141	0.3903	x,y,z
169	H03G	0	H	-0.0040	0.4448	0.4627	x,y,z
170	H03H	0	H	-0.1246	0.4537	0.4412	x,y,z
171	C037	0	C.3	-0.1191	0.3796	0.5573	x,y,z
172	H03I	0	H	-0.1367	0.3404	0.5833	x,y,z
173	H03J	0	H	-0.1792	0.4087	0.5582	x,y,z
174	H03K	0	H	-0.0588	0.4002	0.5801	x,y,z
175	C038	0	C.3	-0.1848	0.3277	0.4463	x,y,z
176	H03L	0	H	-0.1997	0.2889	0.4738	x,y,z
177	H03M	0	H	-0.1673	0.3161	0.3970	x,y,z
178	H03N	0	H	-0.2467	0.3554	0.4464	x,y,z
179	C014	0	C.3	-0.0040	0.1530	0.3496	x,y,z
180	H01B	0	H	-0.0553	0.1505	0.3100	x,y,z
181	H01C	0	H	-0.0155	0.1936	0.3755	x,y,z
182	C015	0	C.3	-0.0196	0.0959	0.4010	x,y,z
183	H015	0	H	-0.0619	0.0627	0.3757	x,y,z
184	C016	0	C.3	0.0887	0.0676	0.4171	x,y,z
185	H016	0	H	0.0833	0.0343	0.4552	x,y,z

186	C017	0	C.3	0.1316	0.0379	0.3475	x,y,z
187	H01D	0	H	0.2053	0.0245	0.3545	x,y,z
188	H01E	0	H	0.0899	-0.0003	-0.3347	x,y,z
189	C018	0	C.3	0.1254	0.0866	0.2875	x,y,z
190	H01F	0	H	0.1920	0.0872	0.2604	x,y,z
191	H01G	0	H	0.0680	0.0754	0.2543	x,y,z
192	C019	0	C.3	0.1642	0.1205	0.4403	x,y,z
193	H01H	0	H	0.2301	0.1015	0.4583	x,y,z
194	H01I	0	H	0.1324	0.1459	0.4792	x,y,z
195	C020	0	C.3	0.1879	0.1643	0.3759	x,y,z
196	H020	0	H	0.2562	0.1497	0.3555	x,y,z
197	C021	0	C.2	-0.0780	0.1155	0.4659	x,y,z
198	H021	0	H	-0.0472	0.1463	0.4969	x,y,z
199	C022	0	C.2	-0.1720	0.0918	0.4826	x,y,z
200	H02A	0	H	-0.2041	0.0610	0.4523	x,y,z
201	H02B	0	H	-0.2068	0.1056	0.5246	x,y,z
202	C023	0	C.3	0.1995	0.2366	0.3924	x,y,z
203	H023	0	H	0.1875	0.2619	0.3479	x,y,z
204	C024	0	C.2	0.3094	0.2485	0.4199	x,y,z
205	C025	0	C.2	0.3970	0.2485	0.3713	x,y,z
206	C026	0	C.2	0.3855	0.2426	0.2962	x,y,z
207	H026	0	H	0.3181	0.2373	0.2754	x,y,z
208	C027	0	C.2	0.4738	0.2446	0.2540	x,y,z
209	O12	0	O.2	0.3217	-0.1101	0.2781	x,y,z
210	O13	0	O.3	0.4932	-0.0996	0.2683	x,y,z
211	C39	0	C.3	0.4233	-0.0978	0.3849	x,y,z
212	H39A	0	H	0.4983	-0.0908	0.3931	x,y,z
213	H39B	0	H	0.4016	-0.1377	0.4078	x,y,z
214	H39C	0	H	0.3834	-0.0621	0.4052	x,y,z
215	C40	0	C.2	0.4030	-0.1017	0.3075	x,y,z
216	C41	0	C.3	0.4800	-0.1024	0.1905	x,y,z
217	H41A	0	H	0.4351	-0.0667	0.1741	x,y,z
218	H41B	0	H	0.4459	-0.1431	0.1767	x,y,z
219	C42	0	C.3	0.5846	-0.0979	0.1572	x,y,z
220	H42A	0	H	0.5773	-0.0991	0.1051	x,y,z
221	H42B	0	H	0.6280	-0.1339	0.1729	x,y,z
222	H42C	0	H	0.6180	-0.0577	0.1714	x,y,z
223	O14	0	O.2	0.3884	0.0699	0.3625	x,y,z
224	O15	0	O.3	0.5383	0.0829	0.4250	x,y,z
225	C43	0	C.3	0.5477	0.0688	0.3022	x,y,z
226	H43A	0	H	0.6215	0.0731	0.3161	x,y,z
227	H43B	0	H	0.5293	0.1028	0.2685	x,y,z
228	H43C	0	H	0.5368	0.0272	0.2795	x,y,z
229	C44	0	C.2	0.4831	0.0737	0.3640	x,y,z
230	C45	0	C.3	0.4762	0.0874	0.4903	x,y,z
231	H45A	0	H	0.4379	0.0470	0.4988	x,y,z
232	H45B	0	H	0.4246	0.1226	0.4865	x,y,z
233	C46	0	C.3	0.5513	0.1001	0.5496	x,y,z
234	H46A	0	H	0.5128	0.1036	0.5947	x,y,z
235	H46B	0	H	0.5887	0.1401	0.5403	x,y,z
236	H46C	0	H	0.6018	0.0649	0.5527	x,y,z
237	O16	0	O.2	-0.3271	0.4746	-0.0533	x,y,z
238	O17	0	O.3	-0.4627	0.4815	0.0086	x,y,z
239	C47	0	C.3	-0.4516	0.5562	-0.0797	x,y,z
240	H47A	0	H	-0.5204	0.5676	-0.0603	x,y,z
241	H47B	0	H	-0.4586	0.5457	-0.1305	x,y,z
242	H47C	0	H	-0.4035	0.5924	-0.0742	x,y,z
243	C48	0	C.2	-0.4086	0.4991	-0.0400	x,y,z
244	C49	0	C.3	-0.4188	0.4297	0.0550	x,y,z
245	H49A	0	H	-0.3586	0.4085	0.0316	x,y,z
246	H49B	0	H	-0.3960	0.4468	0.1017	x,y,z
247	C50	0	C.3	-0.5072	0.3852	0.0636	x,y,z

248	H50A	0	H	-0.4838	0.3474	0.0901	x,y,z
249	H50B	0	H	-0.5328	0.3721	0.0164	x,y,z
250	H50C	0	H	-0.5638	0.4063	0.0899	x,y,z
251	O18	0	O.2	-0.0815	0.9948	0.2622	x,y,z
252	O19	0	O.3	-0.2339	1.0226	0.2289	x,y,z
253	C51	0	C.3	-0.2160	0.9368	0.3137	x,y,z
254	H51A	0	H	-0.2643	0.9098	0.2865	x,y,z
255	H51B	0	H	-0.2539	0.9572	0.3531	x,y,z
256	H51C	0	H	-0.1590	0.9106	0.3329	x,y,z
257	C52	0	C.2	-0.1733	0.9852	0.2675	x,y,z
258	C53	0	C.3	-0.1851	1.0706	0.1708	x,y,z
259	H53A	0	H	-0.1154	1.0862	0.1861	x,y,z
260	H53B	0	H	-0.1784	1.0496	0.1237	x,y,z
261	C54	0	C.3	-0.2627	1.1239	0.1681	x,y,z
262	H54A	0	H	-0.3334	1.1063	0.1623	x,y,z
263	H54B	0	H	-0.2466	1.1518	0.1276	x,y,z
264	H54C	0	H	-0.2591	1.1485	0.2126	x,y,z
265	O2W	0	O.3	-0.1588	1.0320	0.2297	x,y,z
266	O3W	0	O.3	-0.1083	0.9306	0.3543	x,y,z
267	O1W	0	O.3	-0.2902	1.1406	0.1689	x,y,z

Number	Atom1	Atom2	Type	Length	SybylType
1	S1	O1	Unknown	1.442	un
2	S1	O2	Unknown	1.472	un
3	S1	O3	Unknown	1.444	un
4	S1	C2	Unknown	1.793	1
5	O4	C7	Unknown	1.213	2
6	O5	N2	Unknown	1.228	1
7	O6	N2	Unknown	1.230	1
8	O7	N3	Unknown	1.233	1
9	O8	N3	Unknown	1.224	1
10	C1	H1	Unknown	1.000	1
11	C1	C2	Unknown	1.542	1
12	C1	C6	Unknown	1.533	1
13	C1	N1	Unknown	1.460	1
14	C2	H2	Unknown	1.000	1
15	C2	C3	Unknown	1.531	1
16	C3	H3A	Unknown	0.992	1
17	C3	H3B	Unknown	0.989	1
18	C3	C4	Unknown	1.523	1
19	C4	H4A	Unknown	0.990	1
20	C4	H4B	Unknown	0.989	1
21	C4	C5	Unknown	1.521	1
22	C5	H5A	Unknown	0.990	1
23	C5	H5B	Unknown	0.991	1
24	C5	C6	Unknown	1.518	1
25	C6	H6A	Unknown	0.991	1
26	C6	H6B	Unknown	0.990	1
27	C7	C8	Unknown	1.502	un
28	C7	N1	Unknown	1.347	un
29	C8	C9	Unknown	1.381	un
30	C8	C13	Unknown	1.403	un
31	C9	H9	Unknown	0.950	1
32	C9	C10	Unknown	1.395	un
33	C10	C11	Unknown	1.358	un
34	C10	N2	Unknown	1.464	1
35	C11	H11	Unknown	0.950	1
36	C11	C12	Unknown	1.385	un
37	C12	C13	Unknown	1.369	un
38	C12	N3	Unknown	1.480	1
39	C13	H13	Unknown	0.951	1
40	N1	H1A	Unknown	0.881	1
41	S01	O01	Unknown	1.462	un
42	S01	O02	Unknown	1.472	un
43	S01	O03	Unknown	1.452	un
44	S01	C02	Unknown	1.795	1
45	O04	C07	Unknown	1.231	2
46	O05	N02	Unknown	1.213	1
47	O06	N02	Unknown	1.211	1
48	O07	N03	Unknown	1.229	1
49	O08	N03	Unknown	1.237	1
50	N01	H01	Unknown	0.880	1
51	N01	C01	Unknown	1.457	1
52	N01	C07	Unknown	1.336	un
53	C01	H01A	Unknown	1.000	1
54	C01	C02	Unknown	1.551	1
55	C01	C06	Unknown	1.541	1
56	C02	H02	Unknown	1.000	1
57	C02	C03	Unknown	1.515	1
58	C03	H03A	Unknown	0.991	1
59	C03	H03B	Unknown	0.990	1
60	C03	C04	Unknown	1.538	1
61	C04	H04A	Unknown	0.990	1

62	C04	H04B	Unknown	0.991	1
63	C04	C05	Unknown	1.493	1
64	C05	H05A	Unknown	0.990	1
65	C05	H05B	Unknown	0.990	1
66	C05	C06	Unknown	1.530	1
67	C06	H06A	Unknown	0.990	1
68	C06	H06B	Unknown	0.989	1
69	C07	C08	Unknown	1.509	un
70	C08	C09	Unknown	1.400	un
71	C08	C013	Unknown	1.384	un
72	C09	H09	Unknown	0.950	1
73	C09	C010	Unknown	1.385	un
74	C010	C011	Unknown	1.374	un
75	C010	N02	Unknown	1.469	1
76	C011	H011	Unknown	0.951	1
77	C011	C012	Unknown	1.365	un
78	C012	C013	Unknown	1.411	un
79	C012	N03	Unknown	1.458	1
80	C013	H013	Unknown	0.950	1
81	O10	C23	Unknown	1.435	1
82	O10	C34	Unknown	1.375	1
83	O9	C27	Unknown	1.363	1
84	O9	C33	Unknown	1.428	1
85	O11	C34	Unknown	1.214	2
86	N4	H4	Unknown	0.930	1
87	N4	C14	Unknown	1.493	1
88	N4	C18	Unknown	1.504	1
89	N4	C20	Unknown	1.518	1
90	N5	C30	Unknown	1.359	un
91	N5	C31	Unknown	1.324	un
92	N6	H6	Unknown	0.879	1
93	N6	C34	Unknown	1.310	un
94	N6	C35	Unknown	1.489	1
95	C14	H14A	Unknown	0.989	1
96	C14	H14B	Unknown	0.991	1
97	C14	C15	Unknown	1.536	1
98	C15	H15	Unknown	1.001	1
99	C15	C16	Unknown	1.549	1
100	C15	C21	Unknown	1.515	1
101	C16	H16	Unknown	1.001	1
102	C16	C17	Unknown	1.544	1
103	C16	C19	Unknown	1.523	1
104	C17	H17A	Unknown	0.989	1
105	C17	H17B	Unknown	0.990	1
106	C17	C18	Unknown	1.531	1
107	C18	H18A	Unknown	0.989	1
108	C18	H18B	Unknown	0.988	1
109	C19	H19A	Unknown	0.990	1
110	C19	H19B	Unknown	0.989	1
111	C19	C20	Unknown	1.536	1
112	C20	H20	Unknown	1.000	1
113	C20	C23	Unknown	1.538	1
114	C21	H21	Unknown	0.950	1
115	C21	C22	Unknown	1.270	un
116	C22	H22A	Unknown	0.950	1
117	C22	H22B	Unknown	0.950	1
118	C23	H23	Unknown	1.000	1
119	C23	C24	Unknown	1.517	1
120	C24	C32	Unknown	1.360	un
121	C24	C25	Unknown	1.434	un
122	C26	H26	Unknown	0.949	1
123	C26	C27	Unknown	1.362	un

124	C26	C25	Unknown	1.414	un
125	C27	C28	Unknown	1.435	un
126	C28	H28	Unknown	0.950	1
127	C28	C29	Unknown	1.349	un
128	C29	H29	Unknown	0.951	1
129	C29	C30	Unknown	1.413	un
130	C30	C25	Unknown	1.438	un
131	C31	H31	Unknown	0.950	1
132	C31	C32	Unknown	1.415	un
133	C32	H32	Unknown	0.949	1
134	C33	H33A	Unknown	0.981	1
135	C33	H33B	Unknown	0.980	1
136	C33	H33C	Unknown	0.980	1
137	C35	C36	Unknown	1.530	1
138	C35	C37	Unknown	1.553	1
139	C35	C38	Unknown	1.475	1
140	C36	H36A	Unknown	0.980	1
141	C36	H36B	Unknown	0.980	1
142	C36	H36C	Unknown	0.980	1
143	C37	H37A	Unknown	0.979	1
144	C37	H37B	Unknown	0.980	1
145	C37	H37C	Unknown	0.980	1
146	C38	H38A	Unknown	0.980	1
147	C38	H38B	Unknown	0.978	1
148	C38	H38C	Unknown	0.981	1
149	O09	C033	Unknown	1.419	1
150	O09	C027	Unknown	1.365	1
151	O010	C034	Unknown	1.371	1
152	O010	C023	Unknown	1.434	1
153	O011	C034	Unknown	1.214	2
154	N04	H04	Unknown	0.931	1
155	N04	C014	Unknown	1.501	1
156	N04	C018	Unknown	1.509	1
157	N04	C020	Unknown	1.505	1
158	N05	C030	Unknown	1.373	un
159	N05	C031	Unknown	1.298	un
160	N06	H06	Unknown	0.879	1
161	N06	C034	Unknown	1.342	un
162	N06	C035	Unknown	1.476	1
163	C028	H028	Unknown	0.949	1
164	C028	C029	Unknown	1.350	un
165	C028	C027	Unknown	1.407	un
166	C029	H029	Unknown	0.950	1
167	C029	C030	Unknown	1.418	un
168	C030	C025	Unknown	1.408	un
169	C031	H031	Unknown	0.950	1
170	C031	C032	Unknown	1.425	un
171	C032	H032	Unknown	0.951	1
172	C032	C024	Unknown	1.357	un
173	C033	H03C	Unknown	0.980	1
174	C033	H03D	Unknown	0.980	1
175	C033	H03E	Unknown	0.980	1
176	C035	C036	Unknown	1.528	1
177	C035	C037	Unknown	1.526	1
178	C035	C038	Unknown	1.531	1
179	C036	H03F	Unknown	0.980	1
180	C036	H03G	Unknown	0.980	1
181	C036	H03H	Unknown	0.981	1
182	C037	H03I	Unknown	0.981	1
183	C037	H03J	Unknown	0.980	1
184	C037	H03K	Unknown	0.980	1
185	C038	H03L	Unknown	0.981	1

186	C038	H03M	Unknown	0.981	1
187	C038	H03N	Unknown	0.980	1
188	C014	H01B	Unknown	0.990	1
189	C014	H01C	Unknown	0.990	1
190	C014	C015	Unknown	1.548	1
191	C015	H015	Unknown	0.999	1
192	C015	C016	Unknown	1.533	1
193	C015	C021	Unknown	1.484	1
194	C016	H016	Unknown	1.000	1
195	C016	C017	Unknown	1.545	1
196	C016	C019	Unknown	1.531	1
197	C017	H01D	Unknown	0.990	1
198	C017	H01E	Unknown	0.990	1
199	C017	C018	Unknown	1.519	1
200	C018	H01F	Unknown	0.990	1
201	C018	H01G	Unknown	0.988	1
202	C019	H01H	Unknown	0.989	1
203	C019	H01I	Unknown	0.989	1
204	C019	C020	Unknown	1.544	1
205	C020	H020	Unknown	0.999	1
206	C020	C023	Unknown	1.552	1
207	C021	H021	Unknown	0.952	1
208	C021	C022	Unknown	1.335	un
209	C022	H02A	Unknown	0.951	1
210	C022	H02B	Unknown	0.949	1
211	C023	H023	Unknown	1.000	1
212	C023	C024	Unknown	1.514	1
213	C024	C025	Unknown	1.442	un
214	C025	C026	Unknown	1.419	un
215	C026	H026	Unknown	0.950	1
216	C026	C027	Unknown	1.377	un
217	O12	C40	Unknown	1.187	2
218	O13	C40	Unknown	1.366	1
219	O13	C41	Unknown	1.468	1
220	C39	H39A	Unknown	0.980	1
221	C39	H39B	Unknown	0.979	1
222	C39	H39C	Unknown	0.981	1
223	C39	C40	Unknown	1.475	1
224	C41	H41A	Unknown	0.990	1
225	C41	H41B	Unknown	0.991	1
226	C41	C42	Unknown	1.476	1
227	C42	H42A	Unknown	0.980	1
228	C42	H42B	Unknown	0.980	1
229	C42	H42C	Unknown	0.980	1
230	O14	C44	Unknown	1.211	2
231	O15	C44	Unknown	1.355	1
232	O15	C45	Unknown	1.461	1
233	C43	H43A	Unknown	0.981	1
234	C43	H43B	Unknown	0.980	1
235	C43	H43C	Unknown	0.979	1
236	C43	C44	Unknown	1.425	1
237	C45	H45A	Unknown	0.990	1
238	C45	H45B	Unknown	0.991	1
239	C45	C46	Unknown	1.490	1
240	C46	H46A	Unknown	0.980	1
241	C46	H46B	Unknown	0.980	1
242	C46	H46C	Unknown	0.981	1
243	O16	C48	Unknown	1.186	2
244	O17	C48	Unknown	1.201	1
245	O17	C49	Unknown	1.498	1
246	C47	H47A	Unknown	0.980	1
247	C47	H47B	Unknown	0.980	1

248	C47	H47C	Unknown	0.981	1
249	C47	C48	Unknown	1.511	1
250	C49	H49A	Unknown	0.990	1
251	C49	H49B	Unknown	0.989	1
252	C49	C50	Unknown	1.472	1
253	C50	H50A	Unknown	0.981	1
254	C50	H50B	Unknown	0.981	1
255	C50	H50C	Unknown	0.980	1
256	O18	C52	Unknown	1.192	2
257	O19	C52	Unknown	1.316	1
258	O19	C53	Unknown	1.607	1
259	C51	H51A	Unknown	0.979	1
260	C51	H51B	Unknown	0.980	1
261	C51	H51C	Unknown	0.979	1
262	C51	C52	Unknown	1.440	1
263	C53	H53A	Unknown	0.989	1
264	C53	H53B	Unknown	0.989	1
265	C53	C54	Unknown	1.493	1
266	C54	H54A	Unknown	0.980	1
267	C54	H54B	Unknown	0.979	1
268	C54	H54C	Unknown	0.981	1

Danksagung

Zu aller erst gilt mein besonderer Dank Prof. Wolfgang Lindner dafür, daß er mir die Möglichkeit gegeben hat meine Doktorarbeit in seiner Arbeitsgruppe und über interessante Themenstellungen durchführen zu können, sowie für seine umfassende Betreuung, für ein Arbeitsumfeld das geprägt war von keinerlei Mangel an Mitteln und Ausstattung, für seinen steten Fluß an neuen Ideen, und für seine Motivation die eigenen Ergebnisse auf Seminaren und Konferenzen zu präsentieren.

Besonderer Dank gilt auch Prof. Michael Lämmerhofer, der immer Zeit für ausschlußreiche Gespräche sowie einen passenden Rat oder Lösungsvorschlag parat hatte und mit dem die Zusammenarbeit mir große Freude bereitet hat.

Bei Prof. Hanspeter Kählig möchte ich mich bedanken für die zahlreichen Messungen im NMR-Servicebetrieb und darüber hinaus für die gute Zusammenarbeit im Rahmen unserer NMR-Studie. Bedanken möchte ich mich auch bei Prof. Vladimir Arion und Alexander Roller für die Röntgenstrukturanalysen sowie bei Mag. Johannes Theiner für die Durchführung der Elementaranalysen.

Weiters möchte ich danken: dem Christoph für eine wirklich gute Zeit, und zusammen mit dem Alex für ihre Unterstützung beim Zurechtfinden in einem Analytik-Labor sowie für zahlreiche MS-Messungen, der Trixi für Ihre zügige Zusammenarbeit auf Kapillar-Nivau die in zwei Artikeln mündete, dem Norbert und dem Karol für die sehr abwechslungsreiche gemeinsame Zeit im Syntheselabor, und natürlich der gesamten Arbeitsgruppe Lindner: Vielen Dank für das prima Arbeitsklima - und die gemeinsamen Ess- und Trinkaktivitäten!

Mein Dank geht auch an AstraZeneca für mehr wissenschaftliche Freiheit als ich es in einer Industriekooperation erwartet hatte.

Abstract

Liquid chromatography (LC) by means of chiral stationary phases (CSPs) is of central importance both as an analytical tool for the separation of enantiomers and also on a preparative scale to give access to bulk quantities of highly enantiopure chiral compounds.

In this work the development of several novel ion exchanger type CSPs based on synthetic low molecular mass chiral selectors (SOs) as the enantioselective functional entities, and their evaluation for enantiomer separations in HPLC are presented.

At first, strong cation exchanger (SCX) type SOs were prepared that contained a β-amidocyclohexanesulfonic acid as chiral moiety. The corresponding CSPs allowed the baseline enantioseparation of a series of chiral basic drugs. In a separate study on the SCX-type SOs, and in combination with a quinidine-based, oppositely charged anion-exchanger (AX) type SO using HPLC and X-ray diffraction analysis, the molecular recognition mechanism of these AX- and CX-type SOs could be depicted. Furthermore, the SCX-type CSP was evaluated for the nonenantioselective analysis of a series of basic *Cinchona* alkaloids where it turned out to be an alternative, complementary stationary phase to the reversed-phase packing materials commonly used in this context. The described SCX-SO was also applied in a comparison of capillary electrochromatography (CEC) and capillary liquid chromatography (CLC) for enantioseparations as well as in a study that deconvoluted the electrokinetic and chromatographic contributions to analyte migration in enantioselective ion-exchange CEC. Finally, a novel type of ion-exchanger CSP was developed by combining key motifs of both anion- and cation-exchanger type CSPs into one, now zwitterionic SO molecule. The resulting zwitterionic (ZWIX) CSPs not only essentially combined the enantioselective properties of the parent AX- and CX-type CSPs, but in addition also showed excellent enantioselectivities for zwitterionic amino acids and peptides. Mechanistically the zwitterion exchange could be described by a simultaneous double ion pairing event. Due to the overlaid equilibra particular effects on retention and resolution could be observed in the course of mobile phase optimization.

Abstract

Flüssigchromatographie unter Verwendung von chiralen stationären Phasen (CSPs) ist von zentraler Bedeutung sowohl als Werkzeug in der Enantiomerenanalytik als auch für die Gewinnung von hoch enantiomerenreinen chiralen Substanzen im präparativen Maßstab.
In der vorliegenden Arbeit werden die Entwicklung von mehreren neuartigen, auf dem Ionenaustauscherprinzip aufbauenden CSPs und deren Evaluierung für die Enantiomerentrennung in der HPLC vorgestellt. Als funktionelle Einheiten dieser CSPs fungieren synthetische niedermolekulare chirale Selektoren (SOs).
Zunächst wurden SOs vom starken Kationenaustauscher-Typ (strong cation exchanger, SCX) hergestellt die als chirale Gruppe eine β-Aminocyclohexansulfonsäure beinhalteten. Die darauf aufbauenden CSPs ermöglichten die Basislinientrennung einer Reihe von chiralen basischen Wirkstoffen. In einer weiteren Studie über diese SCX-SOs, zu der ein Quinidin-basierter, entgegengesetzt geladener SO vom Anionentauscher-Typ (anion exchanger, AX) hinzugezogen wurde, konnte mit Hilfe von HPLC und Röntgenstrukturanalyse der molekulare Erkennungsmechanismus dieser AX- und CX-SOs aufgezeigt werden. Desweiteren wurde die CSP vom SCX-Typ auch für die nichtenantioselektive Analyse einer Reihe von basischen *Cinchona* Alkaloiden evaluiert. Dabei hat sie sich als alternative, komplementäre stationäre Phase zu den für dieses Trennproblem üblicherweise eingesetzten Chromatographiematerialien vom Umkehrphasentyp herausgestellt. Besagter SCX-SO wurde außerdem in einem Vergleich von Kapillarelektrochromatographie (CEC) und Kapillarflüssigchromatographie (CLC) für die Enantiomerentrennung und in einer Studie eingesetzt, die die elektrokinetischen und chromatographischen Beiträge zur Analytmigration in der enantioselektiven Ionenaustausch-CEC herausarbeitete. Schließlich wurde ein neuartiger Typ einer Ionenaustauscher-basierten CSP entwickelt indem Schlüsselmotive sowohl von Anionentauscher- wie auch Kationentauscher-CSPs in einem, nun zwitterionischen SO-Molekül vereinigt wurden. Die daraus resultierenden zwitterionischen CSPs zeigten nicht nur die im Wesentlichen kombinierten enantioselektiven Eigenschaften der AX- und CX-CSP von denen sie abgeleitet wurden sondern zudem ausgezeichnete Enantioselektivitäten für Aminosäuren und Peptide. Der Zwitterionenaustausch konnte mechanistisch durch simultane doppelte Ionenpaarbildung beschrieben werden. Aufgrund überlagerter Gleichgewichte wurden besondere Effekte bei Retention und Auflösung im Zuge der Optimierung der mobilen Phase beobachtet.

curriculum vitae

Dipl.-Chem. Christian Hoffmann
Institut for Analytical Chemistry & Food Chemistry
University of Vienna
Währingerstrasse 38
A-1090 Vienna
christian.hoffmann@univie.ac.at

Date of birth:	May 21th 1977
Place of birth:	Hof a. d. Saale, Germany
Nationality:	german
Family status:	single

Education

November 1997 - July 2000	chemistry studies at the University of Bayreuth, Germany
August 2000 - June 2001	chemistry studies at the University of Delaware, USA, as a stipend of the University of Bayreuth and graduate student at Prof. Joel P. Schneider
July 2001 - August 2003	chemistry studies at the University of Bayreuth diploma thesis at Prof. Carlo Unverzagt graduation with degree of Diplom-Chemiker, grade „sehr gut“/excellent
since October 2004	PhD thesis at Prof. Wolfgang Lindner, University of Vienna

Sciencific contributions

talks

2. ASAC JunganalytikerInnen Forum, June 2006, Graz, Austria
title: „Design und modulare Synthese von neuartigen chiralen Kationenaustauschermaterialien und deren Anwendung zur Enantiomerentrennung in der HPLC“

17. Doktorandenseminar der GDCh, January 2007, Hohenroda, Germany
title: „Development of novel chiral cation exchangers for enantiomer separations in HPLC“

posters

1st European Chemistry Congress August 2006, Budapest, Hungary
title: „Novel chiral strong cation exchange molecular recognition materials: Design, modular synthesis and application to enantiomer separation in HPLC“

19th Int. Symposium on Chirality ISCD, July 2007, San Diego, USA
title „Chromatographic enantiomer separation of chiral amines with a novel strong cation exchange type chiral stationary phase“

19th Int. Symposium on Chirality ISCD, July 2007, San Diego, USA
title: „Structural elucidation of cation exchange type chiral selectors for enantiomer separation using liquid chromatography, NMR Spectroscopy and X-Ray diffraction analysis“
(awarded best poster)

33rd Int. Symposium on High-Performance Liquid Phase Separations and Related Techniques, HPLC2009, May 2008, Baltimore, USA
title: „A novel strong cation exchange type stationary phase for the separation of basic analytes – comparison with commercially available strong cation exchanger and reversed-phase packing materials for *Cinchona* alkaloids“
(awarded top-twenty poster)

20th Int. Symposium on Chirality ISDC, July 2008, Geneva, Switzerland
title: „Novel zwitterionic chiral ion exchangers for the enantioseparations of chiral acids, bases, and amino acids in HPLC“
(awarded second best poster)

27th Int. Symposium on Chromatography ISC, July 2008, Münster, Germany
title: „Novel zwitterionic chiral ion exchangers: chromatographic evaluations for the enantioseparation of chiral acids, bases, and amino acids in HPLC“
(awarded best poster, joined 1st place)

publications

Journal of Chromatography A 2007, 1161, 242-251
title: “A novel strong cation exchanger type chiral stationary phase for the enantiomer separation of chiral amines by HPLC”
authors: Christian Hoffmann, Michael Lämmerhofer, Wolfgang Lindner

Journal of Separation Science 2008, 31, 3065-3078
title: “Deconvolution of electrokinetic and chromatographic contributions to solute migration in stereoselective ion-exchange capillary electrochromatography on monolithic silica capillary columns”
authors: Beatrix Preinerstorfer, Michael Lämmerhofer, Christian Hoffmann, Dieter Lubda, Wolfgang Lindner

Electrophoresis 2008, 29, 1626-1637
title: “Enantioselective silica-based monoliths modified with a novel aminosulfonic acid-derived strong cation exchanger for electrically driven and pressure-driven capillary chromatography”
authors: Beatrix Preinerstorfer, Christian Hoffmann, Dieter Lubda, Michael Lämmerhofer, Wolfgang Lindner

Analytical Chemistry 2008, in press
title: „Synergistic effects on enantioselectivity of zwitterionic chiral stationary phases for the separation of chiral acids, bases, and amino acids in HPLC”
authors: Christian Hoffmann, Reinhard Pell, Michael Lämmerhofer, Wolfgang Lindner